

CANADIAN THESES ON MICROFICHE

THÈSES CANADIENNES SUR MICROFICHE



National Library of Canada
Collections Development Branch

Canadian Theses on
Microfiche Service

Ottawa, Canada
K1A 0N4

Bibliothèque nationale du Canada
Direction du développement des collections

Service des thèses canadiennes
sur microfiche

NOTICE

The quality of this microfiche is heavily dependent upon the quality of the original thesis submitted for microfilming. Every effort has been made to ensure the highest quality of reproduction possible.

If pages are missing, contact the university which granted the degree.

Some pages may have indistinct print especially if the original pages were typed with a poor typewriter ribbon or if the university sent us an inferior photocopy.

Previously copyrighted materials (journal articles, published tests, etc.) are not filmed.

Reproduction in full or in part of this film is governed by the Canadian Copyright Act, R.S.C. 1970, c. C-30. Please read the authorization forms which accompany this thesis.

**THIS DISSERTATION
HAS BEEN MICROFILMED
EXACTLY AS RECEIVED**

AVIS

La qualité de cette microfiche dépend grandement de la qualité de la thèse soumise au microfilmage. Nous avons tout fait pour assurer une qualité supérieure de reproduction.

S'il manque des pages, veuillez communiquer avec l'université qui a conféré le grade.

La qualité d'impression de certaines pages peut laisser à désirer, surtout si les pages originales ont été dactylographiées à l'aide d'un ruban usé ou si l'université nous a fait parvenir une photocopie de qualité inférieure.

Les documents qui ont déjà l'objet d'un droit d'auteur (articles de revue, examens publiés, etc.) ne sont pas microfilmés.

La reproduction, même partielle, de ce microfilm est soumise à la Loi canadienne sur le droit d'auteur, SRC 1970, c. C-30. Veuillez prendre connaissance des formules d'autorisation qui accompagnent cette thèse.

**LA THÈSE A ÉTÉ
MICROFILMÉE TELLE QUE
NOUS L'AVONS REÇUE**

Canada

THE UNIVERSITY OF ALBERTA

EXPERIMENTAL AND NUMERICAL MODELLING
OF GAS INJECTION IN CONJUNCTION WITH STEAM
FOR THE RECOVERY OF MODERATELY VISCOUS OILS

by

THOMAS G. HARDING

A THESIS

SUBMITTED TO THE FACULTY OF GRADUATE STUDIES AND RESEARCH

IN PARTIAL FULFILLMENT OF THE REQUIREMENTS FOR THE DEGREE

OF DOCTOR OF PHILOSOPHY

IN

PETROLEUM ENGINEERING

DEPARTMENT OF MINING, METALLURGICAL AND PETROLEUM ENGINEERING

EDMONTON, ALBERTA

FALL, 1986

Permission has been granted to the National Library of Canada to microfilm this thesis and to lend or sell copies of the film.

The author (copyright owner) has reserved other publication rights, and neither the thesis nor extensive extracts from it may be printed or otherwise reproduced without his/her written permission.

L'autorisation a été accordée à la Bibliothèque nationale du Canada de microfilmer cette thèse et de prêter ou de vendre des exemplaires du film.

L'auteur (titulaire du droit d'auteur) se réserve les autres droits de publication; ni la thèse ni de longs extraits de celle-ci ne doivent être imprimés ou autrement reproduits sans son autorisation écrite.

ISBN 0-315-32599-2

THE UNIVERSITY OF ALBERTA

RELEASE FORM

NAME OF AUTHOR THOMAS G. HARDING
TITLE OF THESIS EXPERIMENTAL AND NUMERICAL MODELLING OF GAS
INJECTION IN CONJUNCTION WITH STEAM FOR THE
RECOVERY OF MODERATELY VISCOUS OILS
DEGREE FOR WHICH THESIS WAS PRESENTED DOCTOR OF PHILOSOPHY
YEAR THIS DEGREE GRANTED 1986

Permission is hereby granted to THE UNIVERSITY OF ALBERTA
LIBRARY to reproduce single copies of this thesis and to lend
or sell such copies for private, scholarly or scientific
research purposes only.

The author reserves other publication rights, and neither the
thesis nor extensive extracts from it may be printed or
otherwise reproduced without the author's written permission.

TH Harding

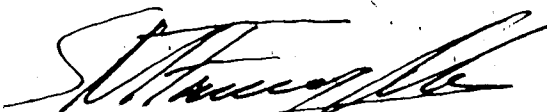
PERMANENT ADDRESS: 2031 Briar Crescent N.W.
Calgary, Alberta
T2N 3V6

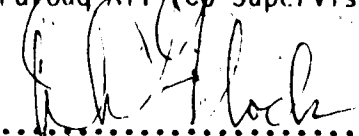
DATED June 27, 1986

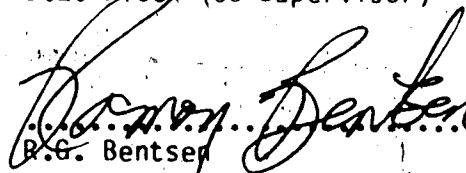
THE UNIVERSITY OF ALBERTA

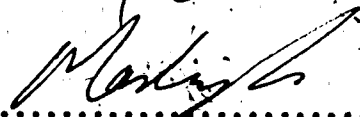
FACULTY OF GRADUATE STUDIES AND RESEARCH

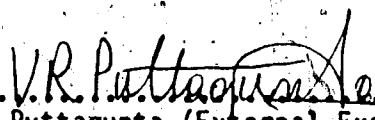
The undersigned certify that they have read, and recommend to the Faculty of Graduate Studies and Research, for acceptance, a thesis entitled EXPERIMENTAL AND NUMERICAL MODELLING OF GAS INJECTION IN CONJUNCTION WITH STEAM FOR THE RECOVERY OF MODERATELY VISCOUS OILS submitted by THOMAS G. HARDING in partial fulfillment of the requirements for the degree of Doctor of Philosophy in Petroleum Engineering.


.....
S.M. Farouq Ali (Co-Supervisor)


.....
D.L. Flock (Co-Supervisor)


.....
R.G. Bentser


.....
J. Masliyah


.....
V.R. Puttagunta (External Examiner)

Date June 27, 1986

To Brynne and Graeme

ABSTRACT

A project involving physical and numerical modelling of steam and gas injection processes was undertaken in order to determine the effect on the steamflood process of the addition of carbon dioxide and nitrogen. The project originated from questions raised as to the effect of flue gases on reservoir performance when employing a downhole steam generator or other equipment which creates a mixture of non-condensable gases and steam.

A series of laboratory experiments was conducted in linear porous media saturated with a moderately viscous refined oil and water. Comparisons were made between steam-only, steam/flue gas (steam, CO₂, N mixtures), steam/CO₂ and steam/N injection processes. The majority of the experiments involved simultaneous injection of the gases with steam but some involved steam injection following a slug of gas. The gas/steam ratios employed in the experiments were those which would result from the recombination of steam and the gas products from the combustion of fuel used to raise the steam. Both pre-and post-waterflooded sand packs were used. A fully implicit thermal numerical simulation model was written to aid in the interpretation of the experimental results. History matching and process sensitivity studies were conducted with the numerical model.

The addition of the gases to steam was found to accelerate oil production response quite markedly and to yield a modest improvement in total oil recovery. The steam/CO₂ injection process was superior to the steam/flue gas process on the basis of oil recovery at the same total molal fluid injection. Steam-oil and water-oil ratios were reduced in

the steam/gas co-injection processes.

The laboratory experiments were found to be sensitive to thermal effects including heat losses, steam quality and injection rate. Other sensitive parameters included: oil saturation, viscosity and volatility; porosity and relative permeability; gas/steam ratio and CO₂/N₂ ratio; and, gas solubility. The processes were relatively insensitive to absolute permeability, rock compressibility and rock heat capacity. History matching of the experiments was done primarily by varying the heat loss and relative permeability parameters.

The performance improvement observed as a result of gas addition to steam is attributed to non-condensable gas drive and solubility effects including viscosity reduction and swelling of oil.

ACKNOWLEDGEMENT

The author wishes to express his sincere appreciation to Dr. S.M. Farouq Ali and Dr. D.L. Flock for their guidance and assistance during this investigation.

The assistance of Mr. G. Walsh and Mr. R. Smith with design and construction of the experimental apparatus is gratefully acknowledged. Oil for the laboratory experiments was provided by the Imperial Oil Strathcona Refinery in Edmonton, Alberta.

Thanks are also due to the management of BP Canada Inc. for allowing the author to use the company's computing facilities during numerical simulation model development and application.

The author is indebted to the following organizations for financial support during the course of this study: The Alberta Oil Sands Technology and Research Authority; BP Canada Inc.; The National Sciences and Engineering Research Council; and, the Petroleum Aid to Education Fund.

The following individuals are recognized for their contributions to the work: Dr. R.K. Mehra for helpful advice on mathematical model formulations; Mr. B. Rubin for assistance during mathematical model debugging; Dr. K.G. Logan for compiling IMSL subroutines for the FPS 164 array processor and for useful comments on the mathematical model debugging process; Mrs. E. Bay for preparation of plots of experimental and numerical simulation results; Mr. P.A. Dykstra for drafting of figures and preparation of photographic plates; and Mrs. L.A. Thompson and Mrs. C. Marshall for typing the manuscript.

A special debt of gratitude is owed to my wife Marne for her unfailing support and encouragement, particularly during the years of full time employment and continued work on this project.

Special thanks are also expressed to other members of my family and to my friends for their caring and consideration. I am grateful to my parents for their moral support and for assistance with household maintenance and improvements during the course of this study.

TABLE OF CONTENTS

	Page
DEDICATION	1v
ABSTRACT	v
ACKNOWLEDGEMENT	vi
LIST OF TABLES	xii
LIST OF FIGURES	xiv
LIST OF PLATES	xvii
NOMENCLATURE	xviii

CHAPTER

I.	INTRODUCTION	1
II.	REVIEW OF LITERATURE	7
	A. Effect of Gases and Steam on Fluid Properties	7
	B. Laboratory Studies of Gas-Steam Injection	11
	C. Numerical Simulation Studies of Gas-Steam Injection	14
	D. Compositional Reservoir Simulation	18
	E. Numerical-Simulation of Thermal Recovery Methods	24
	1. Steam Models	26
	2. In-Situ Combustion Models	30
III.	EXPERIMENTAL EQUIPMENT AND PROCEDURE	35
	A. Introduction	35
	B. Experimental Apparatus	36
	1. Test Cell	37
	2. Steam Generator	42
	3. Gas Injection System	45
	4. Production Handling	46
	C. Materials	47
	D. Experimental Procedure	50
IV.	EXPERIMENTAL RESULTS	58
	A. The Experimental Program	58
	B. Nature of the Experiments	64
	C. The Effect of Gas Additives to Steam	69
	D. The Effect of Flow Rate, Pressure and Carbon Dioxide Presaturation on Simultaneous Steam-Gas Injection Processes	84

	Page
V. MATHEMATICAL MODEL FORMULATION	95
A. General Features of the Model	95
B. Mathematical Formulation	99
C. Physical Properties of Reservoir Fluids and Rock	101
1. Rock Properties	101
2. Fluid Properties	102
a) Viscosity	102
b) Density	102
c) Enthalpy and Internal Energy	110
d) Phase Behaviour	111
3. Fluid-Rock Properties	113
a) Relative Permeability	113
b) Capillary Pressure	114
D. Heat Losses	115
E. Injection and Production Rates	117
F. Solution Method	118
1. Newton-Raphson Technique	118
2. Choice of Primary Variables	121
3. Finite Difference Approximations	123
G. Organization of the Computer Program	123
VI. NUMERICAL SIMULATION RESULTS	129
A. Preliminary Data Set Development	129
1. Process and Reservoir Conditions	129
2. Fluid Properties	133
3. Grid Arrangement and Model Operation	136
B. Preliminary Simulation Results	143
1. Base Case Results	143
2. Grid and Heat Loss Sensitivities	148
3. Reservoir Parameter Sensitivities	150
4. Fluid Property Sensitivities	168
5. Process Sensitivities	173
6. Discussion	178
C. Representative Simulation Runs	186
1. Data Set Development	186
2. History Match Results	189
3. Process and Parameter Sensitivites	189
4. Discussion	195
VII. DISCUSSION OF RESULTS	197
VIII. CONCLUSIONS AND RECOMMENDATIONS	201
IX. REFERENCES	203
APPENDIX A - Material and Equipment Suppliers for Experimental Work	212
APPENDIX B - Design Drawings for Test Cell Used In Laboratory Experiments	216

	page
APPENDIX C - Tables of Experimental Data	219
APPENDIX D - Derivation of Partial Differential Equations for the Mathematical Model	258
APPENDIX E - Mathematical Model in Finite Difference Form	264
APPENDIX F - Mathematical Model, Equations in Standard Form	270
APPENDIX G - Example Simulation Data Set and Computer Output	278
VITA	293

Table		Page
3.1	Properties of Oil	49
4.1	Summary of Experimental Results	59
4.2	Comparison of Steam-Only Injection and Simultaneous Steam-Gas Injection (Prewaterflood)	72
4.3	Comparison of Steam-Only Injection and Simultaneous Steam-Gas Injection (Postwaterflood)	77
4.4	Comparison of Slug and Simultaneous Steam-Gas Injection Processes	83
4.5	Effect of Flow Rate on Simultaneous Steam-Gas Injection Processes	86
4.6	Effect of Pressure and CO ₂ Presaturation on Simultaneous Steam-Gas Injection Processes	91
5.1	Distribution of Components in Fluid Phases	96
5.2	Functional Dependence of Physical Properties	98
6.1	Initial Phase Compositions	130
6.2	Process and Reservoir Data	132
6.3	Pure Component Critical Properties	134
6.4	Pure Component Viscosities	135
6.5	Pure Component Liquid Phase Density Data	137
6.6	Pure Component Liquid Phase Enthalpy Data	138
6.7	Pure Component Vapour Phase Enthalpy Data	139
6.8	Equilibrium K-Value Data	140
6.9	Grid Block Sizes	141
6.10	Program Control Parameters	144
6.11	Notes on Reservoir Parameter Sensitivity Simulation Runs	151
6.12	Fluid Property and Process Sensitivity Simulation Runs	169

6.13	Summary of Reservoir Parameter Sensitivity Results	184
6.14	Summary of Fluid Property and Process Sensitivity Results	185
6.15	Input Data Used for History Matching	187

Figure	Page
3.1 Schematic Diagram of Steamflood Apparatus	38
3.2 Schematic Diagram of Apparatus for Saturating Sand Pack with Water and Measuring Permeability	53
3.3 Schematic Diagram of Apparatus for Flooding Sand Pack with Oil	55
4.1 Inlet Pressure Histories for Simultaneous Steam-Gas Injection	67
4.2 Temperature Profiles - Run 6	68
4.3 Wall and Centre Temperature Profiles - Run 4	70
4.4 Wall and Centre Temperature Profiles - Run 6	71
4.5 Cumulative Production Histories for Simultaneous Steam-Gas Injection (Prewaterflood)	74/75
4.6 Cumulative Production Histories for Simultaneous Steam-Gas Injection (Postwaterflood)	79/80
4.7 Cumulative Production Histories for Steamfloods Following Injection of Carbon Dioxide, Flue Gas and Water	85
4.8 Cumulative Production Histories for Simultaneous Steam/CO ₂ Injection at Two Flow Rates	88
4.9 Cumulative Production Histories for Simultaneous Steam/Flue Gas Injection at Two Flow Rates	89
4.10 Cumulative Production Histories for Simultaneous Steam/Flue Gas Injection at Two Pressures	92
4.11 Cumulative Production Histories for Simultaneous Steam/CO ₂ Injection	93
5.1 Main Program Flow Chart	124
6.1 One Dimensional Grid System	142
6.2 Laboratory and Numerical Model Inlet Pressure Histories	145
6.3 Numerical Model Temperature Profiles - Base Case	146
6.4 Laboratory and Numerical Model Cumulative Oil Production Histories	147

	Page
6.5 Cumulative Oil Production Histories - Grid Sensitivity	149
6.6 Cumulative Oil Production Histories - Heat Loss Sensitivity Cases 1 to 4	152
6.7 Cumulative Oil Production Histories - Heat Loss Sensitivity Cases 5 to 8	153
6.8 Numerical Model Temperature Profiles - Heat Loss Case 7	154
6.9 Cumulative Oil Production Histories - Porosity Sensitivity	155
6.10 Cumulative Oil Production Histories - Absolute Permeability Sensitivity	156
6.11 Inlet Pressure Histories - Absolute Permeability Sensitivity	158
6.12 Cumulative Oil Production Histories - Rock Compressibility Sensitivity	159
6.13 Cumulative Oil Production Histories - Rock Heat Capacity Sensitivity	160
6.14 Numerical Model Temperature Profiles - Rock Heat Capacity Case 1	161
6.15 Numerical Model Temperature Profiles - Rock Heat Capacity Case 2	162
6.16 Cumulative Oil Production Histories - Initial Oil Saturation Sensitivity	163
6.17 Cumulative Oil Production Histories - Residual Oil Saturation Sensitivity	164
6.18 Cumulative Oil Production Histories - Irreducible Water Saturation Sensitivity	165
6.19 Cumulative Oil Production Histories - Critical Gas Saturation Sensitivity	166
6.20 Cumulative Oil Production Histories - Relative Permeability Sensitivity	167
6.21 Cumulative Oil Production Histories - Oil Viscosity Sensitivity	170
6.22 Inlet Pressure Histories - Oil Viscosity Sensitivity	171

Figure		Page
6.23	Cumulative Oil Production Histories - K-Value Sensitivity	172
6.24	Cumulative Oil Production Histories - CO ₂ Liquid Phase Property Sensitivity	174
6.25	Cumulative Oil Production Histories - Injection Rate Sensitivity	175
6.26	Numerical Model Temperature Profiles - Injection Rate Sensitivity Case 2	176
6.27	Cumulative Oil Production Histories - Steam Quality Sensitivity	177
6.28	Cumulative Oil Production Histories - Gas/Steam Ratio Sensitivity	179
6.29	Numerical Model Temperature Profiles - Gas/Steam Ratio Case 1	180
6.30	Numerical Model Temperature Profiles - Gas/Steam Ratio Case 4	181
6.31	Cumulative Oil Production Histories - CO ₂ /N ₂ Ratio Sensitivity	182
6.32	Cumulative Oil Production Histories - Back Pressure Sensitivity	183
6.33	Cumulative Oil Production Histories - History Match of Laboratory Experiments with Numerical Model	190
6.34	Inlet Pressure Histories - History Match of Laboratory Experiments with Numerical Model	191
6.35	Numerical Model Temperature Profiles - History Match of Steam Only Experiment	192
6.36	Numerical Model Temperature Profiles - History Match of Steam/Flue Gas Experiment	193
6.37	Cumulative Production Histories - Parameter and Process Sensitivities	194

LIST OF PHOTOGRAPHIC PLATES

Plate		Page
3.1	Test Cell - Side View	39
3.2	Test Cell - End View	39
3.3	Insulated Test Cell	43
3.4	Control Panel	43

NOMENCLATURE

Latin Symbols

a'	heat or mass transfer area
A	area; constant
b	formation volume factor
B	constant
c	compressibility; concentration
C_p	heat capacity at constant pressure
C_T	thermal expansion coefficient
C_v	heat capacity at constant volume
d, D	diameter
E	one problem formulation constants
\exp	exponential function
f	fraction
f_w	fractional flow of water
F	function
g	gravitational acceleration
h	enthalpy; formation thickness
h'	heat or mass transfer coefficient
i	molar injection rate
J	Jacobian
k	absolute permeability
k_r	relative permeability
K, K	equilibrium ratio
L	length
L_v	latent heat of vaporization
M	molecular weight
N_c	number of components
N	molar flow rate; number
P_v	vapour pressure
P	pressure
P_b	base pressure
P_{cgo}	gas-oil capillary pressure
P_{cow}	oil-water capillary pressure
P_k	convergence pressure
P_{sat}	saturation pressure
PI	productivity index
q	heat transfer rate
q_L	heat loss rate
q_s	heat transfer rate to source or sink
Q	volumetric flow rate
r	radius
r_e	external radius
r_w	wellbore radius
R	universal gas constant
S	saturation; skin effect
S_{or}	residual oil saturation
S_{wir}	irreducible water saturation
t	time

T	temperature; transmissibility
T _{sat}	saturation temperature
U	internal energy; heat transfer coefficient
v	specific volume
V	volume; velocity
x	mole fraction; length
y	vapour phase mole fraction
z	length
Z	compressibility factor

Greek Symbols

α	constant
β	thermal expansion coefficient
γ	specific weight; constant; interfacial tension
δ	time difference operator
δ_i	maximum change of a variable during previous time step
Δ	space difference operator
λ	thermal conductivity; mobility ratio
μ	viscosity
n_i	input norm for variable i in time step selection
Π	product operator
ρ	mass density
$\bar{\rho}$	molar density
Σ	summation operator
ϕ	porosity
ϕ_p	potential of phase p
ω	damping factor in time step selection

Mathematical Symbols

∇	del operator
∂	partial differential operator
\forall	for all the numbers of a set

Subscripts

a	aqueous
av	average
b	boiling point; block
c	critical; component; conduction
cond	conduction
conv	convection
f	formation
g	gas
i	index for component i; injection
in	initial
ip	component i in phase p
i,j,k	block indices

L	liquid
m	mixture
o	oil or oleic; original
p	pore; production; phase index
r	rock; relative; reduced
ref	reference
s	steam; stability
sat	saturation
t	total
v	vapour
w	water
wf	flowing wellbore condition
x,y,z	directional indices

Superscripts

k	iteration counter
n	old time level
n+1	new time level
*	pertaining to overburden/underburden or wellbore condition

I. INTRODUCTION

Much effort has recently been directed towards the development of downhole steam generators (DHSG's) for use in thermal recovery of heavy oil (Bader et al, 1979), (Fox et al, 1981), (Chesters et al, 1981), (Anderson et al, 1982), (Eson, 1982), (Marshall, 1982), (Boden et al, 1984), (Fox and Donaldson, 1985). Considerable progress has been made on the mechanical design and operation of the downhole equipment but questions still remain as to the effect on reservoir performance of injecting the mixtures of flue gases and steam which are produced. The purpose of the present study was to compare steam-only flooding with steam/flue gas injection in a linear system. Particular attention is paid to oil recovery and oil production history in the comparison.

Steam raised in conventional surface generators is seldom injected into oil reservoirs which are more than about 500 metres (1650 feet) deep because of excessive wellbore heat losses. Conventional boilers typically lose 19 percent of the energy derived from fuel as stack losses, 3 to 20 percent in the flowlines and 3 to 20 percent in the wellbore (Eson, 1982). DHSG's located near the producing interval would eliminate these injection heat losses and therefore significantly improve the overall energy efficiency of the steam injection processes. The use of DHSG's would extend the depth to which steam could be used to perhaps 1800 metres (6000 feet) making some deeply buried heavy oil resources amenable to exploitation and thereby increasing recoverable reserves.

The use of insulated tubing in conjunction with surface

steam generation has been employed in some field operations. Cost comparisons have been made between direct-fired high pressure DHSG's and surface generation with insulated tubing (Hart, 1982), (Friefeld et al, 1983) for delivering steam to the sand face. Below about 600 metres (2 000 ft) it appears the DHSG's are cheaper than the other alternative.

Conventional boilers in oilfield operations usually burn lease crude which commonly contains significant quantities of impurities such as sulphur and nitrogen. Air pollution in the form of particulates and the oxides of sulphur and nitrogen results from emission of the flue gases to the atmosphere. In areas such as California which have large steam injection projects, high sulphur content of produced oil and high population density, considerable expense results from the need to scrub stack gases before venting to atmosphere. In 1979, federal regulations in the United States required that if a national ambient air quality standard would be exceeded by a new installation, emissions of that pollutant from existing sources would have to be reduced by at least the amount of the new emissions (Goodley, 1979). The air pollution levels in California have reached such a condition and it is also conceivable that air pollution would reach significant levels in Alberta should large-scale steam injection projects be undertaken in the oil sands.

Recent field tests of DHSG's have demonstrated the potential of these units to reduce air pollution due to the scrubbing action of underground formations (Fox et al, 1981), (Anderson et al, 1982), (Friefeld et al, 1983), (Fox and Donaldson, 1985). The elimination

of particulates, substantial scrubbing of sulphur dioxide, an order of magnitude reduction in the oxides of nitrogen and a two-fold reduction in carbon monoxide have been reported. A portion of the pollutants remain in solution in residual reservoir liquids and in gas which is trapped in the reservoir. Much of the pollutant material is also recovered in solution in the produced liquids (Bader et al, 1979).

The use of DHSG's has been proposed for deep wells to reduce wellbore heat losses, environmentally impacted areas, arctic applications to reduce permafrost melting in steam injection wells, and offshore areas where in addition to reducing heat losses in deep wells, space savings may be realized on platforms and untreated sea water may be used for generating steam (Anon, 1984), (Boden et al, 1984). Of course before using sea water in a thermal application the effects of such a fluid on the formations in question would have to be evaluated.

It has also been suggested that gas injection with steam may improve oil recovery and production performance. Carbon dioxide, which is highly soluble in oil, causes viscosity reduction and swelling of the oil (Klins and Farouq Ali, 1982) (Simon and Graue, 1965). In steam stimulation, solution gas drive effects may be important and non-condensable carbon dioxide may be able to contact regions of the reservoir which have not been heated by steam.

There are also a number of potential disadvantages to the injection of flue gas with steam. Reduction in liquid relative permeabilities occurs due to increased gas saturation. Redford

(1982) has suggested that an optimum CO_2 /steam ratio exists at around $15 \text{ dm}^3/\text{kg}$ and that above this level, lowering of liquid relative permeability causes reductions in oil production rates. The use of oxygen or oxygen-enriched air instead of air for combustion may be considered in order to reduce the volumes of flue gas created. Nitrogen is the largest constituent in the flue gas and does not provide the same potential as CO_2 for process improvement due to its lower solubility in oil. In steamflooding, potential gas handling problems at production wells (gas locking of pumps, casing vent gas collection, etc.) would be reduced if oxygen or oxygen-enriched air were used in the burners. Additional corrosion problems could develop in downhole goods due to the mixing of carbon dioxide, sulphur oxides and steam. It would be expected that a steam/ CO_2 mixture would affect reservoir matrix materials differently than pure steam and that potentially adverse rock-fluid interactions would have to be investigated for particular reservoirs prior to the implementation of steam/flue gas injection. In field applications, gravity override and gas channelling may be aggravated by the combination of steam and non-condensable gases resulting in reductions in sweep efficiencies and therefore total recoveries. Two- and three-dimensional numerical simulation studies would be helpful in assessing the magnitude of this problem. Here again, oxygen enriched air for combustion may partially alleviate the negative aspects of the gas injection.

The use of DHSG's may ultimately be decided on the basis of process improvement or harm caused by the combustion gases in association with steam (Hart, 1982), (Boden et al, 1984). Field

tests have indicated improvements in production rates and steam-oil ratios over steam-only injection but the data are very limited and equivalent test conditions (e.g. steam slug sizes) often were not employed.

In addition to DHSG's, two other methods of generating mixtures of steam and combustion gases have been proposed: the Carmel Energy Vapor Therm Process (Sperry, 1977), (Sperry et al, 1978), (Sperry et al, 1979), (Young and Krajicek, 1979), and the Zimpro-AEC Wet Air Oxidation (WAO) Boiler (Pradt, unpublished), (Balog et al, 1982). A method for generating steam downhole using the wet oxidation process has also been proposed (Clark, 1985). This process requires a minimum pressure of 6 000 kPa to be effective. The disposal of ash created in the process could be a major problem for downhole operation.

The Vapor Therm unit generates a mixture of superheated steam, nitrogen and carbon dioxide at 6205 kPa and 344°C (900 psi and 650°F). In field tests in heavy oil reservoirs the process has achieved significantly improved production rates over primary production in a cyclic stimulation mode of operation. No comparison of Vapor Therm with steam-only stimulation has been made.

The WAO boiler also generates a mixture of CO₂, N₂ and steam (100% quality) by flameless oxidation of a slurry of organic material mixed with compressed air or other oxygen containing gas. Wet air oxidation, a process which has been applied in industrial waste processing, operates at temperatures in the range of 205-316°C (400-600° F) and pressures up to 20.684 MPa (ga) (3000 psig) and

material. The WAO process requires no feedwater treatment and oil-containing produced water can be recycled to the boiler allowing sensible heat recovery. The boilers emit no smoke, SO_2 or NO_x and pollutants are concentrated in an inert ash blowdown. If the reactor is supplied with high purity oxygen instead of air, the WAO plant becomes a CO_2 /steam generator.

In the present study, the effects on oil recovery and production performance of flue gas injection with steam have been investigated in unscaled laboratory experiments in a linear system. The runs involved injection of steam/ CO_2 , steam/ CO_2 / N_2 and steam/ N_2 mixtures as well as steam-only injection for purposes of comparison. In some experiments slugs of gas were followed by steam and in others the gases were injected simultaneously with steam. The oil used in the study was a moderately viscous refined oil. The choice of refined oil, pure silica sand and distilled water for sand pack materials was made in order to reduce potential rock-fluid interactions which would complicate interpretation of the experimental results. All experiments were conducted with sandpacks in a horizontal position. In order to gain further insight into the factors controlling the steam/gas injection processes, a numerical simulation model was written and a sensitivity study conducted to investigate the effect on the processes of various reservoir and operating parameters.

A. Effect of Gases and Steam on Fluid Properties

In the case where a small amount of excess air is used in a downhole steam generator, the effluent gas composition from the burner would have approximately the following composition (Eson, 1982): 62 % by volume of steam, 32% nitrogen, 5% carbon dioxide, 1% oxygen and traces of SO_2 , NO_x . If high purity oxygen were used instead of air the effluent gas composition would be approximately 92% by volume steam, 7% carbon dioxide, 1% oxygen with traces of SO_2 and N_2 .

Carbon dioxide is more soluble in oil than is nitrogen. Jacoby and Rasza (1952) presented equilibrium vaporization ratios (K-values) for mixtures of nitrogen, methane, ethane, carbon dioxide, hydrogen sulphide and a 26.8° API (s.g. = 0.894 @ 60/60) crude oil. Data were obtained at temperatures of 38, 68 and 94°C (100, 150 and 200° F) and various pressures in the range of 1.38 to 34.5 MPa (abs) (200 to 5000 psia). The following data have been taken from their paper to illustrate the relative solubilities of the two gases. These data were collected for a mixture whose composition was 5 mole percent N_2 , 40% natural gas, 5% CO_2 , 5% H_2S , and 45% crude oil.

Pressure (psia)	Temperature ° F	K_{N_2}	K_{CO_2}
500	100	30	3.5
500	200	32	5.0
1000	100	15	2.1
1000	200	18	3.0

The data illustrate the higher solubility of carbon dioxide and also the effect of pressure and temperature on the

solubilities. Increasing pressure and decreasing temperature have the effect of increasing the solubilities. The effect of temperature on nitrogen solubility is less pronounced than is the effect of pressure in the ranges of pressure and temperature considered. At the higher partial pressures of nitrogen which occur with flue gas injection, the total amount of nitrogen in solution may be nearly equal to the total amount of carbon dioxide in solution.

It is well known that gas in solution in oil causes swelling of the oil (Craft and Hawkins, 1959) and reduction in its viscosity. Correlations of solubility, swelling and viscosity reduction of crude oils in equilibrium with carbon dioxide have been presented by Simon and Graue (1965). Their data were collected on nine oils, seven of which were crude and two of which were refined, ranging in gravity from 11.9 to 33.3° API. The ranges of temperature and pressure considered were 38 to 121°C (100 - 250° F) and 10.3 kPa to 15.86 MPa (14.7 to 2300 psia), respectively. Data taken from the paper are shown below for an oil with similar properties to the one used in the present study. [Oil gravity, 17.3° API
Viscosity, 87 cp @ 110° F
10.6 cp @ 200° F
U.O.P., 11.4]

Pressure (psia)	Temp. (° F)	CO ₂ Solubility (mol. frac)	Swelling Factor* (frac)	Dead Oil Viscosity (cp)	Viscosity CO ₂ Sat. (cp)
500	100	0.34	1.06	110	20.0
500	200	0.23	1.03	12.4	1.1
1000	100	0.56	1.155	110	9.6
1000	200	0.40	1.08	12.4	1.0

* vol. @ sat'n pressure and temperature
vol. @ atm. pressure and temperature

The combined effects of temperature and solution gas on viscosity are evident from examination of these data.

Jacobs et al (1980) measured the effect of dissolved carbon dioxide, methane and nitrogen on the viscosity of Athabasca bitumen. Data were collected over the following temperature and pressure ranges:

<u>Gas</u>	<u>Temperature Range (°C)</u>	<u>Pressure Range (MPa)</u>
methane	25 to 170	0.09 to 13.8
nitrogen	40 to 170	0.09 to 6.33
carbon dioxide	25 to 140	0.09 to 5.69

As illustrated by the following table, carbon dioxide reduces the viscosity of bitumen dramatically and especially at low temperatures.

<u>Pressure (MPa)</u>	<u>Viscosity of CO₂ Saturated Bitumen</u>	
	<u>@ 40°C (Pa.s)</u>	<u>@ 120°C (Pa.s)</u>
0.09	60	0.10
2.34	4	0.065
3.72	1.5	0.055
5.69	0.6	0.04

The effect of pressure (i.e. gas in solution) on reducing viscosity is less at temperatures above 100°C. Methane has a less dramatic, but still significant, effect on viscosity. This is due to the lower solubility of methane in oil (Jacoby and Rzasza, 1952). Nitrogen was determined to have a negligible effect on bitumen viscosity.

Empirical correlations of crude oil viscosity in the presence of carbon dioxide and steam have been developed by

Bader et al (1979) and Leung (1983). Bader et al (1979) presented a correlation for a typical heavy crude in the range of pressures of 0 to 13.79 MPa (ga) (0 to 2000 psig) and temperatures of 15 to 316°C (60 to 600° F). They suggest that, in a certain temperature range for a given pressure, as temperature is increased, viscosity actually increases due to reduction in carbon dioxide solubility. As the temperature increases above this range, the temperature effect dominates and viscosity decreases. Preliminary experimental results for three different crude oils confirmed this general trend although differences existed between the computed and experimental values. For his numerical modelling studies of an Athabasca oil sands reservoir, Leung (1983) combined the data from Simon and Graue (1965), Miller and Jones (1981) and Jacobs et al (1980). No laboratory data were available on Kern River oil and for these simulations, solubilities, swelling factors and viscosity effects were all estimated using data by Simon and Graue (1965) and Miller and Jones (1981) as a guide. Lin (1981) has pointed out the need for laboratory data collection of solubility, swelling and viscosity reduction effects with various gases and crude oils over a wide range of temperatures and pressures.

Leung (1983) has also shown that solubilities of CO₂ in water can be considerable; for example, as much as 27 dm³/kg at 6.9 MPa and 38°C (152 SCF/Bbl @ 1000 psi and 100° F). Ignoring this effect in simulations can result in optimistic estimates of improvement in performance of combined steam-CO₂ recovery

processes as compared to steam-only processes.

B. Laboratory Studies of Gas-Steam Injection

Pursley (1974) reported on partially scaled physical model tests simulating 1/8 of 5-spot patterns on 1.25, 10 and 20 acre well spacings. Four tests were conducted to determine the effects on performance of injecting small slugs ($4.8 \text{ dm}^3/\text{kg}$ or 20 SCF/Bbl) of air, methane and CO_2 at a time when the well's productivity had declined following steam stimulation. Dramatic improvement resulted when air and methane were injected in this way. Somewhat less but also significant improvement resulted when using carbon dioxide. It was suggested that this may have been due to higher solubility of CO_2 in water. Substantial reductions in water-oil-ratios (WOR's) were achieved in these tests.

Cumulative Production WOR	Gas
1.7	steam-air
1.8	steam-methane
2.4	steam- CO_2
3.2	steam only

Experiments showed substantially higher oil-steam ratios (OSR's) when methane was injected after steam rather than late in the production cycle. A series of 4, 3-cycle stimulation tests were conducted to determine the effect of injected gas-steam ratio on performance. Methane was injected in each case. It was found that an optimum gas-steam ratio (GSR) of 17.8 to $35.6 \text{ dm}^3/\text{kg}$ (100 to 200 SCF/Bbl) existed. Pursley (1974) suggested that increasing the GSR beyond a certain value would not be advantageous. The results of the experimental

work were said to have shown qualitative agreement with field tests.

Redford (1982) reported on laboratory experiments with additives to steam in an elemental model 45 cm in diameter and 40 cm high. Experiments were conducted with Athabasca tar sand in a manner such as to represent an element of the actual reservoir. Clean 20-40 frac sand was used to initiate a communication path and the pack was produced with a pressure cycling type of operation. With the production control valve open, steam was injected until it appeared at the production well. This well was then closed and the pressure built up to 3.3 MPa. The back pressure was then controlled for about 30 minutes in a manner so that hot water but not steam was produced. A series of pressure build-ups and drawdowns was then initiated. Typically, 20 minutes of straight-through operation was followed by 10 minutes of pressure drawdown in which the injection well was shut-in and pressure allowed to bleed off through the production well. The additives to steam which were used in the experiments were methane, ethane, propane, butane, hexane, heptane, Suncor diluent naptha and carbon dioxide.

The results of these tests showed that using ethane and CO₂ gave significantly improved recoveries over the other additives and the improvement was most evident on the drawdown portions of the cycles. For CO₂ and ethane, average production on the injection portion of the cycles was lower than it was

for steam-only injection while in the case of naphtha it was higher. Larger swept volumes resulted from addition of ethane and CO₂ and substantially cooler fluids were produced on drawdown with these additives being used.

An optimum CO₂/steam ratio of about 35 dm³/kg was found to exist. Below this level, Redford (1982) suggested that the drive effect on pressure blowdown was reduced and that above 35 dm³/kg, reduced heat transfer and increased relative permeability to gas began to dominate. It was found that a combination of CO₂-naphtha-steam had the best overall recovery and that for this mix the optimum CO₂/steam ratio was about 15 dm³/kg. The improved performance using gas additives was attributed to solution gas drive, swelling and viscosity reduction effects of the soluble gases. Undesirable effects of using too much gas included reduced injectivity, reduced relative permeability to liquids and an increased tendency towards channeling of steam.

Fox et al (1981) reported that laboratory experiments conducted to examine recovery with soluble gas/steam drive have shown a more rapid recovery than steam-only drive. The experimental data were not presented.

Hutchinson et al (1983) investigated Utah tar sand steamflood performance in linear systems with CO₂, N₂ or air as additives. Their experimental apparatus was 8.26 cm (3.25 in) in diameter by either 81.92 cm (32.25 in) or 182.62 cm (72.25 in) in length. The runs were mainly adiabatic and were

conducted at temperature and pressure conditions of 231°C (447°F) and 2 758 kPa (400 psi), respectively. Steam injection rates at or close to 1 250 cm³/hr (2.75 lbm/hr) were used for all runs. Gas injection rates were either 170 dm³/hr (0.1 SCF/min) or 850 dm³/hr (0.5 SCF/min) resulting in gas-steam ratios of 140 and 680 dm³/kg (786 and 3 932 SCF/bbl), respectively. It was found that the addition of non-reactive gases to steam produced only slight improvement in oil recovery performance over steam alone. Both concurrent and alternating modes of steam drive with additives were equally effective in oil recovery of the tar sand. Results of air/steam co-injection experiments were complicated by combustion phenomena. Oil recoveries were generally low from these experiments, being in the range of 10 to 15 percent of the original oil in place, indicating poor sweep and displacement efficiency.

C. Numerical Simulation Studies

Klins and Farouq Ali (1982) conducted a 2-D areal numerical simulation study in order to compare the performance of nonthermal CO₂, nitrogen, natural gas or water injection in the recovery of heavy oils with viscosities in the range of 10 to 1000 cp. The simulations were conducted in a range of temperatures and pressures at which the gases were not miscible in the oil but solubility effects were nevertheless important. It was found that CO₂ injection was superior to the other processes for oil viscosities above 70 cp. The gain in recovery over waterflooding was as much as 9 percent for

heavier crudes. Waterflooding was technically superior to pure CO₂ injection for low viscosities due to lack of mobility control when pure CO₂ was driving a low viscosity carbonated oil. Carbon dioxide drive recovered significantly more oil than nitrogen drive at low viscosities because of improved sweep efficiency as a result of viscosity reduction and swelling. Low pressure nitrogen injection operates in a similar manner to waterflooding in that the injected fluid does not mix with the reservoir fluids. Nitrogen injection yields a poorer recovery than waterflooding due to less favourable mobility ratio. It was found that in heavy oil (100-1000 cp) a minimum oil saturation of 50% was required in order to produce significant amounts of oil and that a saturation of over 60% was required for stabilized banking. Very viscous oils were found to yield low recoveries at low initial oil saturations.

The production histories from two comparative simulations of steam-only drive and steam-flue gas drive have been reported for a California-type reservoir (Bader et al, 1979), (Fox et al, 1981). In the steam-only flood, 85% quality steam was injected at 79.5 m³/d (500 B/D) and in the steam-gas flood the injection rates were 47.7 m³/d (300 B/D) of 85% quality steam, 345.5 kg/h (760 lb/h) of CO₂ and 1273 kg/h (2800 lb/h) of N₂. Recovery occurred earlier with the steam-gas process with production time reduced by approximately one-third. No details of the simulations were given.

Weinstein (1974) has presented a one-dimensional, 3-phase flow numerical model which accounts for 2-D heat

transfer and can be used to simulate the steam stimulation process. The model was matched to field data of steam stimulation followed by gas injection in a Cold Lake reservoir. Two cycles of 7949 m^3 (50,000 Bbls) of steam injection followed by $1.41 \times 10^5 \text{ m}^3$ (5 MMSCF) of natural gas were matched following which the model was used to compare the effect of injecting gas before or after the steam. The following results were presented:

Case	Fluids	Avg. Oil Rate (B/D)	Oil Prod. (Bbl)	Oil-Steam Ratio
Steam only	45 M Bbl steam	114	8 300	0.18
Gas first	4.99 MMSCF gas 45 M Bbl steam	137	10 000	0.22
Steam first	45 M Bbl steam 4.99 MMSCF gas	192	14 000	0.31

It can be seen from these data that gas injection has a marked effect on performance and that gas injection following steam is the best alternative. No data on the simultaneous injection of steam and gas were presented.

Leung (1983) has conducted a numerical simulation study of an immiscible displacement process with CO_2 injected simultaneously with steam in a heavy oil reservoir. The study deals primarily with steam stimulation but one steamflood case was also presented. It was found that in high compressibility reservoirs, viscosity reduction was the main contributor to increased production over the steam-only process whereas in normal compressibility reservoirs, the solution gas drive

effect was the main contributor. For an Athabasca tar sand reservoir, a 36% increase in recovery was achieved after 6 cycles at a GSR of $71.24 \text{ dm}^3/\text{kg}$ (400 SCF/Bbl) in comparison to steam-only stimulation. At a GSR of $106 \text{ dm}^3/\text{kg}$ (600 SCF/Bbl), the recovery was slightly lower due to increased gas production. A 16% increase in recovery over 6 cycles was achieved at a GSR of $89.0 \text{ km}^3/\text{kg}$ (500 SCF/Bbl) for a Kern River reservoir. In a 3-D steam drive simulation, CO_2 injection with steam did not improve recovery significantly for a California-type heavy oil reservoir where the stripping effect of steam was the main recovery mechanism. In this simulation steam was injected at $79.5 \text{ m}^3/\text{d}$ (500 B/D) at a gas-steam ratio of $89.0 \text{ dm}^3/\text{kg}$ (500 SCF/Bbl). The injected gas promoted vertical gravity override and steam breakthrough occurred slightly earlier. The CO_2 was seen to concentrate at the leading edge of the steam zone.

Hong and Ault (1984) have simulated non-condensable gas injection with steam in steam flooding operations for both light and heavy oil reservoirs. The results show that the effect of non-condensable gas addition to steam is to accelerate production during the early part of a typical heavy oil project but the cumulative recovery stays about the same as that obtained with steam injection only. The early production increase was attributed to additional reservoir sweep caused by the injected gas. In the light oil case, non-condensable gases accelerated oil recovery and also increased the recovery slightly. This increase was caused by enhanced steam

distillation and viscosity reduction of the oil, by soluble gas. The heavy oil was considered to be a single component dead oil with an initial viscosity of 2 000 cp at initial conditions. The light oil was assumed to be composed of three components and had a viscosity of 5 cp at the initial reservoir temperature of 49°C (120°F).

Singh et al (1984) investigated the injection of steam and CO₂ into a bottom water tar sand reservoir. A small portion of reservoir, 20 metres thick by 24 metres in radius was modelled using 24 grid blocks in an r-z geometry. It was shown that steam/CO₂ injection can be beneficial in some instances in reservoirs of this type.

Stone and Malcolm (1985) presented results of a comparison between physical and numerical model results for a large scale steam-CO₂ co-injection experiment using Athabasca oil sand. The work concluded that for the system studied, the main advantage of CO₂ as an additive lay in its ability to enhance displacement of bitumen but that viscosity reduction due to CO₂ played almost no role in the process. Solution gas drive behaviour of the steam/CO₂ process was seen to be a significant factor.

D. Compositional Reservoir Simulation

Reservoir simulators of the compositional type have been developed by a number of investigators including Roebuck et al (1969), Culham et al (1969), Van-Quy et al (1972), Nolen (1973), Kazemi et al (1978), Fussel and Fussel (1979) and Coats

(Oct. 1980). The models are isothermal and all assume that phase equilibrium exists in the porous medium at all times. With the exception of the model by Van-Ouy et al (1972) diffusion is neglected. A variety of methods are used for predicting fluid properties and a number of different solution schemes are proposed. If water is present, mutual insolubility of water and the hydrocarbon phases is generally assumed.

Roebuck et al (1969) presented an implicit one-dimensional, 3-phase flow model in which capillary effects were considered but gravitational effects were not. The model equations were solved using Newtonian iteration in which partial derivatives in the Jacobian were evaluated numerically.

One- and two-dimensional models which neglected capillary effects were described by Culham et al (1969). Simulations were compared to one-dimensional laboratory experiments of depletion drive oil recovery where no external source of energy was supplied to the process. For the volatile hydrocarbons used in the study (methane and propane), it was found that the assumption of 2-phase (gas and liquid) equilibrium satisfactorily duplicated the experimental results.

The model developed by Van-Ouy et al (1972) was one-dimensional, 2-phase (gas and liquid) and accounted for convection, diffusion and thermodynamic exchange between phases. Capillary and gravitational effects were neglected.

numerical results for several processes including high-pressure gas drive and condensing gas drive.

Nolen (1973) described a three-dimensional compositional model which used the IMPES (implicit pressure, explicit saturation) method to solve the mass balance equations. Fluid densities and equilibrium ratios (K-values) were treated implicitly and viscosities, capillary pressures and relative permeabilities were evaluated explicitly. Nolen pointed out the need to use internally consistent correlations for densities, viscosities and equilibrium ratios for miscible displacement problems where "the approach to miscibility is accompanied by a growing equivalence between the properties of the oil and gas" and where the "K values approach 1.0 as the pressure approaches the convergence pressure". He found that convergence problems arose in miscible displacement simulations when different correlations were used for each of the density and viscosity calculations. In the model, internal consistency was achieved when oil and gas phase densities were calculated using the Lee and Edmister (1971) modification of the Redlich/Kwong (1949) equation of state and oil- and gas-phase viscosities were calculated using the method of Lohrenz et al (1964). Equilibrium ratios were obtained from correlations developed by MacDonald (1971) and Lohrenz et al (1963) to approximate the data contained in the GPSA Engineering Data Book (1972). K-values for methane, carbon dioxide, hydrogen

$$\ln K = \left(1 - \frac{P}{P_k}\right)^m [b_0 + b_1 \ln P + b_2 (\ln P)^2] \quad (2.1)$$

where m is constant and b_0 , b_1 and b_2 are polynomials in temperature. In order to use correlations of this type it is necessary to estimate the convergence pressure, P_k , defined as the critical pressure of a critical mixture. The composition of the critical mixture is first determined and then the critical pressure is found using the correlations of either Simon and Yarborough (1963) or Etter and Kay (1961). Details of the determination of the critical mixture composition were not given by Nolen. The inconsistency between the critical point predicted by the K-value correlations and that implied by the densities calculated from an equation of state could be eliminated by calculating the K-values from the same equation of state which was used to predict the densities. Nolen found it necessary to adjust critical properties and acentric factors of the heavy fractions in order to match laboratory oil density data with the R-K equation of state. Also, it was usually necessary to modify the K-value correlations of selected components in order to match measured phase behaviour.

A three-dimensional, three-phase multicomponent simulator including capillary pressure was reported by Kazemi et al (1978). Model equations were combined to produce an implicit oil-phase pressure equation, an explicit equation for hydrocarbon composition, and explicit saturation equations.

method. Three choices were available for calculating the required physical properties. In the first method, densities, viscosities and equilibrium ratios were tabulated as functions of pressure at reservoir temperature. Properties were described as functions of pressure, temperature and composition in the second method. In the case of densities, compositional dependence was incorporated through use of average molecular weights and for viscosities the concentration of a key component(s) was used. Dependence on composition of K-values was accounted for by including the convergence pressure. The third method was essentially that used by Nolen (1973) as outlined previously. Three-phase relative permeabilities were synthesized from two-phase data using the method of Stone (1973). Adjustment of the coefficients in the phase behaviour equations was done in order to match experimental PVT data.

Fussel and Fussel (1979) presented a three-dimensional, three-phase compositional model incorporating the Redlich and Kwong (1949) equation of state as modified by Zudkevitch and Joffe (1970). Expressions for thermodynamic equilibria and hydrocarbon-phase densities were obtained from the equation of state. The method of Lohrenz et al (1964) was used for viscosities. Water compressibility factor was calculated as:

$$Z_w = \frac{P Z_{w,b}}{P_b} [1 - c_w (P - P_b)] \quad (2.2)$$

where P_b = base pressure

c_w = water compressibility at P_b

$Z_{w,b}$ = water compressibility factor at P_b

imum variable Newton-Raphson method (MVNR) described earlier for single-stage separation calculations by Fussel and Yanosik (1978). Simultaneous solution is performed for a minimum set of unknowns. Transmissibilities are treated explicitly and all other variables are treated implicitly.

Coats (Oct. 1980) has developed an implicit three-dimensional, three-phase compositional model also using the R-K equation of state for phase equilibrium and property calculations. As pointed out by Coats, "the equation of state provides consistency and smoothness as gas- and oil-phase compositions and properties converge near a critical point. This avoids computational problems near a critical point associated with use of different correlations for K-values as opposed to phase densities". The implicit nature of the model is claimed to enhance efficiency and reliability although no comparison was made with semi-implicit formulations due to lack of information on such models. The increased efficiency results from removal of time-step limitations associated with models using explicit transmissibilities. The formulation requires simultaneous solution of a set of $(n_c + 1)$ finite difference equations where n_c is the number of components. The $n_c + 3$ constraint equations which do not involve unknowns from neighbouring grid blocks are removed from the simultaneous solution set by Gaussian elimination leaving the $n_c + 1$ primary equations which do involve unknowns from the neighbouring grid blocks. The primary equation set is solved by the direct

used to handle phase appearance and disappearance in which different problem formulations are used depending on the number of phases in existence in a given grid block. Saturation pressure calculations are performed at each iteration for each grid block where gas saturation or oil saturation is zero to determine the model solution mode (single-phase or two-phase). Relative permeability and capillary pressure are functions of saturations and interfacial tension. The gas/oil interfacial tension is calculated from the Macleod/Sugden correlation found in Reid et al (1977).

E. Numerical Simulation of Thermal Recovery Methods

Farouq Ali and Ferrer (1981) have reviewed the level of expertise in numerical simulation of thermal recovery processes. Simulation areas identified as requiring further elucidation included formation parting, relative permeability variation with temperature, phase behaviour of the fluids and emulsification of the oil in place. It was suggested that implicit formulations be used along with direct solution techniques for thermal recovery problems.

Steam injection stimulators may be placed in two groups where: (1) the oil is a single nonvolatile component; and, (2) the oil is composed of two or more components allowing for prediction of steam distillation. Models of the first type are those by Shutler (1969), Shutler (1970), Abdalla and Coats (1971), Coats et al (1974) and Vinome (1974). Models of the

Ferrer and Farouq Ali (1976), Weinstein et al (1977) and Coats (1978).

The first multiphase in-situ combustion model was a linear formulation developed by Gottfried (1965). Smith and Farouq Ali (1971) followed with a two-dimensional single-phase model which tracked the combustion front movement. An extension of this approach was presented by Eggenschwiler and Farouq Ali (1977). Laboratory results of linear combustion tube tests and corresponding numerical simulations were reported by Smith and Perkins (1973) but few details of the numerical model formulation were given. Adler (1975) described a one-dimensional in-situ combustion model using an extension of Gottfried's (1965) method of determining inter-phase mass transfer rates. Farouq Ali (1977) and Youngren (1980) presented multiphase, multidimensional models of in-situ combustion. General multiphase, multidimensional thermal models capable of simulating steam injection, hot waterflooding and in-situ combustion were presented by Crookston et al (1979), Coats (Dec. 1980), Grabowski et al (1979), Rubin and Buchanan (1985) and Buchanan (1985).

Abou-Kassem (1981) has summarized the assumptions common to most of the steam simulators including (1) mutual insolubility of water and oil phases; (2) negligible effect on the energy equation of kinetic energy and viscous work of the flowing fluid; (3) instant attainment of thermal and phase

equilibria; (4) mass transfer between the oil and gas phases governed by two-phase equilibrium. Mass transfer between water and gas phases determined by Raoult's and Dalton's laws (i.e. the presence of other materials than steam in the gas phase does not alter steam-water phase behaviour). The water-liquid phase is assumed to contain only water (i.e. no solubility of hydrocarbon or other gases in water); (5) mass transfer due to diffusion is negligible; (6) thermal cracking of hydrocarbons is ignored; and, (7) heat losses through lateral reservoir boundaries are negligible. It is the author's belief that assumption (6) may not be valid for steam stimulation in heavy oil where long contact times occur between steam and oil in near-wellbore regions and repeated resaturation of these areas occurs due to the cyclic nature of the process. Coking of the oil at steam temperatures over a period of years may yield substantial amounts of coke and result in permeability reductions. Abou-Kassem (1981) included a thermal cracking formulation in his steamflood model but the formulation did not account for the formation of a fourth, solid-phase or the permeability and porosity reduction which would ensue. Experimental data on the extent of thermal cracking at steam temperatures are required.

1. Steam Models

Spillette and Nielsen (1968) developed a two-dimensional mathematical model of hot waterflooding which was used in a vertical cross-sectional mode. The model, which included the effects of gravity and

capillarity, assumed that no gas phase was present and was used for immiscible displacement studies.

A three-phase, one-dimensional steamflood simulator was presented by Shutler (1969). Interphase mass transfer was allowed between the water and steam phases but hydrocarbon gas was assumed to be insoluble in the liquid phases. The model accounted for one-dimensional heat convection and two-dimensional conduction in the oil sand and adjacent strata. An extension of this simulator to two-dimensions was presented by Shutler (1970).

Abdalla and Coats (1971) described linear and two-dimensional, three-phase steamflood models. The gas phase consisted only of steam when present. Coats et al (1974) presented a three-dimensional steamflood model which used simultaneous solution of the mass and energy balance equations eliminating the need to iterate on mass transfer terms. The model did not include temperature dependent relative permeabilities or steam distillation effects but did include gravity and capillarity.

Runge-Kutta methods were used by Vinsome (1974) to stabilize the IMPES (implicit-pressure, explicit-saturation) solution scheme in a simulator for hot waterflooding and steam injection. All physical properties of the fluids were expressed as analytical functions in order to help control the size of the program.

One-dimensional notation was also used.

Weinstein et al (1977) developed a one-dimensional, three-phase flow model which accounted for steam condensation, solution gas, and distillation effects. Interphase mass transfer was allowed between water and vapour, and oil and vapour. The model did not include gravity, capillarity or temperature dependence of relative permeability. Fluid properties were expressed as cubic spline functions. The use of an explicit mass transfer rate between the oil and vapour rather than a gas solubility factor represented a new method of treating solution gas and distillation effects.

An extension of the model of Coats et al (1974) to account for steam distillation, solution gas and temperature dependent relative permeability was presented by Coats (1976). A more implicit treatment of saturation calculations in the new model increased stability significantly. History dependent hysteresis of gas relative permeability was included. The model had three hydrocarbon components and represented a step towards a fully compositional thermal model. Representation of phase behaviour was deemed to be the weakest element of the work. This was basically the result of a lack of PVT data for heavy oil-steam systems. The authors suggested that insufficient data were available to justify use of sophisticated schemes of the type used in isothermal compositional models.

Ferrer and Farouq Ali (1976) developed a three-phase, two-dimensional, compositional simulator for steam injection processes. Three hydrocarbon components and water were included in the formulation. No component other than water was allowed in the aqueous phase. Surface oil, water and gas compositions were determined by flash calculations at separator conditions.

A highly implicit, three-dimensional model was presented by Coats (1978). The oil was treated as a two-component mixture to accommodate problems involving solution or inert gas or distillation. The earlier model, Coats (1976), was reported to have had stability problems for some compositional cases. The new model showed improved stability and material balances in comparison to the previous model when both were applied to example reservoir problems.

Abou-Kassem and Aziz (1982) examined grid orientation effects in a fully implicit, two-dimensional, compositional, three-phase steam model. Hydrocarbons could be grouped into up to three hypothetical components. Water constituted the fourth component. Thermal cracking at steam temperatures was allowed in the formulation but no coke-like material was produced in the cracking reactions. The model incorporated both five-point and nine-point finite difference schemes for investigation of grid orientation effects. Validation of the simulator consisted

of comparing results with the Intercomp steam model (Coats et al (1974), Coats (1976) and Coats (1978)), which had been validated against experimental and field-scale data, for one-dimensional and two-dimensional modes. Phase appearance and disappearance was handled in two ways: the first was an extension of the method proposed by Crookston et al (1979) called by Abou-Kassem the one-problem formulation and the second was the variable substitution method described by Coats (1978). A comparison of the two methods for one-dimensional problems indicated that there were negligible differences in the results obtained. The first method is simpler to program but less rigorous than the second.

2. In-situ Combustion Models

Gottfried (1965) presented the first general theory for thermal oil recovery in which consideration was given simultaneously to heat transfer and fluid flow. Prior to this work, interest had been focused mainly on the heat transfer aspects of the problem. His model, which required 2 to 3 hours of computer time per problem, treated linear, three-phase flow, aqueous phase change and chemical reaction between the oil and oxygen. The formulation neglected hydrocarbon phase change, intraphase diffusion, capillarity and gravity. Heat transfer was by conduction and convection.

The development of a more complex simulator was

reported by Adler (1975). It considered the oil as a mixture of two components along with the evaporation of these components. Combustion gas consisting of carbon oxides was allowed to be soluble in the oil and water liquid phases. This model assumed that heat transfer in unconsolidated sands was mainly by radiation. Dissolved materials were assigned a saturation which the author claimed to simplify organization of the computer program. The saturation of the combustion gas dissolved in a liquid phase was defined as the difference between the saturation of the solution and the saturation of the pure solvent.

Crookston et al (1979) reported on a two-dimensional, three-phase general thermal model, including gravity and capillarity, which could be used for steam injection and in-situ combustion simulations. The formulation considered six components: oxygen, inert gas, a light hydrocarbon pseudocomponent, a heavy hydrocarbon pseudocomponent, water and coke (solid). Vaporization and condensation were governed by vapor-liquid equilibrium as defined by pressure and temperature-dependent equilibrium ratios (K-values). It was assumed that the solid fuel (coke) occupied negligible volume (i.e. $S_o + S_w + S_g = 1.0$). Four chemical reactions were included and they were: (1) coke formation from the heavy hydrocarbon, (2) oxidation of coke, (3) oxidation of light hydrocarbon, and (4) oxidation of heavy hydrocarbon. Heat transfer mechanisms were conduction and convection. The model used

an automatic time-step selection algorithm.

A three-dimensional, three-phase in-situ combustion simulator was developed by Youngren (1980). Five components were considered: water, oxygen, nonvolatile oil and two arbitrary volatile oil components. None of the last four components were allowed to be in solution in the liquid water phase. The model included oxidation of heavy oil but neglected the formation and oxidation of coke. Any dead oil not displaced from the porous medium was burned as fuel. Gravity and capillarity were included as well as heat transfer by conduction and convection. Automatic time-step selection was based on changes in the dependent variables during the previous time step as in Todd et al (1972). If the change in a dependent variable exceeded a specified maximum, the time step was reduced and the calculations repeated. It was found that automatic time-step selection was far more reliable for the problems studied than was manual selection.

Coats (1980) presented a 3-D, 3-phase general thermal model which allowed any number and identity of components and allowed distribution of any component in any or all of the four phases included: oil, water, gas and coke. Absolute permeability was allowed to vary with coke saturation. Any number of chemical reactions were also possible. Heat transfer in the reservoir was by conduction, convection and radiation. Coats concluded on

the basis of previous experience with steamflood modelling, that total computer time for thermal simulations decreases with the degree of implicitness. This was due to the greater stability of the implicit formulations which allowed large time steps to be taken in the model. Temperature dependence of relative permeabilities and automatic time step selection were also featured.

Grabowski et al (1979) developed a three-dimensional, three-phase, fully implicit general thermal model which included four phases, a variable number of oil components, a variable number of chemical reactions, and gravity and capillary pressure terms. The model contained implicit and sequential implicit solution options. Storage and computation time were reduced by implementation of a bandwidth reducing option for the solution matrix. The automatic time-step solution algorithm was the following:

$$\Delta t^{n+1} = \Delta t^n \min_j \frac{(1 + \omega) \eta_j}{\delta_j + \omega \eta_j} \quad (2.3)$$

where δ_j = maximum of an independent variable during the previous time step

η_j = input norm

ω = damping factor (experience shows ~ 1).

The new time step was limited to double the old by this equation.

Further development and enhancement of the model of Grabowski et al (1979) was reported by Rubin and Buchanan

powerful iterative techniques for solving large-scale thermal problems. The model operates in cartesian, radial and curvilinear coordinate systems.

Buchanan (1985) described a multiphase multicomponent thermal model which is a further extension of the work of Rubin and Buchanan (1985). The model handles various additives to steam as well as in-situ combustion processes. The most novel aspects of this model are the use of global mole fractions as primary variables and the development of interchangeable phase equilibrium and physical property modules which can be designed specifically for the problem being considered.

simulation using physical and numerical models have been discussed by Farouq Ali and Redford (1977). These authors point out that it would be desirable to use scaled physical models in all studies since the results are directly applicable to field situations but that in practice it is not possible to completely scale thermal recovery processes. In a recent paper on scaled model experiments of fireflooding in tar sands (Garon et al, 1982), unscaled effects common to both steamflooding and fireflooding included capillarity, relative permeability, pressure gradients and fluid/solid interactions. Additional unscaled effects for fireflooding involved gas-phase diffusion, reaction kinetics and pyrolysis reactions. The term partially-scaled models has been used to describe those in which some of the scaling criteria have been relaxed. As pointed out by Farouq Ali and Redford (1977), mathematical simulation may be used to gain insight into the importance of the neglected scaling relationships to the experimental results.

Another approach is to use an unscaled physical model to obtain data for mathematical simulation. The unscaled physical model is used to represent a small element of a reservoir which is subjected to certain process conditions. History matching of such "elemental" model experiments can be used to validate a numerical model which can then be applied

field data were available and greater confidence could then be placed in the simulation results.

Experimental Apparatus

The experimental equipment is similar to that which has been described by Redford et al. (1976) and Flock and Lee (1977) except that for the present work a new test cell was constructed and additional equipment was installed for gas flow control, measurement and compression and for automatic back-pressure control.

In the tests, fluid injection rates and back pressures were held constant. This method of operation was thought to be preferable to the previously applied techniques which used constant injection pressure and production rate, due to the difficulty of controlling flow rate of a multiphase mixture of varying composition. The advantage to the old method which uses a constant pressure for steam injection is that better control of steam enthalpy may be achieved. Where the fluid injection rates and back pressures are held constant, as in the present work, the inlet pressure changes gradually throughout the course of the experiment and thus the saturated steam temperature also varies. It was necessary therefore to make small adjustments in boiler temperatures as experiments progressed.

shown in Figure 3.1. The experimental equipment is divided into four sections for presentation: test cell, steam generator, gas injection equipment and the production system. Addresses of Suppliers for the specific materials and equipment are shown in Appendix A. In most instances, local distributors rather than the manufacturer have been listed.

1. Test Cell

The test cell, shown in Plate 3.1, was built at the University of Alberta and was fashioned after the larger diameter units built previously. It was constructed of a 4-foot (121.9 cm) length of nominal 3-inch (7.62 cm) Schedule 80, 321 stainless steel pipe. The internal pipe diameter was 2.9 inches (7.37 cm) and the outside diameter 3.5 inches (8.89 cm). Flanges were made from 1.25-inch (3.18 cm) thick, 316L stainless steel plate which was machined to a diameter of 10 inches (25.4 cm). Design drawings of the test cell are found in Appendix B. Eight bolt holes were drilled in the flanges to house 0.875-inch (2.22 cm) diameter bolts. Although 347 stainless steel was desired for the intended service, and it was preferred that the same material be used throughout, it was necessary to use materials readily available rather than face delays in placing orders outside the country. The materials thus chosen have performed satisfactorily. The test cell was mounted on a stand which allowed rotation to any desired angle.

PI Pressure Indicator
 PT Pressure Transducer
 TI Temperature Indicator
 FT Flow Transmitter
 FC Flow Controller
 PC Pressure Controller

Control Valve
 Manual Valve
 Check Valve

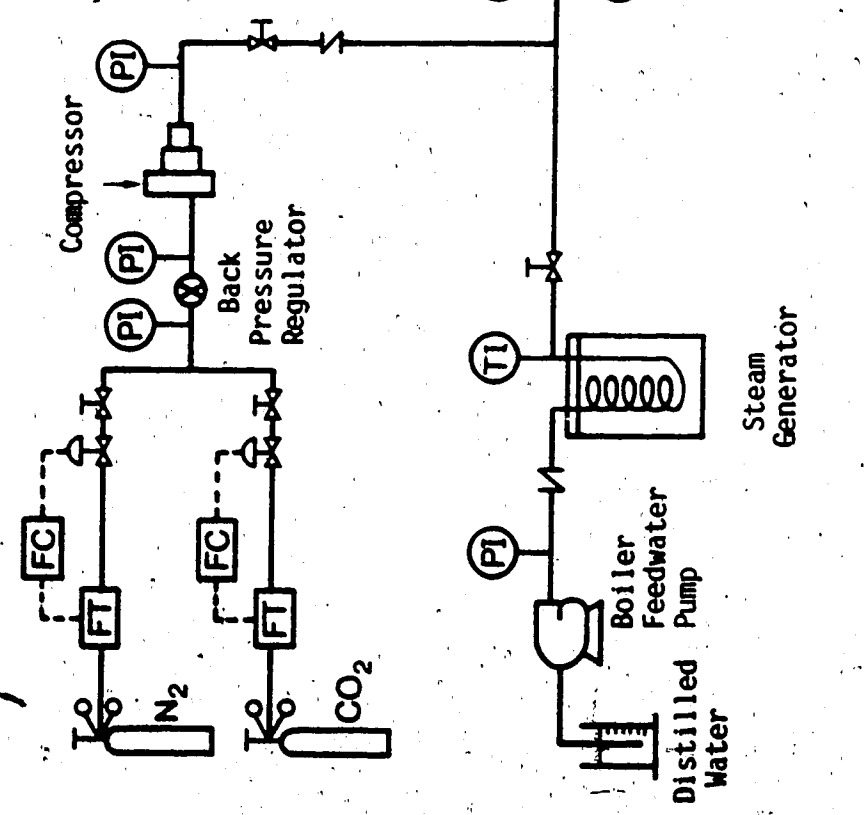


FIGURE 3.1
 SCHEMATIC DIAGRAM OF STEAMFLOOD APPARATUS

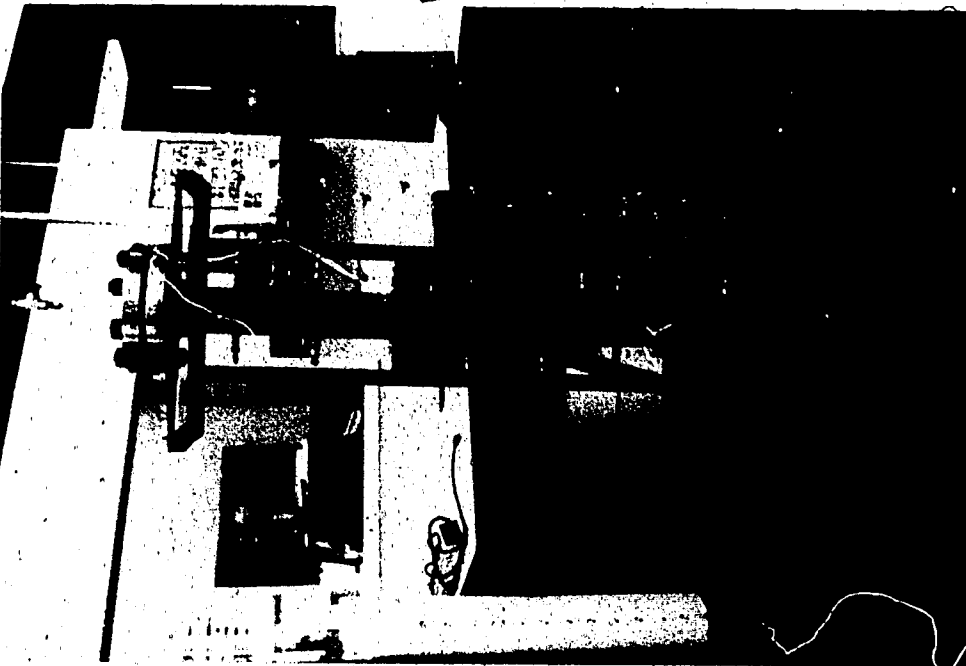


PLATE 3.1 TEST CELL SIDE VIEW



PLATE 3.2 TEST CELL END VIEW

steel were used but these were found to leak on reuse. It was decided to use instead a softer, less expensive RX37 ring of mild steel to be discarded after each experiment. The softer ring does not deform the flange grooves as does a ring of similar hardness to the flanges. Stainless steel spacers were built to take up the additional space created by the larger RX37 rings. It would be desirable in future to build a test cell with raised face flanges for use with the RX37 rings. Screens of 20 x 250 mesh wire cloth were placed at both ends of the sand packs to keep the sand from moving with the fluids.

Plate 3.2 shows the mortar lining which was placed on the inside of the test cell to reduce both heat losses and longitudinal conduction of heat down the thick walled steel pipe during steamflooding. A fairly uniform coating of the cement was obtained by spinning the pipe in a horizontal orientation after applying wet mortar to the inside. The mortar is of a type used for lining pressure vessels for high temperature service. It is composed of 35 percent cement, 5 percent flyash and 60 percent sand and is mixed using 18.5 gallons of water per 100 pounds of dry mix. The resulting inlet and outlet internal diameters of the test cell after application of the mortar were 2.325 inches (5.906 cm) and 2.613 inches (6.638 cm) respectively, yielding an average internal diameter of

2.409 inches (0.272 cm). The inlet end was chosen as that with the thicker mortar in order to provide additional insulating thickness in the region exposed to high temperatures for the longest period of time during steamflooding.

Plate 3.1 is a view of the test cell showing the location of thermowells and pressure taps. Two rows of 15 and 9 of these taps were located on the top and bottom of the cell respectively. On the top row, the taps were spaced 3 inches (7.62 cm) apart and on the bottom row, 6 inches (15.24 cm) apart except at the ends where an additional tap was located. The bottom row was not used in the present study and in the top row, thermocouples were placed such that the first monitored the centre temperature of the sandpack, the second monitored the top edge temperature, the third monitored the center temperature again and so on down the length of the test cell. Thus, a centre temperature was available every six inches (15.24 cm). The thermocouples were located in this way in order to monitor gravity override and heat loss phenomena. The thermowell/pressure taps were constructed using Swagelok welded fittings (SS-400-1-4 MPW) and tube-to-tube adaptors (SS-200-R-4 and SS-100-R-2). The SS-100-R-2 fittings had to be drilled out to accept the type J thermocouples.

Foam-glass insulation was used initially and was shaped to fit around the pipe and thermowells. It was

found to be excessively brittle (cracked when heated) and was abrasive when handled. The foam-glass was replaced by a calcium silicate pipe insulation (Thermo 12) which proved to be more satisfactory. The test cell was covered with two layers of the insulation providing a total thickness of 4 inches (10.16 cm) and it was held in place with nylon-reinforced tape as shown in Plate 3.3.

Following construction, the test cell was hydrostatically tested to 2200 psi (15.17 MPa) at room temperature. The cell is capable of standing this pressure at steam temperature. The flanges in the new test cell were made identical to those of previously built vessels of larger diameter in order that the test cells would all fit the existing stands and could therefore be interchanged as required.

2. Steam Generator

The steam generator consists of a coil of 0.125-inch (0.3175 cm) diameter stainless steel tubing immersed in a heat transfer fluid. The Dowtherm A fluid, manufactured by Dow Chemical Co., has a vapour pressure of 137.8 psig (950 kPa) at its maximum use temperature of 750°F (400°C), and is contained in a pressure vessel whose pressure is monitored during an experiment. The properties of Dowtherm A are listed in the Chemical Engineers' Handbook (1963) on page 3-162. Electric heating rods are used to heat the fluid and power is

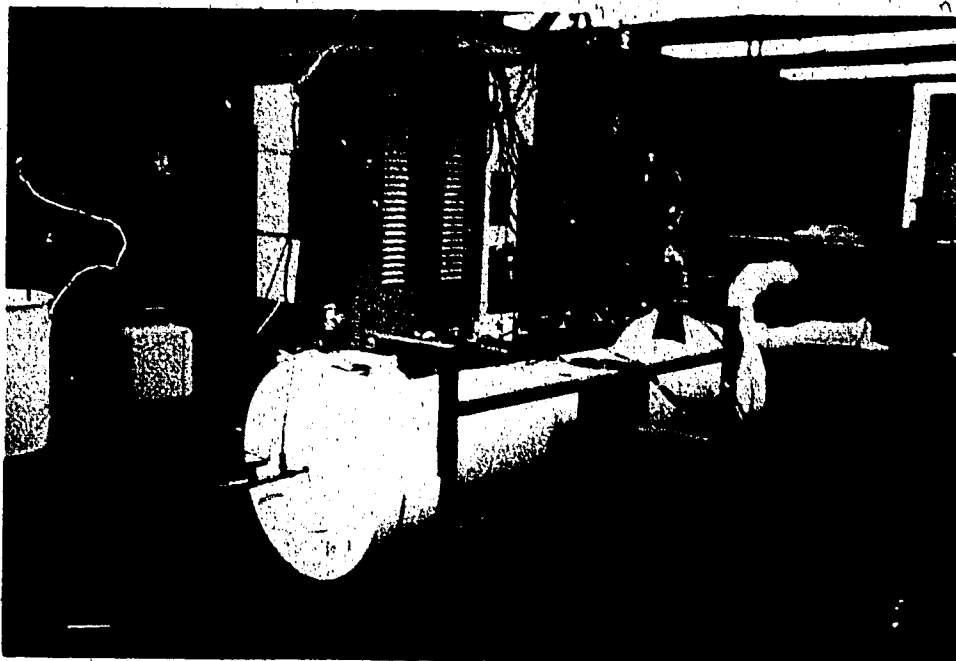


PLATE 3.3 INSULATED TEST CELL

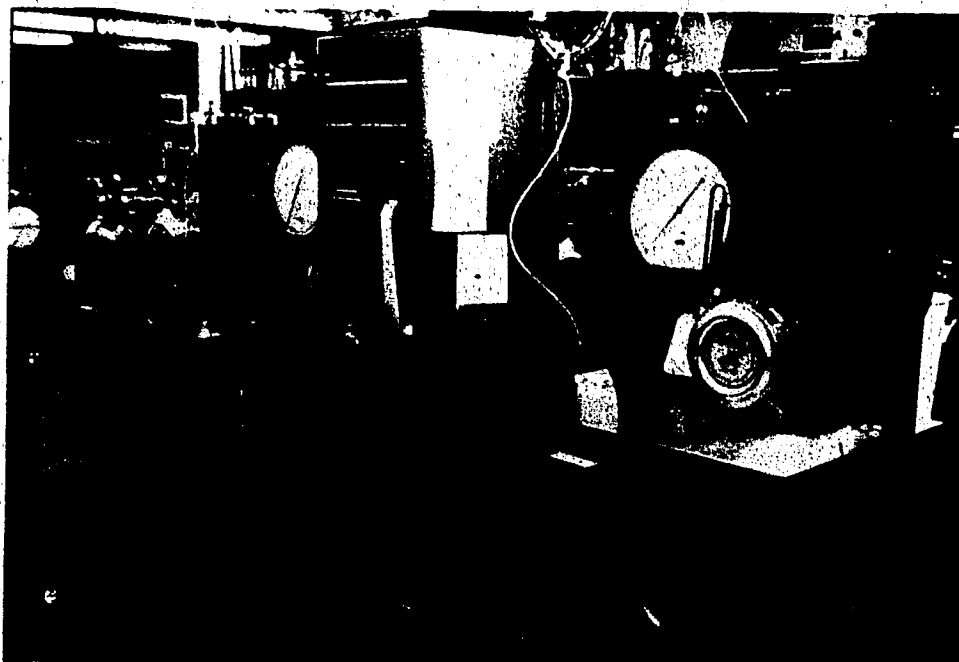


PLATE 3.4 CONTROL PANEL

regulated to these rods by a variable set point temperature controller.

A thermocouple and pressure transducer combination in the inlet line to the test cell are used to determine whether the steam is saturated or superheated. It is necessary to run the experiments so that slightly superheated steam enters the test cell since the equipment does not allow control of saturated steam quality and the enthalpy of the injected steam must be known. Since the inlet pressure of the test cell varies somewhat during the course of an experiment, it is required that the boiler temperature be adjusted periodically in order to maintain an approximately constant level of superheat in the steam.

The 1/4-inch (0.635 cm) steam line from the boiler to the test cell was wrapped with Fibrefax Moist Pak-D ceramic insulation. Further insulating or shortening of this line would be useful as substantial drops in steam temperature were common between the boiler and the test cell requiring that the boiler be operated at a high temperature. The boiler was insulated with a 4-inch (10.16 cm) thickness of foam-glass insulation.

Water was supplied to the boiler by a Milton Roy positive-displacement, variable-speed pump. Distilled water was drawn to the pump suction from graduated cylinders allowing measurement of the volume and injection

rate of the water. As protection against excessive pressures developing in the pump discharge lines due to a blockage or operator error, a Mercoid control switch (300 - 2500 psi) was installed. This unit shuts off the pump if a preset pressure is exceeded.

3. Gas Injection System

Carbon dioxide and nitrogen for use in the experiments were supplied from compressed gas cylinders. Pressure regulators on the cylinders were set at approximately 25 psig (172.4 kPa) and each gas was then fed to a Matheson mass flow controller. According to the operation and service manuals supplied with the equipment, the mass flow controllers use the principles of heat transfer along a capillary tube to develop a flow signal. A small capillary tube around which most of the flow bypasses produces a signal which is proportional to the mass flow rate and the heat capacity of the gas. Provided that the unit has been calibrated for a specific gas in a certain range of flow rates, the signal is proportional to the mass flow rate. Because it is the mass rate of flow which is being monitored, fluctuations in pressure within the ratings of the equipment do not affect the flow control.

The gas stream leaving the flow controllers is fed to the suction side of a JMAR gas compressor. As the

compressor runs on partial vacuum at the flow rates used in the experiments, a back pressure regulator (Tescom 26-2320-24) was placed between the flow controllers and the compressor suction to ensure that the controllers did not experience pressures less than atmospheric. The compressor boosts the gas to whatever discharge pressure is necessary to create flow through the test cell. The gas stream is mixed with steam from the boiler at the inlet to the test cell. An adjustable high-pressure shutdown (Murphy 45-PE-5000 switchgauge) was installed on the compressor discharge to protect against developing excessive pressures.

The gas injection system described could not be used for injecting pure carbon dioxide at pressures above the vapour pressure of CO₂ at room temperature due to the formation of a liquid phase in the compressor.

4. Production Handling

In the initial experiments, all fluids were withdrawn through a single manual regulating valve and the back pressure was controlled manually. Later, a 500 cm³ high-pressure separator was installed to separate the gas and liquid phases. Liquids were withdrawn periodically through the bottom of the separator using a manual valve and gases flowed continuously out the top and into an automatic back-pressure regulating system. The separator

and back-pressure control equipment obviated the need to continuously operate the manual valve and allowed the operator to perform other necessary tasks during the course of an experiment.

The automatic back-pressure control equipment consisted of a pressure transducer on the outlet of the test cell, an EMF to pneumatic converter (Foxboro 33C), a pneumatic pressure controller (Foxboro 40 PR-A4) and a pneumatic control valve (1/4-inch Research Control valve). The 0 to 10-volt signal produced by the pressure transducer was converted to a 3 to 15 psi pneumatic signal in the converter and this signal was then transmitted to the pressure controller. It would be possible to use this type of back-pressure control equipment even when non-condensable gases were not injected into the test cell by merely injecting a small flow of gas into the production line at a point upstream of the back-pressure control valve. Highly effective back-pressure control was obtained using this system. A picture of the control panel is shown in Plate 3.4.

C. Materials

The experiments conducted in this study represent initial investigative work on combined steam and gas injection and it was desired that the sand pack materials be chosen so as to exclude possible unusual effects due to rock/fluid

interactions such as typically occur in actual reservoir materials. Clean silica sand (80-120 mesh) was used in order to avoid such phenomena as clay swelling and migration as well as possible chemical reactions between the steam, carbon dioxide and various minerals in the solid matrix. A refined oil was chosen to eliminate reactions which could occur between the injected fluids and impurities such as sulphur contained in crude oils. Also, refined oils usually have a narrower range of physical properties than crude oils, which simplifies to some extent the treatment required in the numerical simulator. It was felt that interpretation of the experimental results would be made easier by using these materials initially. Of course, a natural extension of the present work would be to use actual reservoir materials from fields which would be amenable to thermal recovery operations.

The oil used was a lubricating oil base stock obtained from the Imperial Strathcona Refinery in Edmonton. Its properties are given in Table 3.1. Density measurements were taken with a Paar DMA 60 density meter and were confirmed using a pycnometer. The viscosity of the dead oil and samples saturated with carbon dioxide at 504 and 802 psig (3475 and 5530 kPa) were measured using a Haake RV3 Rotovisco viscometer which was equipped with a pressure vessel allowing measurements up to 100 atmospheres (10.13 MPa). Calibration of the Haake unit was checked using Dow Corning 200 silicone

Table 3.1
PROPERTIES OF OIL

API Gravity ^(a)	28.32
Density ^(b) @ 25.5°C, g/cm ³	0.88015
Viscosity ^(c) , dead oil @ 24°C, cp	227.9
Viscosity ^(c) , CO ₂ saturated, 24°C, 504 psig, cp	43.6
Viscosity ^(c) , CO ₂ saturated, 26°C, 802 psig, cp	18.5

(a) measured using a Pycnometer.

(b) measured by Anton Paar DMA 60 Density meter.

(c) measured by Haake Rotovisco-viscometer.

fluid calibration standards of 50 and 200 centistoke viscosities.

Oil samples saturated with carbon dioxide were prepared using the following procedure. Two one-gallon (3.78 litre) stainless steel sampling cylinders were filled with oil and then approximately one litre of oil was displaced out of the cylinders by carbon dioxide supplied from a compressed gas cylinder. The cylinders were pressurized with carbon dioxide up to the desired pressure and rotated end for end at about 20 rpm for a period of time. A drop in pressure occurred during the rotating due to carbon dioxide going into solution in the oil. More carbon dioxide was then added to the cylinders to bring them back up to the desired pressure. This process was repeated until no drop in pressure was recorded, indicating that the system was in equilibrium at the desired pressure. The Haake viscometer was then charged with CO₂ and the CO₂-saturated oil displaced into the viscometer pressure vessel. A back-pressure regulator (Tescom 26-1726-24) was used to hold pressure on the vessel while it was being filled with the live oil. The viscosity reduction obtained as a result of carbon dioxide in solution agrees closely with the data of Simon and Graue (1965) for a similar oil.

D. Experimental Procedure

Demetre et al (1982) have reported on wet and dry packing methods using 80-120 mesh sand (Fisher Scientific

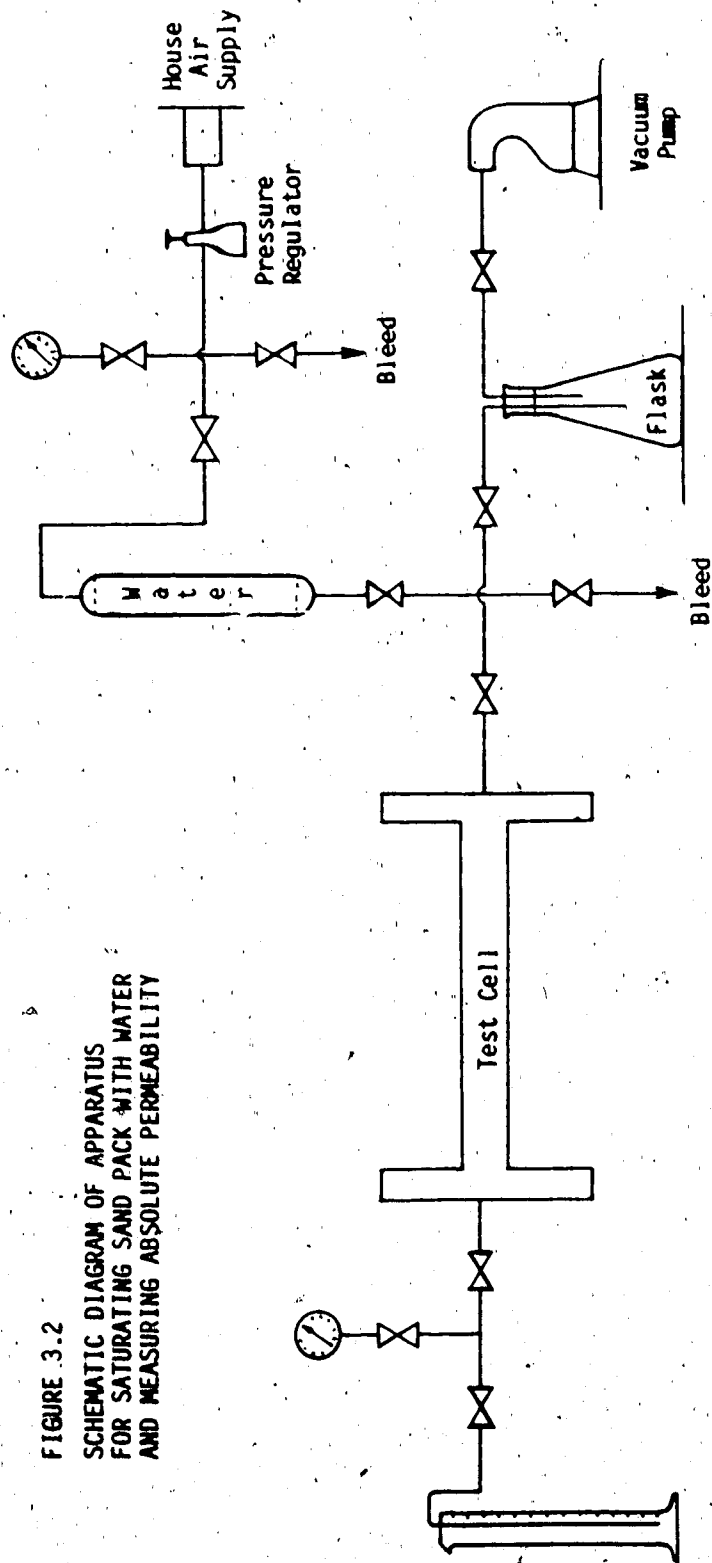
S-151), the same sand used in this study. These authors found that packing the sand by having it settle through a 10 cm layer of water while being continuously vibrated produced sand packs having absolute permeabilities in the range of 14 to 19 darcies. In their method, the coreholder was vibrated for at least 24 hours following packing. The water used in the packing was then removed from the sand pack by passing predried compressed air through for 48 hours. They found that dry packing while vibrating the test cell produced sand packs having properties which were very much dependent upon the length of time the sand pack was vibrated. The absolute permeabilities resulting from dry packing were higher and more variable than with the wet packing procedure.

In the present study, a dry packing technique was used in which the time of vibration of the sand pack was kept essentially constant at around 16 hours (generally from 4:00 p.m. until 8:00 a.m. because of the noise of the vibrator). Absolute permeabilities of 5 to 16 darcies were obtained with the average being 11.3 darcies. Permeabilities in runs 9 to 20 ranged from 9.6 to 15.9 darcies with the average being 12.67 darcies. The advantage to the dry packing technique, provided that it is done using a consistent procedure, is that the drying time following packing is eliminated. Muskat (1981) p. 69 has reported permeability data for 80-100 and 100-120 mesh sands packed to 40% porosity. Permeabilities in the order of 10 darcies were reported which agree well with the data obtained.

The following is a discussion of the steps taken in preparing for and conducting an experiment. The thermowells were cleaned, the thermocouples installed and the outlet end flange attached to the test cell (the spacer and screen were placed at this time). The bolts were torqued first to 200 ft-lbs (271 J) and finally to 325 ft-lbs (441 J) in order to ensure a uniform pressure on the sealing ring. The test cell was oriented vertically and an extender pipe attached to the top flange. A vibrator operating on compressed air was attached to the centre of the test cell. Sand in 1050 gram quantities was poured slowly into the test cell with the vibrator running until 6300 grams of sand had been added. At this point the level of the sand was several centimeters up into the extender piece above the top flange. After vibrating for 16 hours, the extender was removed and the excess sand collected and weighed. The flange was then attached (with spacer and screen) to the inlet end and the sand pack was ready for saturating with water and oil.

A vacuum pump and gauge were then connected to the test cell as shown in Figure 3.2. The vacuum pump was operated for about 3 hours following which it was isolated from the test cell for 0.5 hours in order to see if the pressure would rise indicating that a leak existed somewhere in the apparatus. If no leaks were apparent, water from a graduated cylinder was allowed to enter the test cell giving a measure of the pore volume. Typically the cell would imbibe about 1430 cm³ of water in the first several minutes and then

FIGURE 3.2
SCHEMATIC DIAGRAM OF APPARATUS
FOR SATURATING SAND PACK WITH WATER
AND MEASURING ABSOLUTE PERMEABILITY



an additional perhaps 100 cm^3 in the next 24 hours. It is thought that the initial large water uptake resulted from filling the high permeability silica sand and that the final small amount resulted from water entering the mortar lining. Problems were encountered with this saturating procedure when following packing, the test cell was pressurized with gas to 1000 psig (6895 kPa) to check for leaks. It is thought that some pressurized gas remained in the mortar lining and disrupted the saturating procedure as the gas flowed slowly out of the mortar.

After saturating with water, the absolute permeability to water was measured using the arrangement shown in Figure 3.2. Following the permeability measurement, the test cell was again placed in a vertical orientation and oil displaced into the sand pack from the top using the equipment shown in Figure 3.3. Approximately 3 litres (about 2 pore volumes) of oil was pumped through the sand pack at a rate of 1160 cm^3 per hour. The volumes of oil and water produced from the test cell during this displacement by oil were measured and the oil and water saturations of the sand pack calculated. The test cell was then moved into position for connection to the injection and production systems. The cell was insulated and the thermocouples and pressure transducers connected to the data logger.

To initiate an experiment, the boiler was brought up to temperature and the water injection pump and compressor

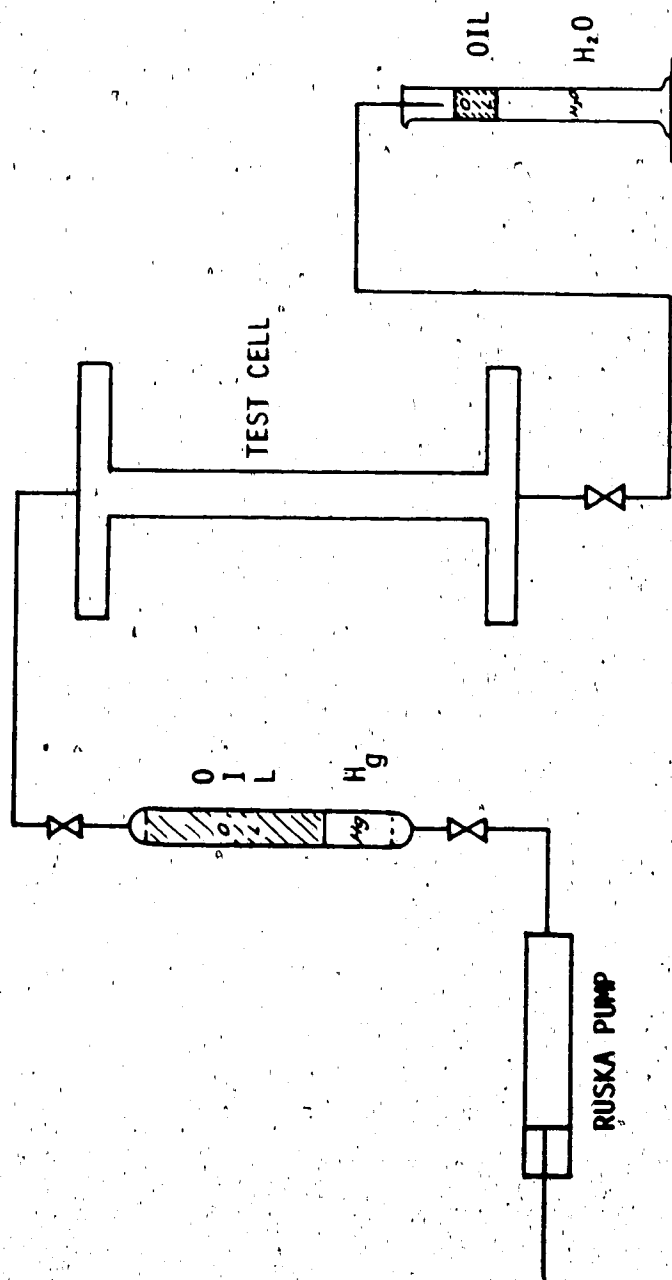


FIGURE 3.3 SCHEMATIC DIAGRAM OF APPARATUS FOR FLOODING SAND PACK WITH OIL

started simultaneously. The mass flow controllers were set to the desired flow rate. The production system was brought into operation once the back pressure had reached the desired operating level. Periodically, the production separator was completely drained of liquid into graduated cylinders and the time of emptying of the separator recorded. The inlet steam line temperature and pressure were monitored closely during a run and adjustments were made to the boiler temperature to keep the steam several degrees above the saturated steam temperature. A scan of the thermocouples and pressure transducers was made every 5 minutes by the data logger and these data were recorded on paper tape. The experiments were terminated when the last thermocouple in the sand pack reached steam temperature. At this point the pump and compressor were shut down and the pressure allowed to bleed off slowly through the production separator.

In the first two experiments, produced oil samples were checked for water content by distillation and were found to contain negligible amounts (less than 0.5%). In subsequent experiments, the production volumes were read directly from the graduated cylinders. Water samples were also analyzed and it was determined that no stable emulsions had been formed.

Once the pressure on the test cell had been reduced to atmospheric, the insulation, flanges, thermocouples and transducers were removed and the sand was cleaned from the test cell using a hand auger. The inside of the cell was

washed with hot water to remove any sand clinging to the mortar and then dried for several hours with hot air from a blow drier. At this point the test cell was ready to repack for the next run.

IV. EXPERIMENTAL RESULTS

A. The Experimental Program

The experiments in the present study were chosen so that comparisons could be made between steamflood performance with the addition of carbon dioxide and nitrogen, and steamflood performance without such gas additives. (Performance comparisons were made on the basis of oil production history and overall recovery.) The ratios of injected gases to steam were approximately those that would be produced by downhole steam generators or that would be encountered in the mixing of boiler flue gases and the generated steam. Mixtures of carbon dioxide, nitrogen and steam represented the effluent that would result if air were used for combustion. Mixtures of carbon dioxide and steam would result if oxygen were used in place of air. The term "flue gas" as used in this work refers to a mixture of carbon dioxide to nitrogen in the molal ratio of 0.267. Table 4.1 summarizes the sand pack properties, run conditions and results for the twenty experiments conducted.

The first experiment was conducted in an old 4 inch (10.16 cm) diameter test cell during the time that the 3 inch (7.62 cm) diameter cell used for the subsequent runs was being built. Necessary repairs were made to the 4 inch cell and new Foamglass insulation was fitted around it. The objective of this first run, which involved the injection of steam only, was simply to obtain operating experience with the equipment and to determine the extent of required modifications to the existing

Table 4.1

SUMMARY OF EXPERIMENTAL RESULTS

RUN NUMBER	1	2	3	4	5	6	7	8	9	10
TYPE	Steam(4")	Steam	Slug CO ₂	Steam	Slug CO ₂	Flue	CO ₂	N ₂	Flue	CO ₂
PACK DENSITY, g/cm ³	1.87	1.52	1.58	1.54	1.56	1.53	1.54	1.54	1.54	1.56
PORE VOLUME, cm ³	3112	1528	1799	1687	1642	1479	1562	1660	1549	1537
POROSITY, %	45.5	40.6	47.8	44.8	43.6	39.3	41.5	44.0	41.1	40.8
PERMEABILITY, d	-	11.0	5.6	13.1	5.5	9.3	7.5	-	10.4	11.0
WATER SAT., % PV	17.7	9.6	27.0	24.9	24.7	14.9	18.5	22.1	18.1	18.8
OIL SAT., % PV	82.3	90.4	73.0	75.1	75.3	85.1	81.5	77.9	81.9	81.2
STEAM INJ. RATE, cm ³ /h	1184	1172	1677	1205	1189	1116	1251	1262	1277	1387
STEAM INJECTED, cm ³	8762	4885	4965	3655	4240	3060	3440	3260	2975	3120
CO ₂ INJ. RATE, dm ³ /h	-	-	283.0	-	187.0	132.5	152.4	-	152.4	152.4
CO ₂ INJECTED, dm ³	-	-	794.7	-	408.0	362.5	419.1	-	355.1	342.7
N ₂ INJ. RATE, dm ³ /h	-	-	-	-	-	521.6	-	572.0	572.4	-
N ₂ INJECTED, dm ³	-	-	-	-	-	1428.0	-	1478.5	1333.6	-
GAS-STEAM RATIO, dm ³ /kg	-	-	158.5	-	96.1	585.5	121.8	453.5	567.6	109.9
BACK PRESSURE, kPa	5192	3371	3350	3364	3350	3323	3406	3554	3475	3399
WATER PRODUCED ¹ , cm ³	7606	4732	4579	3610	3853	2778	3165	3057	3285	3480
OIL PRODUCED ¹ , cm ³	1848	1057	984	1009	1070	1049	1102	1074	1117	1090
OIL RECOVERY, %	72.2	76.5	74.9	79.6	86.5	83.3	86.5	83.1	88.1	87.1
DEPRESS. OIL ² , %	2.9	3.3	3.0	1.3	3.6	-	2.2	0.3	1.0	1.3
STEAM-OIL RATIO, m ³ /m ³	4.74	4.62	5.05	3.62	3.96	2.92	3.12	3.04	2.66	2.86
WATER-OIL RATIO, m ³ /m ³	4.12	4.48	4.65	3.58	3.60	2.65	2.87	2.85	2.94	3.19

1. Does not include fluid produced during depressurization of the test cell.

2. Oil produced during depressurization of the test cell.

Table 4.1 Continued

SUMMARY OF EXPERIMENTAL RESULTS

RUN NUMBER	11	12	13	14	15	16	17	18	19	20
TYPE	N ₂	Slug Flue	CO ₂	Flue	Flue	CO ₂	Slug CO ₂	Steam	N ₂	CO ₂
PACK DENSITY, g/cm ³	1.54	1.54	1.56	1.56	1.54	1.57	1.56	1.56	1.58	1.57
PORE VOLUME, cm ³	1554	1595	1470	1511	1522	1560	1525	1542	1543	1520
POROSITY, %	41.3	42.3	39.0	40.1	40.4	41.4	40.5	40.9	41.0	40.4
PERMEABILITY, d	10.3	9.6	12.8	14.3	15.9	13.1	14.3	15.1	14.2	11.0
WATER SAT., % PV	18.1	21.3	15.5	15.8	15.8	20.9	17.4	18.9	20.4	18.0
OIL SAT., % PV	81.9	78.7	84.5	84.2	84.2	79.1	82.6	81.1	79.6	82.0
STEAM INJ. RATE, cm ³ /h	1270	1103	624	633	1237	1550	1417	1359	1371	1518
STEAM INJECTED, cm ³	2960	3947	4260	4170	3710	3360	3240	3845	3085	3290
CO ₂ INJ. RATE, dm ³ /h	-	152.4	77.4	76.2	153.0	152.4	152.4	-	-	152.4
CO ₂ INJECTED, dm ³	-	381.0	529.0	502.0	459.0	331.0	381.0	-	-	330.0
N ₂ INJ. RATE, dm ³ /h	572.4	572.4	-	288.0	576.0	-	-	-	572.4	-
N ₂ INJECTED, dm ³	1334.0	1431.0	-	1896.0	1728.0	-	-	-	1728.9	-
GAS-STEAM RATIO, dm ³ /kg	451.0	459.0	124.2	575.0	589.5	98.4	117.6	-	414.6	100.4
BACK PRESSURE, kPa	3430	3487	3472	3476	6950	3585	3399	3589	3450	3409
WATER PRODUCED ¹ , cm ³	3455	3752	3980	3903	3424	3201	3189	4226	3533	2903
OIL PRODUCED ¹ , cm ³	(1075) ³	1073	1093	1135	1111	1054	1007	1035	(1066) ³	1078
OIL RECOVERY, %	(84.5)	85.5	88.0	89.2	86.7	89.7	80.0	82.7	(86.8)	86.3
DEPRESS. OIL ² , %	1.2	2.1	1.2	1.5	1.9	1.4	4.1	3.4	1.2	1.0
STEAM-OIL RATIO, m ³ /m ³	2.75	3.68	3.90	3.67	3.34	3.19	3.22	3.71	2.89	3.05
WATER-OIL RATIO, m ³ /m ³	3.21	3.50	3.64	3.44	3.08	3.04	3.17	4.08	3.31	3.71

1. Does not include fluid produced during depressurization of the test cell.
2. Oil produced during depressurization of the test cell.
3. Brackets indicate production estimate.

apparatus. Following this experiment, automatic back pressure control, injection gas flow control and gas compression equipment was ordered. Runs 2 through 7 were made before the automatic back pressure control system was available.

For simultaneous injection of gases and steam at a fixed ratio, the gas flow control equipment was required. In the time required for delivery of this equipment, 4 experiments were performed in the new test cell, two with steam only injection and two with the injection of slugs of carbon dioxide followed by steam. In runs 3 and 5, carbon dioxide flow was measured using an orifice meter composed of a micrometering valve with pressure transducers upstream and downstream of the valve. Carbon dioxide was fed to this system directly from a compressed gas cylinder with the result that the gas flow rates were not constant since they were affected by the varying inlet pressure of the test cell. In run 3 the boiler temperature was too low and as a consequence wet steam of an unknown quality was injected. In run 5 the production lines were not cleaned following an experiment conducted in another program with Athabasca bitumen. A significant but unknown amount of bitumen was therefore removed from these lines by the action of carbon dioxide and oil and this unknown quantity was contained in the production figures. Experiment number 17 was conducted late in the program as a repeat of these earlier runs in order to overcome the problems that had been associated with them. Experiment 12 was similar to 3, 5 and 17 but involved the injection of a slug of flue gas rather than carbon dioxide.

in run 2, the experiment was repeated in run 4 and this run then formed the basis for comparison of steam-only flooding and the simultaneous steam-gas injection processes and in runs 6, 7 and 8. In spite of the somewhat lower steam quality employed in run 2, the results of runs 2 and 4 were qualitatively very similar providing confirmation of the run 4 result on which the fundamental process comparisons are made. Five post-waterflood experiments (numbers 18, 9, 10, 11 and 19) were conducted in order to compare steam-only and steam-gas injection processes for porous media having a lower initial oil saturation. About 2 pore volumes of water was injected in each case prior to the steamfloods. The waterfloods were performed with the outlet at a constant pressure - atmospheric. Run 18 was the base case of waterflood followed by steam-only injection. Runs 9 and 10 involved steam-flue gas and steam-CO₂ injection, respectively. The liquid production valve became blocked with sand about halfway through the steam-N₂ flood in run 11 and some production was lost in clearing the valve. It was necessary to estimate the production for this experiment. Run 19 was to be a successful repeat of run 11 but exactly the same problem developed requiring estimation of lost oil production as well.

Early results suggested that gas solubility effects were not as important as would have been expected (Harding et al, 1983). It was thought that perhaps insufficient time was available for carbon dioxide to enter solution in the oil due to

importance of such effects. Two experiments were conducted at lower flow rates (runs 13 and 14) with steam-CO₂ and steam-flue gas injection and one experiment was conducted at a higher pressure of 1000 psig (6895 kPa)*. This latter experiment (run 15) involved steam-flue gas injection since with the equipment used, it was not possible to inject carbon dioxide at pressures above its vapour pressure at room temperature (about 830 psig). A similar danger of liquifying flue gas in the compressor did not exist due to the large proportion of nitrogen in the gas. In run 16, a steam-CO₂ flood was conducted on a sandpack containing oil saturated with carbon dioxide. The oil was saturated with carbon dioxide at room temperature prior to flooding the test cell with oil. The oil flooding step in the sand pack saturation procedure was conducted through a back pressure regulator in this case. A swelling factor estimate of 1.05 was obtained from the paper by Simon and Graue (1965) for a similar oil and this factor was used to calculate the original dead oil volume of the sandpack for determination of the oil recovery.

The final experiment, number 20, was conducted to examine reproducibility of the recovery figures for runs at similar conditions. Runs 7 and 20 involved simultaneous steam-CO₂ injection and the overall recoveries differed by only

* With the exception of run 1 which was conducted at 750 psig (5171 kPa), all other experiments had back pressures of approximately 500 psig (3448 kPa).

runs were very close although absolute permeability in run 7 was 7.5 darcies and in run 20 was 11.0 darcies.

B. Nature of the Experiments

The properties of the sandpacks for all of the experiments are shown in the top grouping of parameters in Table 4.1. For the experiments in the 3 inch test cell the densities to which the sand was packed ranged from 1.52 to 1.55 g/cm³. Porosities are thought to be somewhat high due to the influence of the mortar lining. It is felt that the lining had a porosity of about 7 percent and that some water entered the mortar during saturation of the sandpack following evacuation. However, porosity figures have not been adjusted to include the effect of the lining. As mentioned in Chapter 3, the magnitude and range of absolute permeabilities of the sand pack were similar to those reported in other studies using the same sand (Demetre et al, 1982). Some groups of runs had initial oil and water saturations which were very close in value (eg., experiments 18, 9, 10 and 11 which all involved waterflooding followed by steam and gas injection).

The gas/steam ratios for injection were chosen to approximate those which would be created in a downhole steam generator. It was assumed that excess air would be minimized in DHSG's because of potential corrosion and that the units would operate at a very high efficiency. Combustion of liquid hydrocarbon fuel would produce about 100 BTU/SCF of air (3.725 MJ/m³) and approximately 1000 BTU/lb (2.326 MJ/kg) would be

generators would be in the order of 10 SCF/lb of steam (529 dm³/kg) in the case of air and twenty percent of this figure or 2 SCF/lb (105 dm³/kg) where oxygen is used. The actual volumes of gas and gas-steam ratios used in the experiments are summarized in Table 4.1. Essentially constant gas-steam ratios were used for all runs including both gas slug and simultaneous gas-steam injection processes.

It is instructive to analyze the stability of the displacement processes basing the analysis on the work of Peters (1979). A stability number for steam injection based on equivalent flow of water is calculated from the following formula and data:

$$N_s = \frac{(\frac{\mu_o}{\mu_w} - 1) V \mu_w D^2}{c^* \gamma k} \quad (4.1)$$

where N_s = stability number

μ_o = oil viscosity = 2.27 g/cm·s

μ_w = water viscosity = 1.0×10^{-2} g/cm·s

D = diameter of system = 6.272 cm

V = superficial velocity = 3.37×10^{-2} cm/s
(typical steam rate)

c^* = wettability number = 306.25
(water-wet system)

γ = Interfacial tension = 24.5 dynes/cm

k = absolute permeability = 1.48×10^{-7} cm².

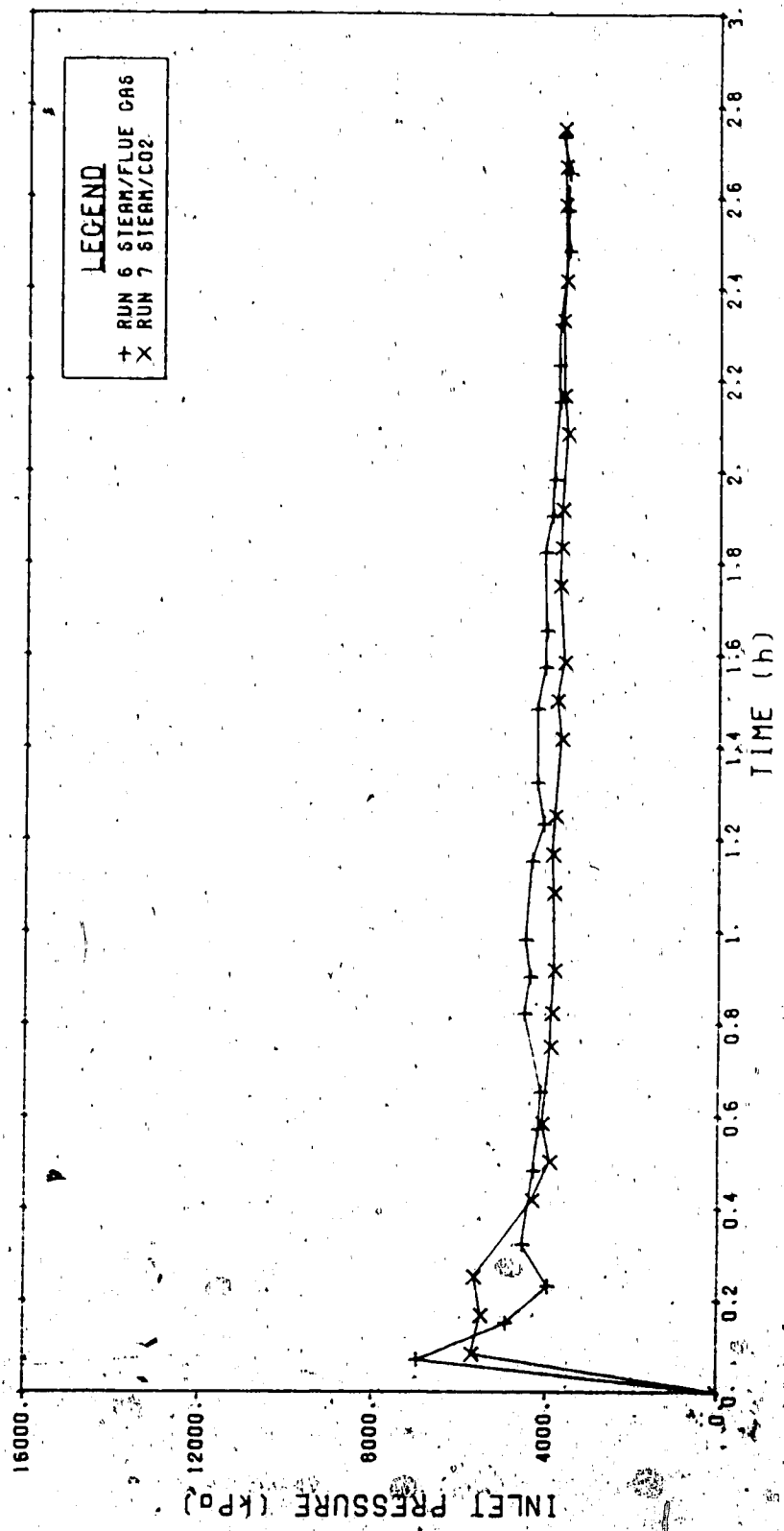
The resultant stability number for this case is 2.698×10^3 , which indicates that the displacement is unstable and is

Consideration of water flow in the gas phase as steam or of the addition of non-condensable gases to the steam would increase the instability and thus it is concluded that all of the experiments were in the unstable displacement category. This was verified during the experiments by early gas and water breakthrough at the production end of the test cell.

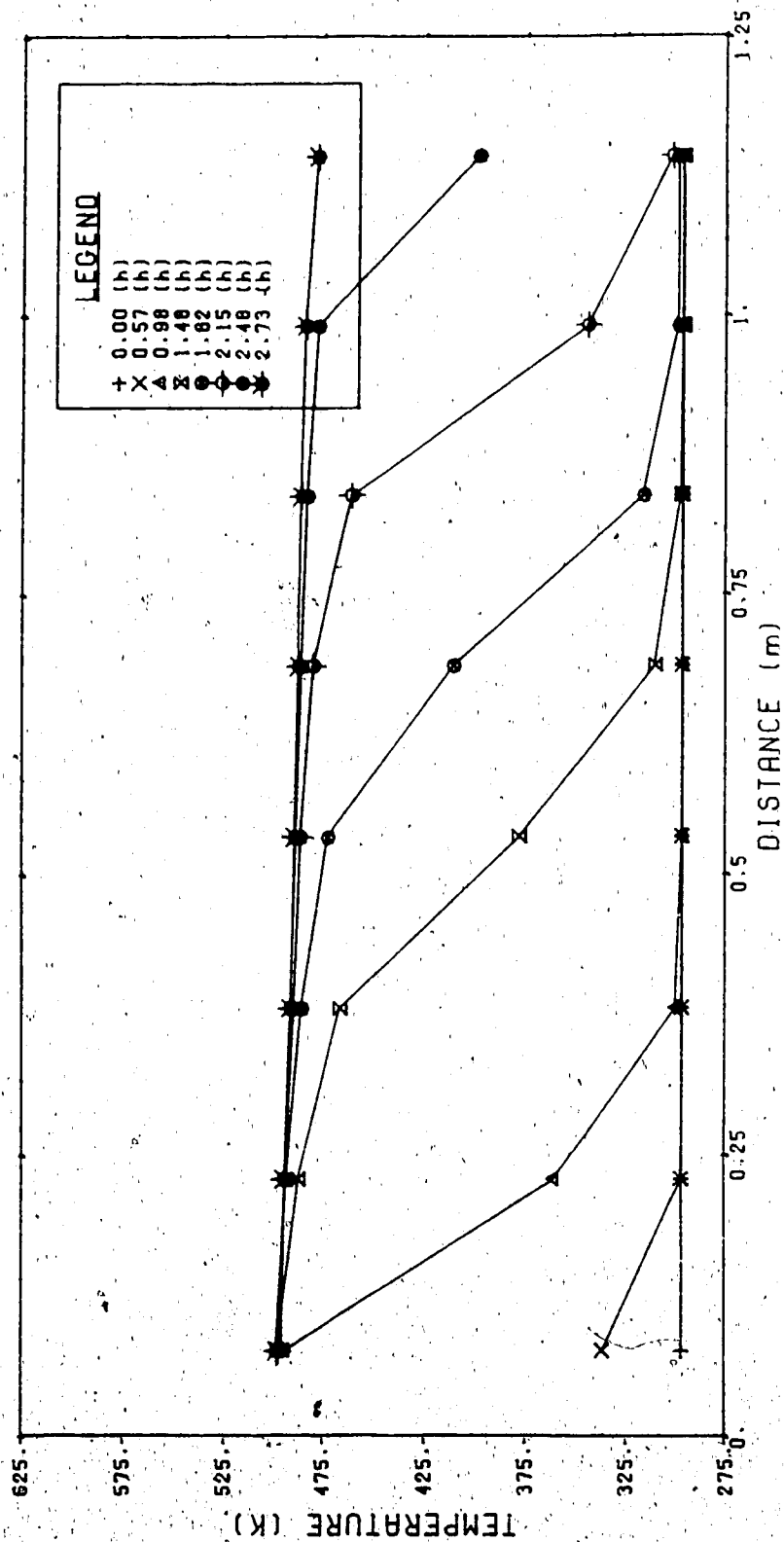
Appendix C contains injection and production data as well as inlet pressure and test cell temperature data for experiments 2 through 20. The inlet pressure histories for two runs have been plotted in Figure 4.1 and the centre line temperature data from experiment 6 are presented in Figure 4.2 in order to illustrate the general character of the tests. At essentially constant back pressures and fluid injection rates, the inlet pressures are high at the beginning of the experiments and gradually decrease as oil is swept from the porous medium (Figure 4.1). Higher inlet pressures occur throughout experiments with larger injection rates as in the case of Run 6 (steam/flue gas) compared to Run 7 (steam/CO₂). In the former the total injection rate was 91.2 mol/h compared to 76.3 for the latter. The temperature profiles (Figures 4.2) show the slow rise to steam temperature of the inlet end characteristic of these experiments. The direct contact between the steam and inlet-end flanges was responsible for this behaviour. All runs were terminated when essentially the whole test cell had reached steam temperature.

It may be recalled from Chapter III that the even

FIGURE 4.1
INLET PRESSURE HISTORIES
FOR SIMULTANEOUS STEAM/GAS INJECTION



2



numbered thermocouples are located on the top surface of the sand pack and the odd numbered ones at the centre. The thermocouples were arranged in this manner to monitor the gravity segregation of fluids and to look at temperature gradients in the direction orthogonal to the fluid flow. Centre line and top wall temperature profiles are presented for two experiments in Figures 4.3 and 4.4. Temperature profiles are plotted for early, intermediate and late times in the tests. Examination of the figures indicates that in general the high temperature front in the centre of the sandpack leads the front on the top surface by 3 to 4 inches (7.6 to 10.2 cm). In the case of simultaneous steam/gas injection, the top wall temperatures along the entire length of the test cell did not reach the same level as the centre temperatures but remained 5 to 10°C lower. Centre and wall temperatures at the end of the experiments were almost identical for the steam-only injection tests. Indications are that there was some segregation of fluids in the simultaneous steam/gas injection cases which caused the lower temperatures at the top of the sandpack.

C. The Effect of Gas Additives to Steam

Oil recoveries and production histories are now examined for sandpacks under the application of steam-only and steam-gas injection. Both pre-waterflood and post-waterflood sandpacks are considered.

Table 4.2 summarizes the data of runs 4, 6, 7 and 8 which were conducted on pre-waterflooded sandpacks at similar

FIGURE 4.4
WALL AND CENTRE TEMPERATURE PROFILES - RUN 6

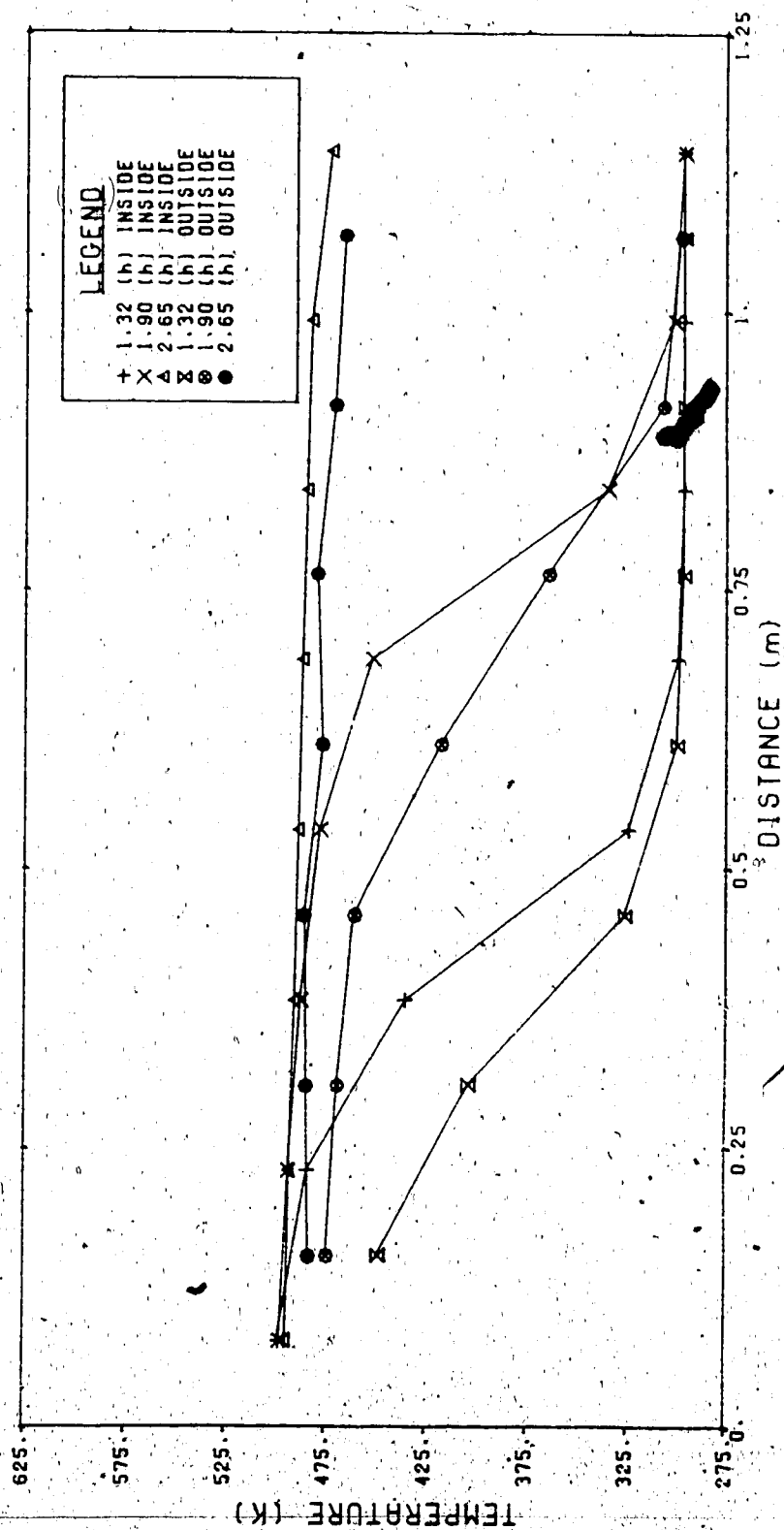


Table 4.2

COMPARISON OF STEAM-ONLY INJECTION
AND SIMULTANEOUS STEAM-GAS INJECTION
(PREWATERFLOOD)

RUN NUMBER	4	7	8	6
TYPE	STEAM	STEAM/CO ₂	STEAM/N ₂	STEAM/FLUE
INITIAL CONDITIONS				
PACK DENSITY, g/cm ³	1.54	1.54	1.54	1.53
PORE VOLUME, cm ³	1687	1562	1660	1479
POROSITY, %	44.8	41.5	44.0	39.3
PERMEABILITY, d	13.1	7.48	-	9.28
WATER SATURATION, % PV	24.9	18.5	22.1	14.9
OIL SATURATION, % PV	75.1	81.5	77.9	85.1
RUN CONDITIONS				
STEAM INJECTION RATE, cm ³ /h	1034	1251	1262	1116
CO ₂ INJECTION RATE, dm ³ /h	-	152.4	-	132.5
N ₂ INJECTION RATE, dm ³ /h	-	-	572	521.6
GAS-STEAM RATIO, dm ³ /kg	-	121.8	453.5	585.5
AVERAGE BACK PRESSURE, kPa	3363	3406	3554	3323
OVERALL RUN				
STEAM INJECTED, cm ³	3655	3440	3260	3060
CO ₂ INJECTED, dm ³	-	419.1	-	362.5
N ₂ INJECTED, dm ³	-	-	1479	1428
WATER PRODUCED, cm ³	3610	3165	3057	2778
OIL PRODUCED, cm ³	1009	1102	1074	1049
OIL RECOVERY, % OOIP ^x	79.6	86.5	83.1	83.3
DEPRESS. OIL, % OOIP ⁺	1.3	2.2	0.3	-
STEAM-OIL RATIO, m ³ /m ³	3.62	3.12	3.04	2.92
WATER-OIL RATIO, m ³ /m ³	3.58	2.87	2.85	2.65
INJ. GAS-OIL RATIO, mol/dm ³ *	201.2	190.4	230.0	238.1

+ Additional oil recovered during depressurization of the test cell.

* Ratio of the injected gases (steam + CO₂ + N₂) in moles to the produced oil in dm³.

x Percentage of the original oil in place.

steam injection rates and back pressures. The lowest recovery was for steam-only at 79.6 percent and the highest for steam/ CO_2 injection, the recovery being 86.5 percent, almost 7 percent higher than the steam-only case. The steam/ N_2 and steam/ flue gas cases yielded recoveries which were very similar and which were intermediate between the recoveries for steam-only and steam/ CO_2 injection. Recoveries may be affected to some extent by variations in initial saturation conditions and permeabilities but there is no trend evident from examination of Table 4.2 of recovery with either of these parameters. Less steam was required to produce the oil in the steam-gas injection processes as reflected in the steam-oil and water-oil ratios. The greater the injected gas-steam ratio, the lower are the steam-oil and water-oil ratios. These indices have important economic implications in application of the processes in actual oil fields. Injected gas to produced oil ratios show that all runs had similar molal throughputs of material due to the reduced requirements for steam in the steam-gas injection runs.

Cumulative production histories for the experiments in Table 4.2 are plotted in Figures 4.5(a) and (b) as functions of cumulative steam injected in pore volumes (Figure 4.5(a)) and cumulative gas injected in moles (Figure 4.5(b))* . In the latter, the molal injection is the sum of steam, carbon dioxide and nitrogen injected. Worthy of note in these figures is the difference in production history between the steam-only and the

* Plotting the data in this manner removes to some extent the effect of differences in flow rate amongst the experiments.

FIGURE 4.5A CUMULATIVE PRODUCTION HISTORIES
FOR SIMULTANEOUS STEAM-GAS INJECTION
(PREWATERFLOOD)

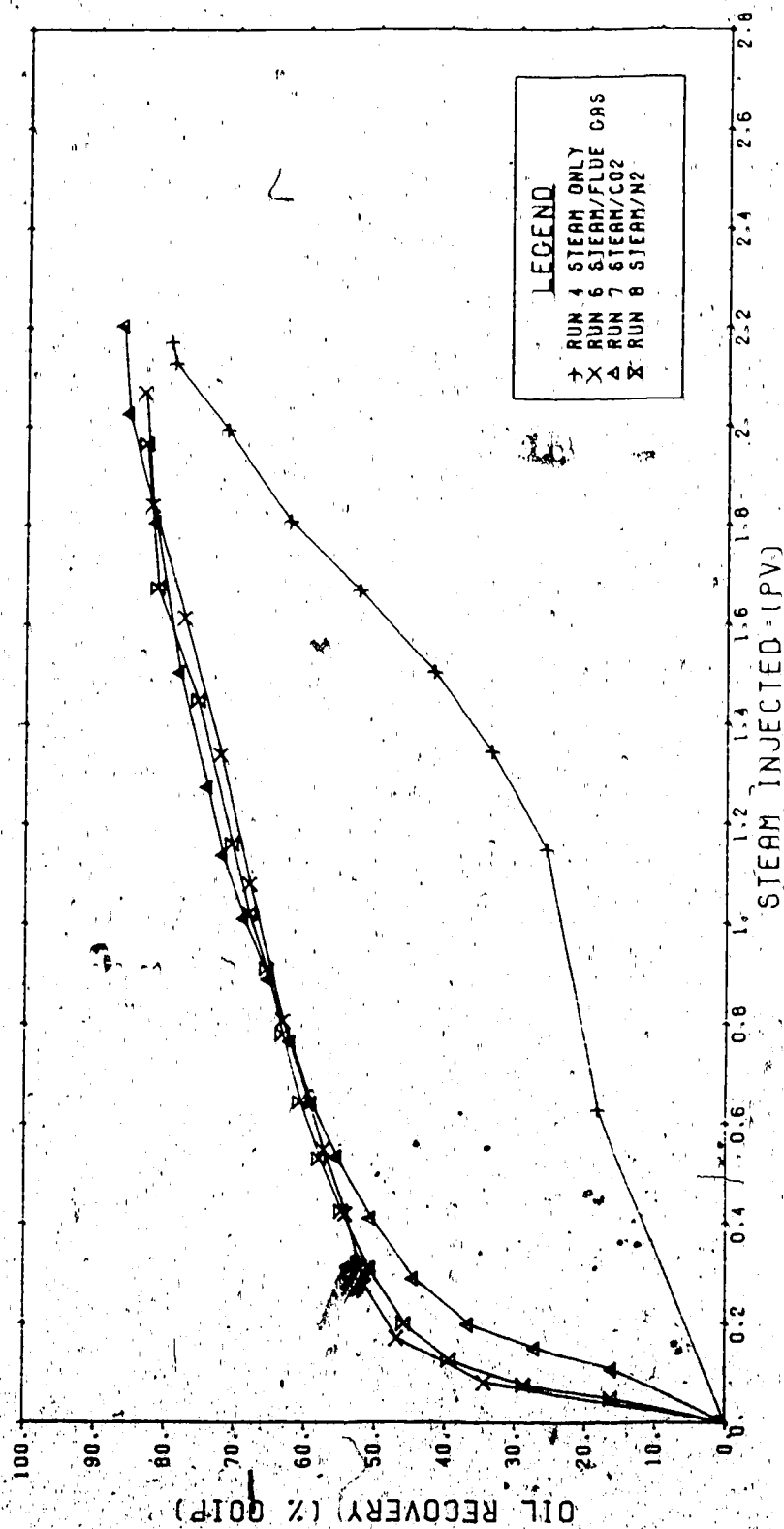
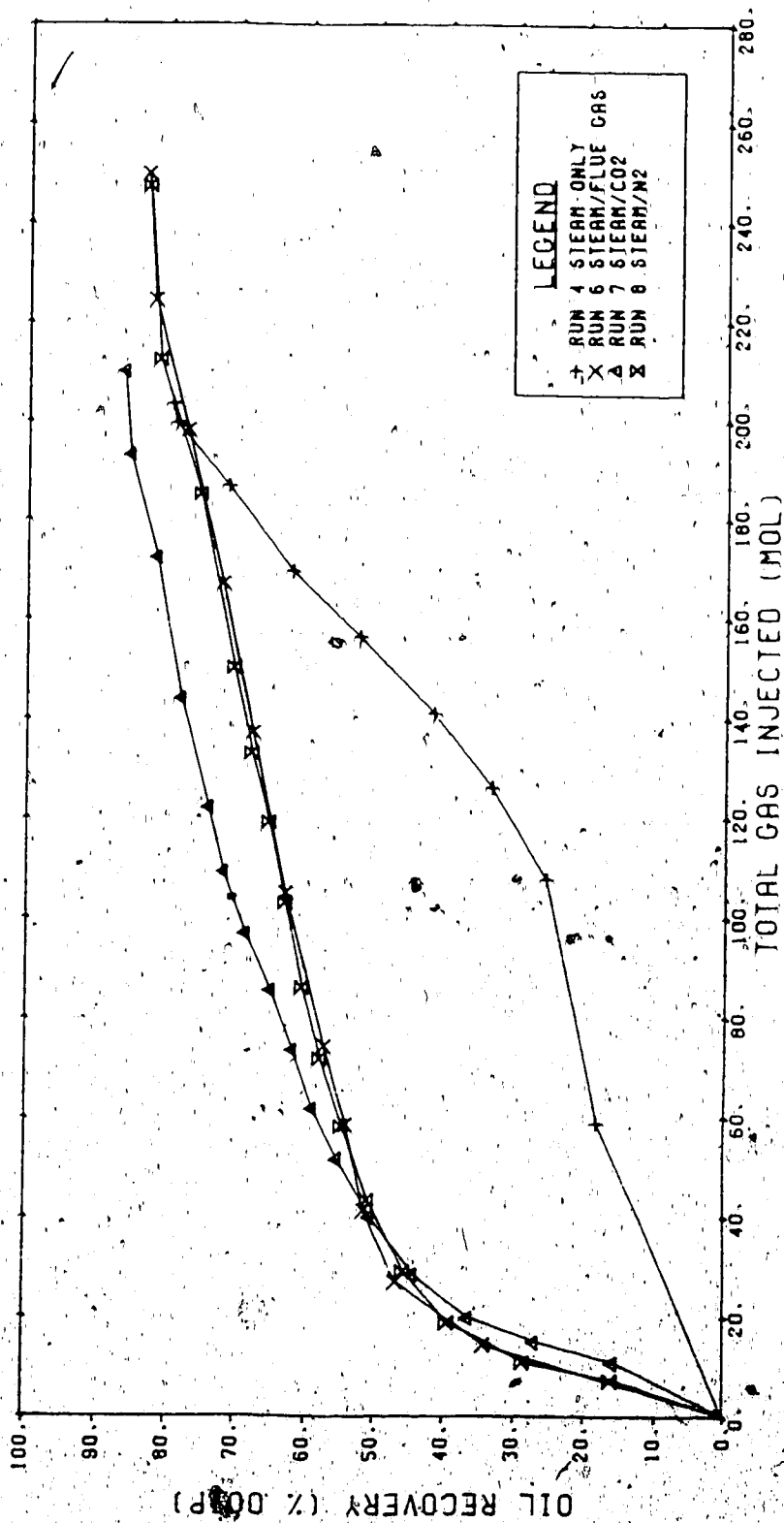


FIGURE 4.5B CUMULATIVE PRODUCTION HISTORIES
FOR SIMULTANEOUS STEAM-GAS INJECTION.
(PREWATERFLOOD)



steam-gas injection cases. All of the steam-gas injection runs show similar performance which is significantly different from that of steam-only. The accelerated production in the steam-gas processes was reported earlier (Harding et al., 1983). Plotting the data on a molal injection basis as in Figure 4.5(b) tends to close the gap somewhat between the steam-only and steam-gas runs but the difference is still significant. It is interesting that in both figures the steam/flue gas and steam/N₂ curves are almost identical. Run 7 (steam/CO₂), although somewhat slower starting than the other steam-gas runs, is the superior process on the basis of total molal input (Figure 4.5(b)). At a cumulative molal throughput of 160 moles, the steam/CO₂ recovery is 81 percent compared to 71 percent for simultaneous steam/flue gas and steam/N₂ processes and the recovery is only 55 percent at the same point for steam-only injection. Run 4 (steam-only) is characterized by a slow rise in the production curve until about half of the steam is injected followed by a steeper rise from that point up to the end of the experiment. This behaviour corresponds to production due to waterflood ahead of the steam zone and then more rapid production once steam temperatures occur in the test cell.

Similar results to the pre-waterflooded cases were obtained in post-waterflooded sandpacks. Table 4.3 shows summary data for the post-waterflood runs 18, 9, 10 and 11. Consistent sandpack properties were obtained in this group of

Table 4.3

COMPARISON OF STEAM-ONLY INJECTION
AND SIMULTANEOUS STEAM-GAS INJECTION
(POST WATERFLOOD)

RUN NUMBER	18	10	11	9
TYPE	STEAM	STEAM/CO ₂	STEAM/N ₂	STEAM/FLUE
INITIAL CONDITIONS				
PACK DENSITY, g/cm ³	1.56	1.56	1.54	1.54
PORE VOLUME, cm ³	1542	1537	1554	1549
POROSITY, %	40.9	40.8	41.3	41.1
PERMEABILITY, d	15.1	11.01	10.25	10.42
WATER SATURATION, % PV	18.9	18.8	18.1	18.1
OIL SATURATION, % PV	81.1	81.2	81.9	81.9
WATERFLOOD				
WATER INJECTION RATE, cm ³ /h	1956	2000	1968	1919
WATER INJECTED, cm ³	4890	3120	5215	4740
OIL PRODUCED, cm ³	563	578	556	558
RECOVERY, % OOIP	45.0	46.3	43.7	44.0
STEAMFLOOD CONDITIONS				
STEAM INJECTION RATE, cm ³ /h	1359	1387	1270	1277
STEAM INJECTED, cm ³	3845	3120	2960	2975
CO ₂ INJECTION RATE, dm ³ /h	-	152.4	-	152.4
CO ₂ INJECTED, dm ³	-	342.9	-	355.1
N ₂ INJECTION RATE, dm ³ /h	-	-	572.4	572.4
N ₂ INJECTED, dm ³	-	-	1334	1334
GAS-STEAM RATIO, dm ³ /kg	-	110	451	568
AVERAGE BACK PRESSURE, kPa	3589	3399	3430	3475
STEAMFLOOD PERFORMANCE				
WATER PRODUCED, cm ³	4226	3480	(3455)	3285
OIL PRODUCED, cm ³	472	508	(519)	559
OIL RECOVERY, % OOIP	37.7	40.8	(40.8)	44.1
OIL RECOVERY, % ORAW*	68.6	75.8	(72.5)	78.7
STEAM-OIL RATIO, m ³ /m ³	8.15	6.14	(5.70)	5.32
WATER-OIL RATIO, m ³ /m ³	8.95	6.85	(6.66)	5.88
INJ. GAS-OIL RATIO, mol/dm ³	453.2	371.2	(431.6)	430.6
WATERFLOOD PLUS STEAMFLOOD				
TOTAL OIL RECOVERY, % OOIP	82.7	87.1	(84.5)	88.1
DEPRESS. RECOVERY, % OOIP	3.4	1.3	1.2	1.0

* % of oil remaining after waterflooding.

() Production estimate.

runs with porosities ranging from 40.8 to 41.3 percent and permeabilities from 10.25 to 15.1 darcies. The initial saturations were very close indeed. Oil recoveries resulting from the waterflooding portions of these runs ranged from 43.7 to 46.3 percent.

Steamflood oil recoveries are reported as a percentage of the oil remaining after waterflooding. Steam-gas injection was marginally superior to steam-only injection for post-waterflooded runs as was the case for pre-waterflood conditions. Steam/flue gas yielded the highest recovery in the post-waterflood runs. Because of higher water saturations at the beginning of the steamfloods, steam-oil and water-oil ratios were high for these experiments but still dropped with increasing amounts of gas injected. The differences in the SOR and WOR between the steam-only and steam/CO₂ cases is greater than the differences in SOR and WOR between the steam/CO₂ and steam/flue gas runs as was evident also in Table 4.2 for the pre-waterflood experiments. Total oil recoveries combining the waterflood and steamflood results show only slight improvement over the total recoveries for the pre-waterflood cases. This indicates that steam determines the ultimate residual oil saturation for this linear system.

Figures 4.6(a) and (b) are similar to 4.5(a) and (b) except that now the data for the post-waterflood cases are being presented. The production history for steam-only injection (Run 18) exhibits a very slow rise until heat begins

FIGURE 4.6A CUMULATIVE PRODUCTION HISTORIES
FOR SIMULTANEOUS STEAM-GAS INJECTION
(POSTWATERFLOOD)

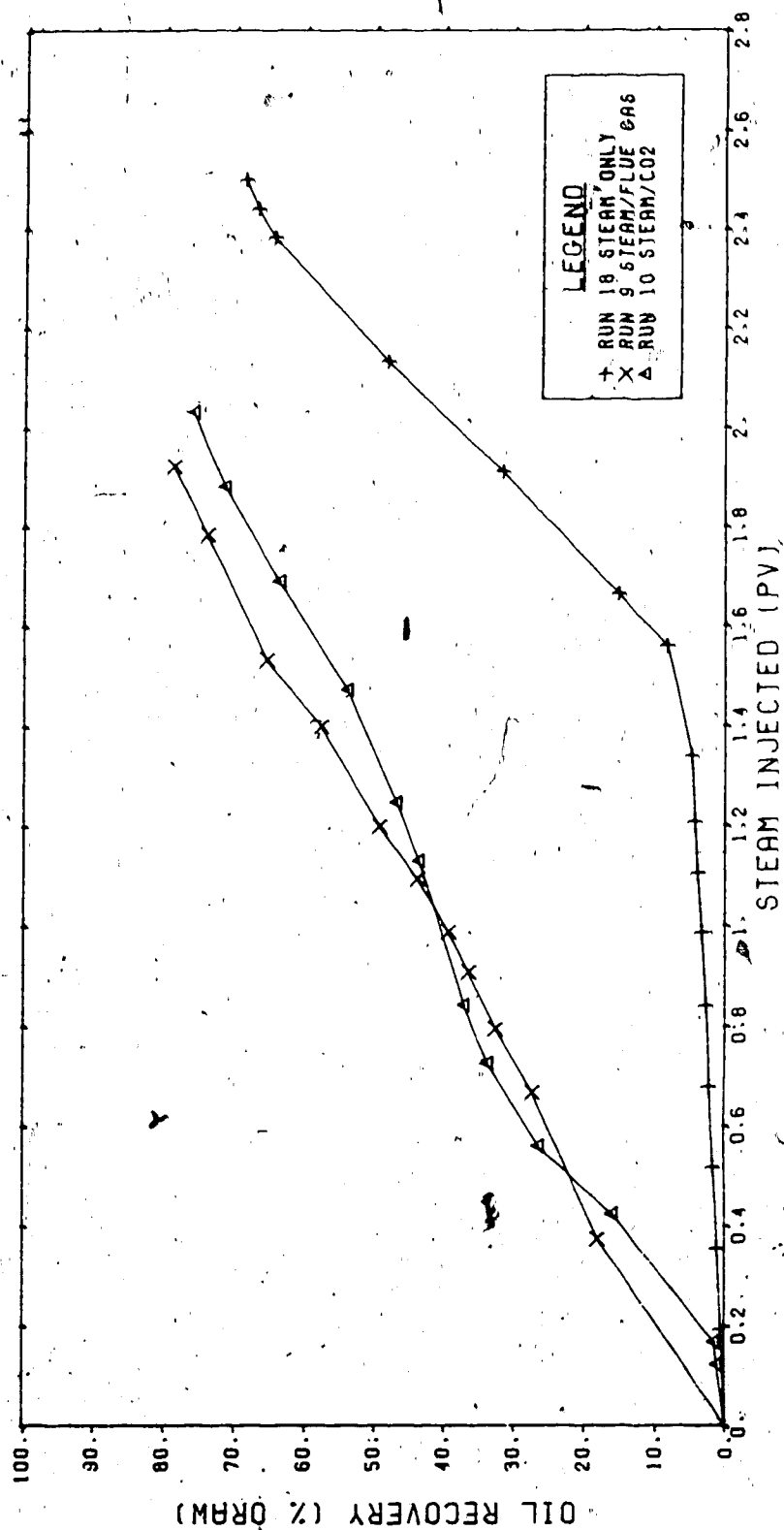
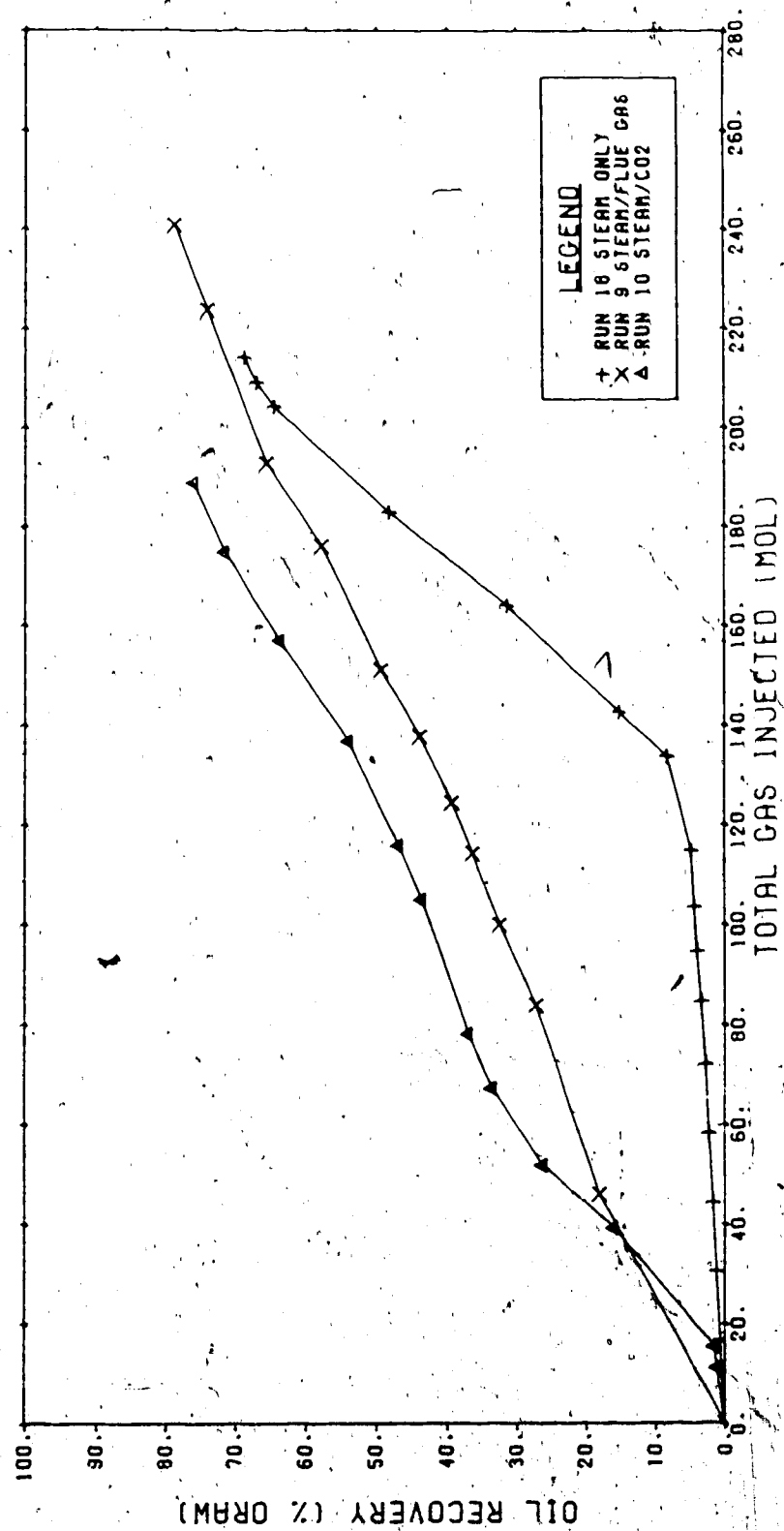


FIGURE 4.6B CUMULATIVE PRODUCTION HISTORIES
FOR SIMULTANEOUS STEAM-GAS INJECTION
(POSTWATERFLOOD)



to mobilize oil. An oil bank begins to come through at the producing end of the test cell after about 1.5 pore volumes of steam have been injected. The oil is then produced very rapidly during the final pore volume of injection. Gas is of great benefit in speeding up the rate of oil production in these runs as was the case in the pre-waterflood experiments. After one pore volume of steam had been injected, recoveries with steam-gas were about 40 percent of the oil remaining after waterflooding whereas with steam-only at this point the recovery is only about 4 percent ORAW. At one and one-half pore volumes of steam, the steam-only figure is only 7 percent and steam-gas is at a level of 60 percent - a remarkable acceleration of production. Following water injection the initial rise in the production curve is not as steep for steam-gas injection as was the case for pre-waterflood sandpacks. Run 10 (steam/CO₂) shows superior performance in oil production rate to Run 9 (steam/flue gas) when compared on the basis of total molar injection (Figure 4.6(b)).

In comparing the performance of the steam-gas injection processes it was concluded earlier (Harding et al, 1983) that gas solubility effects were not as important as the mere presence of a non-condensable gas phase. The initially high oil production rates observed in steam-gas injection runs on pre-waterflooded sandpacks may be explained by considering the relatively large volume occupied by the non-condensable gases in comparison with the volume occupied by condensed steam in the

porous medium. In the pre-waterflood runs, only oil is mobile at the initial conditions and much of it is produced in a very short time when compressed, non-condensable gases are injected into the sand packs. On the basis of equivalent amounts of steam and gas injected, the steam/ CO_2 process is superior to steam/flue gas and steam/ N_2 as a result of solubility effects. When production performance is plotted as in Figures 4.5(a) and 4.6(a) the solubility effects of carbon dioxide are marked by the much larger volume of gas injected in the cases where nitrogen was used. Considering the post-waterflood runs, it would appear that oil mobilized by thermal effects is not allowed to bank in the steam-gas injection processes as it does in steam-only flooding but rather it seems that any mobilized oil is swept by the gases to the production end of the test cell. From a mechanistic point of view, this may be a significant advantage which steam-gas injection has over steam-only flooding.

A comparison of the injection of gas slugs prior to steam with simultaneous steam-gas injection is made in Table 4.4. Cases for combinations of steam and carbon dioxide (runs 7 and 17) and steam and flue gas (runs 5, 6 and 12) are presented. Steam-oil and water-oil ratios are higher for the runs where the gas was injected as a slug prior to steam injection. In run 12 the large discrepancy between the SOR and WOR for the total run compared to the steamflood only results from the high oil recovery obtained during the gas slug injection (41.2 percent). The oil recovery from slug CO_2

Table 4.4

**COMPARISON OF SLUG AND SIMULTANEOUS
STEAM-GAS INJECTION PROCESSES**

RUN NUMBER	7	17	6	12
TYPE	SIM. STEAM/CO ₂	SLUG CO ₂ /STEAM	SIM. STEAM/FLUE	SLUG FLUE/STEAM
INITIAL CONDITIONS				
PACK DENSITY, g/cm ³	1.54	1.56	1.53	1.54
PORE VOLUME, cm ³	1562	1525	1479	1595
POROSITY, %	41.5	40.5	39.3	42.3
PERMEABILITY, d	7.48	14.30	9.28	9.61
WATER SATURATION, % PV	18.5	17.4	14.9	21.3
OIL SATURATION, % PV	81.5	82.6	85.1	78.7
RUN CONDITIONS				
STEAM INJECTION RATE, cm ³ /h	1251	1417	1116	1103
STEAM INJECTED, cm ³	3440	3240	3060	3947
CO ₂ INJECTION RATE, dm ³ /h	152.4	152.4	132.5	152.4
CO ₂ INJECTED, dm ³	419.1	381.0	362.5	381.0
N ₂ INJECTION RATE, dm ³ /h	-	-	521.6	572.4
N ₂ INJECTED, dm ³	-	-	1428	1431
CO ₂ /STEAM RATIO, dm ³ /kg	121.8	117.6	118.5	96.5
N ₂ /STEAM RATIO, dm ³ /kg	-	-	466.6	362.5
GAS/STEAM RATIO, dm ³ /kg	121.8	117.6	585.5	459.0
AVERAGE BACK PRESSURE, kPa	3406	3399	3323	3487
PERFORMANCE				
WATER PRODUCED, cm ³	3165	3189	2778	3752
OIL PRODUCED, cm ³	1101.5	1007	1049	1073
OIL RECOVERY, % OOIP	86.5	80.0	83.3	85.5
DEPRESS. OIL, % OOIP	2.2	4.1	-	2.1
STEAM-OIL RATIO, m ³ /m ³	3.12	3.22(4.14)	2.92	3.68(7.10)
WATER-OIL RATIO, m ³ /m ³	2.87	3.17(4.08)	2.65	3.50(6.75)
INJ. GAS-OIL RATIO, mol/m ³	190.4	224.9	238.1	279.7

() Figures in brackets are calculated on the basis of oil produced only in the steamflooding portion of the experiment.

injection in run 17 was only 17.9 percent. No conclusion may be drawn from these data as to the effect on recovery of injecting the gases simultaneously or as a slug since in run 17 the total recovery from slug injection was lower than the simultaneous injection (run 7) but in run 12 the total recovery from slug injection was higher than in the simultaneous injection case (run 6). It takes much less time to recover oil using simultaneous injection and the economics would therefore be improved by this approach.

Figure 4.7 shows the cumulative oil recovery during steamflooding as a percentage of the oil remaining after previous flooding with carbon dioxide, flue gas, or water. The steamfloods following gas injection respond more quickly and steadily than does the one which follows waterflooding. Run 17 steamflood performance is superior to that of run 12 perhaps because of the unusually low recovery obtained from the carbon dioxide slug injection in run 17.

D. The Effect of Flow Rate, Pressure and Carbon Dioxide Presaturation on Simultaneous Steam-Gas Injection Processes

A comparison is made in Table 4.5 of high- and low-rate tests using simultaneous steam/CO₂ and steam/flue gas injection. One run of each type was conducted at about 1200 cm³/h of steam and the others were operated at about one-half of this rate. Gas-steam ratios were essentially the same within the pairs of experiments being compared. The low rate runs required more steam, as reflected in the higher steam-oil

FIGURE 4.7 CUMULATIVE PRODUCTION HISTORIES
FOR STEAMFLOODS FOLLOWING INJECTION OF CARBON DIOXIDE,
FLUE GAS AND WATER.

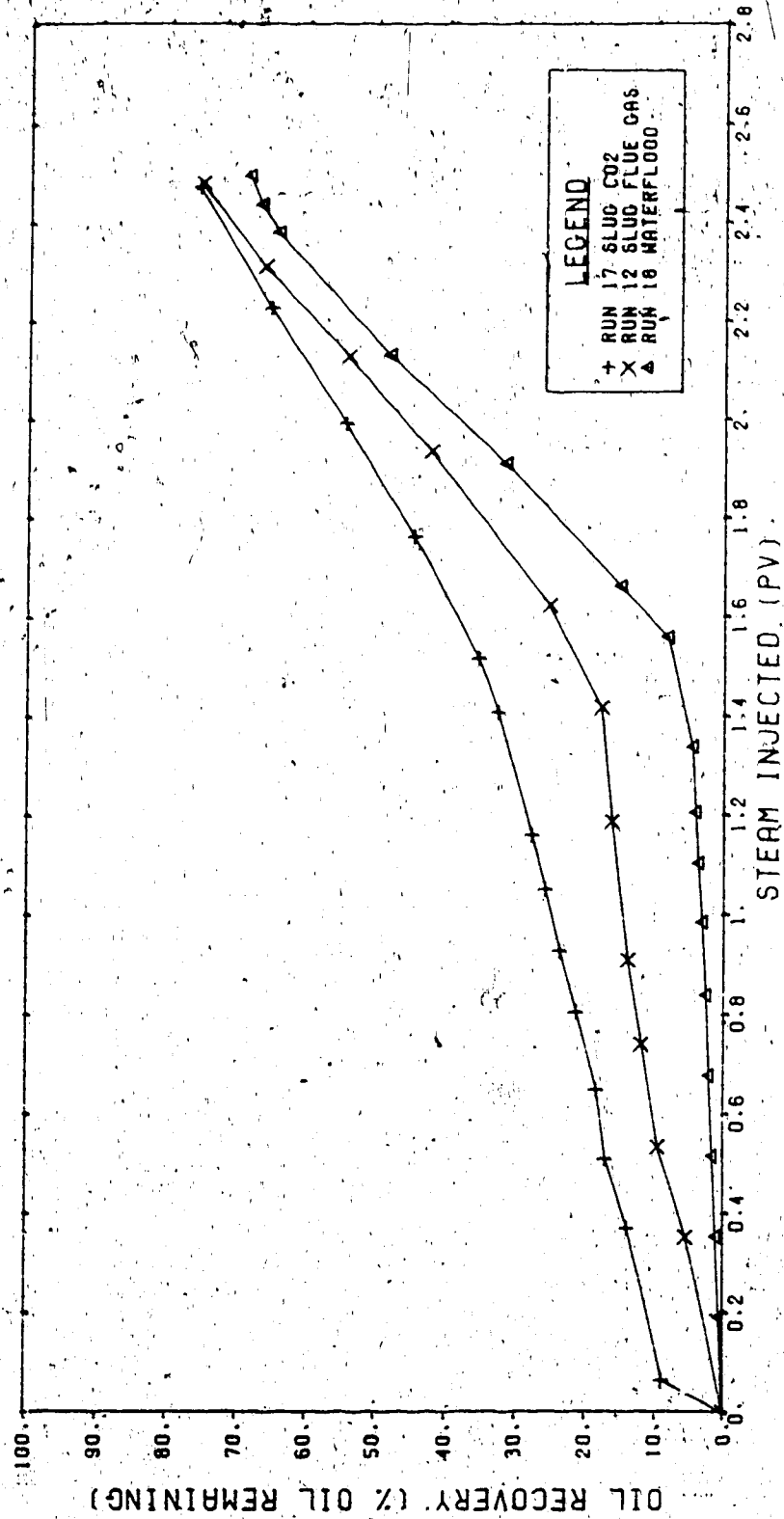


Table 4.5

**EFFECT OF FLOW RATE ON SIMULTANEOUS
STEAM-GAS INJECTION PROCESSES.**

RUN NUMBER	7	13	6	14
TYPE	STEAM/CO ₂ (H)	STEAM/CO ₂ (L)	STEAM/FLUE (H)	STEAM/FLUE (L)
INITIAL CONDITIONS				
PACK DENSITY, g/cm ³	1.54	1.56	1.53	1.56
PORE VOLUME, cm ³	1562	1470	1479	1511
POROSITY, %	41.5	39.0	39.3	40.1
PERMEABILITY, d	7.48	12.8	9.28	14.3
WATER SATURATION, % PV	18.5	15.5	14.9	15.8
OIL SATURATION, % PV	81.5	84.5	85.1	84.2
RUN CONDITIONS				
STEAM INJECTION RATE, cm ³ /h	1251	624	1116	633
STEAM INJECTED, cm ³	3440	4260	3060	4170
CO ₂ INJECTION RATE, dm ³ /h	152.4	77.4	132.5	76.2
CO ₂ INJECTED, dm ³	419.1	529.0	362.5	502.0
N ₂ INJECTION RATE, dm ³ /h	-	-	521.6	288.0
N ₂ INJECTED, dm ³	-	-	1428	1896
GAS/STEAM RATIO, dm ³ /kg	121.8	124.2	585.5	575.0
AVERAGE BACK PRESSURE, kPa	3406	3472	3323	3476
PERFORMANCE				
WATER PRODUCED, cm ³	3165	3980	2778	3903
OIL PRODUCED, cm ³	1101.5	1093	1049.0	1135
OIL RECOVERY, % OOIP	86.5	88.0	83.3	89.2
DEPRESS. OIL, % OOIP	2.2	1.2	-	1.5
STEAM-OIL RATIO, m ³ /m ³	3.12	3.90	2.92	3.67
WATER-OIL RATIO, m ³ /m ³	2.87	3.64	2.65	3.44
INJ. GAS-OIL RATIO, mol/m ³	190.5	235.1	238.1	298.4

and water-oil ratios, to achieve steam temperatures over the entire test cell. This was due to heat losses slowing movement of the steam front. Comparing SOR and WOR for the two low rate runs (13 and 14), superior performance results from the use of steam/flue gas injection as was the case with the high rate runs (6 and 7). The oil recovery is slightly higher for run 14 compared to run 13 which was not the case for the high rate runs. Both runs 13 and 14 show higher recoveries over their respective high rate companion cases.

Figure 4.8 compares cumulative production histories for the two steam/CO₂ runs (7 and 13) on the basis of total molal injection and Figure 4.9 makes a similar comparison for the two steam/flue gas experiments (6 and 14). One might expect that performances of the lower rate cases would be superior to the higher rate cases because of increased time for carbon dioxide to enter solution in the oil. The results show the opposite effect in that at any fixed value of total molal injection, the oil recovered is higher for the high rate cases. Heat losses in the lower rate runs are probably the dominating factors in this behaviour. Any small improvement caused by increased amounts of carbon dioxide in solution are overshadowed by the thermal effects. It is also possible that both the high- and low-flow rates are greater than would be required to allow significant amounts of carbon dioxide to enter solution in the oil. A greater difference in behaviour is evident in the steam/CO₂ than in the steam/flue gas runs perhaps because

FIGURE 4.8 CUMULATIVE PRODUCTION HISTORIES
FOR SIMULTANEOUS STEAM/CO₂ INJECTION
AT TWO FLOW RATES

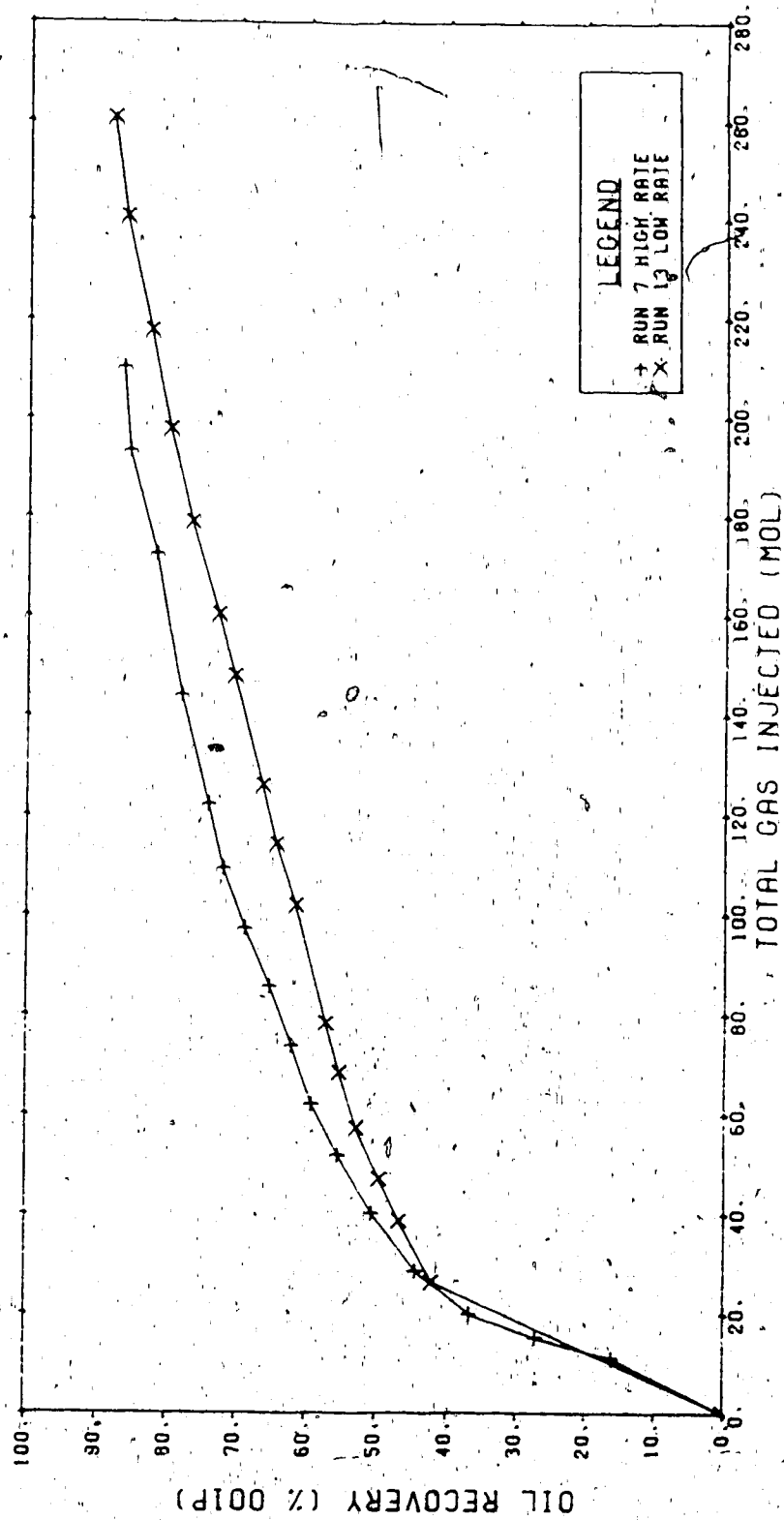
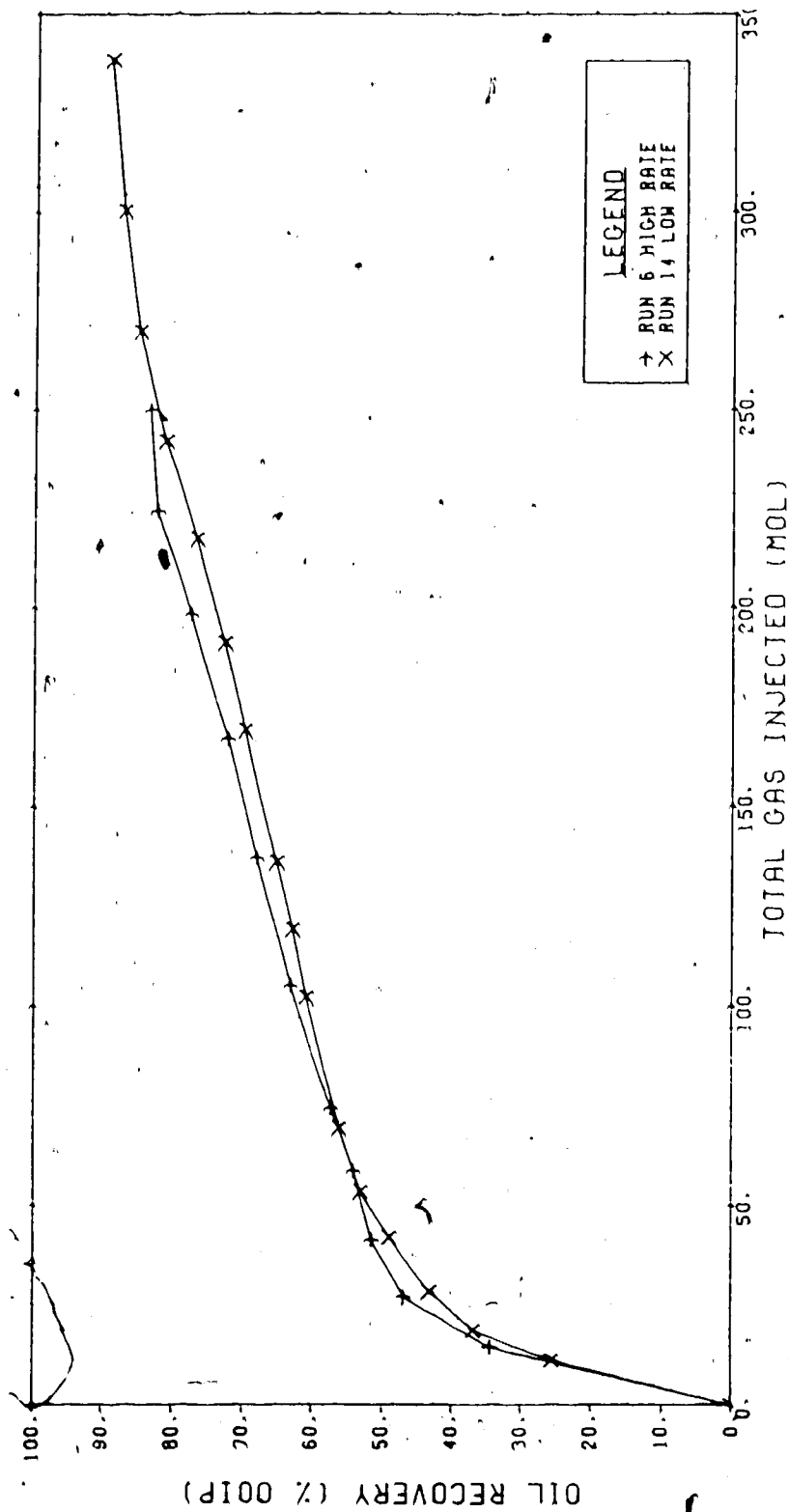


FIGURE 4.9 CUMULATIVE PRODUCTION HISTORIES
FOR SIMULTANEOUS STEAM/FLUE GAS INJECTION
AT TWO FLOW RATES



runs where injected non-condensable gas volumes are substantially higher.

A summary of data for two steam/flue gas runs, one conducted at a back pressure of 3323 kPa (run 6) and one at 6950 kPa (run 15) is contained in Table 4.6. Similar gas-steam ratios and injection rates were used in these experiments. An increase in recovery was obtained in the higher pressure experiment as well as an increase in the steam-oil and water-oil ratios. In Figure 4.10, cumulative production histories for these two runs are plotted. It would be expected that the higher pressure case would have superior performance due to increased gas in solution. However, this effect is overshadowed by the larger gas drive of the lower pressure run caused by the larger volume occupied by the gas at lower pressure.

Table 4.6 also compares two steam/CO₂ runs with the sandpack saturated with carbon dioxide in one case (run 16) and not saturated in the other (run 7). There was only a slight improvement in total recovery in the pre-saturated case occurring late in the experiment (Figure 4.11). The two curves in Figure 4.11 are almost identical except for this small difference at the end of the runs. This indicates that even if the oil becomes saturated with carbon dioxide that it makes little difference to the performance of the experiments.

EFFECT OF PRESSURE AND CO₂ PRESATURATION
ON SIMULTANEOUS STEAM-GAS INJECTION PROCESSES

RUN NUMBER	6	15	7	16
TYPE	STEAM/FLUE LOW PRES.	STEAM/FLUE HIGH PRES.	STEAM/CO ₂ UNSATURATED	STEAM/CO ₂ PRESATURATED
INITIAL CONDITIONS				
PACK DENSITY, g/cm ³	1.53	1.54	1.54	1.57
PORE VOLUME, cm ³	1479	1522	1562	1560
POROSITY, %	39.3	40.4	41.5	41.4
PERMEABILITY, d	9.28	15.90	7.48	13.10
WATER SATURATION, % PV	14.9	15.8	18.5	20.9
OIL SATURATION, % PV	85.1	84.2	81.5	79.1
RUN CONDITIONS				
STEAM INJECTION RATE, cm ³ /h	1116	1237	1251	1550
STEAM INJECTED, cm ³	3060	3710	3440	3360
CO ₂ INJECTION RATE, dm ³ /h	132.5	153.0	152.4	152.4
CO ₂ INJECTED, dm ³	362.5	459.0	419.1	331.0
N ₂ INJECTION RATE, dm ³ /h	521.6	576.0	-	-
N ₂ INJECTED, dm ³	1428	1728	-	-
GAS/STEAM RATIO, dm ³ /kg	585.5	589.5	121.8	98.4
AVERAGE BACK PRESSURE, kPa	3323	6950	3406	3585
PERFORMANCE				
WATER PRODUCED, cm ³	2778	3424	3165	3201
OIL PRODUCED, cm ³	1049	1111	1101.5	1054
OIL RECOVERY, % OOIP	83.3	86.6	86.5	89.7
DEPRESS. OIL, % OOIP	-	1.9	2.2	1.4
STEAM-OIL RATIO, m ³ /m ³	2.92	3.34	3.12	3.19
WATER-OIL RATIO, m ³ /m ³	2.65	3.08	2.87	3.04
INJ. GAS-OIL RATIO, mol/m ³	238.1	273.4	190.4	191.0

FIGURE 4.10 CUMULATIVE PRODUCTION HISTORIES
FOR SIMULTANEOUS STEAM/FLUE GAS INJECTION
AT TWO PRESSURES

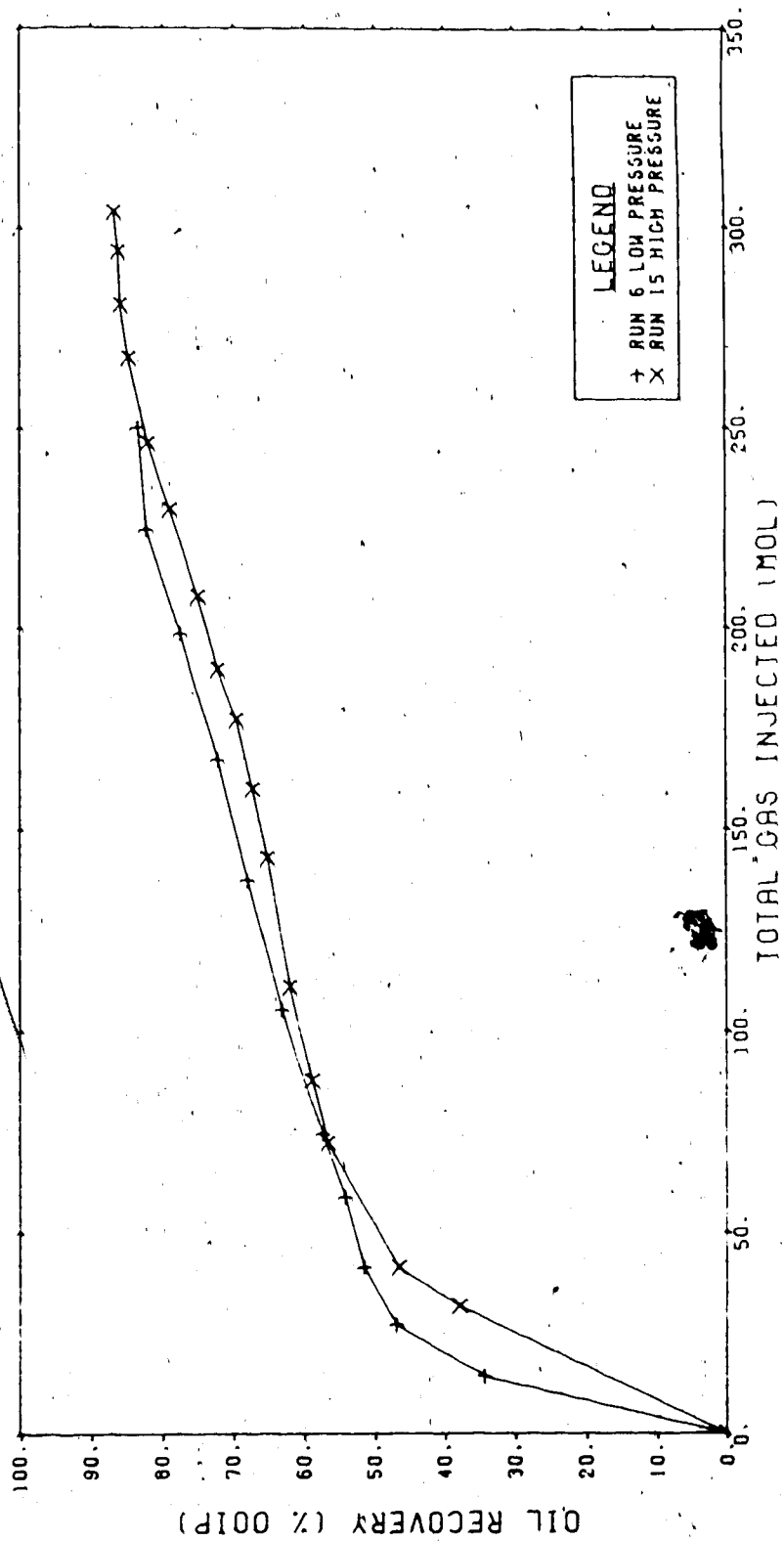
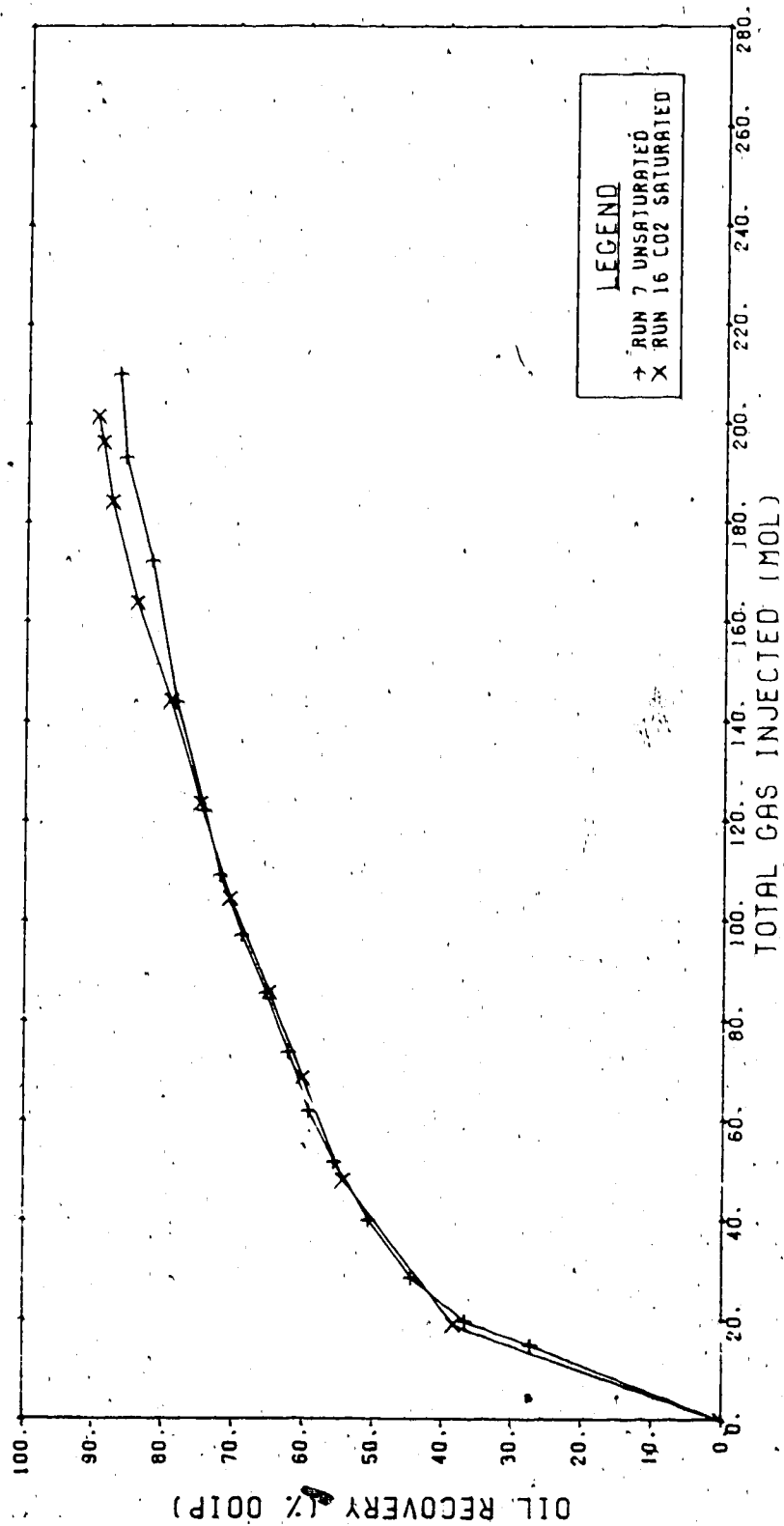


FIGURE 4.11 CUMULATIVE PRODUCTION HISTORIES
FOR SIMULTANEOUS STEAM/CO2 GAS INJECTION



considering the effect of flow rate, pressure and carbon dioxide pre-saturation on the process, one may conclude from these data that solubility effects in this system are of less importance than gas drive and thermal effects.

V. MATHEMATICAL MODEL FORMULATION

A. General Features

A mathematical model of the steamflood process was developed which allowed injection of any or all of the system components along with steam. The purpose of the mathematical model development and application work was to gain further insight into the nature of the laboratory tests and to assist in explaining the phenomena observed in the experiments. The simulator modelled the flow of three phases (aqueous, oleic and vapour) and was designed for the following five components: (1) water, (2) light oil, (3) heavy oil, (4) carbon dioxide and (5) nitrogen.

Gravity and capillary pressure phenomena were included and heat transfer in the porous medium was modelled as a combination of conduction and convection. Heat losses to confining materials were by conduction only.

Interphase mass transfer was governed by pressure and temperature dependent equilibrium ratios (K-values). The oil and water components were considered to be mutually insoluble. Carbon dioxide and nitrogen were allowed to exist in all phases and the vapour phase contained all components. Table 5.1 illustrates the distribution of components in the three phases. Volatility of oil components was included to properly model steamflood behaviour since steam distillation may be an important recovery mechanism in steamflooding [(Coats, 1974), (Coats, 1976), (Weinstein et al, 1977)]:

Table 5.1.

DISTRIBUTION OF COMPONENTS IN FLUID PHASES

<u>NO.</u>	<u>COMPONENT</u>	<u>PHASES</u>		
		<u>AQUEOUS</u>	<u>OLEIC</u>	<u>VAPOUR</u>
1	Water	x_{1a}	-	y_1
2	Light Oil	-	x_{20}	y_2
3	Heavy Oil	-	x_{30}	y_3
4	Carbon Dioxide	x_{4a}	x_{40}	y_4
5	Nitrogen	x_{5a}	x_{50}	y_5

Differential equations describing the simultaneous flow of heat and the multiphase fluid flow were derived from the laws of energy and mass conservation. These equations were then discretized using finite difference techniques. The generalized Newton-Raphson iterative method for a system of nonlinear partial differential equations was employed in obtaining a solution to the problem. Direct techniques were used at each iteration. The model was fully implicit in that all parameters dependent upon the unknown variables were updated at each iteration.

The model is two-dimensional, capable of being run in one or two dimensions. Both areal and vertical cross-sectional simulations are possible. One-dimensional operation allowed examination of the laboratory process and the two-dimensional mode could be used to examine the application of steam/gas injection in field scale simulations. Both regular and irregular grid block sizes may be modelled. The model employs a block-centered grid system with a five-point discretization scheme. Automatic time step control is featured.

Fluid properties were described using correlations where possible in order to control the size of the program (Vinsome, 1974). In some cases options exist for the method of calculation of a physical property and for certain parameters a choice may be made between use of a correlation and a tabulation of data. The functional dependence of physical properties is illustrated in Table 5.2.

Table 5.2

FUNCTIONAL DEPENDENCE OF PHYSICAL PROPERTIES

<u>VARIABLE</u>	<u>DEFINITION</u>	<u>FUNCTIONAL DEPENDENCE</u>
ϕ	porosity	P
λ_f	formation thermal conductivity	T, S_a , ϕ
μ_a	aqueous phase viscosity	T, x_{4a}
μ_o	oleic phase viscosity	T, x_{20} , x_{30} , x_{40} , x_{50}
μ_v	vapour phase viscosity	P, T, y_1 , y_2 , y_3 , y_4 , y_5
ρ_a	aqueous phase density	P, T, x_{1a} , x_{4a} , x_{5a}
ρ_o	oleic phase density	P, T, x_{20} , x_{30} , x_{40} , x_{50}
ρ_v	vapour phase density	P, T, y_1 , y_2 , y_3 , y_4 , y_5
h_a	aqueous phase enthalpy	T, x_{1a} , x_{4a} , x_{5a}
h_o	oleic phase enthalpy	T, x_{20} , x_{30} , x_{40} , x_{50}
h_v	vapour phase enthalpy	T, y_1 , y_2 , y_3 , y_4 , y_5
k_{ra}	aqueous phase rel. perm.	T, S_a
k_{ro}	oleic phase rel. prm.	T, S_a , S_v
k_{rv}	vapour phase rel. perm.	T, S_v
M_a	aqueous phase mol. weight	x_{1a} , x_{4a} , x_{5a}
M_o	oleic phase mol. weight	x_{20} , x_{30} , x_{40} , x_{50}
M_v	vapour phase mol. weight	y_1 , y_2 , y_3 , y_4 , y_5
U_a	aqueous phase internal energy	T, x_{1a} , x_{4a} , x_{5a}
U_o	oleic phase internal energy	T, x_{20} , x_{30} , x_{40} , x_{50}
U_v	vapour phase internal energy	T, y_1 , y_2 , y_3 , y_4 , y_5
U_r	rock internal energy	T
K	equilibrium ratios	P, T

The following additional assumptions were made in formulating the model:

1. Thermal equilibrium is reached instantaneously.
2. The contribution of kinetic energy and the work done by viscous forces is negligible.
3. Thermal cracking of hydrocarbons is ignored.
4. Mass transfer due to molecular and thermal diffusion is negligible.

8. Mathematical Formulation

Appendix D contains derivations of the partial differential equations which describe mass and energy transport for the system of interest in this study. The equations which comprise the present model are summarized below and include a mass balance for each component, the energy balance, mole fraction and saturation constraints, capillary pressure relations and phase equilibrium relations.

1. Mass Conservation

Component 1 - Water

$$\nabla \left(x_{1a} \frac{A k k_{ra} \rho_a}{M_a \mu_a} \nabla \phi_a + x_{1v} \frac{A k k_{rv} \rho_v}{M_v \mu_v} \nabla \phi_v \right) + Q_1^* = -V_b \frac{\partial}{\partial t} \left[\phi \left(\frac{x_{1a} \rho_a S_a}{M_a} + \frac{x_{1v} \rho_v S_v}{M_v} \right) \right] \quad (5.1)$$

Components 2 and 3 - Light Oil and Heavy Oil

$$\begin{aligned} & \nabla \left(x_{i0} \frac{A k k_{ro} \rho_o}{M_o \mu_o} \nabla \phi_o + x_{iv} \frac{A k k_{rv} \rho_v}{M_v \mu_v} \nabla \phi_v \right) \Delta + Q_i^* \\ & = V_b \frac{\partial}{\partial t} \left[\phi \left(\frac{x_{i0} \rho_o S_o}{M_o} + \frac{x_{iv} \rho_v S_v}{M_v} \right) \right] \quad i = 2, 3 \quad (5.2) \end{aligned}$$

Components 4 and 5 - Carbon Dioxide and Nitrogen

$$\begin{aligned} & \nabla \left(x_{ia} \frac{A k k_{ra} \rho_a}{M_a \mu_a} \nabla \phi_a + x_{io} \frac{A k k_{ro} \rho_o}{M_o \mu_o} \nabla \phi_o + \right. \\ & \quad \left. x_{iv} \frac{A k k_{rv} \rho_v}{M_v \mu_v} \nabla \phi_v \right) \Delta + Q_i^* \\ & = V_b \frac{\partial}{\partial t} \left[\phi \left(\frac{x_{ia} \rho_a S_a}{M_a} + \frac{x_{io} \rho_o S_o}{M_o} + \frac{x_{iv} \rho_v S_v}{M_v} \right) \right] \\ & \quad i = 4, 5 \quad (5.3) \end{aligned}$$

$$\begin{aligned} \text{where } \nabla \phi_p &= \nabla p_p - \gamma_p \nabla Z \quad \nabla p = a, o, v \\ \text{and } \gamma_p &= \rho_p g \end{aligned}$$

2. Energy Conservation

$$\begin{aligned} & \nabla (A \lambda \nabla T) \cdot \Delta + \nabla \left(\frac{A k k_{ra} \rho_a \eta_a}{M_a \mu_a} \nabla \phi_a + \frac{A k k_{ro} \rho_o \eta_o}{M_o \mu_o} \nabla \phi_o \right. \\ & \quad \left. + \frac{A k k_{rv} \rho_v \eta_v}{M_v \mu_v} \nabla \phi_v \right) \cdot \Delta + q_S + q_L + (\dot{Q}_a \eta_a + \dot{Q}_o \eta_o + \dot{Q}_v \eta_v) \\ & = V_b \frac{\partial}{\partial t} \left[(1 - \phi) \bar{\rho}_r U_r + \phi \left(\frac{S_a \rho_a U_a}{M_a} + \frac{S_o \rho_o U_o}{M_o} + \frac{S_v \rho_v U_v}{M_v} \right) \right] \\ & \quad (5.4) \end{aligned}$$

3. Phase Saturation Constraint

$$S_a + S_o + S_v = 1.0 \quad (5.5)$$

4. Mole Fraction Constraints

$$\begin{aligned} \sum_i x_{ia} &= 1.0 & i &= 1, 4, 5 & \text{aqueous phase} \\ \sum_i x_{io} &= 1.0 & i &= 2, 3, 4, 5 & \text{hydrocarbon phase} \\ \sum_i x_{iv} &= 1.0 & i &= 1, 2, 3, 4, 5 & \text{vapour phase} \end{aligned} \quad (5.6)$$

5. Capillary Pressures

$$P_{cow} = P_o - P_a \quad (5.7)$$

$$P_{cgo} = P_v - P_o \quad (5.8)$$

6. Distribution Coefficients

$$\begin{aligned} \text{Water} & \quad x_{1v} = K_{1a} x_{1a} \\ \text{Heavy Oil} & \quad x_{2v} = K_{2o} x_{2o} \\ \text{Light Oil} & \quad x_{3v} = K_{3o} x_{3o} \\ \text{Carbon Dioxide} & \quad x_{4v} = K_{4a} x_{4a} \\ & \quad x_{4v} = K_{4o} x_{4o} \\ \text{Nitrogen} & \quad x_{5v} = K_{5a} x_{5a} \\ & \quad x_{5v} = K_{5o} x_{5o} \end{aligned} \quad (5.9)$$

C. Physical Properties of Reservoir Fluids and Rock

1. Rock Properties

Porosity was calculated as in most previous thermal models:

$$\phi = \phi_{in} [1 + c_r (P - P_{in})] \quad (5.10)$$

where c_r = rock compressibility = constant

ϕ_{in} = porosity at initial pressure P_{in}

Absolute permeability, and rock density were assumed to be constant.

Rock internal energy was calculated as in Crookston et al (1979) and Abou-Kassem (1981) where:

$$U_r = C_{pr} (T - T_{in}) \quad (5.11)$$

Rock heat capacity (C_{pr}) was assumed to be constant.

Formation thermal conductivity was calculated as in Crookston et al (1979) where for the permeable strata:

$$\lambda_{sat.,T} = 26.31 [\exp (0.6\rho + 0.6 S_a)] T^{-0.55} \quad (5.12)$$

and $\lambda_{sat.,T}$ = thermal conductivity of partially water-saturated rock in $\frac{\text{millicalories}}{\text{s} \cdot \text{cm} \cdot \text{K}}$

T = temp. in K

$\rho = \rho_r (1 - \phi)$

ρ_r = dry rock density, g/cm³

S_a = water sat. (fraction)

This technique for calculating thermal conductivity was developed by Tikhomirov (1968) and was recommended by Farouq Ali (1970).

2. Fluid Properties

a) Viscosity

Water viscosity was calculated using the method developed by Hawkins et al (1940) where:

$$\mu_w(T) = \frac{2.185}{0.04012 T + 0.00000515 T^2 - 1} \quad (5.13)$$

T in °F

μ_w in cp

correction for the viscosity change as a result of carbon dioxide in solution was then applied. Data for the effect of CO₂ on water viscosity was obtained from Dodds et al (1956) and Tumasyan et al (1969)

$$\mu_a = \mu_w (1 + A \cdot x_{4a} + B \cdot x_{4a}^2) \quad (5.14)$$

where A, B = constants

x_{4a} = aqueous phase concentration of CO₂

Oil phase viscosity was calculated as in Crookston et al (1979), Coats (Dec. 1980) and Grabowski et al (1979) using the Arrhenius equation:

$$\mu = \frac{N_c}{\prod_{i=1}^N \mu_i^{x_i}} \quad (5.15)$$

Oil component viscosities were calculated from expressions of the following type:

$$\mu_i = A \exp (B/T) \quad (5.16)$$

and steam, CO₂ and N₂ pure component viscosities were calculated as:

$$\mu_i = AT^B \quad (5.17)$$

Vapour phase pure component viscosities were all calculated as functions of temperature using Equation 5.17. An option was available for calculating steam

recommended by Farouq Ali (1970):

$$\mu_{mp} = AT - B \quad T < 800 \text{ K} \quad (5.18)$$

$$\mu_{mp} = \frac{C T^{1.5}}{D - T + ET^2} \quad T > 800 \text{ K} \quad (5.19)$$

where $A = 0.361$

$B = 10.2$

$C = 39.37$

$D = 3315$

$E = 0.001158$

T in K

μ_{mp} in micropoise at 1 atmosphere.

The viscosity of the vapour phase mixture was then calculated from the Hering and Zipperer (1936) equation:

$$\mu_v = \frac{\sum \mu_i y_i \sqrt{M_i}}{\sum y_i \sqrt{M_i}} \quad (5.20)$$

where μ_i = pure component viscosity

M_i = pure component molecular weight

y_i = gas phase mole fraction of component i

A pressure correction was then applied using the method of Dean and Stiel (1965):

$$(\mu_m - \mu_{mf}) C_m = 0.000108 \cdot X \cdot (e^{1.439 \rho_{rm}} - e^{-1.111 \rho_{rm}^{1.858}}) \quad (5.21)$$

μ_{m1} = mixture viscosity at 1 atm. from
Herning-Zipperer equation

ρ_{rm} = psuedo-reduced mixture density

$$= \rho_m / \rho_{cm}$$

$$C_m = (T_c)_m^{0.16667} (M)_m^{-0.5} (P_c)_m^{-0.6667}$$

$$\rho_{cm} = (P_c)_m R^{-1} (T_c)_m^{-1} (Z_c)_m^{-1}$$

$$Z_{cm} = \sum_{i=1}^{N_c} y_i Z_{ci}$$

$$P_{cm} = \sum_{i=1}^{N_c} y_i P_{ci}$$

$$T_{cm} = \sum_{i=1}^{N_c} y_i T_{ci}$$

$$M_m = \sum_{i=1}^{N_c} y_i M_i$$

The above procedure was used by Crookston et al (1979).

b) Density

Aqueous phase density may be calculated in the numerical model in one of two ways. The first method is essentially that used by Ferrer and Farouq Ali (1976) in which Amagat's law of partial volumes was assumed. That is,

$$v_a = \sum_{i=1}^{N_c} x_{ia} v_{ia} \quad (5.22)$$

$$C_{1a} = \frac{P_{1a}}{P} \quad (1 - C_{1a}) = \frac{P_{1n}}{P} \quad (5.22)$$

for liquid phase pure water. The other two components which may exist in the aqueous phase are carbon dioxide and nitrogen and the partial volumes of these substances are obtained from the vapour phase density calculations. The second method for aqueous phase density determination employs the Peng-Robinson equation of state (Peng and Robinson, 1976) which may be written as:

$$Z^3 + (B - 1)Z^2 + (A - 3B^2 - 2B)Z - (AB - B^2 - B^3) = 0 \quad (5.23)$$

$$\text{where } Z = \frac{PV}{RT}$$

$$A = \frac{aP}{R^2T^2}$$

$$B = \frac{bP}{RT}$$

For mixtures, the parameters a and b are expressed as:

$$a = \sum_i \sum_j x_i x_j (1 - \sigma_{ij}) a_i^{1/2} a_j^{1/2} \quad (5.24)$$

$$b = \sum_i x_i b_i \quad (5.25)$$

$$\text{where } a_i = a_{ci} \alpha_i$$

$$a_{ci} = 0.45724 R^2 T_{ci}^2 / P_{ci}$$

$$\alpha_i^{1/2} = 1 + \kappa (1 - T_{ri}^{1/2})$$

$$\kappa = 0.37464 + 1.54226 \omega_i - 0.26992 \omega_i^2$$

$$b_i = 0.07780 R T_{ci} / P_{ci}$$

yield three real roots, the largest of which is taken as the compressibility factor of the vapour and the smallest of which is taken as the compressibility factor for the liquid.

The cubic equation in one unknown has the form

$$x^3 + bx^2 + cx + d = 0 \quad (5.26)$$

If the coefficients are real numbers, then at least one of the roots must be real. The equation may be reduced by the substitution

$$x = y - \frac{b}{3}$$

to the form

$$y^3 + py + q = 0$$

$$\text{where } p = \frac{1}{3} (3c - b^2)$$

$$q = \frac{1}{27} (27d - 9bc + 2b^3)$$

The equation has the solutions

$$y_1 = A + B$$

$$y_2 = -\frac{1}{2}(A + B) + i\sqrt{3}/2 (A - B)$$

$$y_3 = -\frac{1}{2}(A + B) - i\sqrt{3}/2 (A - B)$$

$$\text{and } A = \sqrt[3]{-q/2 + \sqrt{R}}$$

$$B = \sqrt[3]{-q/2 - \sqrt{R}}$$

$$R = (p/3)^3 + (q/2)^2$$

if $R > 0$, there is one real root and two conjugate complex roots.

if $R = 0$, there are three real roots of which at least two are equal.

if $R < 0$, the above formulae are impractical - in this case the roots are given by

$$X_K = \pm \sqrt[3]{P/3} \cos [(\phi/3) + 120 K], K = 0, 1, 2$$

$$\text{where } \phi = \cos^{-1} \frac{q^2/4}{-p^3/27}$$

if $q > 0$, the upper sign applies

if $q < 0$, the lower sign applies.

The compressibility factor for the mixture at the temperature and pressure of interest is obtained from the analytical solution of the cubic equation.

Oleic phase density is obtained in a similar manner to that described above for the aqueous phase.

Compressibility factor for the vapour phase may be obtained in one of three ways. The first and most simple is to use the Papay equation, the accuracy of which has been compared to other methods by Takacs (1976). The Papay equation takes the form:

$$Z = 1 - \frac{3.52 P_r}{10^{0.9813} T_r} + \frac{0.274 P_r^2}{10^{0.8157} T_r} \quad (5.27)$$

The second option is to use the method of Hall and Yarborough (1974) as recommended by Dake (1978). In this technique, the compressibility factor is obtained

from the Starling-Carnahan equation of state which is solved using the Newton-Raphson technique. If this second method is used, the Papay equation gives the initial guess for the Newton-Raphson procedure. The Hall-Yarborough equations are:

$$Z = \frac{0.06125 P_{pr} t e^{-1.2 (1-t)^2}}{y} \quad (5.28)$$

where P_{pr} = the pseudo-reduced pressure

t = the reciprocal pseudo-reduced temperature $\frac{T_{pc}}{T}$

y = "reduced" density which can be obtained as the solution of the equation:

$$\begin{aligned} & - 0.06125 P_{pr} t e^{-1.2 (1-t)^2} + \frac{y + y^2 + y^3 - y^4}{(1 - y)^3} \\ & - (14.76t - 9.76t^2 + 4.58t^3) y^2 \\ & + (90.7t - 242.2t^2 + 42.4t^3) y^{(2.18 + 2.82t)} = 0 \end{aligned}$$

This latter non-linear equation is solved for y using the Newton-Raphson procedure which is outlined in Dake (1978), pp. 19-20.

The third alternative for vapour phase density calculation is to use the Peng-Robinson equation of state. In using the solution of the cubic equation for Z , which is the Peng-Robinson equation, there is one real root and two conjugate complex roots when only a single phase exists. In a region containing two phases,

three real roots exist, the largest positive root being the vapour phase Z-factor and the smallest positive root being the liquid phase Z-factor.

c) Enthalpy and Internal Energy

Liquid and vapour pure component water enthalpies are calculated as

$$h_{1a} = 45.006 (T - 77) \quad (5.29)$$

$$\text{and } h_{1v} = h_{1a} + L_{v1}$$

$$\text{where } h_{1a} = 45.006 (T_{\text{sat}} - 77)$$

$$L_{v1} = 3792.42 (705.4 - T_{\text{sat}})^{0.38}$$

$$\text{and } T_{\text{sat}} = 116.0 p^{0.224014}$$

$$(T \text{ in } ^\circ\text{F and } p \text{ in psja})$$

Light oil and heavy oil component liquid and vapour enthalpies are calculated as

$$h_{1v} = h_{1o} + L_{vo}$$

$$h_{1o} = \int_{T_{\text{ref}}}^T C_{pi} dT \quad (5.30)$$

$$\text{where } C_{pi} = a_i + b_i T + c_i T^2$$

$$\text{and } L_{vi} = L_{v \text{ ref}} \left(\frac{1 - T/T_c}{1 - T_b/T_c} \right)^{0.38}$$

Carbon dioxide and nitrogen component enthalpies are calculated as

$$h_{iL} = h_{iv} - L_{vi} \quad (5.31)$$

$$h_{iv} = \int_{T_{ref}}^T C_{pi} dT$$

$$\text{where for CO}_2 \quad C_{pi} = a + b_1 T - \frac{C_1}{T^2}$$

$$\text{and for N}_2 \quad C_{pi} = a + b_1 T + C_1 T^2$$

$$\text{and } L_{vi} = L_{v,ref} \left(\frac{1 - T/T_c}{1 - T_b/T_c} \right)^{0.38}$$

Phase enthalpies are then calculated as

$$h_p = \sum_{i=1}^{N_c} x_{ip} h_{ip} \quad (5.32)$$

The internal energy of the liquid phases is taken to be equivalent to the enthalpy. Vapour phase internal energy is computed as in Rubin (1979):

$$U_v = h_v - R(T - T_0) \quad (5.33)$$

d) Phase Behaviour

Temperature and pressure dependent K-values may be obtained either from tabulated data or from correlations of the following type used by Crookston et al (1979) and Coats (1980).

$$K_{lv} = \frac{A}{P} \left(\frac{T - B}{C} \right)^D \text{ for water} \quad (5.34)$$

$$K_{ij} = \frac{A}{P} \exp \left(B - \frac{C}{T - D} \right)^E + F \text{ for oils, CO}_2, \text{ N}_2$$

A table look-up program conducts a binary search in a two-dimensional table and then linearly interpolates to obtain a value. The procedure is based on the subroutine TABBIN given in Aziz and Settari (1979), p. 448.

Phase appearance and disappearance was handled using the one-problem formulation method of Crookston et al (1979) which was extended by Abou-Kassem (1981). The latter author compared in one-dimension the one-problem formulation with the more rigorous method of Coats (1978) involving variable substitution and found negligible differences in results. Following the approach of Abou-Kassem (1981) we write:

$$K_i = \begin{cases} \hat{K}_i x_a x_v & i = 1 \\ \hat{K}_i x_0 x_v & i = 2, 3, 4, 5 \end{cases} \quad (5.35)$$

$$\begin{aligned} \text{where } x_0 &= \frac{S_0}{S_0 + E_0} \\ x_a &= \frac{S_a}{S_a + E_a} \\ x_v &= \frac{S_v + E_v}{S_v + 10^{-30}} \end{aligned}$$

The E_a , E_0 , E_v are small numbers of the order of 10^{-5} and the \hat{K}_i 's are temperature and pressure dependent equilibrium ratios. The effect of adjusting the K-values in this manner is to create a situation in which individual phases are not allowed to disappear.

completely but a small saturation of each phase is maintained at all conditions.

3. Fluid-Rock Properties

a) Relative Permeability

Relative permeabilities are evaluated using either the analytical method of Coats (Dec. 1980) or tabulated two-phase data. The correlations of Coats (Dec. 1980) include temperature dependence and take the following form:

$$k_{rw} = k_{rwro}(T) \left[\frac{S_w - S_{wir}(T)}{1 - S_{orw}(T) - S_{wir}(T)} \right]^{n_w} \quad (5.37)$$

$$k_{row} = k_{roiw}(T) \left[\frac{1 - S_{orw}(T) - S_w}{1 - S_{orw}(T) - S_{wir}(T)} \right]^{n_{ow}} \quad (5.38)$$

$$k_{rog} = k_{roiw}(T) \left[\frac{1 - S_{wir}(T) - S_{org}(T) - S_g}{1 - S_{wir}(T) - S_{org}(T)} \right]^{n_{og}} \quad (5.39)$$

$$k_{rg} = k_{rgro} \left[\frac{S_g - S_{gc}}{1 - S_{wir} - S_{org} - S_{gc}} \right]^{n_g} \quad (5.40)$$

where $k_{rwro}(T)$ = relative permeability to water at residual oil saturation

$k_{roiw}(T)$ = relative permeability to oil at irreducible water saturation

$S_{wir}(T)$ = irreducible water saturation

$S_{orw}(T)$ = residual oil saturation to water

$S_{org}(T)$ = residual oil saturation to gas

S_{gc} = critical gas saturation

n_w, n_{ow}, n_{og}, n_g = exponents on saturations.

Temperature dependent parameters are linear functions of

temperature:

$$X = A + B(T - T_1) \quad (5.41)$$

where A, B are constants.

Relative permeability to oil is calculated using the second method of Stone (1973) where:

$$k_{ro} = k_{roiw}(T) \frac{k_{row}}{k_{roiw}(T)} + k_{rw} \frac{k_{rog}}{k_{roiw}(T)} - k_{rg} \\ - (k_{rw} + k_{rg}) \quad (5.42)$$

When two-phase tabulated data are used, the tables are interpolated using splines and the oil phase relative permeability is also calculated using the above method of Stone (1973).

b) Capillary Pressure

Capillary pressures are calculated using the analytical expressions of Coats (Dec. 1980) or from tabulated two-phase data. The analytical expressions of Coats (Dec. 1980) are:

$$P_{cow} = \frac{[C_1 + C_2 (1 - S_w) + C_3 (1 - S_w)^3]}{[1 - C_4 (T - T_1)]} \times \quad (5.43)$$

$$P_{cgo} = \frac{[C_5 + C_6 S_g + C_7 S_g^3]}{[1 - C_8 (T - T_1)]} \times \quad (5.44)$$

where C_1 to C_8 are constants.

The temperature dependence here assumes that interfacial tension is a linear function of temperature. As in the case of relative permeability tabulated data are fitted to splines for purposes of interpolation.

D. Heat Losses

In the present study, heat losses from the 1-D laboratory apparatus were calculated in the following manner [(Gottfried (1965), Abdalla and Coats (1971))]:

$$q_L = U_{av} A \Delta T \quad (5.46)$$

where q_L = heat loss

U_{av} = overall heat transfer coefficient

A = area = $2\pi r \Delta x$

$\Delta T = T - T_a$

T = grid block temperature

T_a = ambient temperature

r = internal radius of mortar lining

Δx = grid block length

As in Abdalla and Coats (1971), different overall heat transfer coefficients were used for the vapour and liquid phases.

$$\text{i.e. } U_{av} = U_v S_v + U_L (1 - S_v) \quad (5.47)$$

Heat losses to the over- and under-burden in reservoir modelling was accomplished by the same method as used by Abou-Kassem (1981). This method involves analytical solution of the transient heat conduction problem in one-dimension and use of

the principle of superposition. The following equations result:

$$q_L^{n+1} = bA \sum_{m=1}^n \frac{T_m - T_{m-1}}{\sqrt{t_{n+1} - t_{m-1}}} + \frac{T_{n+1} - T_n}{\sqrt{t_{n+1} - t_n}} \quad (5.48)$$

$$\text{where } q_L^1 = bA_1 \frac{T_1 - T_0}{\sqrt{t_1 - t_0}}$$

$$\text{and } b = \sqrt{\frac{\lambda_r^* \rho_r^* C_{pr}^*}{\pi}}, \quad T_0 = T_i$$

In order to model the effect on the laboratory experiments of heat losses from the injected steam to the inlet end flange, a special heat source/sink term was placed in the energy balance equation. The heat source/sink term was obtained by considering the metal flanges to be a lumped heat-capacity system (Holman, 1981); that is, the system may be considered to be reasonably uniform in temperature as would occur where resistance to heat conduction is small compared with the convection resistance at the surface. The major temperature gradient thus occurs in the fluid layer at the surface of the solid. Convection heat loss from the steam is evidenced by an increase in the internal energy of the flanges.

$$q = hA(T_S - T) = C\rho V \frac{dT}{dt} \quad (5.49)$$

where h = convective heat transfer coefficient

A = heat transfer area

T_S = steam temperature

T = flange temperature

$t = \text{time}$

If $T = T_0$ at $t = t_0 = 0$, the equation may be solved by separation of variables for the flange temperature as a function of time.

$$T = T_S - (T_S - T_0) \exp \frac{hA}{C\rho V} t \quad (5.50)$$

The heat loss is then calculated from

$$q = hA(T_S - T) \quad (5.51)$$

With this model, heat losses to the flanges are large at early times and diminish as time progresses and the flanges approach steam temperature.

E. Injection and Production Rates

The model accounts for injection of any combination of the components at constant rates. An injection or production well may exist at any grid block.

Production occurs against a specified back pressure.

Molar mass production rates of the components are given by

(Abou-Kassem, 1981, p. 68):

$$q_i^{n+1} = \frac{x_{1a} \rho_a q_a}{M_a}^{n+1} + \frac{x_{1o} \rho_o q_o}{M_o}^{n+1} + \frac{y_1 \rho_v q_v}{M_v}^{n+1} \quad (5.52)$$

$$q_H = (n_a \rho_a q_a) + (n_o \rho_o q_o) + (n_v \rho_v q_v) \quad (5.53)$$

where the q_a , q_o , q_v are volumetric flow rates. The volumetric rates of the individual phases are:

$$q_a^{n+1} = PI (P_a^{n+1} - P_{wf}) \frac{k_{ra}^{n+1}}{\mu_a} \quad (5.54)$$

$$q_o^{n+1} = PI (P_o^{n+1} - P_{wf}) \frac{k_{ro}^{n+1}}{\mu_o} \quad (5.55)$$

$$q_v^{n+1} = PI (P_v^{n+1} - P_{wf}) \frac{k_{rv}^{n+1}}{\mu_v} \quad (5.56)$$

$$\text{where } PI = \frac{2\pi kh}{\ln \frac{r_e}{r_w} - 1/2 + S}$$

In two-dimensional cross-sectional reservoir simulations production occurs in only one block at the well location.

F. Solution Method

1. Newton-Raphson Technique

Rubin (1979) has described the generalized Newton-Raphson method for solution of a system of non-linear equations and a summary appears here.

Let F be a real function of a single variable Z in the form:

$$F(Z) = 0 \quad (5.57)$$

expansion about the point Z^0 :

$$F(Z) = F(Z^0) + \frac{dF}{dZ} (Z - Z^0) \quad (5.58)$$

The equation may also be written in the form:

$$F(Z^{k+1}) = F(Z^k) + \frac{dF(Z^k)}{dZ} (Z^{k+1} - Z^k) \quad (5.59)$$

where k is an iteration counter. Since at convergence $F(Z^{k+1}) = 0$, we can write:

$$(Z^{k+1} - Z^k) \frac{dF(Z^k)}{dZ} = -F(Z^k) \quad (5.60)$$

$$\text{and } Z^{k+1} = Z^k - F(Z^k) \frac{dF(Z^k)}{dZ} \quad (5.61)$$

Quadratic convergence to the solution is obtained with this method provided that the initial approximation is chosen carefully.

Similar logic may be applied to a function in several variables where we may state:

$$\begin{aligned} F(X^{k+1}, Y^{k+1}, Z^{k+1}, \dots) &= F(X^k, Y^k, Z^k, \dots) \\ &+ \frac{\partial F(X^k, Y^k, Z^k, \dots)}{\partial X} (X^{k+1} - X^k) \\ &+ \frac{\partial F(X^k, Y^k, Z^k, \dots)}{\partial Y} (Y^{k+1} - Y^k) \end{aligned}$$

$$+ \dots \quad (5.62)$$

If we let the variables be represented by a vector, \vec{Z} , the equation becomes

$$F(\vec{Z}^{k+1}) = F(\vec{Z}^k) + J(\Delta\vec{Z}^k) \quad (5.63)$$

$$\text{where } \Delta\vec{Z}^k = \vec{Z}^{k+1} - \vec{Z}^k$$

and J = Jacobian vector consisting of partial derivatives of the variables.

Again, since $F(\vec{Z}^{k+1}) = 0$ at convergence:

$$J(\Delta\vec{Z}^k) = -F(\vec{Z}^k) \quad (5.64)$$

The above approach may be generalized to a set of functions in several variables such as in the present problem. In this case the Jacobian becomes a matrix and we may write:

$$J(\Delta\vec{Z}^k) = -F(\vec{Z}^k) \quad (5.65)$$

where $F(\vec{Z}^k)$ is a vector of functions.

The Jacobian becomes a banded matrix of partial derivatives which may be obtained analytically or numerically. In this work they are evaluated numerically using a tangent approximation of the actual derivatives; that is,

$$\frac{\partial F}{\partial Z} = \frac{F(\vec{Z}_k + \vec{\epsilon}_k) - F(\vec{Z}_k)}{\epsilon_k} \quad (5.66)$$

10^{-4} corresponding in size to the particular order chosen for the variables.

The problem may be solved by Gaussian elimination for \vec{Z}^k and convergence is obtained when the $\Delta\vec{Z}^k$ are less than specified tolerances. Following each iteration, the variables are updated in the following manner:

$$\vec{Z}^{k+1} = \vec{Z}^k + \Delta\vec{Z}^k \quad (5.67)$$

and all properties dependent upon the variables are updated to the latest iterate level making the technique fully implicit.

Options exist in the model to use either natural grid block ordering or D4 ordering (Price and Coats, 1974) in the direct solution of the equations at each iteration.

2. Choice of Primary Variables

The unknown variables in the equation set requiring solution may be summarized as follows:

<u>Unknowns</u>	<u>Number</u>
ϕ_a, ϕ_o, ϕ_v	3
T	1
S_a, S_o, S_v	3
x_{1a}, x_{1o}, x_{1v}	<u>$3n^*$</u>

TOTAL $3n + 7$ unknowns

* n = number of components

which may be used for solution of the problem:

<u>Equations</u>	<u>Number</u>
molar balances	n
energy balance	1
saturation constraint	1
capillary pressures	2
mole fraction constraints	3
distribution coefficients	<u>2n</u>
TOTAL	3n + 7 equations

Vapour phase saturation, S_v , may be eliminated from the set of unknowns by using the saturation constraint.

Aqueous and vapour phase potentials, ϕ_a and ϕ_v , are eliminated using the capillary pressure relations. Two of the mole fraction unknowns are eliminated using the two liquid phase mole fraction constraint equations. The vapour phase mole fraction constraint is retained in the equation

~~set.~~ The 2n distribution coefficient equations are used to make the final reduction down to n+2 primary variables. The set of unknown variables chosen for the present problem are: ϕ_o (or P_o), T, S_a , S_o , x_{4v} , x_{5v} and x_{3o} .

The ordering of the primary variables and the equation set was done in such a manner as to maximize the diagonal dominance of the matrix. To this end, the equations were ordered as follows:

2. Molar balance for water (Component 1);
3. The sum of the molar balances for the two oil components (Components 2 and 3);
4. Energy balance;
5. Molar balance for carbon dioxide (Component 4);
6. Molar balance for nitrogen (Component 5); and,
7. Molar balance for heavy oil (Component 3).

3. Finite Difference Approximations

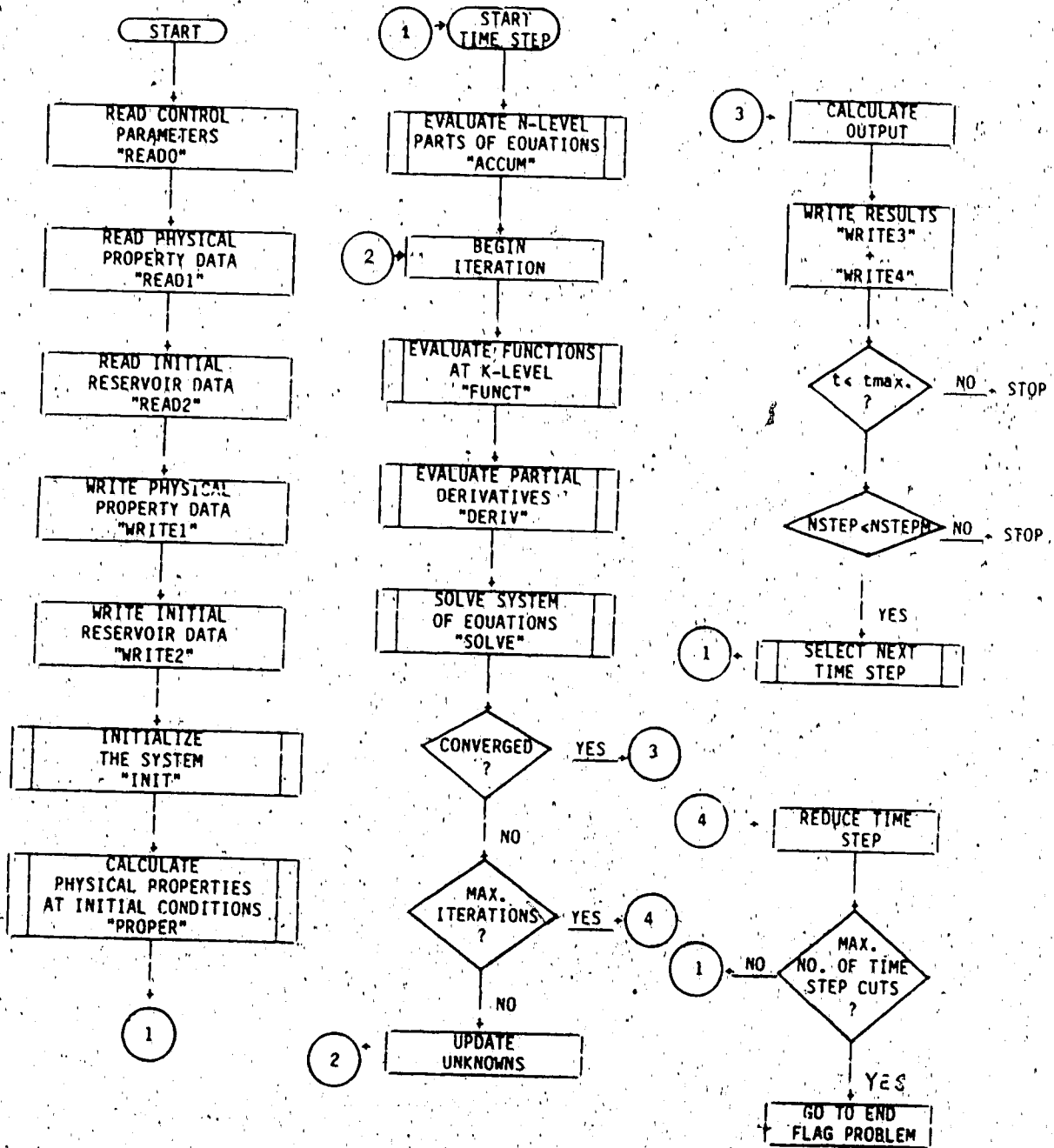
Appendix E contains finite difference approximations to the seven equations outlined in the previous section. An example of the expansion of the finite difference approximations is given for the energy balance equation and definitions of the transmissibilities are provided.

Appendix F shows rearrangement of the equations into a "standard form" and defines the non-zero coefficients for each equation.

G. Organization of the Computer Program

A Fortran IV computer program was written to numerically simulate the steamflood process with gas additives. The structure of the main program is shown in Figure 5.1. If convergence is not reached in a specified number of iterations, the time step is reduced, and the calculations are repeated. Time step cuts may be performed only a specified number of times. Once convergence is obtained, the results are printed

MAIN PROGRAM FLOW CHART



out, a new time step is chosen and the next time step is begun. Automatic time step selection is performed in the main program and follows the procedure of Grabowski et al (1979). A description of the major subprograms comprising the numerical model is contained in the following discussion.

READ0 Subroutine

Program control parameters are read including the number of grid blocks, components and phases, well locations, and parameters identifying which program options are to be used.

READ1 Subroutine

Reads all data required for calculation of the physical properties of the phases.

READ2 Subroutine

Reads initial reservoir data at each grid block including block dimensions, elevation, absolute permeability, and porosity. Also specified are initial pressure, temperature, phase saturations and phase compositions.

WRITE1 Subroutine

Writes all data required for calculation of the physical properties of the phases and corresponds basically to subroutine READ1.

WRITE2 Subroutine

Writes grid block initialization data and basically corresponds to subroutine READ2.

WRITE3.Subroutine

Writes time step information including the time step size, maximum changes in variables, and number of iterations to convergence. Also written are the injection and production rates and volumes of the phases as well as the components.

WRITE4 Subroutine

Writes the reservoir grid summary following a time step and includes the new pressures, temperatures, saturations, compositions and heat losses.

INIT Subroutine

Provides initialization of certain arrays and parameters and includes some conversion of units. Subroutine CTRANS which calculates the constant parts of the transmissibilities is invoked by subroutine INIT. Spline coefficients for tabulated relative permeabilities and capillary pressures are evaluated if required by calling subroutine SPLINE.

PROPER Subroutine

All physical properties at one grid block are evaluated here. This subroutine invokes many other subprograms, mostly functions, in order to accomplish its objective. There is basically one subprogram for each physical property required for each phase.

PRODUC Subroutine

Evaluates production rates at a grid block.

HEATL1 Function

Evaluates heat losses for the laboratory model at a grid block.

HEATL2 Function

Evaluates heat losses for the reservoir model at a grid block.

HEATSK Function

Evaluates the special heat source/sink term in the energy equation based upon a lumped heat capacity system.

TRANS Subroutine

Evaluates transmissibilities over the grid as it determines the upstream grid block locations.

ACCUM Subroutine

Evaluates the accumulation terms in the functions.

FUNCT Subroutine

Evaluates the functions in the system of equations over the entire grid by making appropriate calls to PROPER, PRODUC, HEATL1 or HEATL2, HEATSK, and TRANS.

DERIV Subroutine

Calculates the partial derivatives of the functions and locates them in a Jacobian.

SOLVE Subroutine

Based on the GBAND subroutine given in Aziz and Settari

(1979), this subroutine uses Gaussian elimination to solve the system of equations at each iteration.

VI. NUMERICAL SIMULATION RESULTS

A. Preliminary Data Set Development

A data set was developed to conduct numerical model tests runs and to determine the parameter and process sensitivities. These serve as a guide in conducting a history match of the laboratory experiments. This data set was structured to roughly represent the conditions and properties of the porous media used in the laboratory tests. It was desired to see if qualitatively the same behaviour would be observed in the numerical model as in the experiments. Sensitivity studies of process and physical property variables were conducted involving all of the parameters which it was anticipated would have a significant effect on the results. A copy of the preliminary data set is contained in Appendix G.

1. Process and Reservoir Conditions

The preliminary data set allowed for steam formation and condensation. The light oil component was mildly volatile and the heavy oil component was treated as a dead oil. Carbon dioxide was allowed to be soluble in both oil and water while nitrogen was considered to be insoluble.

The initial phase mole fractions (Table 6.1) were determined by conducting a three phase flash calculation governed by the equilibrium K-values at the initial system temperature and pressure (Peng and Robinson, Dec. 1976). Trace quantities with mole fractions less than 10^{-12} are shown as zero in Table 6.1.

TABLE 6.1
INITIAL PHASE COMPOSITIONS

<u>COMPONENT</u>	<u>AQUEOUS PHASE</u>	<u>OLEIC PHASE</u>	<u>VAPOUR PHASE</u>
1 Water	$9.999\ 999 \times 10^{-1}$	0.0	$1.092\ 176 \times 10^{-2}$
2 Light Oil	0.0	$4.689\ 779 \times 10^{-1}$	$7.099\ 846 \times 10^{-5}$
3 Heavy Oil	0.0	$5.310\ 216 \times 10^{-1}$	0.0
4 Carbon Dioxide	$5.441\ 047 \times 10^{-7}$	$5.441\ 047 \times 10^{-7}$	$8.157\ 327 \times 10^{-4}$
5 Nitrogen	0.0	0.0	$9.881\ 985 \times 10^{-1}$

temperature were similar to those of the laboratory tests (see Table 4.1). Rock density was taken from Crookston et al. (1979) and rock heat capacity from Coats (Dec. 1980). The initial value used for rock compressibility was similar to that used by Hong and Ault (1984) in their light-oil reservoir problem. Steam and gas injection rates were representative of those used in the laboratory work. A steam rate of 1.543×10^{-2} mol/s is equal to 1 000 cm³/h water equivalent. The gas injection rates represented approximately one tenth of the stoichiometric amounts used in the experiments and the injected gas was composed of 25% CO₂ and 75% N₂. Injected steam enthalpy represented 80% quality steam whereas in the laboratory tests approximately 100% quality steam was used. Injected gas enthalpies were chosen to represent the enthalpies of the pure components at the temperature and pressure of the steam. Back pressure and productivity index were representative of lab conditions.

Capillary pressures were zero and relative permeabilities were based on the following simple formulae.

$$k_{rw} = k_{rw0} \left(\frac{S_w - S_{wir}}{1 - S_{wir}} \right)^{EX_{krw}} \quad (6.1)$$

Porosity, percent	45.0
Absolute Permeability, μm^2	10.0
Initial Oil Saturation, %PV	79.869
Initial Water Saturation, %PV	20.040
Initial Pressure, kPa (gauge)	0.0
Initial Temperature, $^{\circ}\text{C}$	25.0
Rock Density, kg/m^3	2.729×10^3
Rock Heat Capacity, $\text{kJ}/\text{kg}\cdot\text{K}$	0.835
Rock Compressibility, $1/\text{kPa}$	4.350×10^{-6}
Injection Rates, mol/s	
Steam	1.543×10^{-2}
CO_2	1.782×10^{-4}
N_2	5.347×10^{-4}
Injected Fluid Enthalpies, J/mol	
Steam	4.489×10^4
CO_2	9.734×10^3
N_2	6.120×10^3
Back Pressure, kPa (gauge)	3.364×10^3
Productivity Index, m^2/m	0.250
$k_{\text{rwro}} = k_{\text{roiw}} = k_{\text{rgro}} = 1.0$	$U_v = 2.0 \text{ J}/\text{s}\cdot\text{m}^2\cdot\text{K}$ $U_L = 5.0 \text{ J}/\text{s}\cdot\text{m}^2\cdot\text{K}$
$EX_{\text{krw}} = EX_{\text{krow}} = EX_{\text{krg}} = 2.0$	$T_0 = 298.16 \text{ K}$
$S_{\text{wir}} = S_{\text{or}} = 0.20$	$h = 2.50 \times 10^3 \text{ J}/\text{s}\cdot\text{m}^2\cdot\text{K}$
$S_{\text{gc}} = 0.01$	$A = 3.14 \times 10^{-3} \text{ m}^2$ $\left(\frac{hA}{C_p V}\right) = -3.0 \times 10^{-4} \text{ 1/s}$

$$k_{rg} = k_{rgro} \left(\frac{S_g - S_{gc}}{1 - S_{gc}} \right)^{L_{krg}} \quad (6.3)$$

No temperature dependence of relative permeability end points was included. The values of parameters used in the above equations are shown in Table 6.2.

Overall heat transfer coefficients for liquid and vapour phases per equation (5.47) are also given in Table 6.2 along with data required for equations (5.50) and (5.51) involving the lumped heat capacity model for heat losses to the inlet flange.

2. Fluid Properties

Required pure component properties are shown in Table 6.3. The light oil assumes properties of n-pentane and the heavy oil those of n-decane (Reid et al, 1977).

The effect of CO₂ on water viscosity was assumed to be zero. Data for oleic and vapour phase component viscosity calculations using equations (5.16) and (5.17) are shown in Table 6.4. These data were obtained from Farouq Ali (1970) and Katz et al (1959), p. 169. Data for hydrocarbon viscosities in the vapour phase assumed pentane for the light oil and decane for the heavy oil. Data for hydrocarbon viscosities in the oleic phase were derived

COMPONENT	MW (kg/mol)	PC (kPa(abs))	TC (K)	ZC	AF	TB (K)
1 Water	0.018016	22104.59	647.44	0.231	-0.100	373.3
2 Light Oil	0.072146	3374.98	469.96	0.269	-0.272	309.4
3 Heavy Oil	0.142276	2206.32	619.44	0.255	-0.487	447.3
4 Carbon dioxide	0.044010	7398.07	304.44	0.275	-0.284	194.83
5 Nitrogen	0.028016	3392.22	126.20	0.291	-0.437	77.56

TABLE 6.4

PURE COMPONENT VISCOSITIES

<u>COMPONENT</u>		<u>OLEIC PHASE</u>	<u>VAPOUR PHASE</u>
1	Water		$\mu_{1V} = 1.70 \times 10^{-5} \text{ 1.11}$
2	Light Oil	$\mu_{20} = 1.929 \times 10^{-2} \text{ exp } (2.897 \times 10^3/T)$	$\mu_{2V} = 3.38 \times 10^{-5} \text{ 0.93}$
3	Heavy Oil	$\mu_{30} = 1.929 \times 10^{-2} \text{ exp } (2.897 \times 10^3/T)$	$\mu_{3V} = 3.27 \times 10^{-5} \text{ 0.87}$
4	Carbon Dioxide	$\mu_{40} = 4.413 \times 10^{-1} \text{ exp } (5.781 \times 10^2/T)$	$\mu_{4V} = 1.057 \times 10^{-4} \text{ 0.81}$
5	Nitrogen	$\mu_{50} = 1.413 \times 10^{-1} \text{ exp } (9.030 \times 10^1/T)$	$\mu_{5V} = 2.530 \times 10^{-4} \text{ 0.71}$

 μ in cp

T in K

method of Hilsenrath et al (1955) and using the Dean and Stiel (1965) pressure correction.

Liquid phase densities were calculated using Amagat's law of partial volumes (equation 5.22). Pure component data for liquid density calculations are shown in Table 6.5. Equation (5.27) was used to calculate vapour phase compressibility factor.

Data for calculating liquid and vapour phase enthalpies are contained in Tables 6.6 and 6.7, respectively. These data are for use in equations (5.29) to (5.32) inclusive.

Equilibrium K-values (distribution coefficients) are shown in Table 6.8 for use in equation (5.34) with temperatures in °R and pressures in psia.

3. Grid Arrangement and Model Operation

A one dimensional grid of 17 blocks was chosen. The grid block sizes are shown in Table 6.9 and illustrated in Figure 6.1. The centres of blocks 2 to 15 correspond to the thermocouple locations in the laboratory apparatus. The other dimensions of the blocks are also shown. The cross sectional area of the rectangular surfaces across which the flow took place was equivalent to the cross sectional area of the experimental test cell.

TABLE 6.5

PURE COMPONENT LIQUID PHASE DENSITY DATA

COMPONENT	COEFFICIENT OF THERMAL EXPANSION $\frac{(1/K)}{(K)}$	COMPRESSIBILITY $\frac{(1/kPa)}{(K)}$	DENSITY AT		REFEREN P [K]
			REFERENCE CONDITIONS $\frac{(mol/m^3)}{(K)}$	TEMP. $\frac{(K)}{(K)}$	
1 Water	8.82×10^{-4}	4.496×10^{-7}	5.55×10^4		273.16
2 Light Oil	7.20×10^{-4}	7.250×10^{-7}	8.73×10^3		273.16
3 Heavy Oil	7.20×10^{-4}	7.250×10^{-7}	5.14×10^3		237.16
4 Carbon Dioxide	7.20×10^{-4}	7.250×10^{-7}	2.50×10^4		273.16
5 Nitrogen	7.20×10^{-4}	7.250×10^{-7}	3.66×10^3		273.16

TABLE 6.6

PURE COMPONENT LIQUID PHASE ENTHALPY DATA

COMPONENT	$\frac{a}{\text{J}} \cdot \text{mol}^{-1}$	$\frac{b}{\text{J}} \cdot \text{mol}^{-1} \cdot \text{K}^{-1}$	$\frac{c}{\text{J}} \cdot \text{mol}^{-1} \cdot \text{K}^{-2}$	REFERENCE TEMPERATURE (K)
2 Light Oil	1.54×10^2	4.544×10^{-1}	0.0	298.1
3 Heavy Oil	2.423×10^2	1.1448	0.0	298.1
4 Carbon Dioxide	1.882×10^1	0.0	0.0	298.1
5 Nitrogen	2.720×10^1	4.180×10^{-3}	0.0	298.1

$$C_{pL} = a_i + b_i T + c_i T^2 \text{ for components 2 and 3}$$

$$C_{pV} = a_i + b_i T - \frac{c_i}{T^2} \text{ for component 4}$$

$$\text{and } C_{pV} = a_i + b_i T + c_i T^2 \text{ for component 5}$$

TABLE 6.7

PURE COMPONENT VAPOUR PHASE ENTHALPY DATA

COMPONENT	a	b	c	L_v (J/mol)	REFERENCE TEMPERATURE (K)
1 Water	34.415	6.28×10^{-4}	5.6×10^{-6}	4.3830×10^4	298.16
2 Light Oil	22.36	6.28×10^{-2}	0.0	2.5773×10^4	298.16
3 Heavy Oil	22.36	6.28×10^{-2}	0.0	3.9280×10^4	298.16
4 Carbon Dioxide	43.26	1.1464×10^{-2}	8.179×10^5	1.715×10^4	298.16
5 Nitrogen	27.20	4.187×10^{-3}	0.0	5.577×10^3	298.16

for use in equations 5.30 to 5.32

TABLE 6.8

EQUILIBRIUM K-VALUE DATA

<u>COMPONENT</u>		<u>A</u>	<u>B</u>	<u>C</u>	<u>D</u>	<u>E</u>
1	Water	1.0	456.69	116.0	4.464	-
2	Light Oil	1.0	12.127	6738.91	167.13	1.0
3	Heavy Oil	0.0	14.510	6598.76	45.29	1.0
4	Carbon Dioxide in Water	1.0	11.126	604.15	0.0	1.0
	in Oil	1.0	11.126	604.15	0.0	1.0
5	Nitrogen in Water	0.0	10.159	-385.32	0.0	1.0
	in Oil	0.0	10.159	-385.32	0.0	1.0

Temperature in °R
 Pressures in psia
 for use in equation (5.34)

GRID BLOCK SIZES

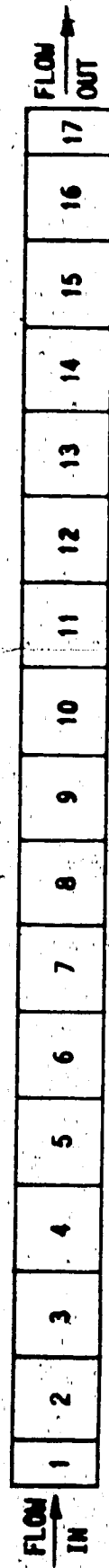
<u>BLOCK</u>	<u>DX</u> <u>(m)</u>	<u>CUMULATIVE</u> <u>DISTANCE</u> <u>(m)</u>	<u>BLOCK</u> <u>CENTRES</u> <u>(m)</u>
1	0.0381	0.0381	0.01905
2	0.0762	0.1143	0.07620
3	0.0762	0.1905	0.15240
4	0.0762	0.2667	0.22860
5	0.0762	0.3429	0.30480
6	0.0762	0.4191	0.38100
7	0.0762	0.4953	0.45720
8	0.0762	0.5715	0.53340
9	0.0762	0.6477	0.60960
10	0.0762	0.7239	0.68580
11	0.0762	0.8001	0.76200
12	0.0762	0.8763	0.83820
13	0.0762	0.9525	0.91440
14	0.0762	1.0287	0.99060
15	0.0762	1.1049	1.06680
16	0.0762	1.1811	1.14300
17	0.0381	1.2192	1.20015

1.2192

DY = 0.05558 m

DZ = 0.05558 m

FIGURE 6.1 ONE DIMENSIONAL GRID SYSTEM



Scale

$$\frac{0.1524 \text{ m}}{6 \text{ in.}}$$

Program convergence tolerances, time step selector norms and levels of change in primary variables for calculation of numerical derivatives are shown in Table 6.10. The problem solution at each iteration was obtained by using the IMSL subroutine library program LEOT2B.

B. Preliminary Simulation Results

1. Base Case Results

The model described in the previous section was run and took 1834 CPU seconds on an FPS 164 array processor. Figure 6.2 shows the injection pressure history for the run and Figure 6.3 shows the temperature profile development. Comparing injection pressure history from the simulator and the laboratory experiments (Figure 4.1), and keeping in mind the differences in the two cases, the behaviour between numerical and physical models is qualitatively similar. Temperature histories in Figures 4.3 and 6.3 may also be compared. Here it is observed that the numerical model predicts less steep temperature gradients and slower movement of the steam front through the grid than in the laboratory case indicating that the heat losses assumed in the numerical model were too large.

Figure 6.4 illustrates the oil production performance of the base case compared to experimental runs 4 and 6. The figure shows that the general character of the curves is similar but that the simulator fails to achieve the oil recovery of the laboratory experiments. This is

TABLE 6.10

PROGRAM CONTROL PARAMETERS

<u>EQUATION</u>	<u>PRIMARY VARIABLE</u>	<u>CONVERGENCE TOLERANCES</u>	<u>TIME STEP SELECTOR NORMS</u>	<u>CHANGE FOR PARTIAL DERIVATIVE CALCULATION</u>
1	ρ	0.1 kPa	500 kPa	0.1
2	S_a	0.0005	0.01	0.001
3	S_o	0.0005	0.01	0.001
4	T	0.1 K	5.0 K	0.1
5	Y_4	0.0005	0.035	0.0001
6	Y_5	0.0005	0.035	0.0001
7	X_{30}	0.0005	0.035	0.0001

maximum iterations in inner loop 8

maximum allowed time step cuts 5

maximum time steps 1 000

maximum iterations 5 000

FIGURE 6.2
LABORATORY AND NUMERICAL MODEL
INLET PRESSURE HISTORIES

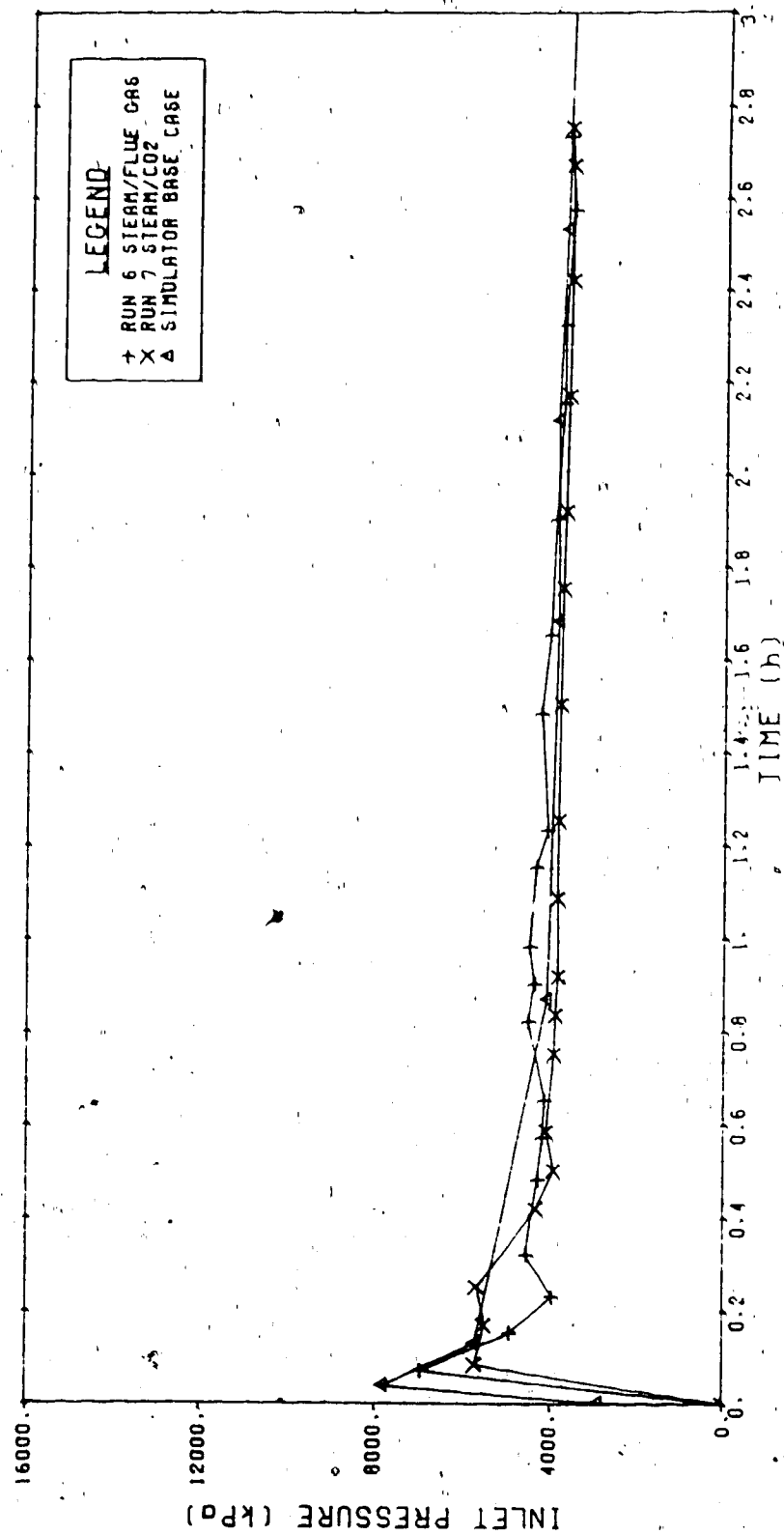


FIGURE 6.3 NUMERICAL MODEL TEMPERATURE PROFILES
BASE CASE

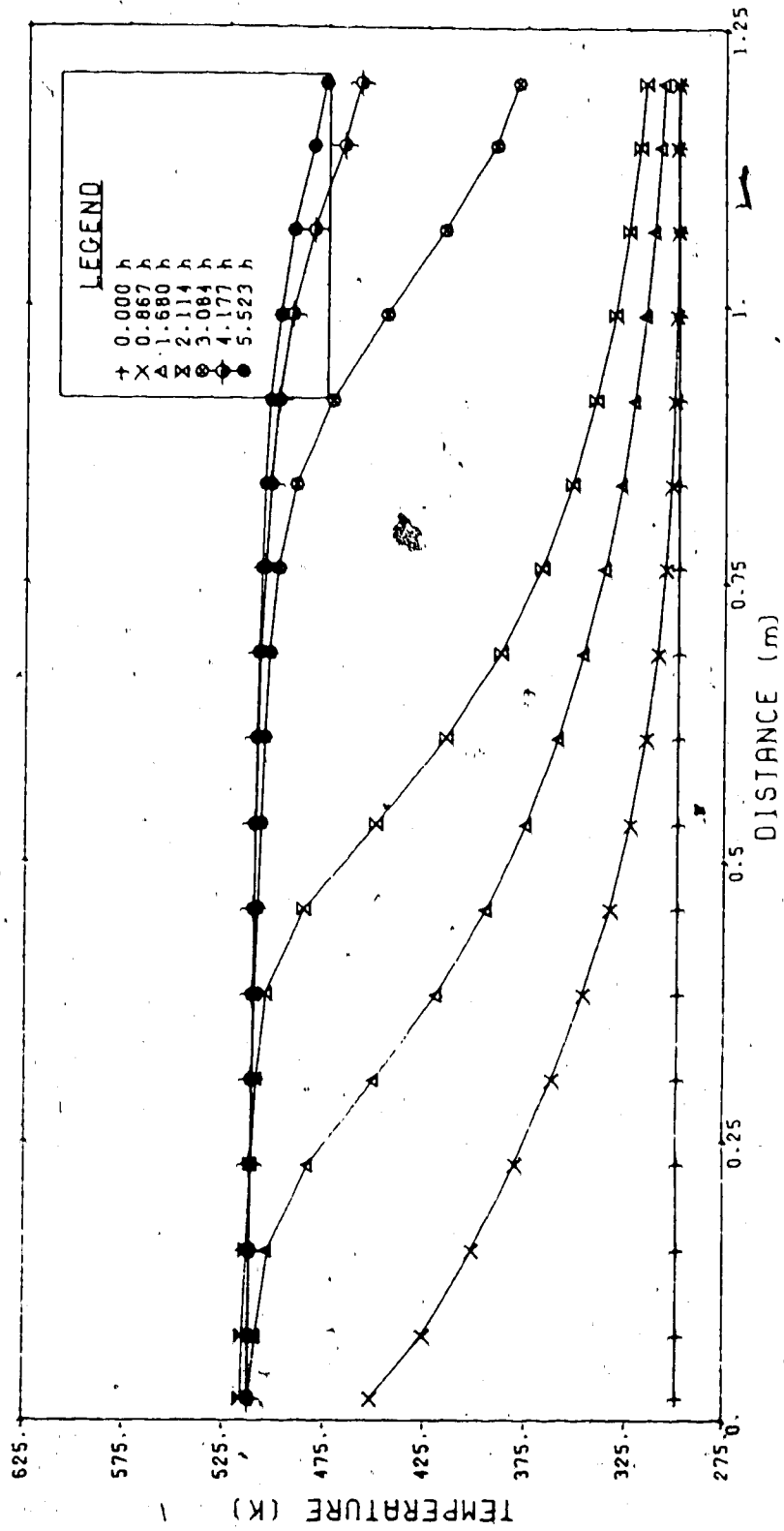
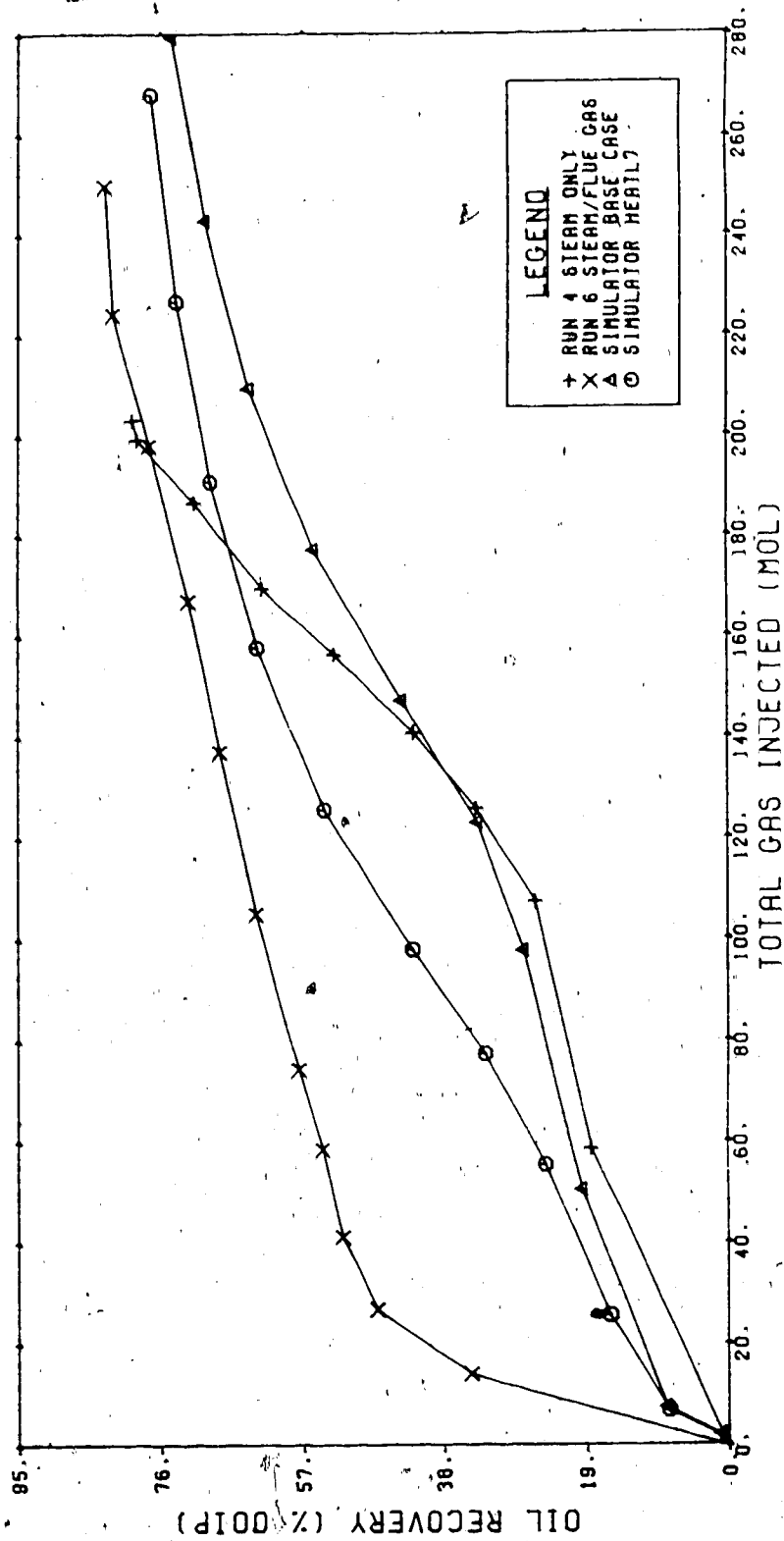


FIGURE 6.4
LABORATORY AND NUMERICAL MODEL
CUMULATIVE OIL PRODUCTION HISTORIES



and to lower quality steam injection in the numerical model. It should be remembered that the gas/steam ratio in the simulator was about one tenth that of the steam/flue gas experiment.

The preliminary data set was deemed to yield a close enough representation to the laboratory results to be used for process and parameter sensitivity studies.

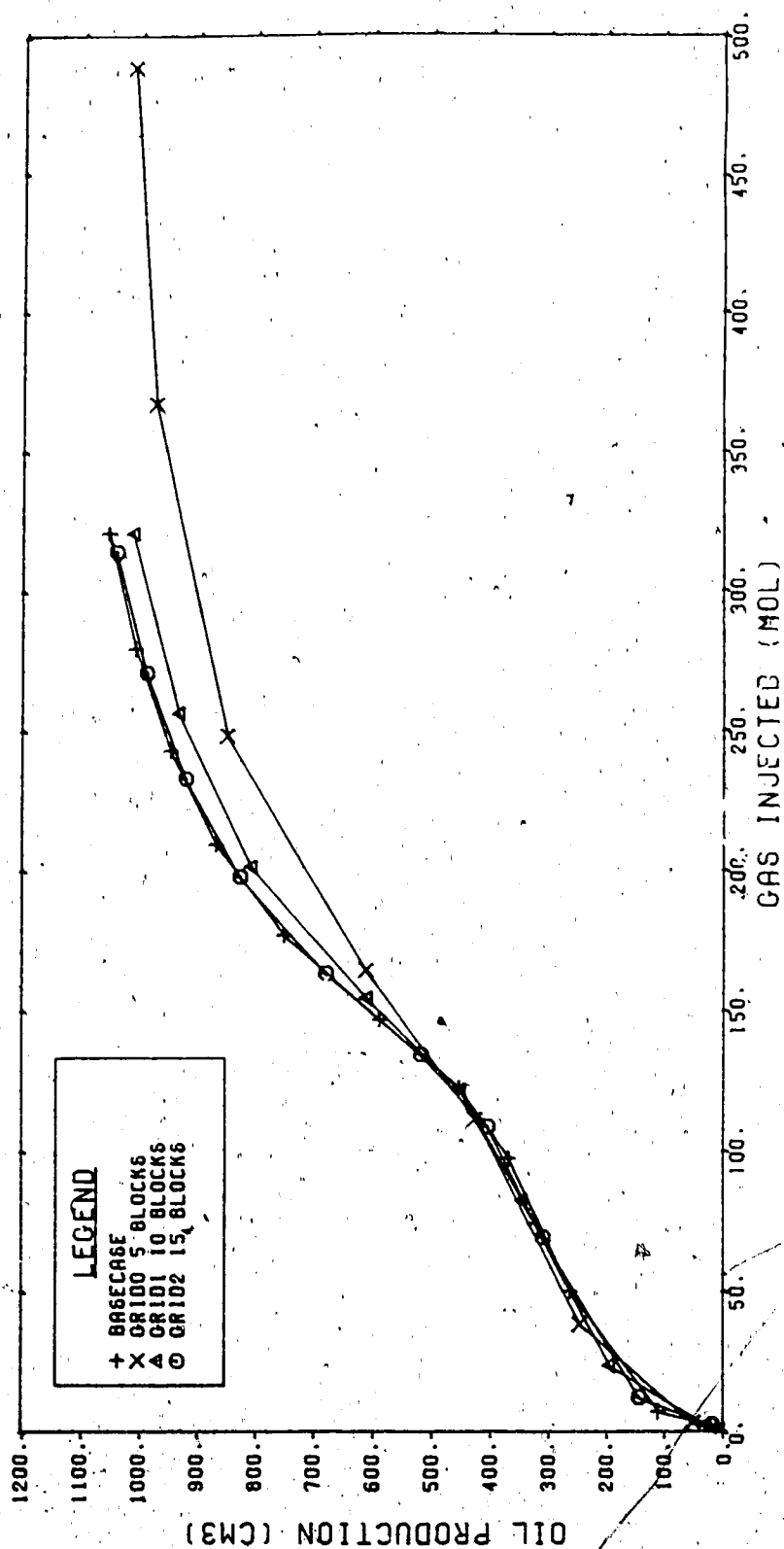
2. Grid and Heat Loss Sensitivities

The preliminary data set was run for grids of 5, 10 and 15 grid blocks in addition to the chosen 17 block grid. It may be observed from Figure 6.5 that the results for the 10 and 15 block cases are very similar while those for the 5 block case show some difference. The 15 and 17 grid block cases are practically identical. On the basis of these runs it was determined that acceptable accuracy may be achieved from the 17 block grid.

This conclusion is consistent with those of Grabowski et al (1979) and Coats (Dec. 1980) who found little difference in results for 10, 20 and 30 grid blocks applied to one-dimensional combustion tube simulations. Rubin and Buchanan (1985) chose a 20 block ~~10~~ grid for history matching the combustion tube data of Smith and Perkins (1973).

It would be expected that a finer grid would be

FIGURE 6.5 CUMULATIVE OIL PRODUCTION HISTORIES
GRID SENSITIVITY



required for fireflood modelling where the temperature and saturation gradients are even more steep than in steam flooding.

Eight simulation runs were conducted in which various heat loss control parameters were changed. Table 6.11 describes the changes that were made to the data set and Figures 6.6 and 6.7 illustrate the effects of these changes on cumulative oil production. Figure 6.8 shows temperature profiles for run HEATL7. Improved representation of heat front movement was obtained for this case in comparison to the base case. In Figure 6.4 the cumulative oil production curve for run HEATL7 also more nearly represents the production behaviour of the steam/gas laboratory experiments. The heat loss parameters are seen to have very significant effects on the process performance.

3. Reservoir Parameter Sensitivities

Also shown in Table 6.11 are the changes made to the base case to identify the effects of changes in reservoir parameters. Changes were made to porosity, absolute permeability, initial oil saturation, rock compressibility and heat capacity, and relative permeability curve shapes and end points. Figure 6.9 shows that reductions in porosity significantly reduce oil production response as would be expected because of reduced oil in place. Figure 6.10 shows that absolute permeability changes in the range

TABLE 6.11

NOTES ON RESERVOIR PARAMETER SENSITIVITY
SIMULATION RUNS

<u>CASE</u>	<u>CHANGED DATA</u>	<u>NOTES</u>
HEATL1	UHG x 2.5	overall gas phase heat transfer coefficient
HEATL2	UHG x 0.5	
HEATL3	UHL x 2.0	overall liquid phase heat transfer coefficient
HEATL4	UHL x 0.5	
HEATL5	CI x 1.6	time constant for heat sink term
HEATL6	CI x 0.33	
HEATL7	HI x 0.40	heat transfer coefficient for heat sink term
HEATL8	HI x 2.0	
POR01	ϕ x 0.444	porosity reduced
POR02	ϕ x 0.666	
PERM1	k x 0.20	absolute permeability
PERM2	k x 0.50	
PERM3	k x 2.0	
COMP1	C _r x 10 ⁻²	rock compressibility reduced
CAP1	C _{pr} x 0.5	rock heat capacity
CAP2	C _{pr} x 2.0	
S01	S _o x 0.75	oil saturation reduced
S02	S _o x 0.50	
SOR1	S _{or} x 0.50	residual oil saturation
SOR2	S _{or} x 1.50	
SWIR1	S _{wir} x 0.50	irreducible water saturation
SWIR2	S _{wir} x 0.75	
SWIR3	S _{wir} x 0.95	
SGC1	S _{gc} x 2.0	critical gas saturation
SGC2	S _{gc} x 5.0	
SGC3	S _{gc} x 0.50	
REL P1	EX _{krw} = EX _{krow} = EX _{krg} = 3.0	
REL P2	EX _{krw} = EX _{krow} = EX _{krg} = 4.0	
REL P3	EX _{krw} = 3.0; EX _{krow} = 2.0; EX _{krg} = 4.0; S _{gc} = 0.05	

FIGURE 6.6 CUMULATIVE OIL PRODUCTION HISTORIES
HEAT LOSS SENSITIVITY CASES 1 TO 4

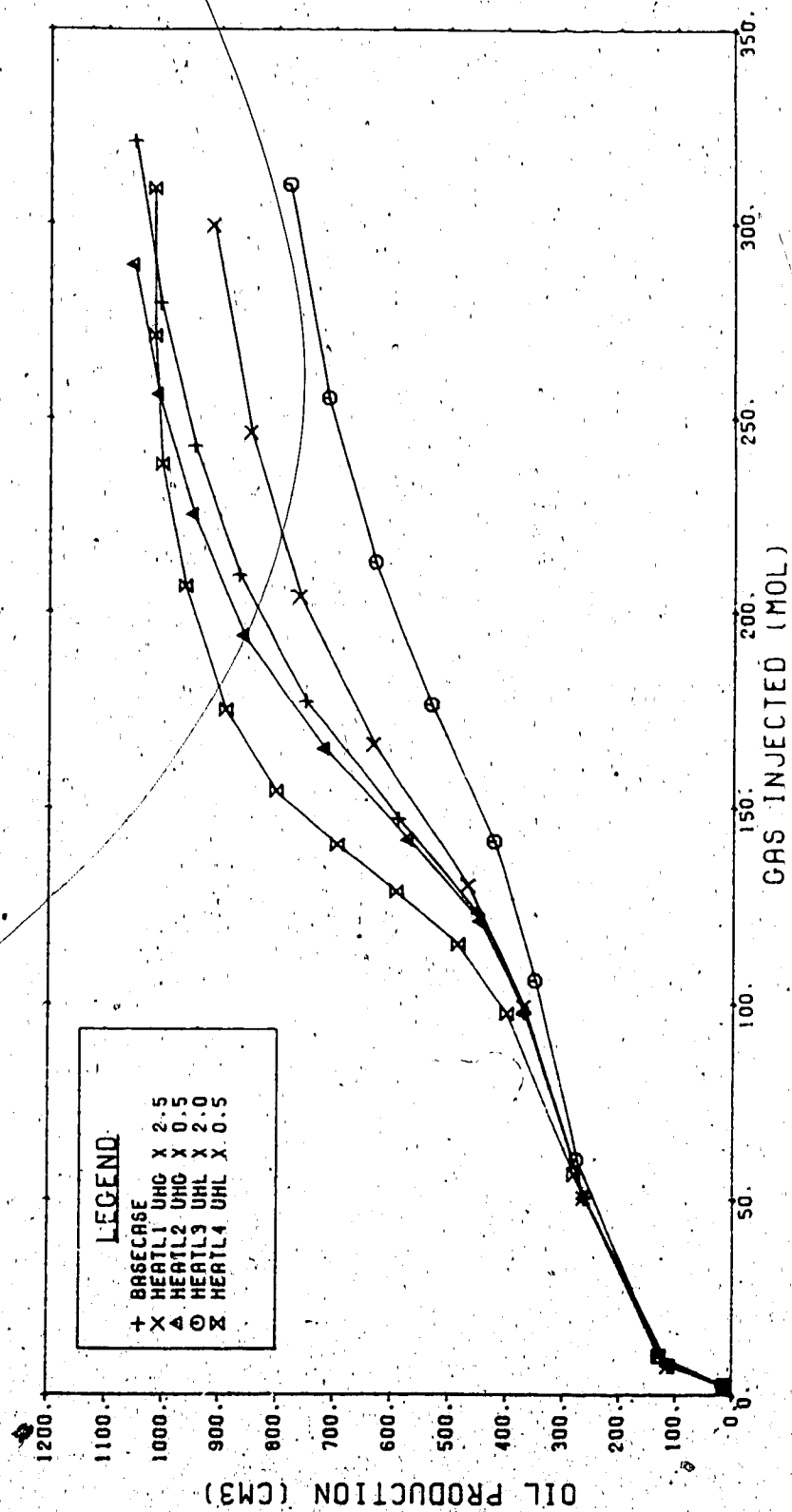


FIGURE 6.7 CUMULATIVE OIL PRODUCTION HISTORIES
HEAT LOSS SENSITIVITY CASES 5 TO 8

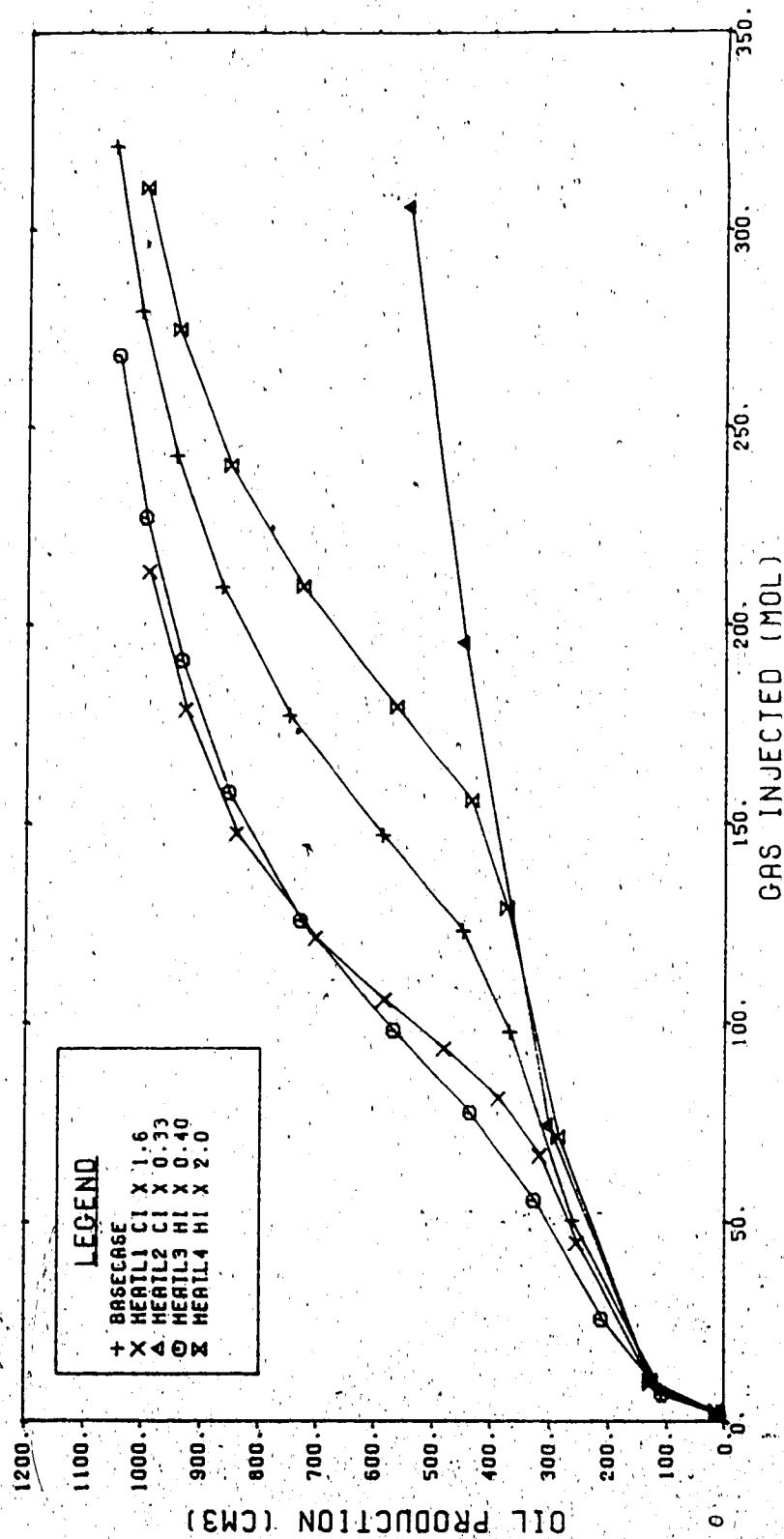


FIGURE 6.9 CUMULATIVE OIL PRODUCTION HISTORIES
POROSITY SENSITIVITY

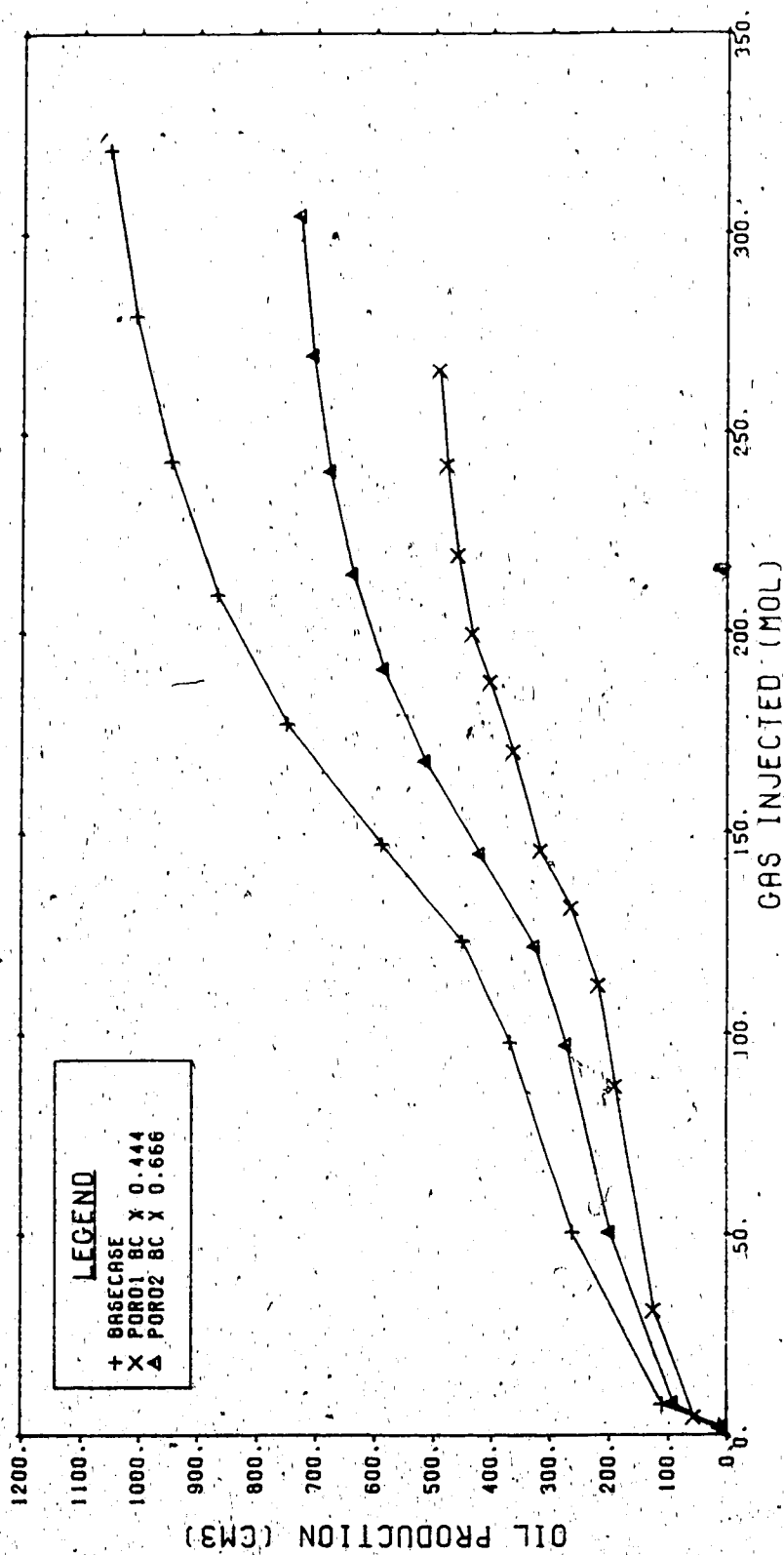
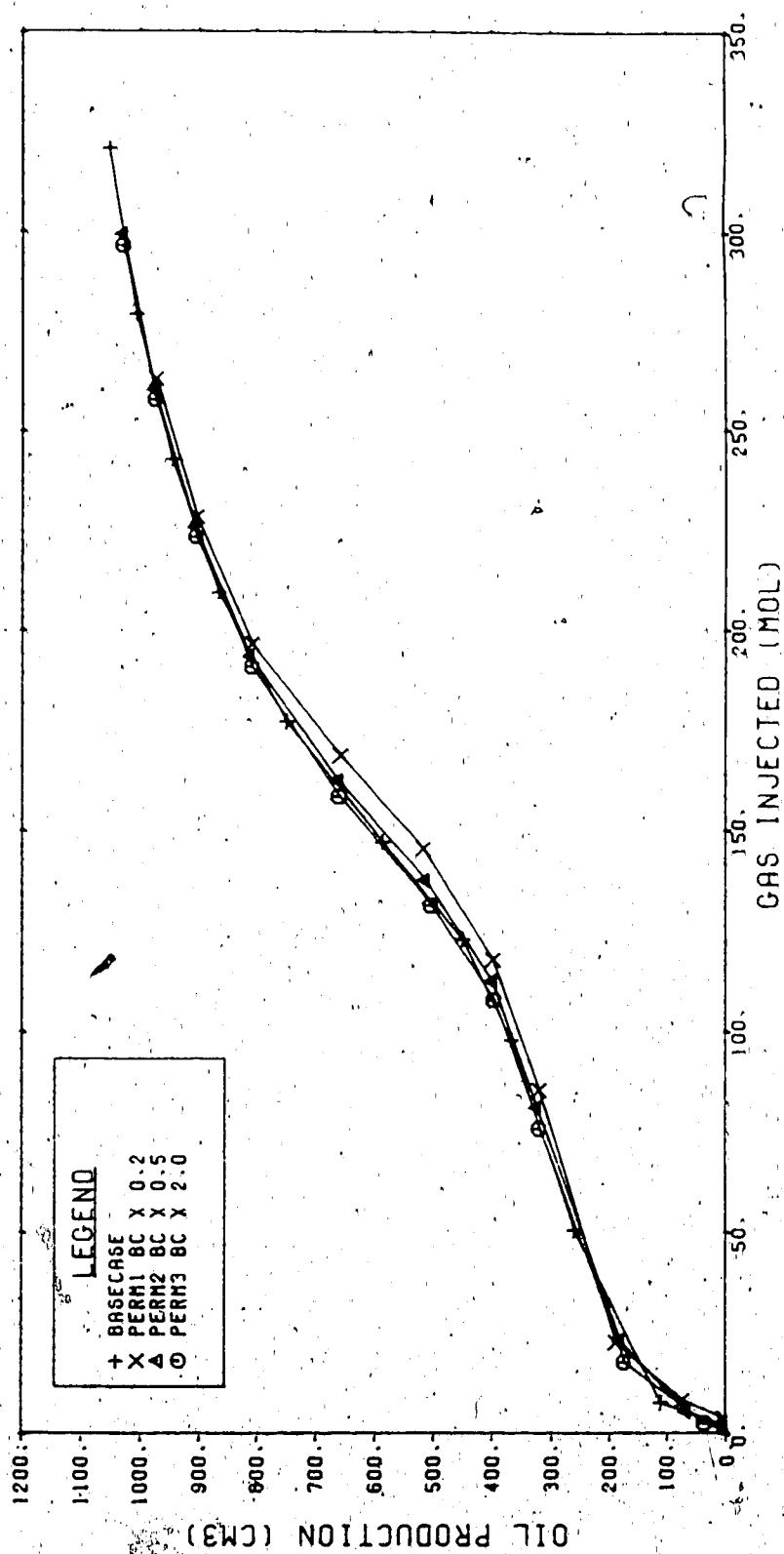


FIGURE 6.10 CUMULATIVE OIL PRODUCTION HISTORIES
ABSOLUTE PERMEABILITY SENSITIVITY



2.0 to 20.0 μm^2 have little effect on oil production performance. Predictably Figure 6.11 shows a marked increase in inlet pressure with reduced absolute permeability. However, this parameter is known to be important in field scale modelling. Figure 6.12 shows that decreasing rock compressibility by two orders of magnitude had little effect on the results. Figures 6.13 to 6.15 show the effect of rock heat capacity on oil production and temperature profiles. Raising the heat capacity of the rock slows heat front advance, steepens the temperature gradients and slows oil production slightly.

The marked effect on oil production of initial oil saturation changes is shown in Figure 6.16 and the effect of changes in residual oil saturation is shown in Figure 6.17. Ultimate recovery is affected by the residual oil saturation but not the general character of the process. Raising irreducible water saturation increases the initial oil production rate but does not affect the ultimate recovery as illustrated in Figure 6.18. This is due to the initial water mobility being decreased at the initial water saturation which results in the displacement of more oil. The same arguments apply to the data illustrated in Figure 6.19. Raising critical gas saturation resulted in more oil production initially but the ultimate recovery was largely unaffected.

Figure 6.20 illustrates the effect of modifying the exponents in the relative permeability curves per equations

FIGURE 6.11 INLET PRESSURE HISTORIES
ABSOLUTE PERMEABILITY SENSITIVITY

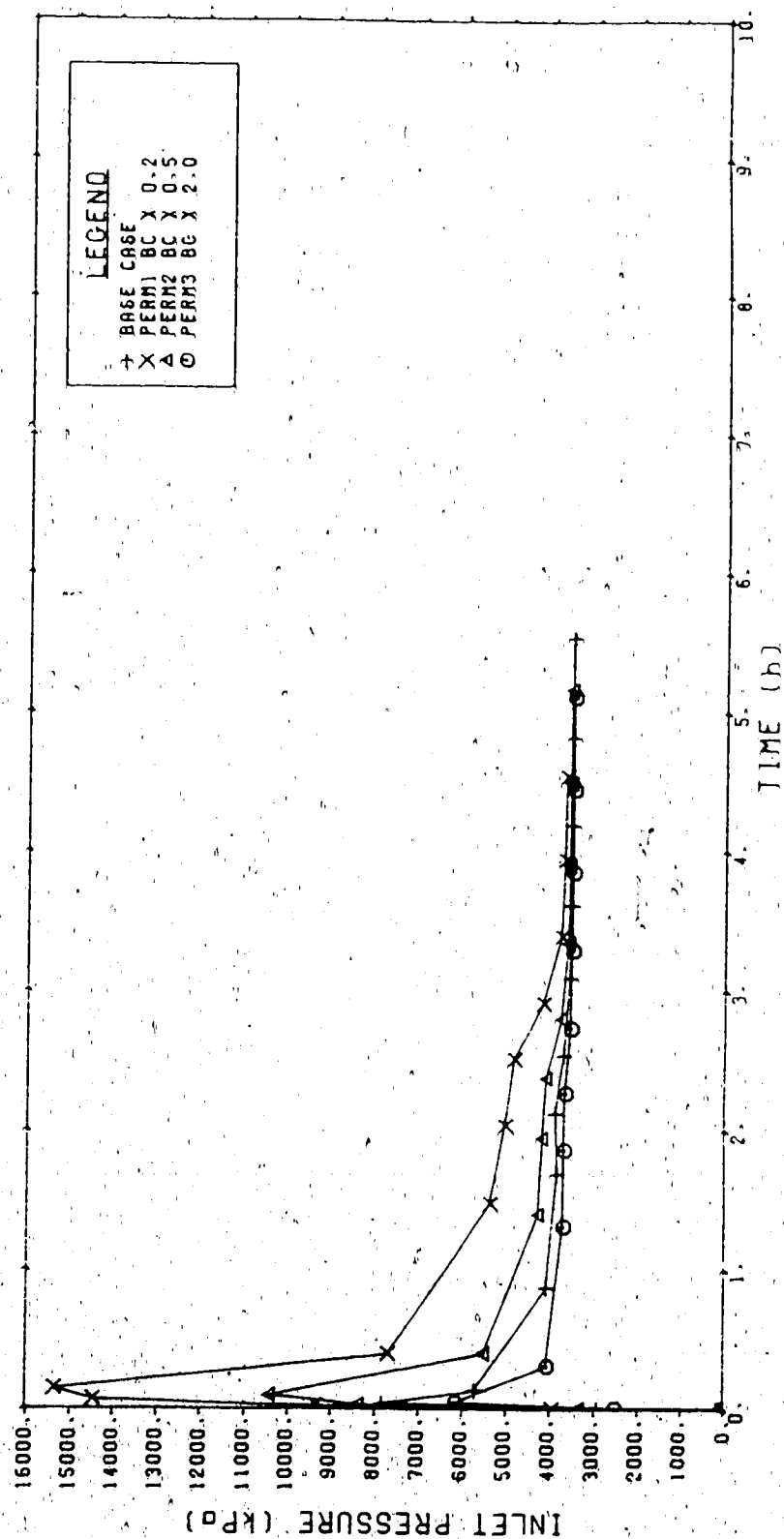


FIGURE 6.12 CUMULATIVE OIL PRODUCTION HISTORIES
ROCK COMPRESSIBILITY SENSITIVITY

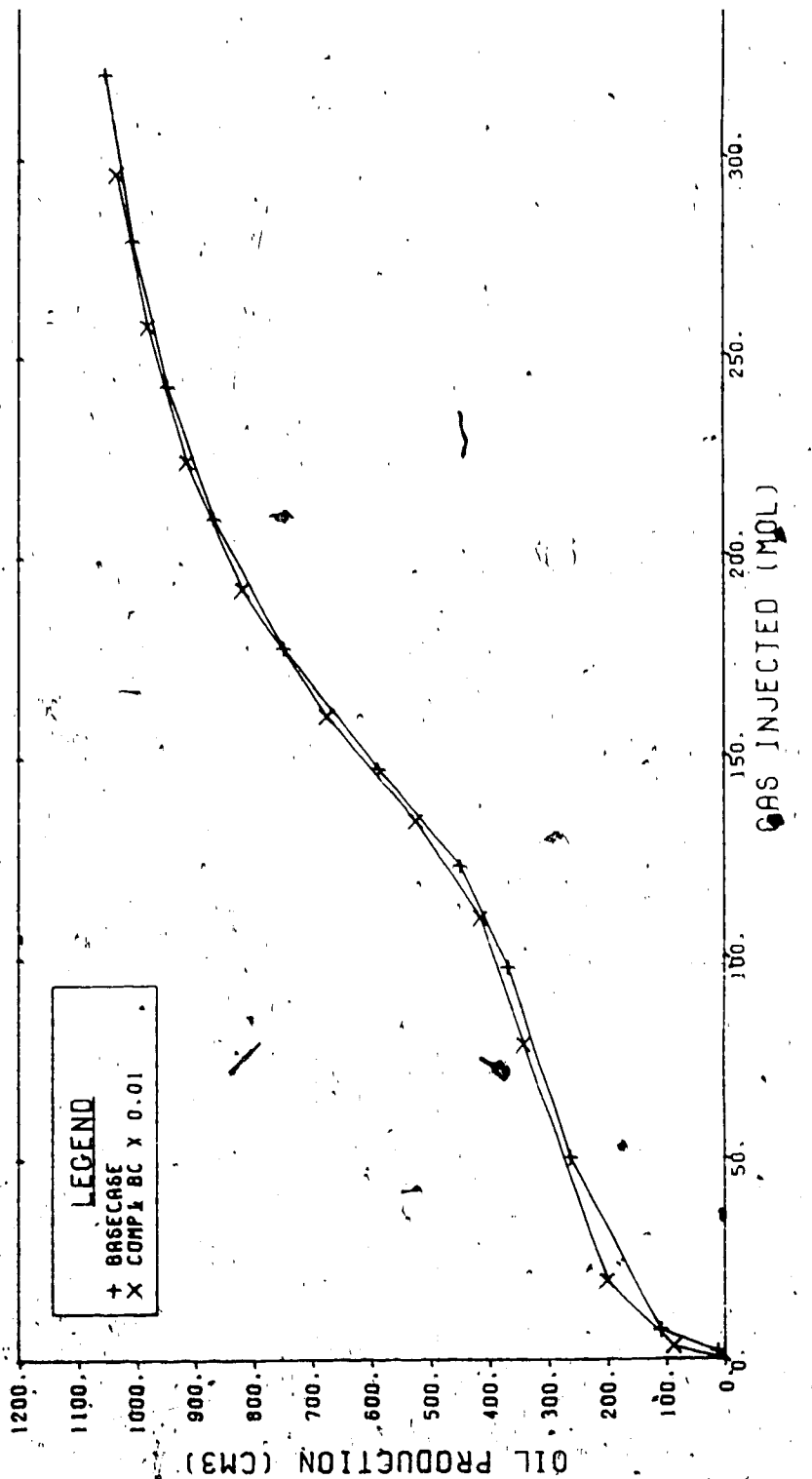
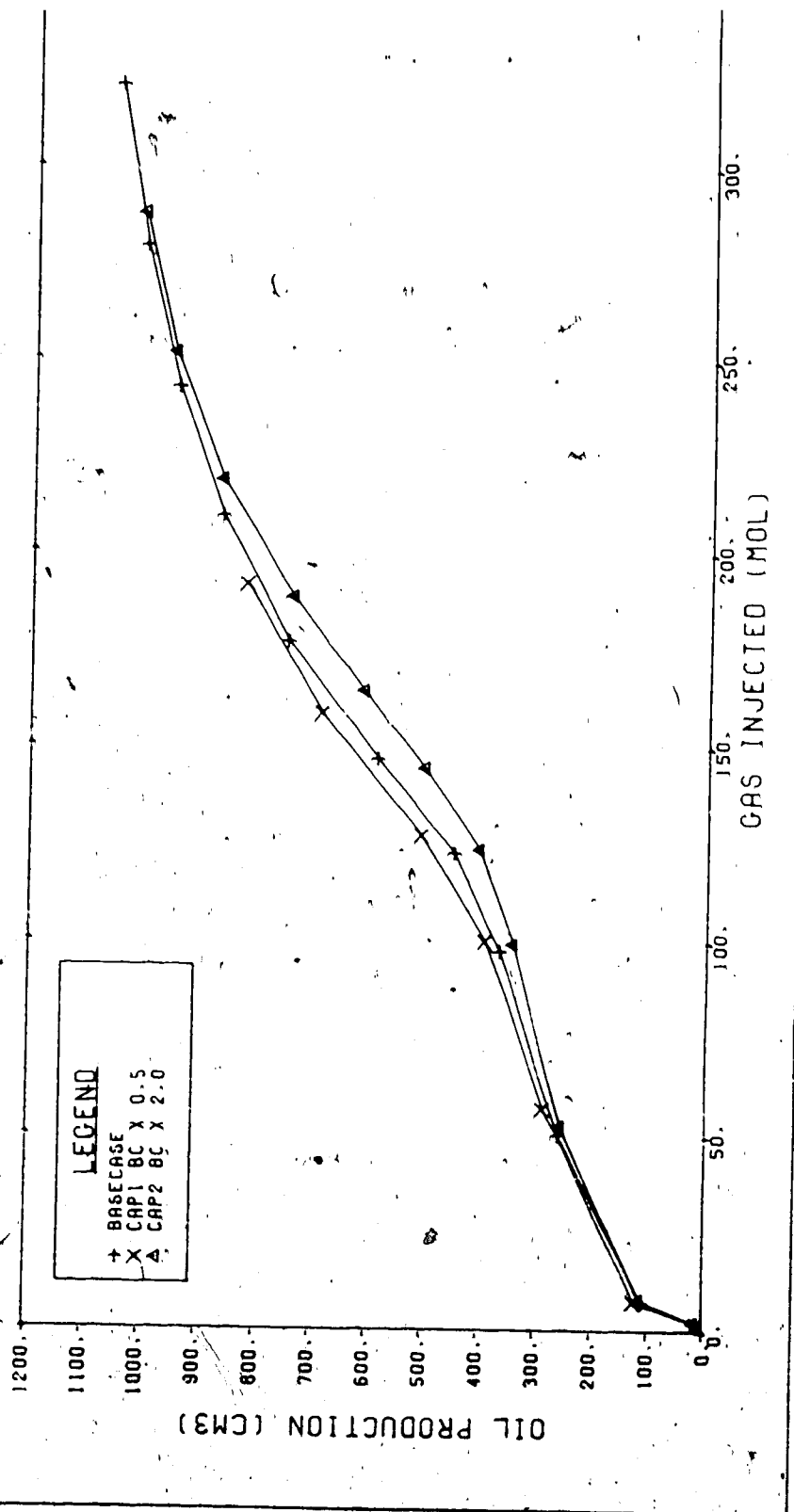


FIGURE 6.13 CUMULATIVE OIL PRODUCTION HISTORIES
ROCK HEAT CAPACITY SENSITIVITY



15



FIGURE 6.16 CUMULATIVE OIL PRODUCTION HISTORIES
INITIAL OIL SATURATION SENSITIVITY

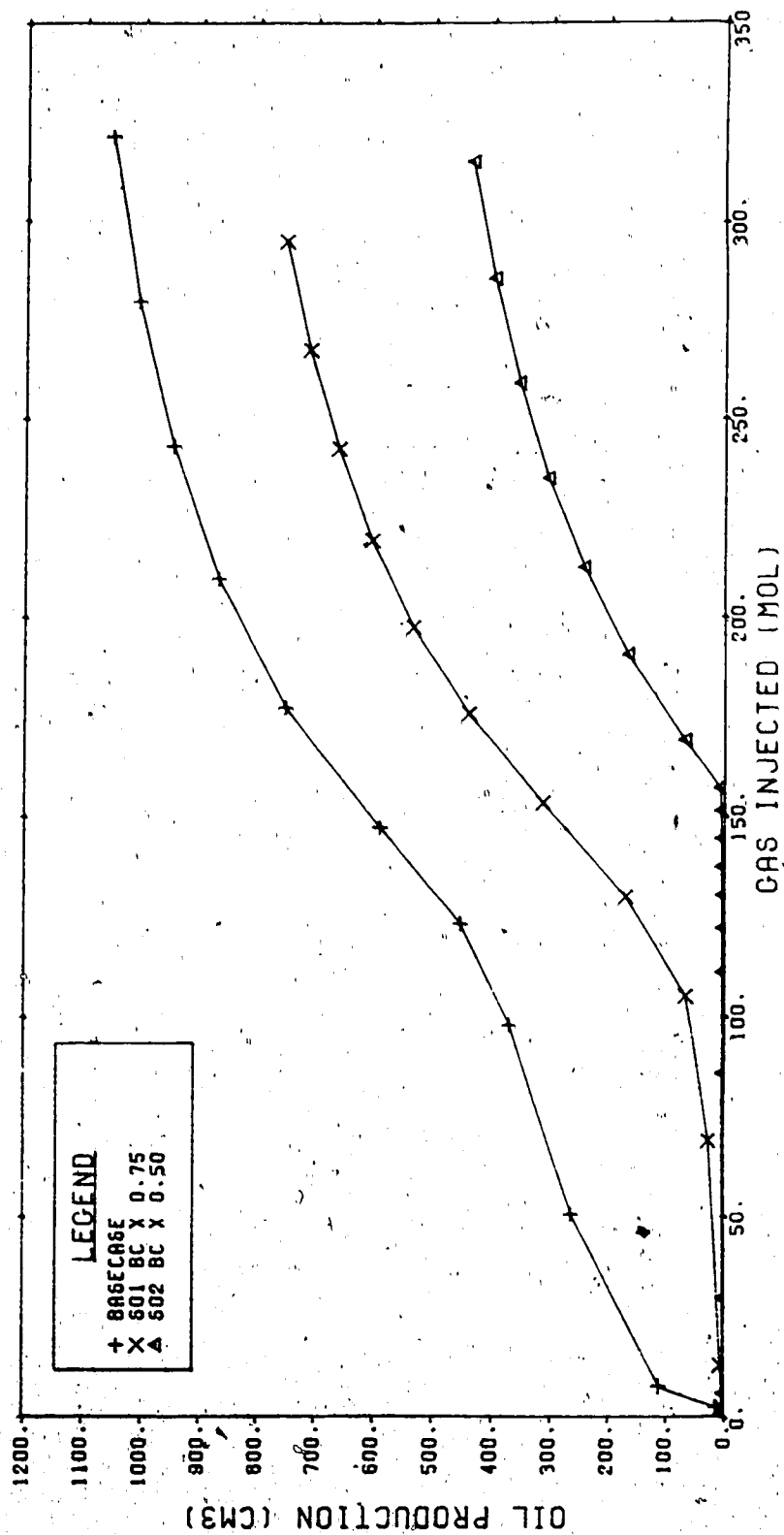


FIGURE 6.17 CUMULATIVE OIL PRODUCTION HISTORIES
RESIDUAL OIL SATURATION SENSITIVITY

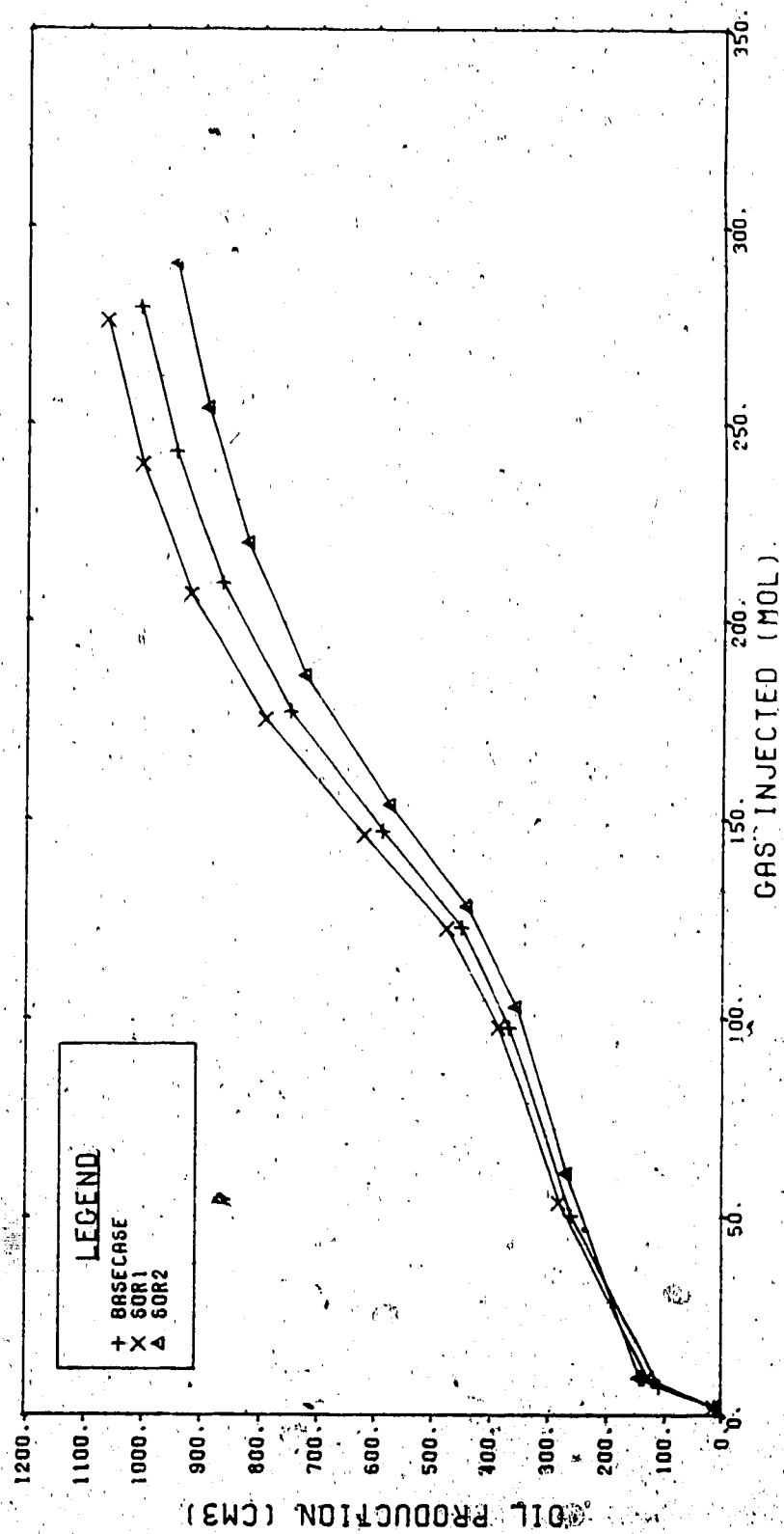


FIGURE 6.18 CUMULATIVE OIL PRODUCTION HISTORIES
IRREDUCIBLE WATER SATURATION SENSITIVITY

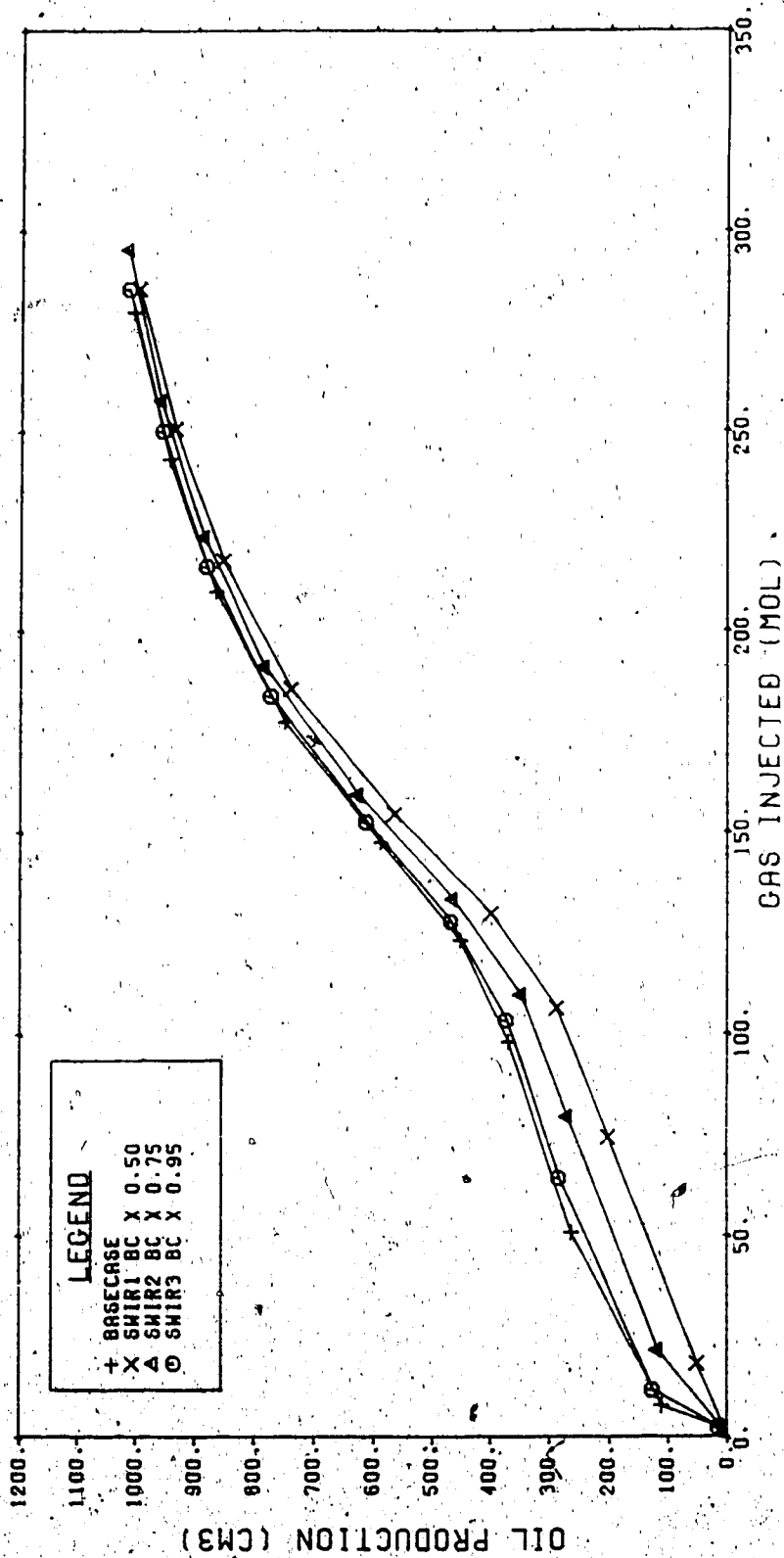


FIGURE 6.19. CUMULATIVE OIL PRODUCTION HISTORIES
CRITICAL GAS SATURATION SENSITIVITY

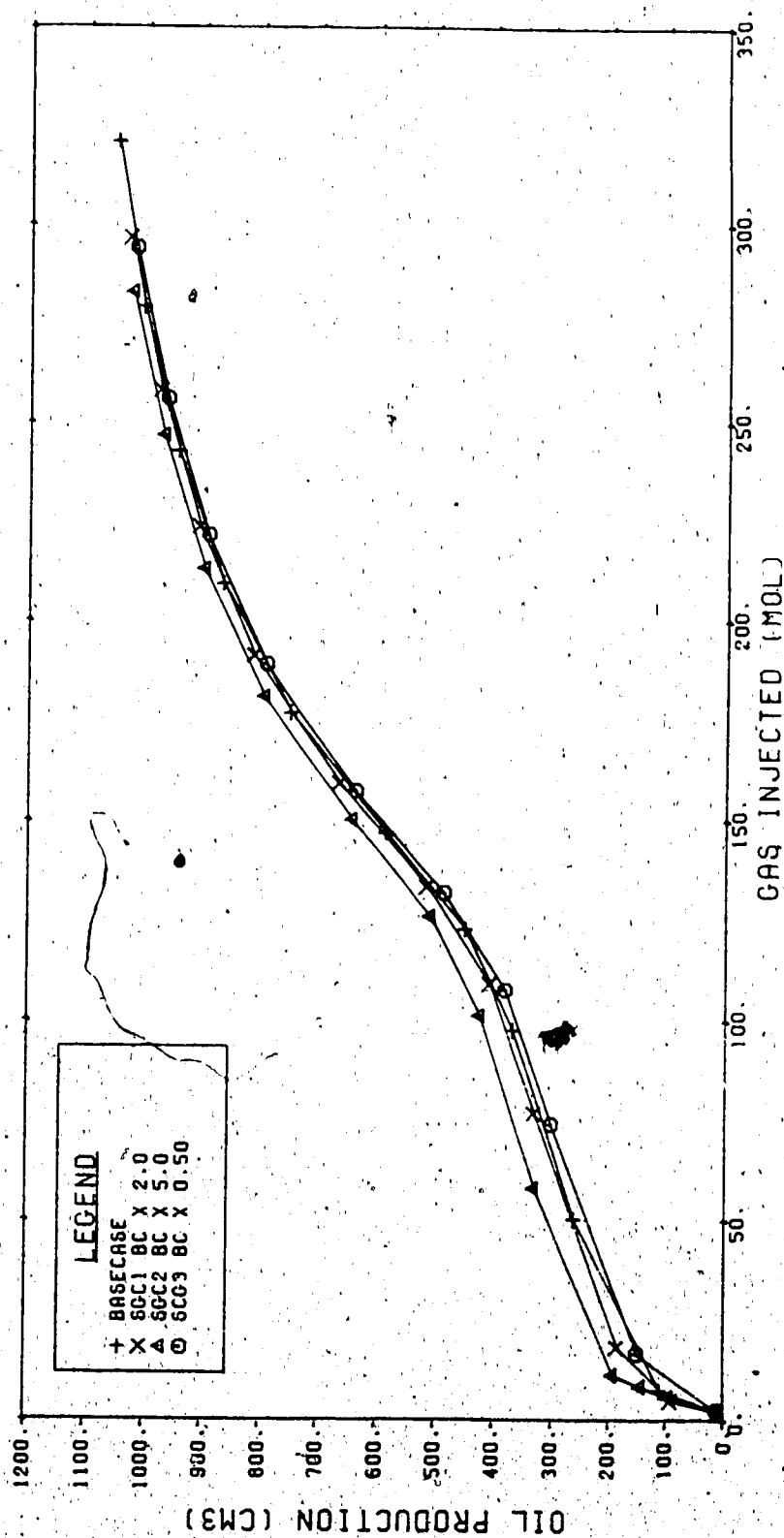
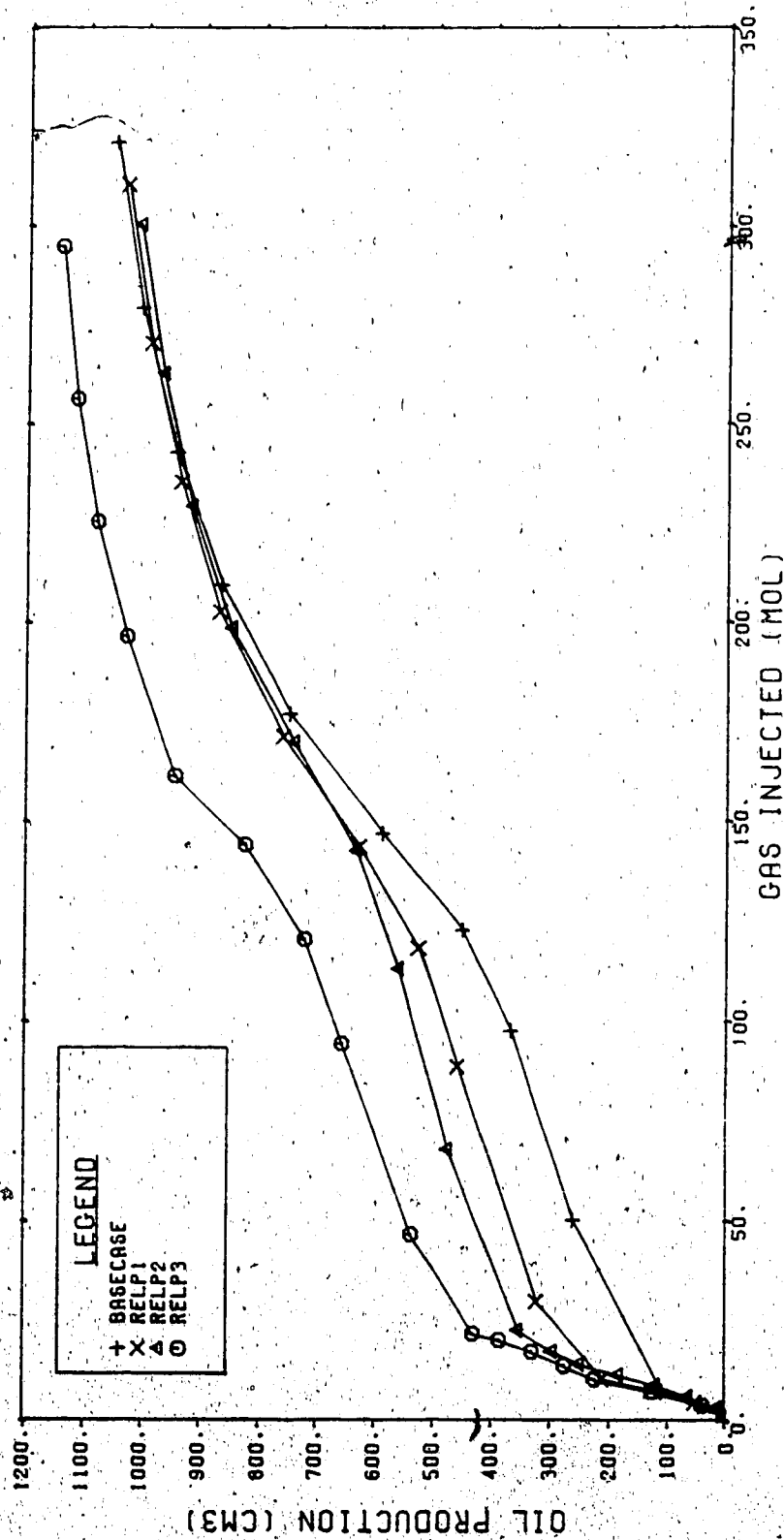


FIGURE 6.20
CUMULATIVE OIL PRODUCTION HISTORIES -
RELATIVE PERMEABILITY SENSITIVITY



0.1 to 0.5. Table 6.11 indicates the changes which were made to the exponents. It may be recalled that the base case simulation used exponents of 2.0 for all phases. The effect of increasing all of the exponents is to make the water and gas mobilities increase more slowly above the critical saturations and as a consequence to displace more oil early in the simulation run. Increasing the exponents for water and gas while leaving the exponent for oil at 2.0 (run RELP3) promotes the displacement of oil throughout. It is evident from Figures 6.17 through 6.20 that the shape and critical saturations assigned to the relative permeabilities have a significant impact on the results.

4. Fluid Property Sensitivities

Table 6.12 summarizes the fluid property and process sensitivity simulation runs.

The effect of viscosity on oil production performance is recorded in Figure 6.21. Viscosities range from 10 to 1 000 cp. The process, as would be expected is highly sensitive to this parameter in terms of both oil production rate and recovery following a certain amount of fluid injection. Inlet pressure histories for the different oil viscosity cases are shown in Figure 6.22.

As illustrated by the curves in Figure 6.23 the solubility of carbon dioxide had little effect on the process. Raising the CO₂ solubility compared to the base case had virtually no effect nor did removing CO₂ solubility

TABLE 6.12

FLUID PROPERTY AND PROCESS SENSITIVITY
SIMULATION RUNS

CASE	CHANGED DATA	NOTES
VISC1	$\mu_o \times 0.03125$	oil viscosity
VISC2	$\mu_o \times 0.3125$	
VISC3	$\mu_o \times 3.125$	
PHASE1	K_{CO_2}	CO ₂ insoluble in aqueous phase
PHASE2	K_{CO_2}	CO ₂ more soluble in oil and water
PHASE3	$K_{light\ oil}$	light oil more volatile
CO2V		viscosity of CO ₂ in liquid phase increased
CO2S1		CO ₂ more soluble in oil and water (as in PHASE 2) and CO ₂ viscosity in liquid decreased
CO2S2		Same as CO2S1 but with density of liquid CO ₂ reduced (i.e. swelling effect increased)
RATE1	steam and gas injection rates $\times 1.5$	
RATE2	steam and gas injection rates $\times 0.5$	
QUAL1	steam quality 0%	
QUAL2	steam quality 20%	
QUAL3	steam quality 50%	
QUAL4	steam quality 90%	gas-steam ratio changes
QUAL5	steam quality 100%	
GSR1	G/S $\times 0.01$	
GSR2	G/S $\times 0.10$	
GSR3	G/S $\times 0.50$	
GSR4	G/S $\times 1.50$	CO ₂ -N ₂ ratio changes
GSR5	G/S $\times 10.0$	
CNR1	CO ₂ 1%; N ₂ 99%	
CNR2	CO ₂ 10%; N ₂ 90%	
CNR3	CO ₂ 50%; N ₂ 50%	back pressure changes
CNR4	CO ₂ 75%; N ₂ 25%	
BP1	$P_{wf} \times 2.0$	
BP2	$P_{wf} \times 0.5$	

FIGURE 6.21 CUMULATIVE OIL PRODUCTION HISTORIES
OIL VISCOSITY SENSITIVITY

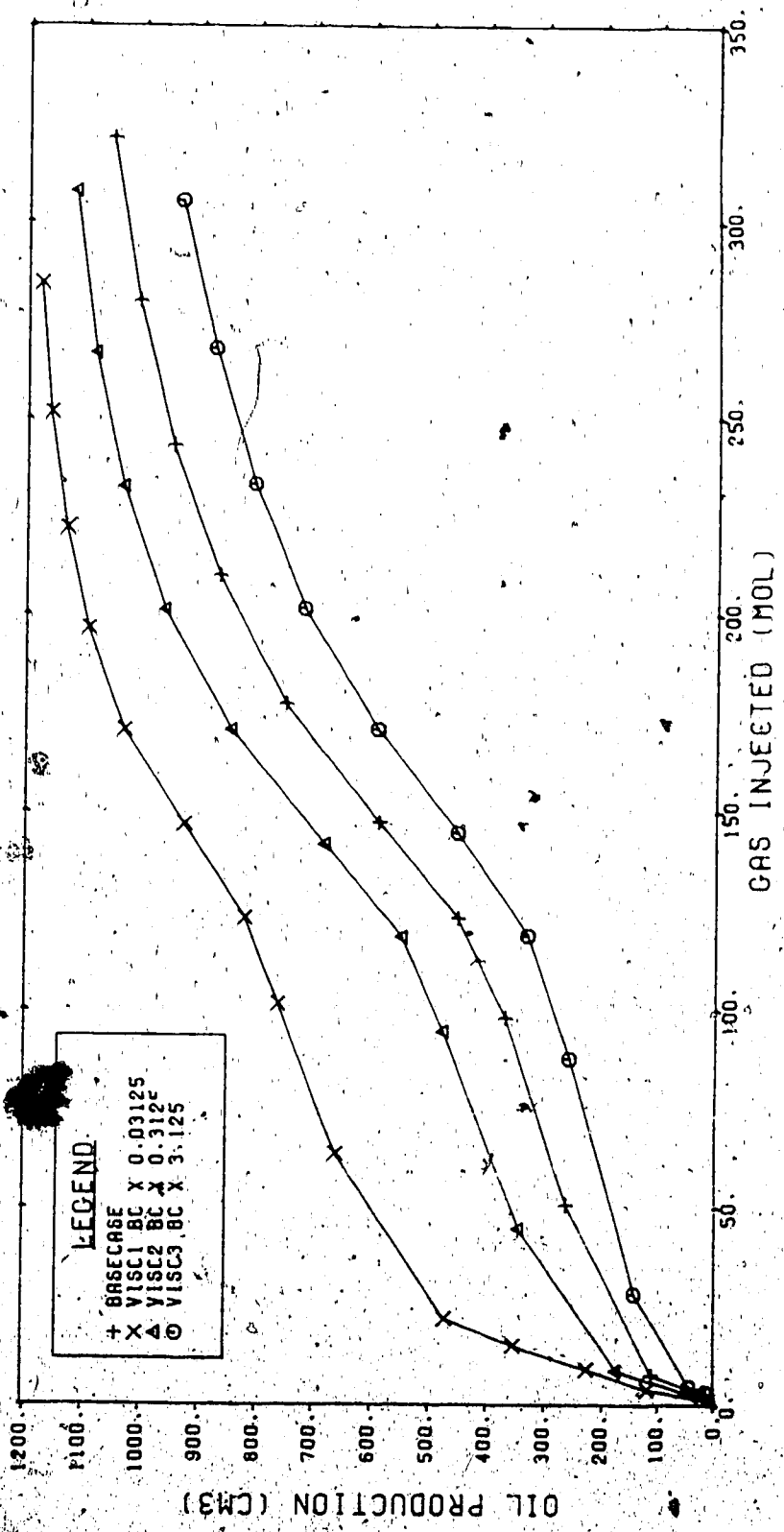


FIGURE 6.22 INLET PRESSURE HISTORIES
OIL VISCOSITY SENSITIVITY

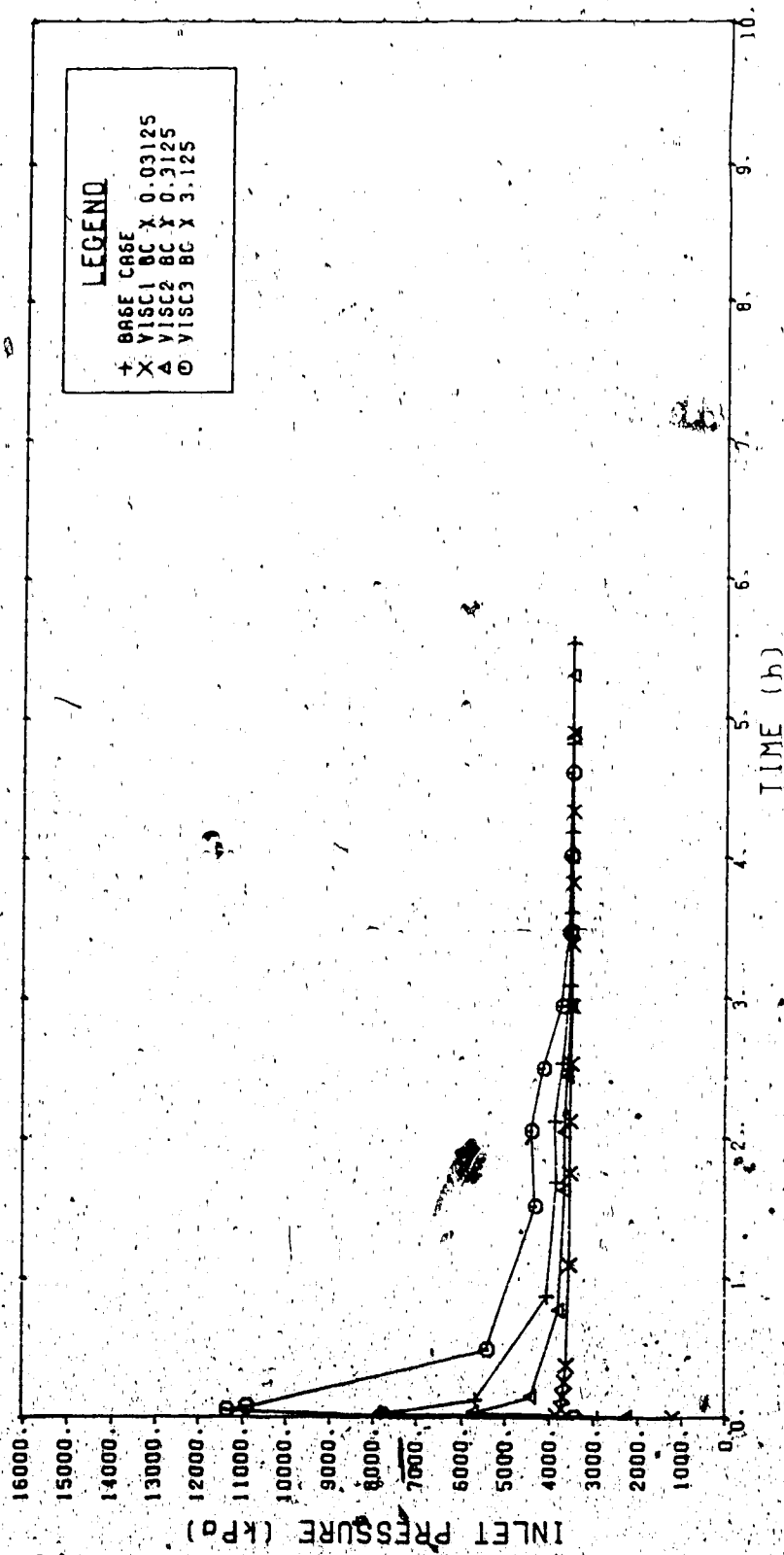
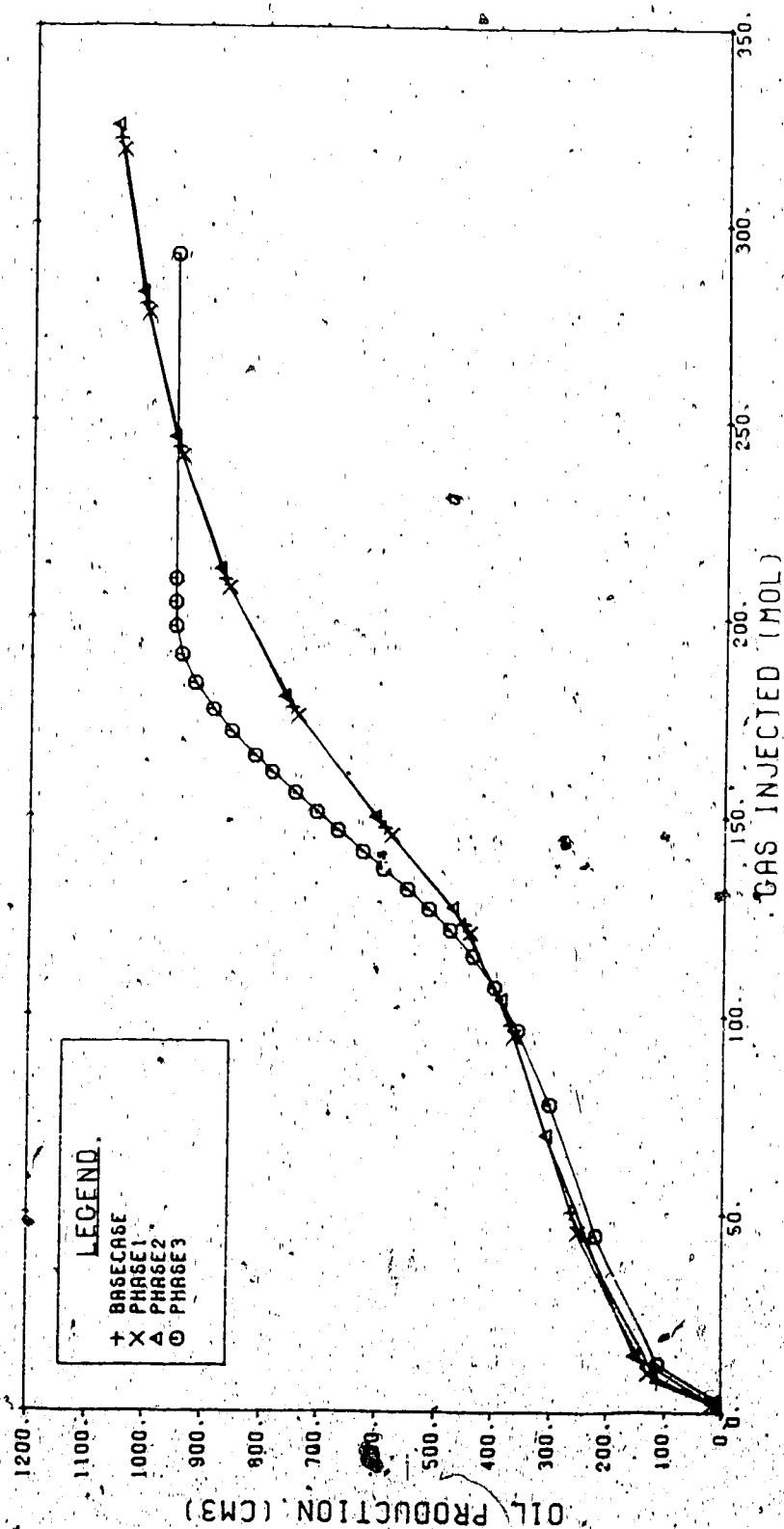


FIGURE 6.23 CUMULATIVE OIL PRODUCTION HISTORIES
K - VALUE SENSITIVITY



in the aqueous phase. Increased light oil volatility altered the performance by accelerating oil production in the latter part of the run.

In the simulations shown in Figure 6.24, the viscosity of CO_2 in the liquid phase was reduced (run C02V) compared to the base case by using the data of Hong and Ault (1984). The same viscosity reduction was retained in the next run (C02S1) and in addition the solubility of CO_2 in liquids was increased in the same manner as in a previous run (PHASE 2). Further, in run C02S2 the CO_2 liquid phase density was reduced to simulate the effect of greater swelling of oil when the amount of CO_2 in solution in oil increases. It is clear from the results that CO_2 viscosity reduction and swelling had little effect on the process.

5. Process Sensitivities

Figure 6.25 shows the effect of increasing and decreasing fluid injection rates while keeping the gas/steam ratio constant. Increasing rates had little effect on the results but decreasing the rates had a significant effect. This is mainly attributable to the slow propagation of the heat front at the low injection rates as shown in Figure 6.26.

Oil production rate and recovery are directly affected by steam quality as shown in Figure 6.27. This is due solely to the rate of heating.

FIGURE 6.24
CUMULATIVE OIL PRODUCTION HISTORIES -
CO₂ LIQUID PHASE PROPERTY SENSITIVITY

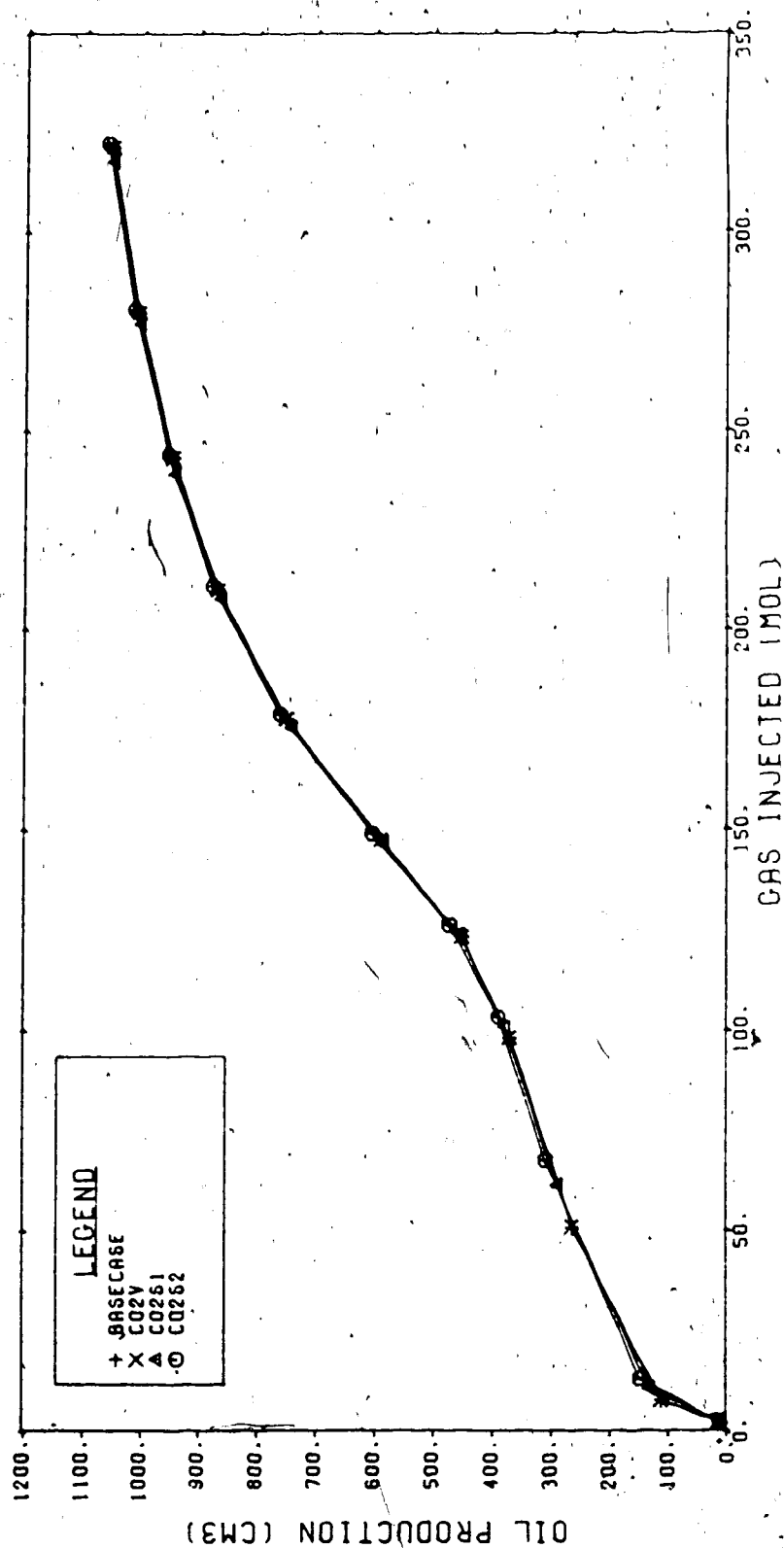


FIGURE 6.25 CUMULATIVE OIL PRODUCTION HISTORIES
INJECTION RATE SENSITIVITY

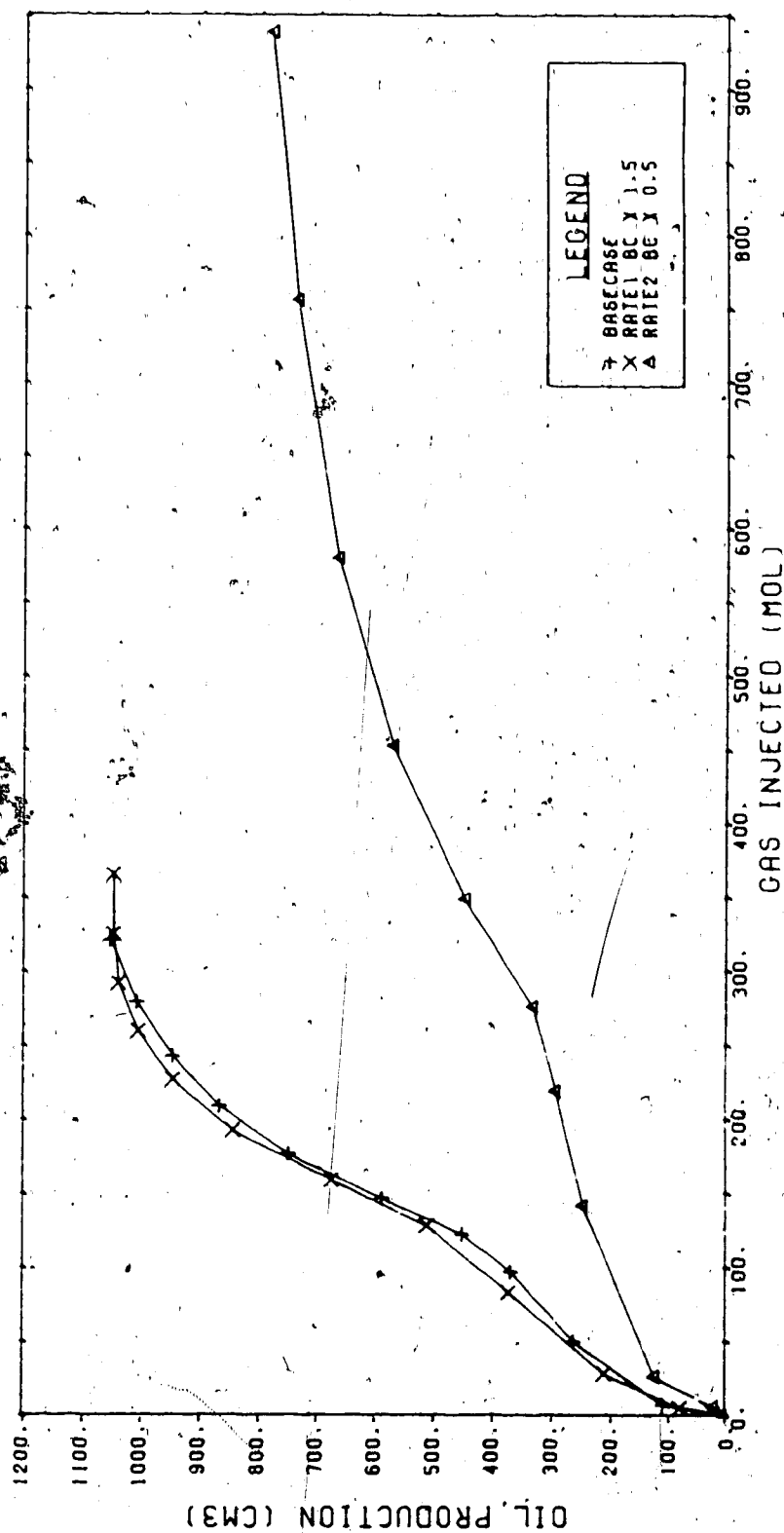


FIGURE 6.26 NUMERICAL MODEL TEMPERATURE PROFILES
INJECTION RATE SENSITIVITY CASE 2

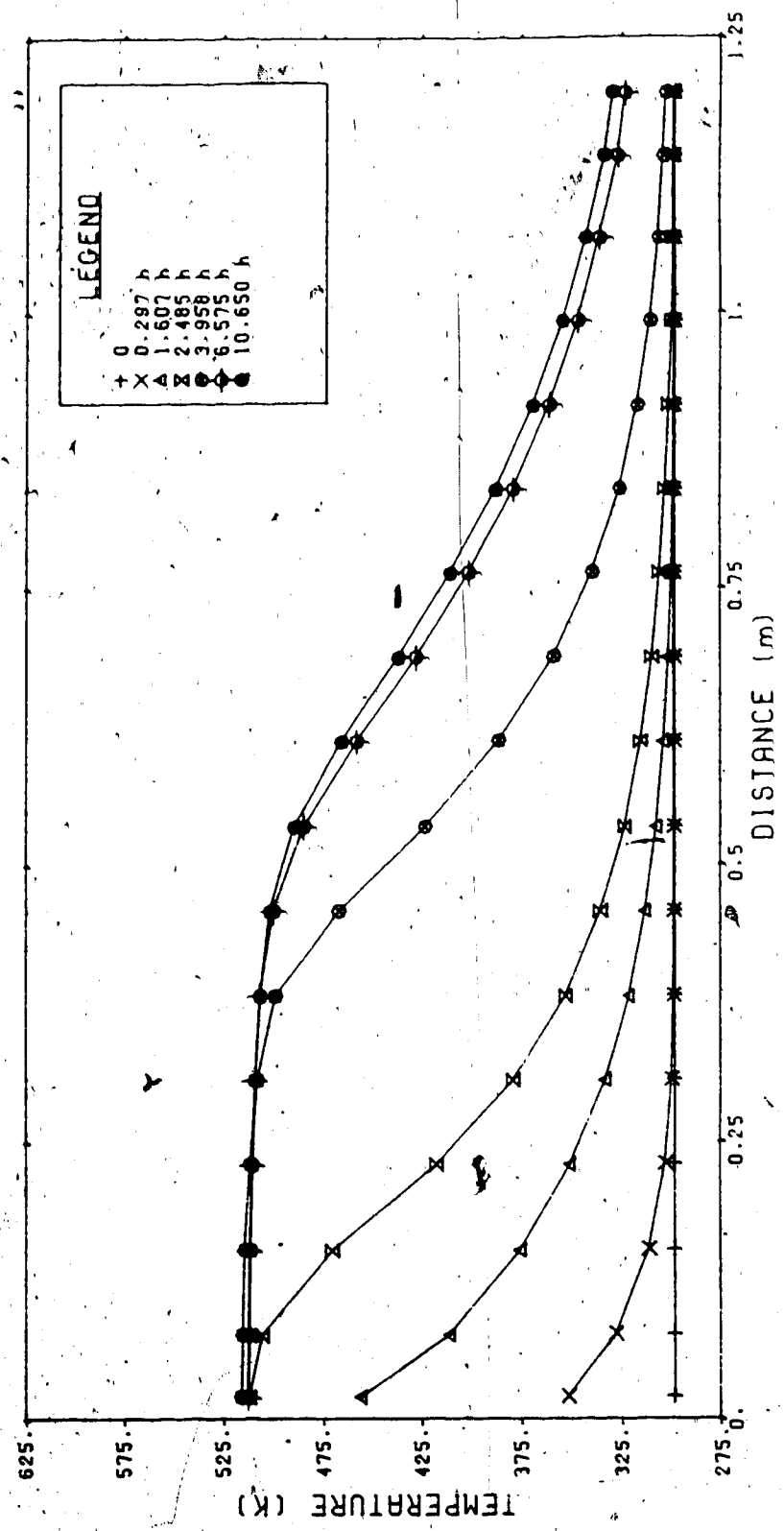
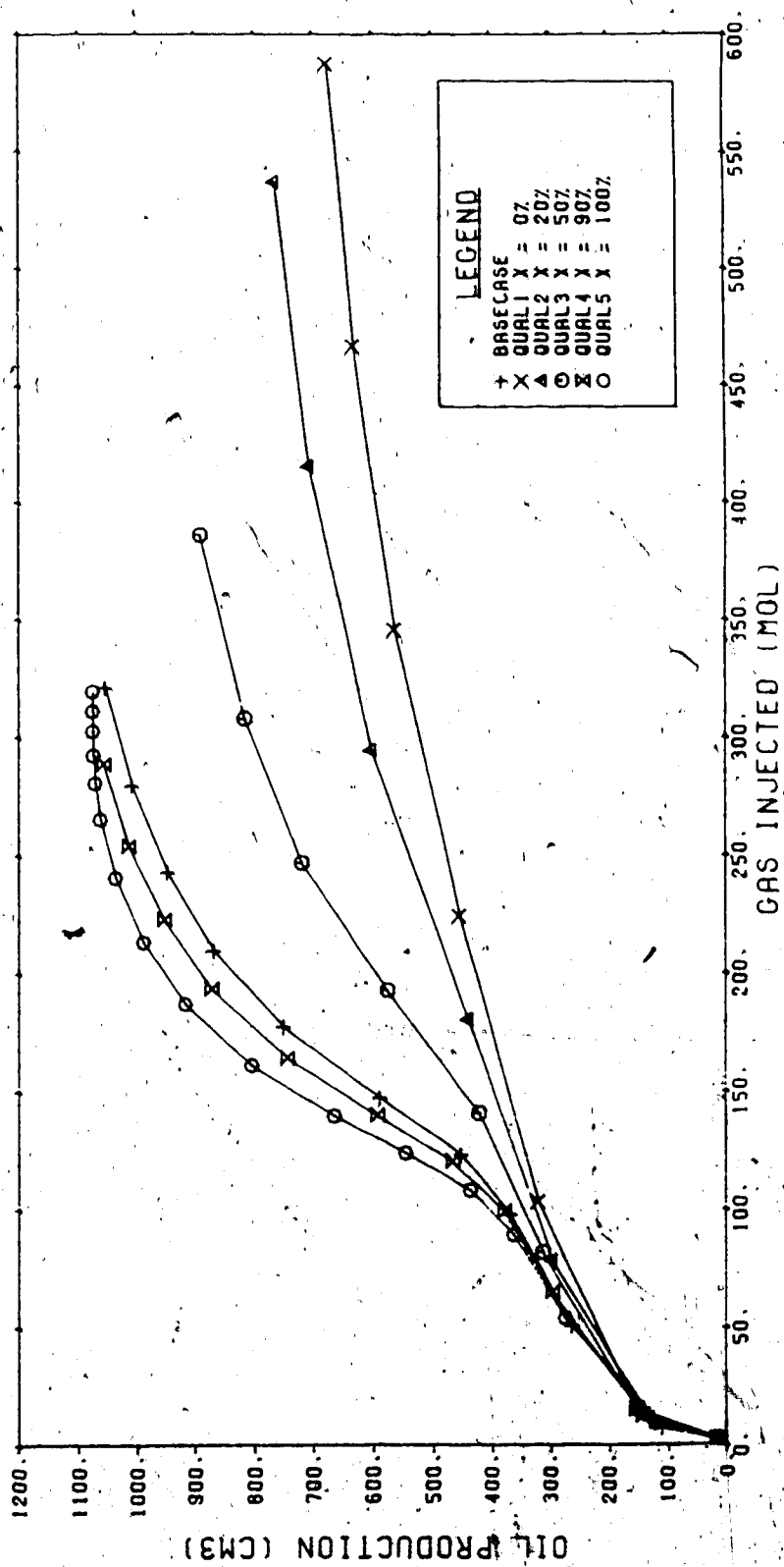


FIGURE 6.27 CUMULATIVE OIL PRODUCTION HISTORIES
STEAM QUALITY SENSITIVITY



Increasing the gas/steam ratio slightly increases early production response as illustrated in Figure 6.28. High gas injection rates tend to flatten out the temperature profiles as shown in Figures 6.29 and 6.30.

Figure 6.31 shows that changing the CO_2/N_2 ratio of the injected gas has no effect on the results.

Figure 6.32 indicates the effect of back pressure on oil production performance. The lower pressure case shows superior performance to the base case because of the increased volume occupied by the gas. Similarly the high pressure case shows inferior performance to the base case.

6. Discussion

Tables 6.13 and 6.14 summarize the results of the numerical simulation sensitivity studies. It is clear that thermal effects including heat loss, injected steam quality and rate are very important to the process. Coupled to this is the naturally strong dependence of the predominantly thermal process to oil viscosity. Porosity and initial oil saturation which affect the amount of oil originally in place are also understandably important parameters. The process is very sensitive to relative permeability curve parameters.

The sensitivity studies conducted thus far positioned the author to undertake a more representative modelling of the process using the numerical model.

FIGURE 6.28
CUMULATIVE OIL PRODUCTION HISTORIES -
GAS/STEAM RATIO SENSITIVITIES

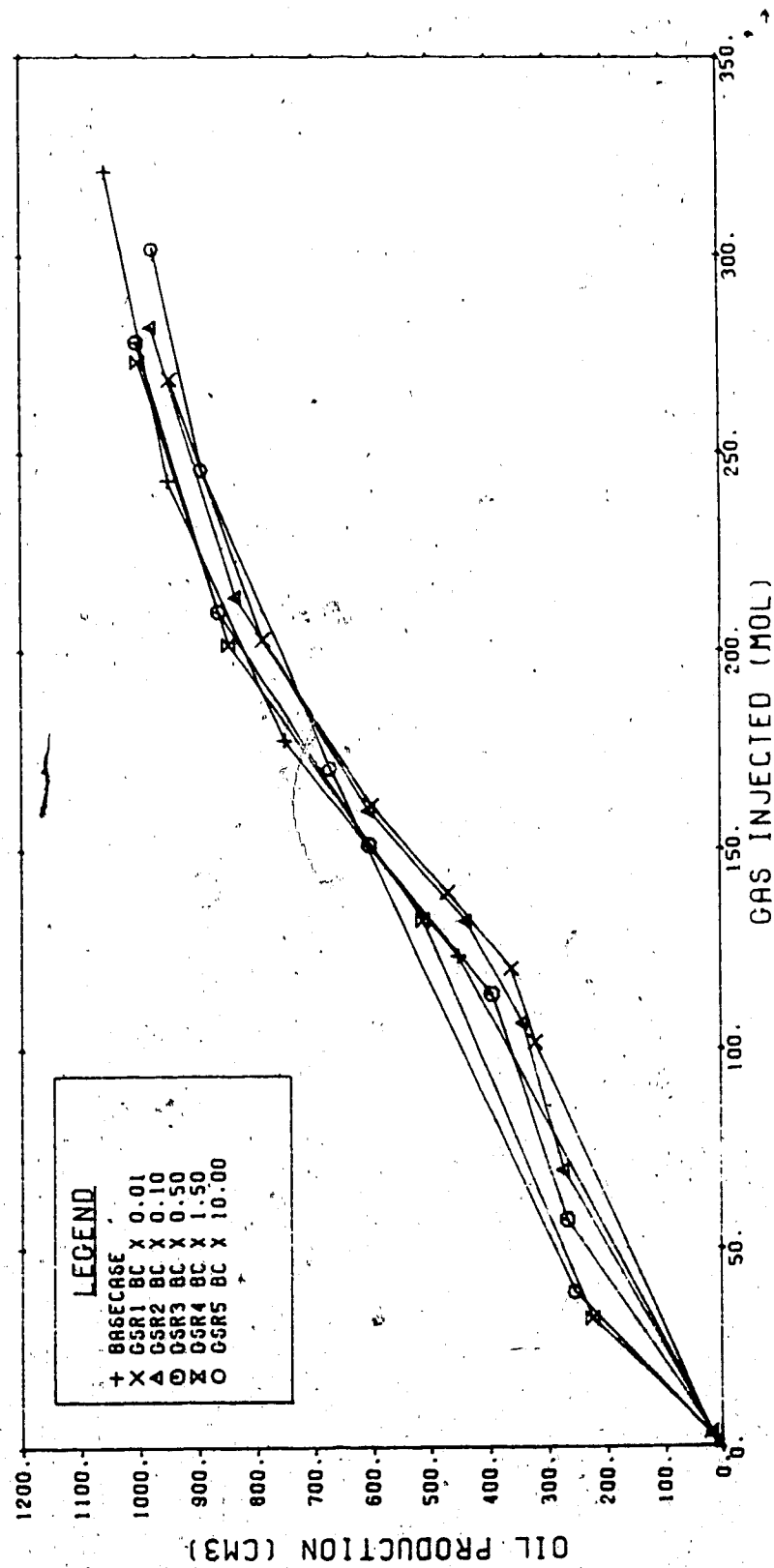


FIGURE 6.29 NUMERICAL MODEL TEMPERATURE PROFILES
GAS/STEAM RATIO CASE 1

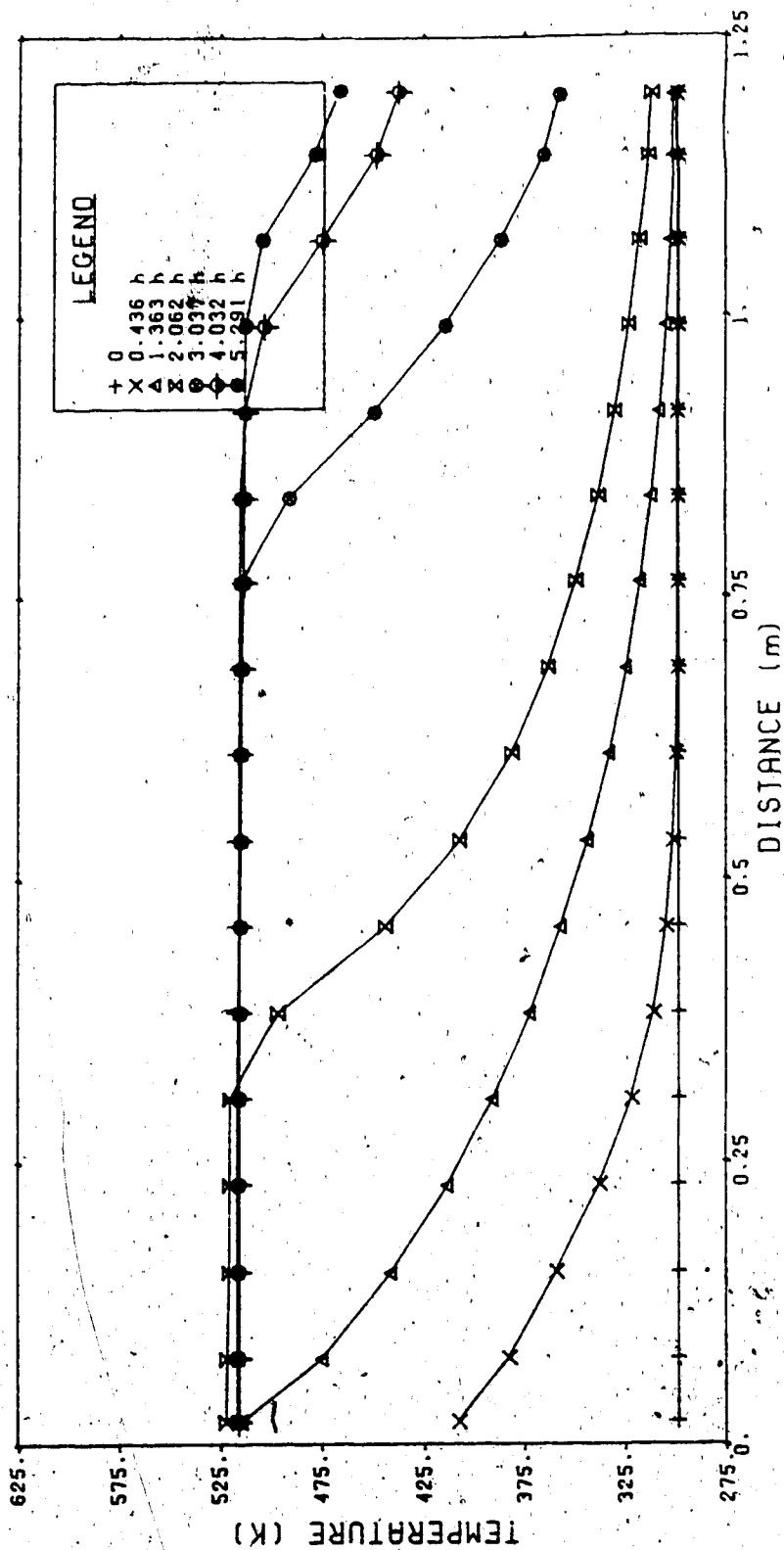


FIGURE 6.30 NUMERICAL MODEL TEMPERATURE PROFILES
GAS/STEAM RATIO CASE 4

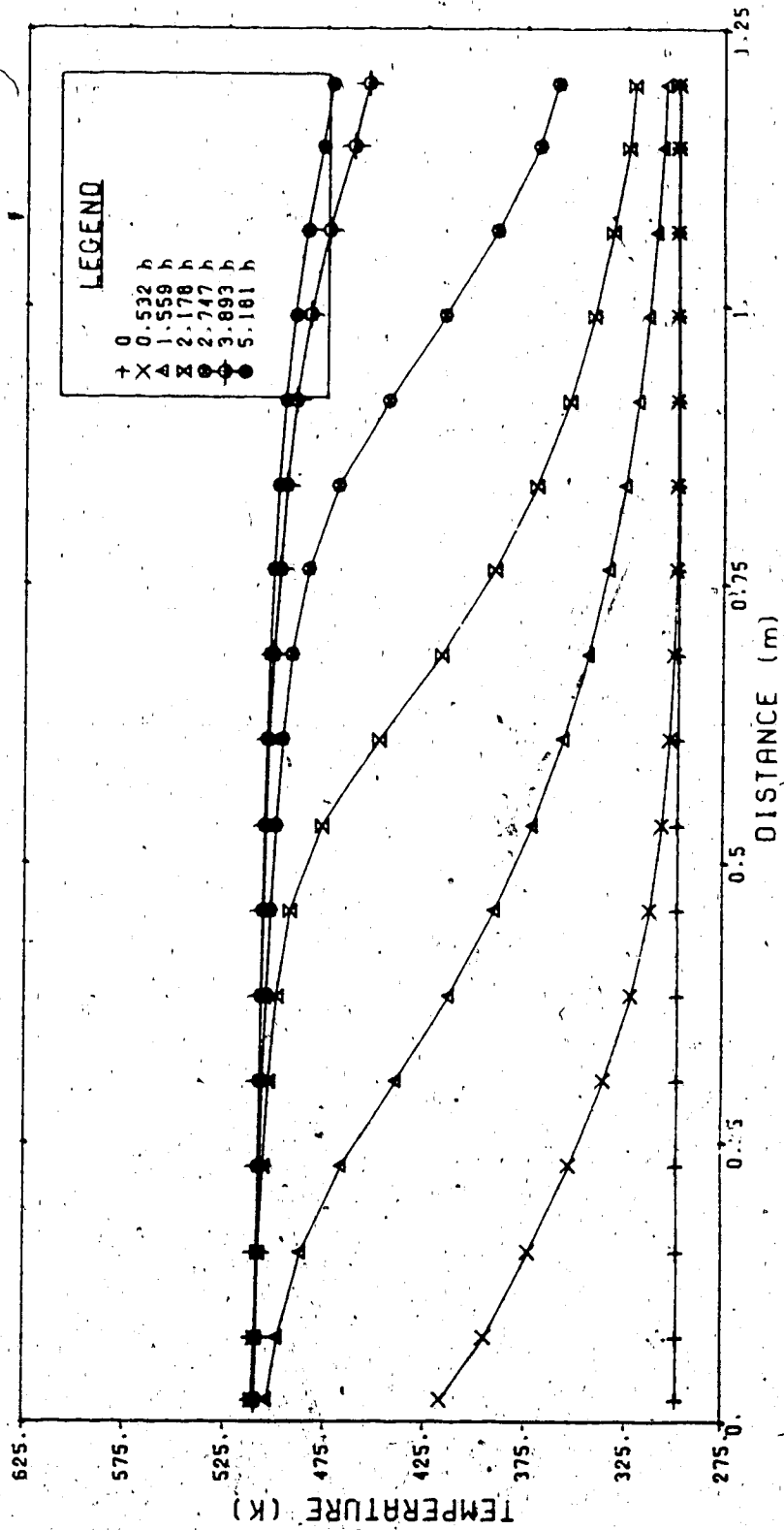


FIGURE 6.31 CUMULATIVE OIL PRODUCTION HISTORIES
CO₂/N₂ RATIO SENSITIVITY

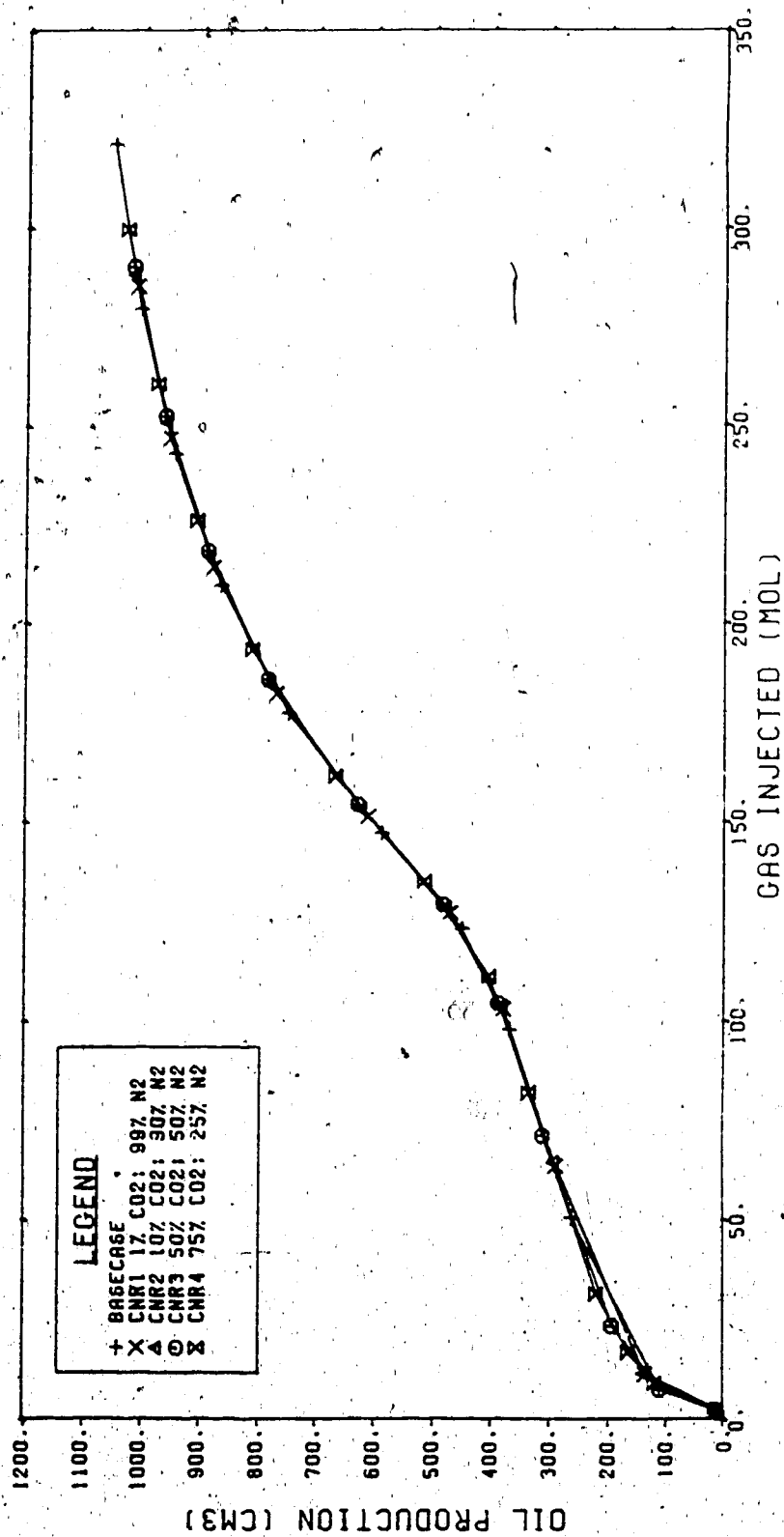


FIGURE 6.32 CUMULATIVE OIL PRODUCTION HISTORIES
BACK PRESSURE SENSITIVITY

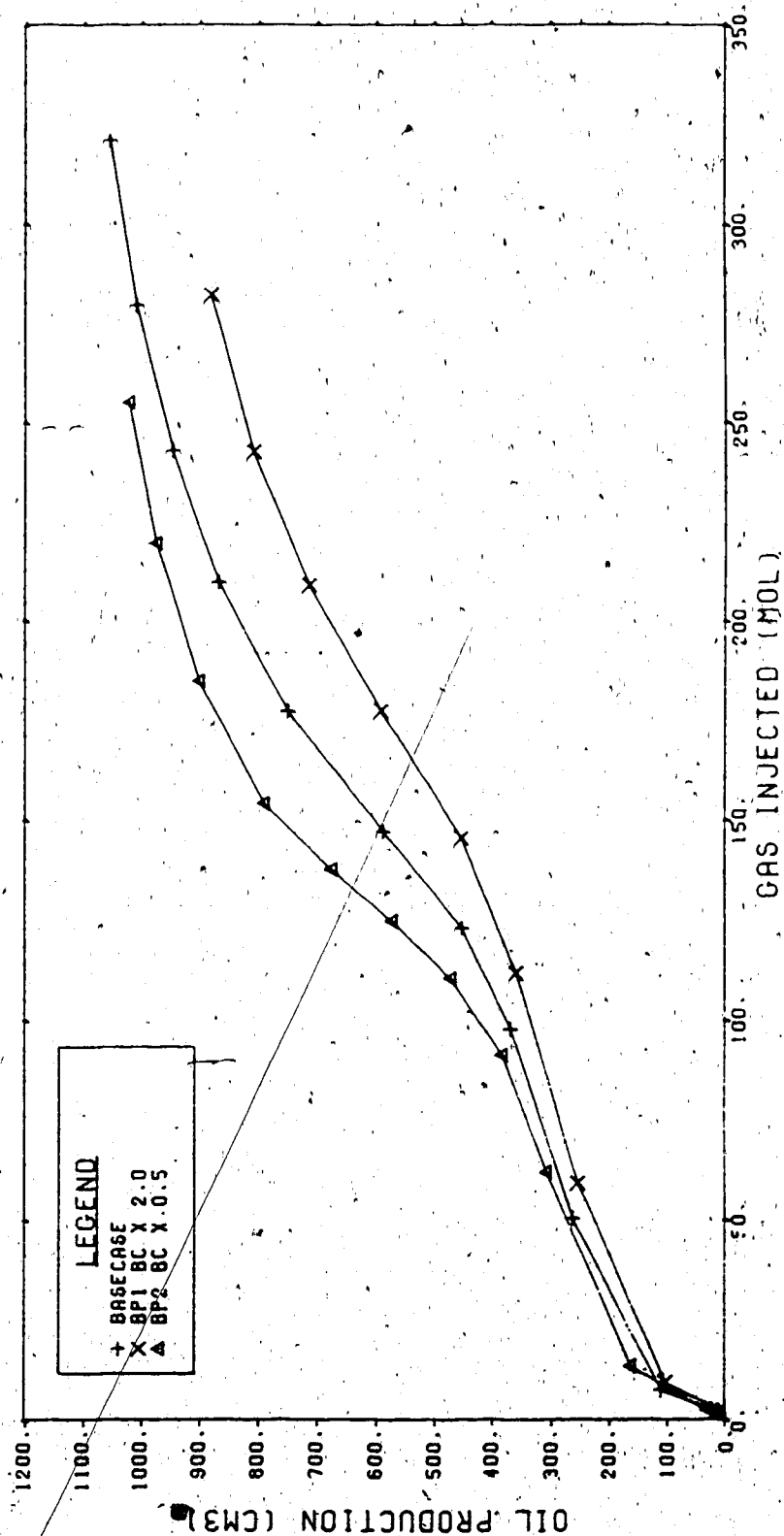


TABLE 6.13

SUMMARY OF RESERVOIR PARAMETER SENSITIVITY RESULTSSENSITIVITY CASECONCLUSIONS

Grid	17 block one-dimensional grid provides adequate accuracy
Heat Loss	major effect on heat front movement and oil production
Porosity	major effect due to difference in oil in place
Absolute Permeability	negligible effect
Rock Compressibility	negligible effect
Rock Heat Capacity	minor effect; changes steepness of temperature profiles
Initial Oil Saturation	major effect
Residual Oil Saturation	minor effect; alters ultimate oil recovery
Irreducible Water Saturation	minor effect; alters initial oil production rate
Critical Gas Saturation	minor effect; alters initial oil production rate
Relative Permeability Curve Shape	major effect

TABLE 6.14

SUMMARY OF FLUID PROPERTY AND PROCESS SENSITIVITY RESULTS

<u>SENSITIVITY CASE</u>	<u>CONCLUSIONS</u>
Oil Viscosity	major effect on oil production rate and recovery
CO ₂ Solubility	negligible effect
Light Oil Volatility	major effect; accelerates oil production rate late in run
Fluid Rates	major effect by reducing injection rates
Steam Quality	major effect
Gas/Steam Ratio	minor effect
CO ₂ /N ₂ Ratio	negligible effect
Back Pressure	major effect due to volume occupied by gas

At this point the simulator has not demonstrated to the same extent the gas drive acceleration of oil recovery experienced in the laboratory tests. The next section outlines efforts to do this.

0. Representative Simulation Results

1. Data Set Development

In order to confirm the validity of numerical simulation results a history match of the laboratory data was conducted. The experimental runs 4 (steam-only) and 6 (steam/flue gas) were history matched using the mathematical model. Actual run conditions and sand pack properties of the two laboratory experiments were used in the numerical simulator. The same heat loss parameters, fluid property data, phase behaviour description and relative permeability exponents were used when simulating the two experiments. Only the relative permeability end points differed to reflect the different initial conditions which existed in the experiments. Table 6.15 identifies differences in input data between the base case simulation run for the sensitivity study (RELTST1), the experimental test 4 simulation (HMS01), and the experimental test 6 simulation (HMEG1).

Several other changes were made to the history matching data sets in comparison to the base case for the sensitivity study. In the base case the oil phase viscosities for the light oil and heavy oil components were

Table 6.15

INPUT DATA USED FOR HISTORY MATCHING

	BASE CASE (RELTST1)	STEAM ONLY MATCH (HMS01)	STEAM/FLUE MATCH (HMEG)
Porosity, percent	45.0	44.8	39.3
Absolute Permeability, μm^2	10.0	12.9	18.4
Initial Oil Saturation, %PV	79.869	75.007	85.008
Initial Water Saturation, %PV	20.040	24.902	14.901
Rock Heat Capacity, kJ/kg.K	0.835	1.00	1.00
Rock Compressibility, 1/kPa	4.350×10^{-6}	4.35×10^{-7}	4.35×10^{-7}
Injection Rates, mol/s			
Steam	1.543×10^{-2}	1.859×10^{-2}	1.722×10^{-1}
CO ₂	1.782×10^{-4}	1.643×10^{-5}	1.643×10^{-3}
N ₂	5.347×10^{-4}	6.468×10^{-5}	6.468×10^{-3}
Injected Fluid Enthalpies, J/mol			
Steam	4.489×10^4	4.979×10^4	4.982×10^4
CO ₂	9.734×10^3	9.734×10^3	9.734×10^3
N ₂	6.120×10^3	6.120×10^3	6.120×10^3
Back Pressure, kPa (gauge)	3.364×10^3	3.323×10^3	3.323×10^3
k_{rwro}	1.0	1.0	1.0
k_{ro1w}	1.0	1.0	1.0
k_{rgo}	1.0	0.4	0.4
S_{wir}	0.200	0.249	0.149
S_{or}	0.200	0.070	0.050
S_{gc}	0.010	0.100	0.100
EX_{krw}	2.0	1.25	1.25
EX_{krow}	2.0	1.75	1.75
EX_{krq}	2.0	3.75	3.75
U_v , J/s.m ² .K	2.0	4.0	4.0
U_L , J/s.m ² .K	5.0	4.5	4.5
h , J/s.m ² .K	2.50×10^3	7.50×10^3	7.500×10^3
$(hA/C_p V)$, 1/s	-3.0×10^{-4}	-4.0×10^{-4}	-4.0×10^{-4}

assumed to be the same, and were described as:

$$\mu_{l.o.} = \mu_{h.o.} = 1.929 \times 10^{-2} \exp (2.897 \times 10^3 / T) \quad (6.4)$$

In the history matching data sets the oil components had different viscosities and were set to yield the same initial viscosity of the mixture as in the base case. The history matching viscosities were described as:

$$\mu_{l.o.} = 1.929 \times 10^{-3} \exp (2.897 \times 10^3 / T) \quad (6.5)$$

$$\mu_{h.o.} = 2.979 \times 10^{-2} \exp (2.897 \times 10^3 / T) \quad (6.6)$$

The viscosity of carbon dioxide when present in the oil phase was described in the history matching simulations as in Hong and Ault (1984) and therefore:

$$\mu_{CO_2} = 4.438 \times 10^{-2} \exp (5.971 \times 10^2 / T) \quad (6.7)$$

This expression yielded a larger viscosity reduction effect due to carbon dioxide compared to the base case. In the base case the density of carbon dioxide in the liquid phase was $25.0 \times 10^3 \text{ mol/m}^3$ and this was decreased to $10.87 \times 10^3 \text{ mol/m}^3$ to improve representation of oil swelling due to the presence of carbon dioxide in solution.

The history match was achieved primarily by adjusting heat loss parameters and relative permeability curve shapes and end points.

2. History Match Results

Figure 6.33 compares the cumulative oil production histories for experimental runs 4 (steam-only) and 6 (steam/flue gas) with the simulation history match data sets for these cases. It may be observed that although the matches are not exact, the characteristically high oil production in the early part of the steam/flue gas experiment is observed. Injection pressure histories for the same cases described above are shown in Figure 6.34. Temperature profiles for the steam-only (HMS01) and steam/flue gas (HMEG1) simulation cases are shown in Figures 6.35 and 6.36, respectively.

3. Process and Parameter Sensitivities

The more representative and realistic data sets used in the history match simulations were tested for sensitivity to gas/steam ratio, CO_2/N_2 ratio and CO_2 solubility to compare with the results from the earlier sensitivity study. Figure 6.37 shows the effect of changing these conditions on the performance of the steam-gas injection process.

Reducing the gas/steam ratio by a factor of 10 has a much more noticeable effect on the history match data than it did in the sensitivity study (see Figure 6.28). It should be remembered that the relative permeabilities used for the history match demonstrate the gas drive effect on oil recovery whereas the sensitivity study runs did not

FIGURE 6.33 CUMULATIVE OIL PRODUCTION HISTORIES -
HISTORY MATCH OF LABORATORY EXPERIMENTS
WITH NUMERICAL SIMULATION MODEL

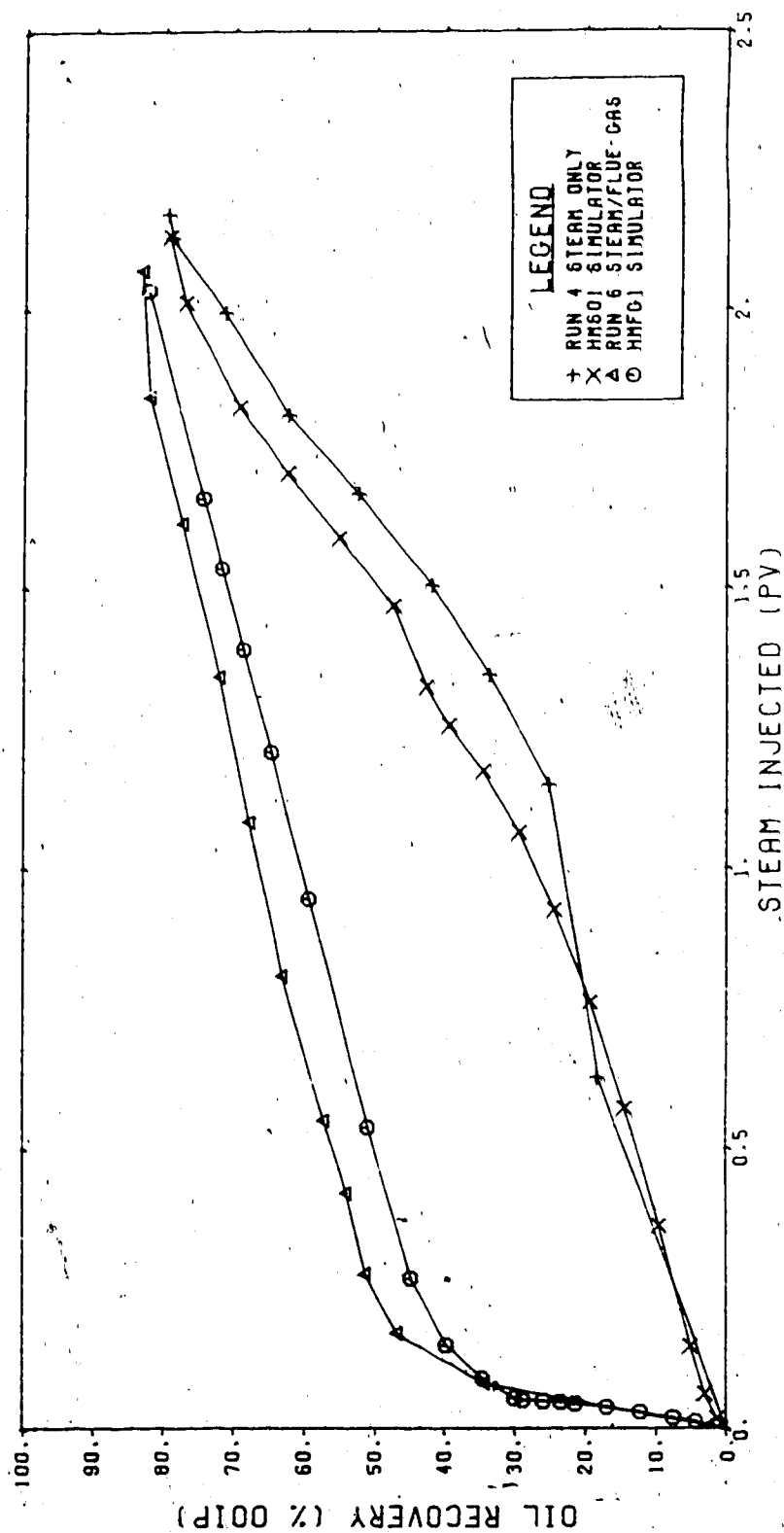


FIGURE 6.34' INLET PRESSURE HISTORIES -
HISTORY MATCH OF LABORATORY EXPERIMENTS
WITH NUMERICAL SIMULATION MODEL

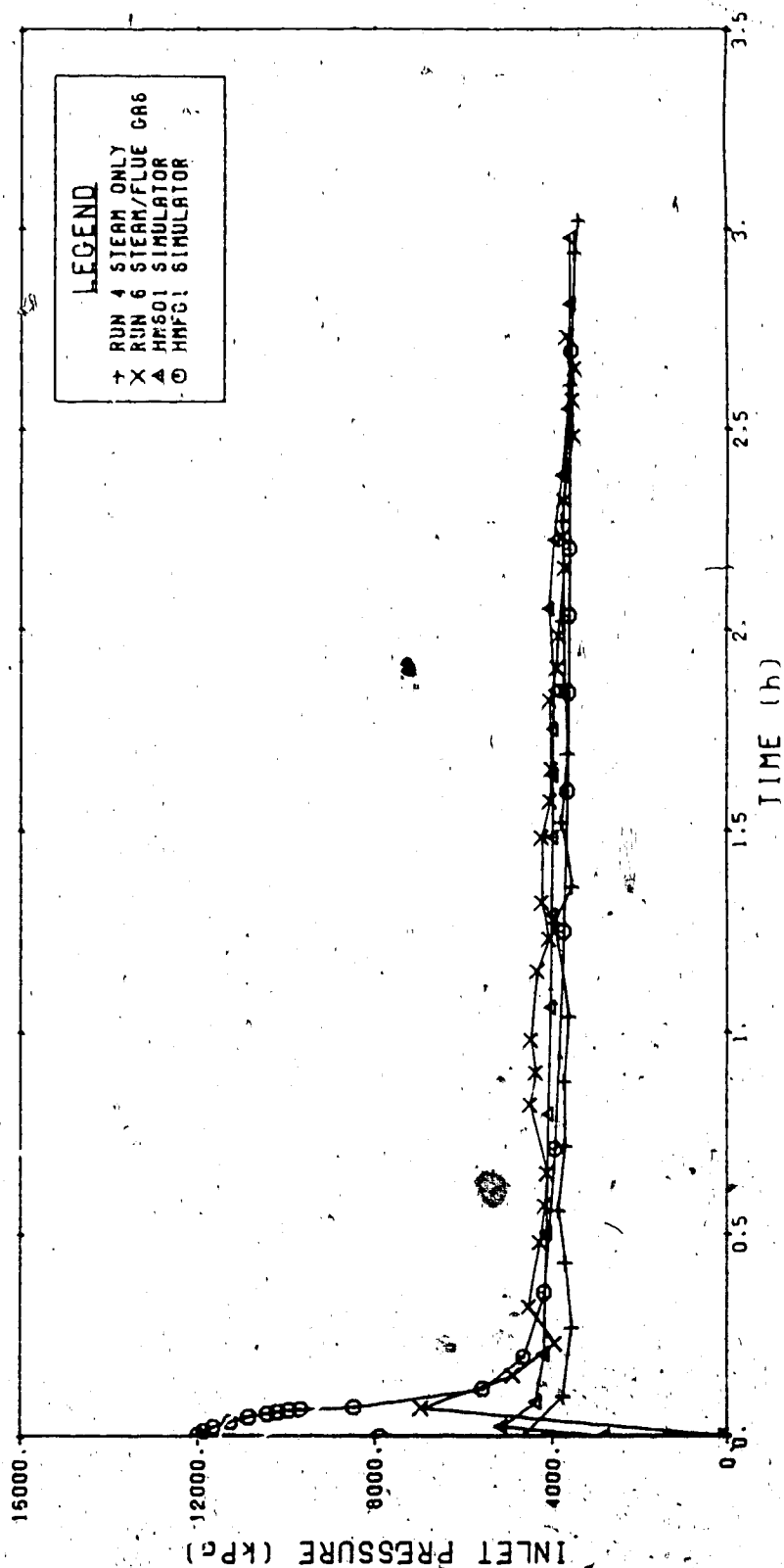


FIGURE 6.35
 NUMERICAL MODEL TEMPERATURE PROFILES
 HISTORY MATCH OF STEAM ONLY EXPERIMENT

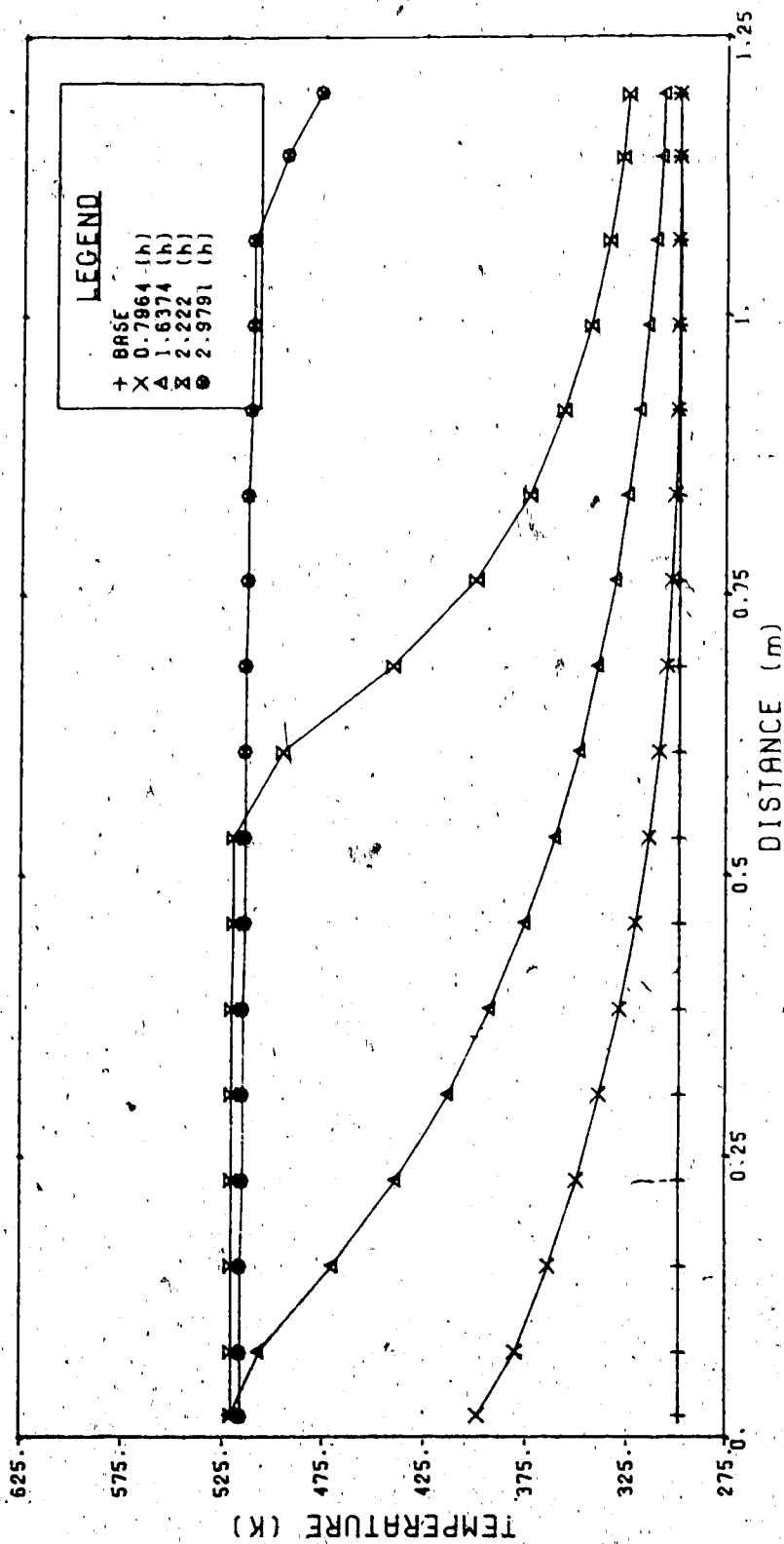


FIGURE 6.36
 NUMERICAL MODEL TEMPERATURE PROFILES
 HISTORY MATCH OF STEAM/FLUE GAS EXPERIMENT

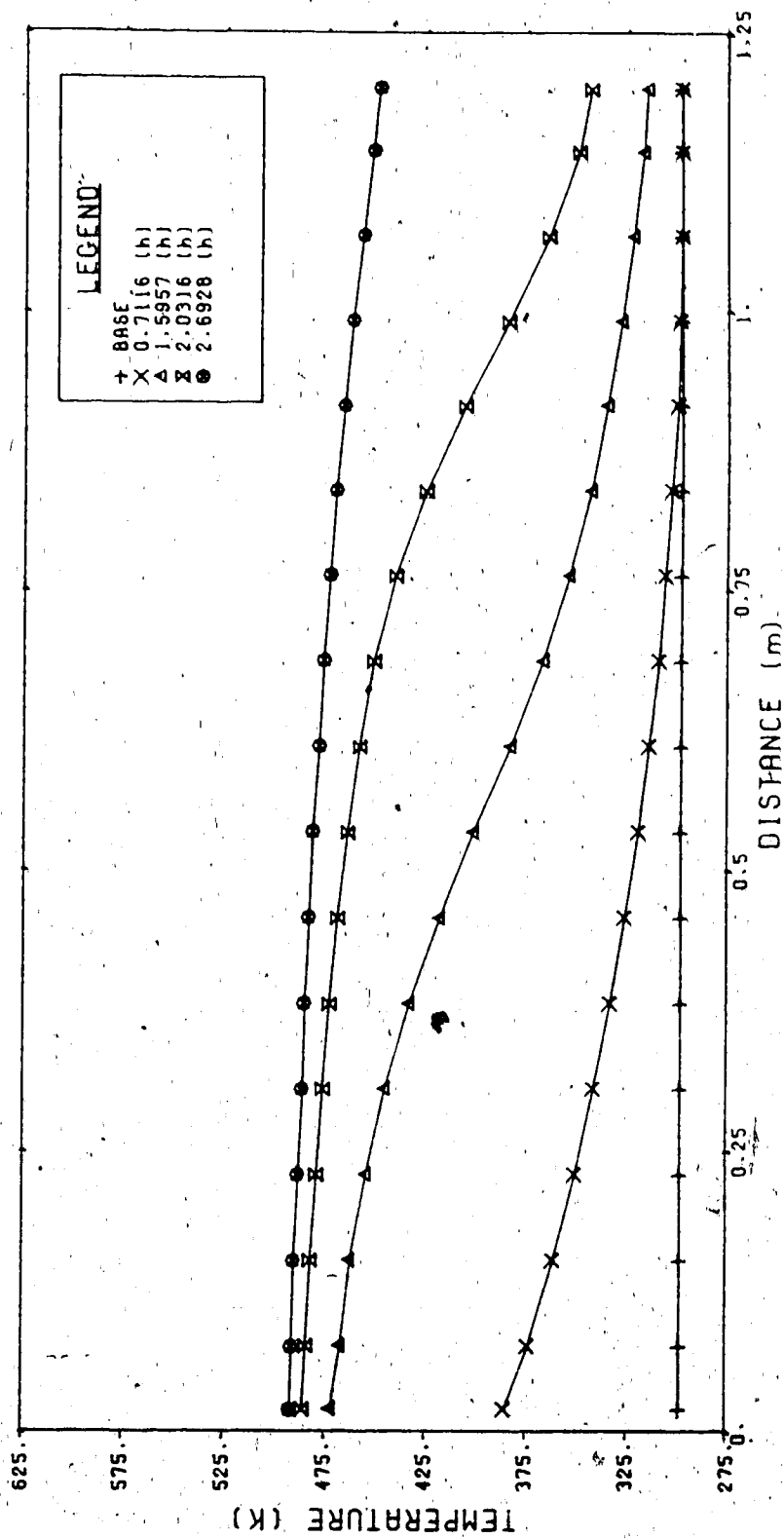
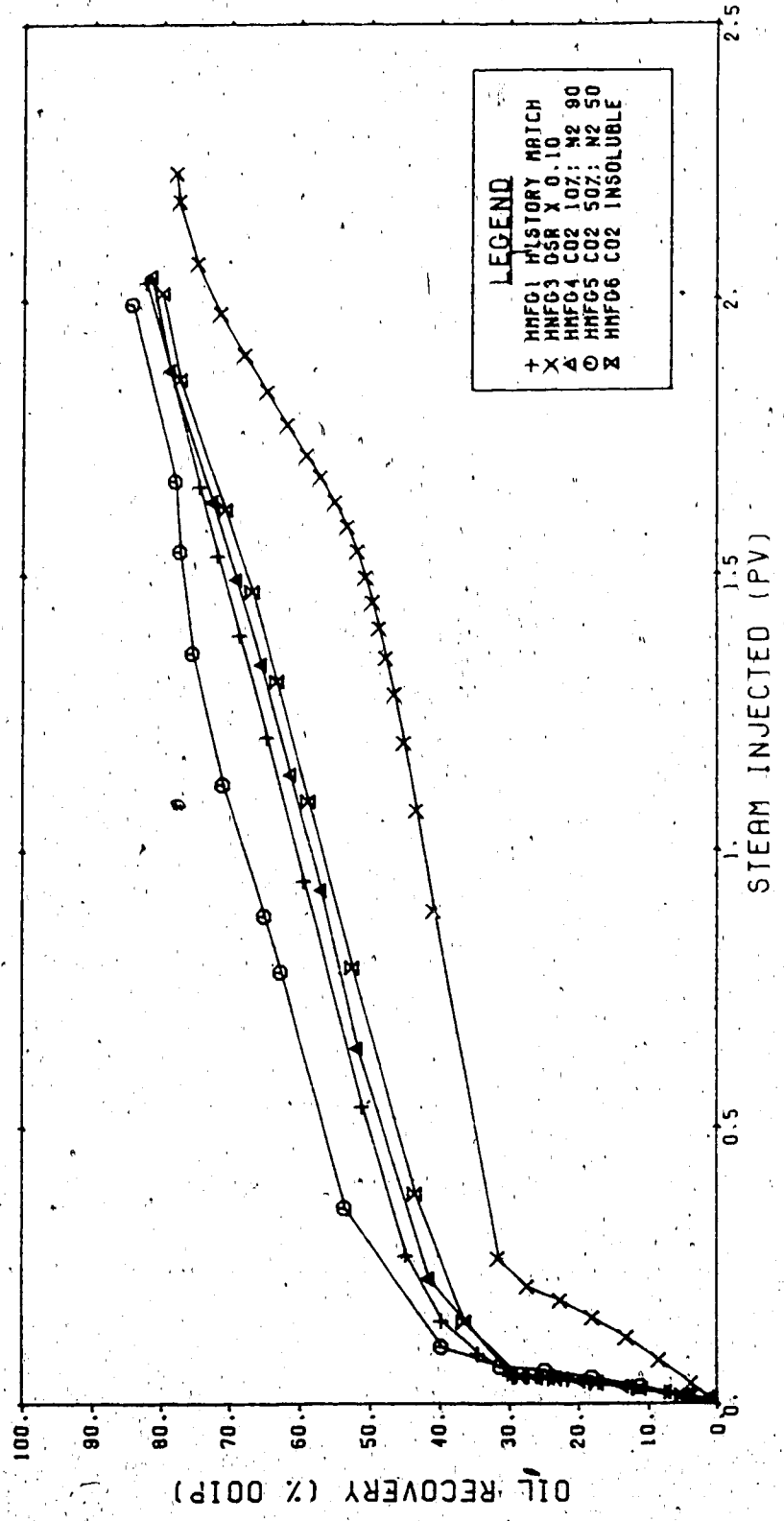


FIGURE 6.37
CUMULATIVE OIL PRODUCTION HISTORIES
PARAMETER AND PROCESS SENSITIVITIES.



show this effect to nearly the same extent.

The effect of CO₂/N₂ ratio is also much more pronounced in the later simulations than in the sensitivity study (Figure 6.31). A decrease in the concentration of CO₂ from 25 percent (HMFG1) to 10% (HMFG4) caused a small reduction in oil recovery throughout. Increasing the concentration of CO₂ in the injected gas to 50 percent (HMFG5) had a marked effect. It may be observed that the performance of this simulation run almost perfectly matches the laboratory experiment number 6 (see Figure 6.33). Increasing the viscosity reduction effect or the solubility of the CO₂ would have a similar effect to raising its concentration in the injected gas. Removing CO₂ solubility entirely (HMFG6) had a further modest effect in reducing oil recovery performance.

4. Discussion

It is evident from examination of Figure 6.37 that the process improvements demonstrated by flue gas or carbon dioxide co-injection with steam are attributable to both gas drive and solubility effects. In the case of steam/CO₂ injection (e.g. experiment run 7), the gas/steam ratio was lower compared to the steam/flue gas experiments but the partial pressure of CO₂ was higher yielding larger amounts of CO₂ in solution. Therefore viscosity reduction and swelling would be more important in the latter case. The performance of both the steam/CO₂ and steam/flue gas

experiments was markedly different from the steam only experiment (Figure 4.5). The simulator has demonstrated that the only way for the steam/CO₂ and steam/flue gas experiments to yield such similar results is for the effect of reduced gas/steam ratio in the steam/CO₂ test to be exactly compensated for by the increased gas solubility effects.

Improvements in the history matches would be possible by reducing the critical gas saturation and raising the relative permeability to gas while at the same time increasing the viscosity reduction and swelling effects of the carbon dioxide. This would have the effect of reducing the inlet pressure peak in the history match while maintaining or even enhancing the early oil production response from steam/gas injection. Temperature profiles may be steepened by reducing gas phase heat capacities and by modifying the balance between heat losses along the test cell and those to the inlet end flange.

VII DISCUSSION OF RESULTS

The purpose of the present work was to identify the effects of the injection of gases with steam in the steamflood process as would result from the use of downhole steam generators or other equipment which would lead to the injection of stoichiometric amounts of combustion gas with steam. A review of the literature revealed that there was no experimental data of the type described in this work in the public domain at the time of its publication (June, 1982 and September, 1983).

A series of laboratory experiments was conducted in a one-dimensional system with a moderately viscous oil. The majority of the experiments involved the simultaneous injection of steam and gas additives but some tests were also done with slugs of gas followed by steam. The experiments compared steam-only flooding, with steam/CO₂, steam/N₂, and steam/CO₂/N₂ (or steam/flue gas) injection on sand packs flooded with oil down to critical water saturation and sand packs which had been previously water flooded.

In both pre- and post-waterflooded sand packs the addition of the gases to steam yielded significant acceleration of oil production. When cumulative oil recovery is plotted as a function of steam injected, there is relatively little difference evident when comparing the simultaneous steam/CO₂, steam/N₂ and steam/flue gas results (Figures 4.5A and 4.6A). When these data are plotted as functions of total gas injected in moles (Figures 4.5B and 4.6B), the steam/CO₂ process is clearly superior to the others.

The steam-only experiments are characterized by a slow oil production rate early in the experiments and then a rapid production of oil towards the end as the steam front progresses down the length of the apparatus. The steam/gas injection experiments show a very rapid early production response which levels off to a steady but modest rate leading to the end of the experiments.

There is a small but consistent improvement in overall recovery in the steam/gas injection cases compared to steam-only with steam/CO₂ yielding the highest recovery. When oil recovered during test cell depressurization is included in the comparison, the steam/CO₂ case shows even higher recovery and less difference is evident amongst the steam-only, steam/flue gas and steam/N₂ run recoveries for the pre-waterflood experiments. Steam-oil and water-oil ratios are consistently lower in the steam/gas processes compared to steam-only.

The results of the laboratory experiments may be explained on the basis of gas drive and solubility effects. It is postulated that the improvement in oil production rates is the result of non-condensable gas drive which promotes oil production and at the same time reduces the flow of water. The superior performance of the steam/CO₂ experiment which was conducted at a lower gas/steam ratio than the steam/flue gas test may be explained by including oil viscosity reduction and swelling effects of the soluble CO₂. The ultimate recovery is dictated primarily by the residual oil saturation following heating to steam temperatures.

Steamflooding following waterflooding (Figure 4.7) shows poor initial oil production response since the steamflood behaves initially like a waterflood until the thermal effects begin to dominate in the latter half of the experiment. The steamfloods following slug gas injection perform better because the initial waterflood-like stage of the steamflood is able to displace more oil.

The performance of two steam/flue gas experiments at two pressures is shown in Figure 4.10. The oil production in the high pressure case begins more slowly but exceeds the low pressure case on a cumulative basis 25 percent into the run. This behaviour may be explained by considering that the gas drive effect is lower in the high pressure case initially because of the smaller volume occupied by the gas. However, more gas enters solution in the oil at the higher pressure and this effect begins to alter the comparison in favour of the high pressure case due to solubility effects. This behaviour comparison is similar to that between the steam/CO₂ and steam/flue gas run. In essence, the high pressure flue gas behaves like a smaller volume, but higher solubility, gas such as in the steam/CO₂ test.

It appears that although the residence time of the gas in the experimental cell was low in all tests, there was sufficient time for soluble gas to enter solution in the viscous oil and thus contribute to oil production through viscosity reduction and swelling.

A fully implicit thermal reservoir simulation model was written to aid in the interpretation of the experimental results. There are few models of this type whose formulation allows solubility of all components in water as well as oil. The simulator models the flow of 3 phases and 5 components. The model was used to history match two of the laboratory experiments. Parameter and process sensitivities were also examined using the model.

It was demonstrated that the laboratory process was very sensitive to thermal effects including heat losses and injected steam quality and rate. Porosity, oil saturation, viscosity and volatility were important parameters along with relative permeabilities. Absolute permeability, rock heat capacity and compressibility were found to have relatively minor influence.

The initial sensitivity study showed that gas/steam ratio and CO₂ solubility effects were also unimportant. However, following history matching of the laboratory experiments, a different conclusion was reached. The history match data set had more representative relative permeabilities as well as improvements in modelling of viscosity reduction and swelling effects due to CO₂ in solution. The history match was obtained primarily by varying heat loss and relative permeability data. The numerical model achieved its purpose in allowing better interpretation of the laboratory experiments as described above.

VIII CONCLUSIONS AND RECOMMENDATIONS

The physical and numerical modelling of steam/gas injection processes conducted in this study support the following conclusions:

1. In the system studied, injection of flue gas or carbon dioxide simultaneously with steam in approximately stoichiometric amounts results in much accelerated oil production response.
2. A modest improvement in total oil recovery results from the steam/gas floods compared to steam-only injection. The steam/CO₂ process yielded the highest recovery.
3. Steam-oil and water-oil ratios are reduced through use of gas additives.
4. Improvement in steamflood performance occurs for both pre- and post-waterflooded sand packs.
5. On the basis of total molar fluid injection, the steam/CO₂ process is superior to the steam/flue gas process.
6. The improvement in performance of the steam/gas processes is attributable to non-condensable gas drive and to solubility effects including viscosity reduction and swelling.
7. The laboratory steamflood process is sensitive to the following effects: heat losses; steam quality and injection rate; oil saturation, viscosity and volatility; porosity and relative permeability; gas/steam ratio and CO₂/N₂ ratio; and gas solubility.
8. The laboratory steamflood process was relatively insensitive to absolute permeability, rock compressibility and heat capacity.

Further development of steam/gas injection process reservoir engineering technology would involve the following laboratory work:

1. Studies using real core material and a variety of field crude samples in the viscosity range from 100 to 10 000 mPa.s.
2. Investigation of the effect of alternating slugs of gas and steam.
3. Optimization of gas/steam and CO₂/N₂ ratios for specific reservoir cases.
4. Identification of gravity override and gas channelling phenomena in 2 or 3 dimensional test beds.
5. Quantification of potential solution gas drive benefits by operating the back pressure in a cycling mode as in Redford (1982) and by conducting steam stimulation experiments with gas additives.

The steam/gas injection has shown enough potential for process improvement to warrant further investigation and possible field trials. Prior to conducting field tests, field scale numerical modelling in 2 or 3 dimensions should be undertaken. Cost benefit analyses of the use of such processes could then be undertaken.

IX. REFERENCES

Anon.: "Development of a Downhole Steam Generator System", Report SAND 83-7121 prepared by Foster-Miller, Inc. for Sandia National Laboratories, Albuquerque, New Mexico, April 1984.

Abdalla, A. and Coats, K. H.: "A Three-Phase, Experimental and Numerical Simulation Study of the Steamflood Process", SPE 3600 presented at the 46th Annual Fall Meeting, New Orleans, Oct. 3-6, 1971.

Abou-Kassem, J. H.: "Investigation of Grid Orientation in a Two-Dimensional, Compositional, Three-Phase Steam Model", Ph. D. Thesis, The University of Calgary, April 1981.

Abou-Kassem, J. H. and Aziz, K.: "Sensitivity of Steamflood Model Results to Grid and Time Step Sizes", SPE 11080 presented at the 57th Annual Fall Technical Conference and Exhibition, New Orleans, Sep. 26-29, 1982.

Adler, G.: "A Linear Model and a Related Very Stable Numerical Method for Thermal Secondary Oil Recovery", Journal of Canadian Petroleum Technology, July-Sep. 1975, pp. 56-65.

Anderson, H. R., Stosur, J. J. and Marshall, B. W.: "U.S. Department of Energy R and D on Downhole Steam Generation for the Recovery of Heavy Oil", UNITAR Second International Conference on Heavy Crude and Tar Sands, Caracas, 1982.

Aziz, K. and Settari, A.: Petroleum Reservoir Simulation, Applied Science Publishers, London, 1979.

Bader, B. E., Fox, R. L. and Stosur, J. J.: "The Potential of Downhole Steam Generation to the Recovery of Heavy Oils", UNITAR First International Conference on the Future of Heavy Crude and Tar Sand, Edmonton, 1979.

Balog, S. E., Kerr, R. K. and Pradt, L. A.: "The Wet Air Oxidation Boiler for Enhanced Oil Recovery", Journal of Canadian Petroleum Technology, Sep.-Oct., 1982, pp. 73-79.

Boden, J. C., Fearnley, P. J., McMahon, M. and Riddiford, F. A.: "Downhole Steam Generator for Enhanced Oil Recovery", Proceedings, 2nd E.C. Symposium, Luxemburg, December 5-7, 1984.

Buchanan, W. L.: "Simulating Steam Additive EOR Processes", SPE 13522 presented at the Reservoir Simulation Symposium, Dallas, Texas, Feb. 10-13, 1985.

Chemical Engineers Handbook, Fourth Edition. Editors R. H. Perry, C. H. Chilton and S. D. Kirkpatrick, McGraw-Hill Book Company, 1963.

Chesters, D. A., Clark, C. J. and Riddiford, F. A.: "Downhole Steam Generation Using a Pulsed Burner", Proceedings, European Symposium on Enhanced Oil Recovery, Bournemouth, England, September 21-23, 1981.

Clark, S. W.: "Wet Oxidation Downhole Steam Generator for Recovery of Deep Heavy Oil", UNITAR Third International Conference on Heavy Crude and Tar Sands, Long Beach, California, 1985.

Coats, K. H., George, W. D., Chu, C. and Marcum, B. E.: "Three-Dimensional Simulation of Steamflooding", Trans. AIME, v. 257, 1974, pp. 573-592.

Coats, K. H.: "Simulation of Steamflooding with Distillation and Solution Gas", Society of Petroleum Engineers Journal, Oct. 1976, v. 16, n. 5, pp. 235-247.

Coats, K. H.: "A Highly Implicit Steamflood Model", Society of Petroleum Engineers Journal, Oct. 1978, v. 18, n. 5, pp. 369-383.

Coats, K. H.: "An Equation of State Compositional Model", Society of Petroleum Engineers Journal, Oct. 1980, pp. 363-376.

Coats, K. H.: "In-Situ Combustion Model", Society of Petroleum Engineers Journal, Dec. 1980, pp. 533-554.

Craft, B. C. and Hawkins, M. F.: Applied Petroleum Reservoir Engineering, Prentice-Hall, Inc., Englewood Cliffs, N. J., 1959.

Crookston, R. B., Culham, W. E. and Chen, W. H.: "A Numerical Simulation Model for Thermal Recovery Processes", Society of Petroleum Engineers Journal, Feb. 1979, pp. 37-58.

Culham, W. E., Farouq Ali, S. M. and Stahl, C. D.: "Experimental and Numerical Simulation of Two-Phase Flow with Interphase Mass Transfer in One and Two Dimensions", Society of Petroleum Engineers Journal, Sep. 1969, pp. 323-337.

Dake, L. P.: Fundamentals of Reservoir Engineering, Elsevier Scientific Publishing Company, New York, 1978, pp. 19-20.

Dean, D. E. and Stiel, L. I.: "The Viscosity of Nonpolar Gas Mixtures at Moderate and High Pressures", American Institute of Chemical Engineers Journal, May 1965, v. 11, pp. 526-531.

Demetre, G. P., Bentsen, R. G. and Flock, D. L.: "A Multi-Dimensional Approach to Scaled Immiscible Fluid Displacement", Journal of Canadian Petroleum Technology, July-Aug. 1982, v. 21, n. 4, pp. 49-61.

Dodds, W. S., Stutzman, L. F. and Sollami, B. J.: "Carbon Dioxide Solubility in Water", Journal of Industrial and Engineering Chemistry, 1956, v. 1, pp. 92-95.

Eggenschwiler, M. and Farouq Ali, S. M.: "Two-Dimensional, Single Phase Simulation of a Fireflood", CIM Special Volume 17, The Oil Sands of Canada-Venezuela, 1977, pp. 487-495.

Engineering Data Book, Ninth Edition. Gas Processors' Suppliers' Association, Tulsa, Oklahoma, 1972.

Eson, R. L.: "Downhole Steam Generator - Field Tests", SPE 10745 presented at the California Regional Meeting, San Francisco, March 24-26, 1982.

Etter, D. D. and Kay, W. B.: "Critical Properties of Mixtures of Normal Paraffin Hydrocarbons", Journal of Chemical and Engineering Data, 1961, pp. 409-414.

Farouq Ali, S. M.: Oil Recovery by Steam Injection, Producers Publishing Company, Bradford, Pa (1970).

Farouq Ali, S. M.: "Multiphase, Multidimensional Simulation of In-Situ Combustion", SPE 6896 presented at the 52nd Annual Fall Technical Conference and Exhibition, Denver, Oct. 9-12, 1977.

Farouq Ali, S. M. and Redford, D. A.: "Physical Modelling of In-Situ Recovery Methods for Oil Sands", CIM Special Volume 17, The Oil Sands of Canada-Venezuela, 1977, pp. 319-326.

Farouq Ali, S. M. and Ferrer, J.: "State-of-the-Art of Thermal Recovery Models", Trans. ASME, Dec. 1981, v. 103, pp. 296-300.

Ferrer, J. C. and Farouq Ali, S. M.: "A Three-Phase Two-Dimensional, Compositional Thermal Simulator for Steam Injection Processes", paper No. 7613 presented at the 27th Annual Technical Meeting of the Petroleum Society of CIM, Calgary, June 7-11, 1976.

Flock, D. L. and Lee, J.: "An Experimental Investigation of Steam Displacement of a Medium Gravity Crude Oil", CIM Special Volume 17, The Oil Sands of Canada-Venezuela, 1977, pp. 386-394.

Fox, R. L., Donaldson, A. B. and Mulac, A. J.: "Development of Technology for Downhole Steam Production", SPE/DOE 9776 presented at the Second Joint Symposium on Enhanced Oil Recovery, Tulsa, April 5-8, 1981.

Fox, R. L. and Donaldson, A. B.: "Production of Heavy Crude Using Downhole Steam Generators", UNITAR Third International Conference on Heavy Crude and Tar Sands, Long Beach, California, 1985.

Friefeld, J. M., Stabinsky, L. and Pilger, P. F.: "Field Test of a Direct-Fired Downhole Steam Generator", Proceedings, Pacific Coast Oil Show and Conference, Bakersfield, California, Nov. 15-17, 1983, 13 pp.

Fussel, D. D. and Yanosik, J. L.: "An Iterative Sequence for Phase-Equilibria Calculations Incorporating the Redlich-Kwong Equation of State", Society of Petroleum Engineers Journal, June 1978, pp. 173-182.

Fussel, L. T. and Fussel, D. D.: "An Iterative Technique for Compositional Reservoir Models", Society of Petroleum Engineers Journal, Aug. 1979, pp. 211-220.

Garon, A. M., Geisbrecht, R. A. and Lowry, W. E., Jr.: "Scaled Model Experiments of Fireflooding in Tar Sands", Journal of Petroleum Technology, Sep. 1982, v. 34, n. 9, pp. 2158-2166.

Goodley, A.: "Air Quality Impact of Thermally-Enhanced Heavy Oil Recovery in California, U. S. A.", UNITAR First International Conference on the Future of Heavy Crude and Tar Sand, Edmonton, 1979.

Gottfried, B. S.: "A Mathematical Model of Thermal Oil Recovery in Linear Systems", Society of Petroleum Engineers Journal, Sep. 1965, pp. 196-210.

Grabowski, J. W., Vinsome, P. K., Lin, R. C., Behie, A. and Rubin, B.: "A Fully Implicit General Purpose Finite-Difference Thermal Model for In-Situ Combustion and Steam", SPE 8396 presented at the 54th Annual Fall Meeting Technical Conference and Exhibition, Las Vegas, Sep. 23-26, 1979.

Grabowski, J. W., Rubin, B. and Harding, T. G.: "A Preliminary Numerical Simulation Study of In-Situ Combustion in a Cold Lake Oil Sands Reservoir", Journal of Canadian Petroleum Technology, April-June 1981, pp. 79-89.

Hall, K. R. and Yarborough, L.: "How to Solve Equation of State for Z-factors", Oil and Gas Journal, Feb. 18, 1974, pp. 86-88.

Harding, T. G., Farouq Ali, S. M. and Flock, D. L.: "Steamflood Performance in the Presence of Carbon Dioxide and Nitrogen", Journal of Canadian Petroleum Technology, Sep.-Oct. 1983, pp. 30-37.

Hart, C. M.: "A Comparative Evaluation of Surface and Downhole Steam Generation Techniques", SPE/DOE 10704 presented at the Third Joint Symposium on Enhanced Oil Recovery, Tulsa, April 4-7, 1982.

Hawkins, G. A., Solberg, H. L. and Potter, A. A.: "The Viscosity of Water and Superheated Steam", Trans. ASME, 1940, v. 62, p. 677.

Herning, F. and Zipperer, L.: "Calculation of the Viscosity of Technical Gas Mixtures from the Viscosity of Individual Components", Gas u. Wasserfach, 1936, v. 79, n. 49, p. 69.

Hilsenrath, J. et al: Tables of Thermal Properties of Gases, National Bureau of Standards, Circular 564, Nov. 1955, pp. 10, 460-461.

Holman, J. P.: Heat Transfer, 5th Edition, McGraw-Hill, Inc., New York, 1981, p. 109.

Hutchinson, H. L., Ip, D. T. and Shirazi, M.: "Experimental Study of Coinjection of Steam with Air or Other Coinjections into Asphalt Ridge Tar Sands", SPE 11850 presented at the Rocky Mountain Regional Meeting, Salt Lake City, Utah, May 23-25, 1983.

Hong, K. C. and Ault, J. W.: "Effects of Noncondensable Gas Injection on Oil Recovery by Steamflooding", Journal of Petroleum Technology, Dec. 1984, pp. 2160-2170.

Jacobs, F. A., Donnelly, J. K., Stanislav, J. F. and Svrcek, W. Y.: "Viscosity of Gas-Saturated Bitumen", Journal of Canadian Petroleum Technology, Oct.-Dec. 1980, pp. 45-50.

Jacoby, R. H. and Rasza, M. J.: "Equilibrium Vaporization Ratios for Nitrogen, Methane, Carbon Dioxide, Ethane, and Hydrogen Sulphide in Absorber-Oil-Natural Gas and Crude Oil-Natural Gas Systems", Trans. AIME, 1952, v. 195, pp. 99-110.

Katz, D. L. et al: Handbook of Natural Gas Engineering, McGraw-Hill Book Company, New York, 1959, p. 96.

Kazemi, H., Vestal, C. R. and Shank, G. D.: "An Efficient Multicomponent Numerical Simulator", Society of Petroleum Engineers Journal, Oct. 1978, pp. 355-368.

Klins, M. A. and Farouq Ali, S. M.: "Heavy Oil Production by Carbon Dioxide Injection", Journal of Canadian Petroleum Technology, Sep.-Oct. 1982, pp. 64-72.

Lée, B-I and Edminster, W. E.: "New Three Parameter Equation of State", Industrial and Engineering Chemistry Fundamentals, 1971, v. 10.

Leung, L. C.: "Numerical Evaluation of the Effect of Simultaneous Steam and CO₂ Injection on the Recovery of Heavy Oil", Journal of Petroleum Technology, Sep. 1983, pp. 1591-1599.

Lin, R.: "Gas-Steam Stimulation in Heavy Oil Reservoirs", Presentation made at the AOSTRA workshop on Computer Modelling, University of Alberta, Edmonton, Jan. 28-30, 1981.

Lohrenz, J., Clark, G. C. and Francis, R. J.: "A Compositional Material Balance for Combination Drive Reservoirs with Gas and Water Injection", Journal of Petroleum Technology, Nov. 1963, pp. 1233-1238.

Lohrenz, J., Bray, B. G. and Clark, C. R.: "Calculating Viscosities of Reservoir Fluids from Their Compositions", Journal of Petroleum Technology, Oct. 1964, pp. 1171-1176.

MacDonald, R. C.: "Reservoir Simulation with Interphase Mass Transfer", Report No. UT-71-a, Texas Petroleum Research Committee, 1971.

Marshall, B. W.: "Operational Experiences of a Downhole Steam Generator", SPE 10744 presented at the California Regional Meeting, San Francisco, March 24-26, 1982.

Miller, J. S. and Jones, R. A.: "A Laboratory Study to Determine Physical Characteristics of Heavy Oil after CO₂ Saturation", SPE/DOE 9789 presented at the 2nd Joint Symposium on Enhanced Oil Recovery, Tulsa, Oklahoma, April 5-8, 1981.

Muskat, M.: Physical Principles of Oil Production, IHRDC, Boston, 1981.

Nolen, J. S.: "Numerical Simulation of Compositional Phenomena in Petroleum Reservoirs", SPE 4274 presented at the 3rd Symposium on Numerical Simulation of Reservoir Performance, Houston, Jan. 11-12, 1973.

Peng, D-Y and Robinson, D. B.: "Two and Three Phase Equilibrium Calculations for Systems Containing Water", Canadian Journal of Chemical Engineering, Dec. 1976, pp. 595-599.

Peng, D-Y and Robinson, D. B.: "A New Two-Constant Equation of State", Ind. Eng. Chem. Fund., 1976, v. 15, n. 1, p. 59-64.

Peters, E. J.: "Stability Theory and Viscous Fingering in Porous Media", Ph. D. Thesis, University of Alberta, Edmonton, 1979.

Pradt, L. A.: "Generation of CO₂ and Inert Gas for EOR by WAO", unpublished.

Price, H. S. and Coats, K. H.: "Direct Methods in Reservoir Simulation", Society of Petroleum Engineers Journal, June 1974, pp. 295-308.

Pursley, S. A.: "Experimental Studies of Thermal Recovery Processes", presented at the Symposium on Heavy Crude Oil, Maracaibo, Venezuela, July 1974.

Redford, D. A., Flock, D. L., Peters, E. and Lee, J.: "Laboratory Model Flow-Test Systems of In-Situ Recovery from Alberta Oil Sands", Annual Meeting of the Canadian Chemical Society, Montreal, 1976.

Redford, D. A.: "The Use of Solvents and Gases with Steam in the Recovery of Bitumen from Oil Sands", Journal of Canadian Petroleum Technology, Jan.-Feb. 1982, v. 21, n. 1, pp. 45-53.

Redlich, O. and Kwong, J. N. S.: "On the Thermodynamics of Solutions V. An Equation of State, Fugacities of Gaseous Solutions", Chem. Rev., Feb. 1949, v. 44, pp. 233-244.

Reid, R. C., Prausnitz, J. M. and Sherwood, T. K.: The Properties of Gases and Liquids, Third Edition, McGraw-Hill Book Company, New York, 1977.

Roebuck, I. F., Jr., Henderson, G. E., Douglas, J., Jr. and Ford, W. T.: "The Compositional Reservoir Simulator: Case I - The Linear Model", Society of Petroleum Engineers Journal, March 1969, pp. 115-130.

Rubin, B.: "One-Dimensional Simulation of the In-Situ Combustion Process", M. Sc. Thesis, The University of Calgary, 1979, 82 pp.

Rubin, B. and Buchanan, W. L.: "A General Purpose Thermal Model", Society of Petroleum Engineers Journal, Apr. 1985, pp. 202-214.

Shutler, N. D.: "Numerical, Three-Phase Simulation of the Linear Steamflood Process", Society of Petroleum Engineers Journal, June 1969, pp. 232-246.

Shutler, N. D.: "Numerical Three-Phase Model of the Two-Dimensional Steamflood Process", Society of Petroleum Engineers Journal, Dec. 1970, pp. 405-417.

Simon, R. and Yarborough, L.: "A Critical Pressure Correlation for Gas-Solvent-Reservoir Oil Systems", Journal of Petroleum Technology, 1963, pp. 556-560.

Simon, R. and Graue, D. J.: "Generalized Correlations for Predicting Solubility, Swelling and Viscosity Behaviour of CO₂ - Crude Oil Systems", Journal of Petroleum Technology, Jan. 1965, pp. 102-106.

Singh, B., Malcom, J. D. and Heidrick, T. R.: "Injection-Production Strategies for Reservoir Having a Bottom Water Zone", SPE 13623 presented at the California Regional Meeting, Long Beach, April 11-13, 1984.

Smith, J. T. and Farouq Ali, S. M.: "Simulation of In-Situ Combustion in a Two-Dimensional System", SPE 3594 presented at the 46th Annual Fall Meeting, New Orleans, Oct. 3-6, 1971.

Smith, F. W. and Perkins, T. K.: "Experimental and Numerical Simulation Studies of the Wet Combustion Recovery Process", Journal of Canadian Petroleum Technology, July-Sep. 1973, pp. 44-54.

210

Sperry, J. S.: "Development and Field Testing of the Vapor Therm Process, Iola, Kansas", presented at the 3rd Annual ERDA Symposium on Enhanced Oil and Gas Recovery and Improved Drilling Methods, Tulsa, August 1977.

Sperry, J. S., Poston, R. S. and Young, F. S.: "Development and Field Testing of the Vapor Therm Process in the Carlyle Pool - Allen County, Kansas", presented at the 4th Annual DOE Symposium on Enhanced Oil and Gas Recovery and Improved Drilling Methods, Tulsa, Aug. 27-31, 1978.

Sperry, J. S., Young, F. S. and Poston, R. S.: "Field Testing of the Vapor Therm Process", presented at the 5th Annual DOE Symposium, Tulsa, Aug. 1979.

Spillette, A. G. and Nielsen, R. L.: "Two-Dimensional Method for Predicting Hot Waterflood Recovery Behaviour", Journal of Petroleum Technology, June 1968, pp. 627-638.

Stone, H. L.: "Probability Method for Estimating Three-Phase Relative Permeability", Journal of Petroleum Technology, Feb. 1970, p. 214.

Stone, H. L.: "Estimation of Three-Phase Relative Permeability and Residual Oil Data", Journal of Canadian Petroleum Technology, Oct.-Dec. 1973, pp. 53-61.

Stone, T. and Malcolm, J. D.: "Simulation of a Large Steam-CO₂ Co-injection Experiment", Journal of Canadian Petroleum Technology, Nov.-Dec. 1985, pp. 51-59.

Takacs, G.: "Comparisons Made for Computer Z-factor Calculations", Oil and Gas Journal, Dec. 20, 1976, pp. 64-66.

Tikhomirov, V. M.: "Thermal Conductivity of Rock and Its Relation to Liquid Saturation, Density and Temperature", Neftganoé Khozaistau, April 1968, v. 46, n. 4, p. 36.

Todd, M. R., O'Dell, P. M. and Hirasaki, G. J.: "Methods for Increased Accuracy in Numerical Reservoir Simulators", Society of Petroleum Engineers Journal, Dec. 1972, pp. 515-530.

Tumasyan, A. B., Panteleev, V. G. and Meinster, G. P.: "Effect of Carbon Dioxide on the Physical Properties of Petroleum and Water", Nefteprom. Delo, 1969, p. 20.

Van-Quy, N., Simandoux, P. and Corteville, J.: "A Numerical Study of Diphasic Multicomponent Flow", Society of Petroleum Engineers Journal, April 1972, pp. 171-184.

Vinsome, P. K. W.: "A Numerical Description of Hot-Water and Steam Drives by the Finite-Difference Method", SPE 5248 presented at the 49th Annual Fall Meeting, Houston, Oct. 6-9, 1974.

Weinstein, H. G.: "Mathematical Models for Thermal Recovery Processes", presented at Symposium on Heavy Crude Oil, Maracaibo, Venezuela, July 1974.

Weinstein, H. G., Wheeler, J. A. and Woods, E. G.: "Numerical Model for Thermal Processes", Society of Petroleum Engineers Journal, Feb. 1977, pp. 65-78.

Willman, B. T., Valleroy, V. V., Runberg, G. W., Cornelius, A. J. and Powers, L. W.: "Laboratory Studies of Oil Recovery by Steam Injection", Journal of Petroleum Technology, July 1961, p. 681.

Young, F. S. and Krajicek, R. W.: "The Vapor Therm Process for Recovery of Viscous Crude Oil", UNITAR First International Conference on the Future of Heavy Crude and Tar Sand, Edmonton, 1979.

Youngren, G. K.: "Development and Application of an In-Situ Combustion Reservoir Simulator", Society of Petroleum Engineers Journal, Feb. 1980, pp. 39-51.

Zudkevitch, D. and Joffe, J.: "Correlation and Prediction of Vapor-Liquid Equilibria with the Redlich-Kwong Equation of State", American Institute of Chemical Engineers Journal, Jan. 1970, pp. 112-119.

APPENDIX A

MATERIAL AND EQUIPMENT SUPPLIERS FOR EXPERIMENTAL WORK

Item	Supplier
3" dia., sch. 80, 321 s.s. pipe, 4 ft. long	Specialty Steels 9759 - 51 Avenue Edmonton, Alberta T6E 4Z5
20" x 20" x 1-1/4", 316L s.s. plate	Uddeholm Steels Ltd. 2071 Viceroy Place Richmond, B.C. V6V 1Y9
7/8" N.C. x 5" studs 7/8" N.C. nuts 7/8" flat washers	Universal Fastening 4612 - 97 Street Edmonton, Alberta
R37, 304 s.s. ring seal	MHK Industries Ltd. 9610 - 60 Avenue Edmonton, Alberta T6E 0C3
10 lbs., 1/8", #310 ss. low carbon welding rods	Consumers Welding Supplies 9810 - 62 Avenue Edmonton, Alberta T6E 0E3
Swagelok fittings ss-400-1-4 MPW ss-200-R-4 ss-100-R-2 Whitey valve ss-3RLF4	Edmonton Valve and Fitting Ltd. 4518 - 101 Street Edmonton, Alberta T6E 5G9
RX37, mild steel ring seals	Norwesco Industries 9817 - 47 Avenue Edmonton, Alberta T6E 5M7
20 x 250 mesh, type 316 s.s. filter cloth (0.011/0.0085 wire diameter)	Cambridge International, Inc. P. O. Box 399 Cambridge, Maryland U. S. A. 21613
Torque wrench	S. J. Dyer Specialties 10505 - 114 Street Edmonton, Alberta T5H 3J6
Insulation - Foam-glass - Thermo 12 - Fibrefax Moist Pak-D	Crossroads Industries 14723 - 128 Avenue Edmonton, Alberta
Watlow Firerod heaters	Instrument Service Laboratories 9307 - 35 Avenue Edmonton, Alberta

Thermocouples - type J

Model 49 Proportioning controller,
0-600°C

Milton Ray DRM1-44-59-SM pump

Model 8250 Modular Flow controller
Model 8240 Mass Flow controller
Tescom 26-2320-24 b.p. regulator

Mercoild Control switch
Series DS-221-2
Range 135 (300-2500 psi)
c/w flange no. 17-26

Murphy switchgauge 45-PE-5000

V1-350 Varius air compressor

Heise gauges

Doric Digifrend 220 Datalogger

Research Control Valve
1/4" NPT, 316 s.s. body

Edmonton, Alberta

Thermoelectric Canada Ltd.
8425 Argyll Road
Edmonton, Alberta
T6C 4B2

Omega Engineering Inc.
Box 4047 Springdale Station
Stamford, Connecticut
U.S.A. 06907

Zazula Process Equipment Ltd.
1526 - 10 Avenue S. W.
Calgary, Alberta
T3C 0J5

Matheson of Canada Ltd.
P. O. Box 6240, Station C
Edmonton, Alberta
T5B 4K6

The Mercoild Corp.
4201 Belmont Avenue
Chicago, Illinois
U. S. A. 60641

Cantech Controls Ltd.
10604 - 105 Avenue
Edmonton, Alberta

JMAR Compressors Inc.
5760 Cedarbridge Way
Richmond, B.C.
V6X 2A7

Barber Engineering and Controls
Inc.
8803 - 58 Avenue
Edmonton, Alberta

Intertechnology
Box 219
Don Mills, Ontario
M3C 2S4

Spartan Controls Ltd.
8525 Davies Road
Edmonton, Alberta
T6E 4N3

300 SERIES EMV/PNEUMATIC TRANSMITTER
40 PR-A4 Pneumatic controller

roxboro Canada Inc.
7911 Argyll Road
Edmonton, Alberta
T6C 4A9

218 WII proportioning pump
2.5 to 560 cm³/hr
2 pumps

Ruska International Export Inc.
P. O. Box 36010
6121 Hillcroft
Houston, Texas
U. S. A. 77036

Vactorr 75 vacuum pump

GCA/Precision Scientific
Chicago, Illinois
U. S. A. 60647

80-120 mesh silica sand

Fisher Scientific Co. Ltd.
10720 - 178 Street
Edmonton, Alberta T5L 4K1

Vibrator

Leader Equipment Ltd.
17630 - 102 Avenue
Edmonton, Alberta
T6E 5C8

Oil

Imperial Oil Enterprises Ltd.
Strathcona Refinery
P. O. Box 1020
34 Street & Hwy. 16A East
Edmonton, Alberta
T5J 2M1

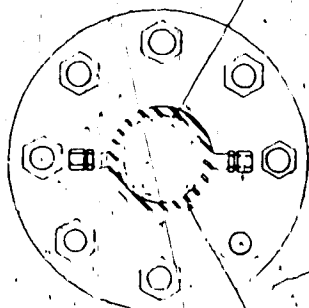
Mortar for lining the test cell

Shaw Pipe Protection (Alberta)
Ltd.
Box 5560, Station "L"
Edmonton, Alberta
T6C 4E9

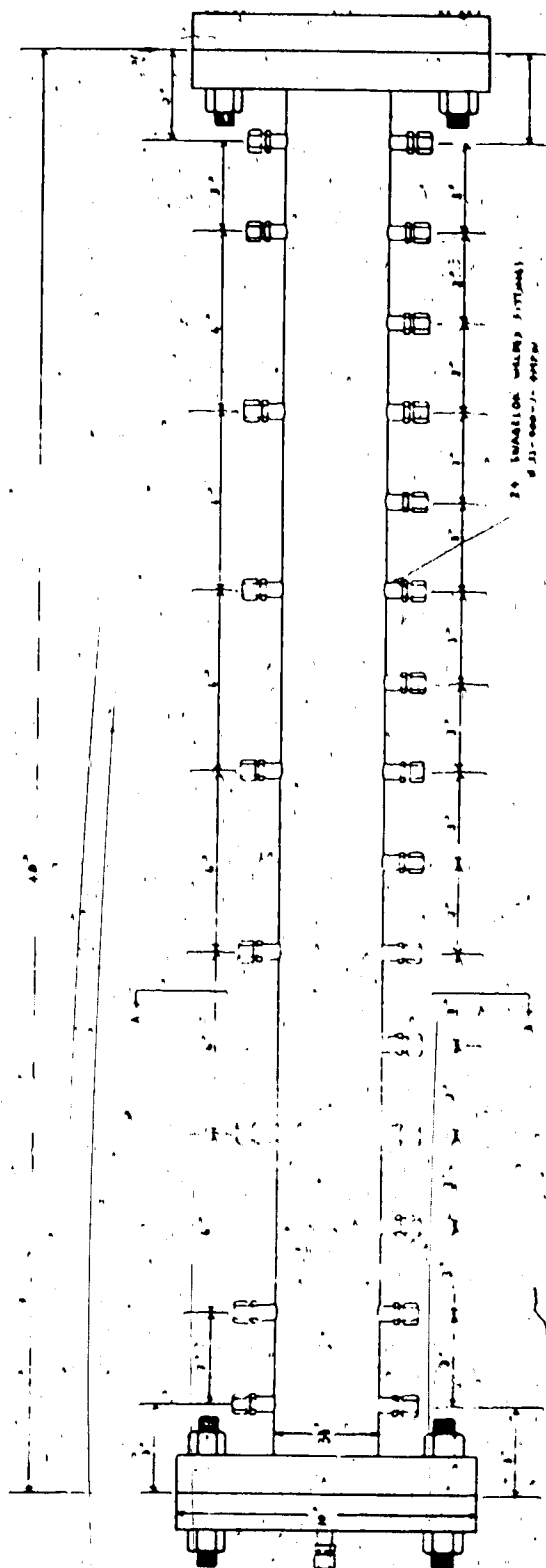
APPENDIX B

DESIGN DRAWINGS FOR TEST CELL USED IN LABORATORY EXPERIMENTS

SECTION A-A



12 BOLTS TO PIPE
3/4" DIA

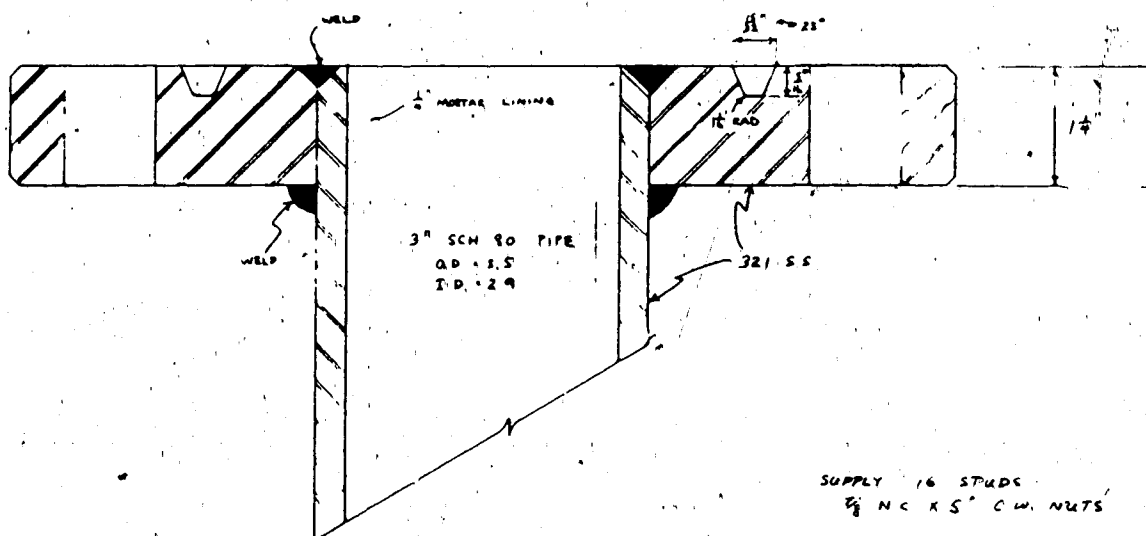


24 BOLT PATTERN (SEE DETAIL)
Ø 31'-00" - 31'-04"

3 MAX IN
2000 PSI 780 PS
COME FROM PDA

1/4" DIA x 1/4" DIA

JH
Page



CORE HOLDER (3 INCH.)

APPENDIX C

TABLES OF EXPERIMENTAL DATA

TYPE: STEAM ONLY

TIME Hour	STEAM INJECTED		GAS INJECTED Moles	TOTAL INJECTED Moles	WATER PRODUCED cm ³	OIL PRODUCED cm ³	OIL RECOVERY % OOIP
	PV	Moles					
0.70	0.433	36.76	-	36.76	226	284	20.5
1.23	0.761	64.60	-	64.60	602	400	28.9
1.75	1.082	91.85	-	91.85	1024	471	34.1
2.28	1.410	119.69	-	119.69	1447	541	39.1
2.68	1.657	140.66	-	140.66	1880	606	43.8
3.05	1.886	160.10	-	160.10	2310	676	48.9
3.37	2.084	176.91	-	176.91	2733	749	54.2
3.73	2.307	195.84	-	195.84	3126	853	61.7
4.12	2.548	216.30	-	216.30	3572	918	66.4
4.55	2.814	238.88	-	238.88	4012	975	70.5
5.17	3.200	271.64	-	271.64	4732	1057	76.5
Postrun					5622	1103	79.8

RUN NUMBER: 2

TIME Hour	INLET PRESS. Psig	THERMOCOUPLES, °C															
		Inlet	1	2	3	4	5	6	7	8	9	10	11	12	13	14	15
0.00	673.5	97.1	24.8	21.5	21.4	21.2	21.2	21.2	21.3	21.3	21.3	21.3	21.3	21.3	21.3	21.2	21.2
0.15	608.4 ^a	135.3	25.5	22.0	21.5	21.2											
0.33	579.5	254.0	30.6	23.3	21.6	21.3	21.2										
0.50	558.2	251.0	46.4	25.9	21.8	21.8											
0.67	607.4	255.3	77.8	49.1	21.9												
0.83	566.7	251.2	108.1	66.9	-	26.3	23.6	21.6									
1.00	543.3	247.8	133.8	83.4	-	33.2	28.5	22.3									
1.48	518.2	248.4	153.7	122.8	-	61.1	52.5	32.1	30.1	23.5	23.0	21.7					
1.65	523.6	245.8	169.0	139.6	-	72.5	63.3	38.4	35.7	25.6	24.9	22.2	22.0	21.5			
1.82	530.8	248.7	186.0	149.6	-	83.7	71.1	45.2	40.4	28.5	26.8	23.1	22.7	21.7			
1.98	534.9	248.0	198.2	156.9	-	93.8	80.5	51.8	46.3	31.7	29.5	24.2	23.6	22.0	21.9	21.5	
2.15	510.0	247.2	210.6	166.3	-	104.6	91.6	59.2	54.3	35.7	33.4	25.8	25.2	22.6	22.4	21.7	
2.32	564.3	250.5	218.3	176.5	-	116.2	101.3	67.6	60.7	40.8	36.8	28.0	26.8	23.5	23.0	21.9	21.8
2.48	537.5	248.6	230.3	197.9	-	129.4	116.5	78.2	72.4	47.5	43.4	31.5	30.1	24.9	24.4	22.5	22.3
2.65	520.3	247.4	225.0	245.9	-	146.5	132.0	91.0	87.7	56.2	52.5	36.3	35.0	27.1	26.5	23.5	23.2
2.82	511.3	246.0	246.4	246.0	-	200.0	153.6	103.3	99.9	65.9	61.3	41.7	40.1	29.9	29.0	24.6	24.2
3.32	497.0	244.6	245.0	244.6	-	245.0	244.4	242.5	198.4	110.3	113.6	67.5	69.4	44.7	44.9	32.0	32.1
3.82	499.2	245.2	245.2	244.8	-	245.2	244.7	244.6	245.1	244.7	244.7	175.6	145.0	69.3	64.1	44.8	41.5
4.32	491.9	244.1	244.5	244.1	244.2	244.5	244.0	243.9	244.3	244.0	243.8	243.8	244.1	241.8	243.5	99.3	117.2
4.82	493.1	243.9	244.4	244.1	244.2	244.4	243.9	243.9	244.4	244.1	244.0	244.0	244.4	243.9	244.3	226.7	206.7
5.15	489.1	243.8	244.0	243.7	243.8	243.9	243.5	243.6	243.9	243.6	243.6	243.5	243.8	243.5	243.8	237.7	243.8

RUN NUMBER: 3

TYPE: SLUG CO₂/STEAMFLOOD

TIME Hour	STEAM INJECTED		GAS INJECTED	TOTAL INJECTED	WATER PRODUCED	OIL PRODUCED	OIL RECOVERY
	PV	Moles	Moles	Moles	cm ³	cm ³	% OOIP
1.27	-	-	-	-	0	365	27.8
2.93	0.016	1.60	35.48	37.08	0	435	33.1
3.55	0.590	58.97	35.48	94.45	308	607	46.2
3.87	0.885	88.45	35.48	123.93	771	634	48.2
4.17	1.165	116.44	35.48	151.92	1265	640	48.7
4.45	1.430	142.92	35.48	178.40	1775	642	48.8
4.75	1.709	170.81	35.48	206.29	2272	675	51.3
5.13	2.066	206.49	35.48	241.97	2717	723	55.0
5.42	2.330	232.87	35.48	268.35	3763	820	62.4
5.83	2.719	271.75	35.48	307.23	4579	984	74.8
Postrun					5219	1024	77.9

RUN NUMBER: 3

INLET		THERMOCOUPLES, °C														
TIME	Hour	1	2	3	4	5	6	7	8	9	10	11	12	13	14	15
2.87	508.3	132.1	22.2	22.8	23.4	24.2	24.4	24.3	24.3	24.3	24.2	-	24.1	24.1	23.9	23.7
2.95	530.0	248.1	34.1	29.5	23.5											
3.04	568.9	251.7	67.5	43.7	27.2	24.6										
3.20	526.7	247.8	112.4	55.6	38.5	27.4	24.5									
3.29	525.5	247.4	124.0	64.2	46.2	30.0	27.9	24.7								
3.37	523.4	247.4	131.8	73.3	55.4	33.6	32.3	25.2	24.6							
3.54	522.5	247.4	152.0	90.8	74.7	44.4	42.8	28.3	29.2	25.0	24.8					
3.62	549.1	249.9	161.0	99.9	84.6	51.2	48.0	31.0	32.1	25.6	25.9	24.9				
3.70	549.6	250.0	164.4	109.8	94.2	59.1	53.8	34.3	35.5	26.7	27.1	25.0				
3.87	544.8	250.6	169.1	128.0	112.5	76.1	68.2	42.6	42.8	30.2	30.7	25.9	24.9	25.1	24.9	25.2
3.95	562.9	251.0	174.1	135.5	120.6	84.3	76.8	47.7	47.5	32.6	33.2	26.7	25.0	25.3	25.0	25.2
4.04	560.1	251.0	180.3	142.7	128.1	92.4	85.2	53.9	52.9	35.6	36.0	27.8	25.5	25.6	25.0	25.2
4.20	561.8	251.0	191.1	156.5	142.7	107.8	100.7	67.8	66.1	42.9	42.7	31.2	26.6	26.6	25.4	25.5
4.29	560.7	251.0	196.2	162.9	145.9	115.4	108.2	75.3	73.4	47.6	47.0	33.3	27.6	27.5	25.6	25.6
4.37	566.8	251.3	201.8	169.3	157.1	122.9	115.8	82.5	81.0	52.9	52.3	36.0	28.7	28.7	25.9	26.1
4.54	559.5	251.1	206.3	175.6	164.0	130.3	123.1	89.6	88.1	58.6	57.8	39.1	30.1	30.1	26.5	26.5
4.62	496.3	243.9	223.6	241.8	179.0	145.0	139.8	104.1	104.0	71.3	72.5	47.2	34.6	34.8	28.5	28.7
4.70	500.4	244.7	238.1	243.9	192.2	152.1	148.1	111.4	112.1	77.9	80.2	52.0	37.4	37.8	29.9	30.2
4.87	487.6	243.2	243.8	243.5	243.4	240.4	240.4	129.4	140.0	94.5	107.6	65.9	47.0	53.0	35.6	39.0
4.99	498.7	244.8	244.3	244.5	244.2	244.3	244.2	183.2	153.6	107.8	115.9	77.7	55.9	59.7	41.3	42.5
5.07	497.3	244.5	244.0	244.2	244.0	244.0	243.9	228.2	243.9	132.5	121.5	86.1	63.1	64.1	46.1	45.5
5.24	504.4	245.6	245.0	245.0	245.0	245.9	244.9	244.8	233.4	244.8	244.8	133.0	75.8	78.4	55.2	57.0
5.32	510.4	246.3	246.0	246.1	245.9	245.8	245.8	245.6	240.9	245.4	245.4	183.7	88.4	94.0	60.0	61.3
5.49	496.2	244.5	244.1	244.4	244.0	243.9	243.9	243.8	243.5	243.8	243.8	243.6	190.7	243.8	82.9	91.5
5.57	493.7	244.1	243.8	243.9	243.7	243.8	243.6	243.5	243.2	243.5	243.5	243.3	243.1	243.5	146.7	135.5
5.65	498.0	244.6	244.5	244.7	244.4	242.2	242.2	244.0	243.8	243.9	243.6	243.8	243.6	243.6	188.5	243.7

RUN NUMBER: 4

TYPE: STEAM ONLY

TIME Hour	STEAM INJECTED		GAS INJECTED Moles	TOTAL INJECTED Moles	WATER PRODUCED cm ³	OIL PRODUCED cm ³	OIL RECOVERY % OOIP
	PV	Moles					
0.52	0.625	58.58	-	58.58	263	229	18.1
1.37	1.146	107.41	-	107.41	1143	337	25.6
1.69	1.342	125.78	-	125.78	1613	424	33.5
1.95	1.502	140.77	-	140.77	1998	530	41.8
2.22	1.667	156.23	-	156.23	2356	665	52.5
2.45	1.808	169.45	-	169.45	2731	790	62.4
2.75	1.992	186.69	-	186.69	3114	905	71.4
2.97	2.127	199.35	-	199.35	3517	1002	79.0
3.04	2.169	203.28	-	203.28	3610	1009	79.6
Postrun					4194	1025	80.9

RUN NUMBER: 4

TIME Hour	INLET Psig	THERMOCOUPLES, °C														
		1	2	3	4	5	6	7	8	9	10	11	12	13	14	15
0.00	675.0	123.4	26.1	22.8	22.2	22.2	22.5	22.0	22.0	22.2	22.3	22.3	22.3	22.3	22.3	22.3
0.10	541.6	248.1	26.5	23.6	22.2											
0.27	512.4	249.3	49.0	27.2	23.0	22.3										
0.43	533.7	249.0	79.2	40.1	26.0	23.0	22.3									
0.56	558.0	251.7	110.7	57.8	35.0	25.5	23.0	22.3								
0.72	534.2	250.8	138.0	79.1	48.4	31.3	25.2	22.9								
0.88	538.0	252.2	164.9	101.1	65.4	41.5	30.4	24.5	22.7							
1.04	552.2	253.4	189.4	125.0	85.0	56.0	38.9	28.1	24.2	23.0						
1.27	569.4	262.7	215.7	211.9	107.7	73.8	51.5	35.3	27.4	24.5	23.0					
1.36	511.1	254.7	243.8	243.2	122.8	83.6	58.2	39.4	29.9	25.8	23.5	22.5				
1.52	546.3	256.6	248.3	249.3	183.9	112.0	75.2	50.4	36.6	30.0	25.6	23.2	22.7			
1.69	527.1	266.0	247.1	247.2	247.0	209.7	110.4	71.6	50.3	41.0	32.1	25.2	24.3	22.8		
1.86	537.5	267.4	248.2	248.3	248.1	248.0	248.2	101.6	69.0	54.2	40.8	29.4	27.1	23.9	23.5	
2.02	542.4	268.8	248.8	248.9	248.7	248.7	248.7	234.1	115.1	76.1	54.0	35.9	32.1	26.0	23.4	23.3
2.27	541.3	270.7	248.7	248.7	248.6	248.5	248.4	248.7	236.2	248.6	248.7	62.3	53.8	33.4	25.6	24.9
2.61	514.2	264.5	245.7	245.8	245.5	245.6	245.4	245.7	245.3	245.5	245.6	228.9	245.6	177.1	223.7	46.2
2.94	498.9	263.6	243.9	243.9	243.8	243.8	243.7	243.9	243.5	243.8	243.8	243.5	243.8	243.7	243.8	221.4
3.02	486.8	262.8	242.4	242.5	242.4	242.4	242.3	242.4	242.2	242.3	242.4	242.2	242.4	242.3	242.4	242.8

RUN NUMBER: 5

TYPE: SLUG CO₂/STEAMFLOOD

TIME Hour	STEAM INJECTED		GAS INJECTED	TOTAL INJECTED	WATER PRODUCED	OIL PRODUCED	OIL RECOVERY
	PV	Moles	Moles	Moles	cm ³	cm ³	% OOIP
0.15	-	-	-	-	2	95	7.6
0.27	-	-	-	-	2	178	14.3
0.63	-	-	-	-	2	251	20.1
1.22	-	-	-	-	2	339	27.1
1.87	-	-	-	-	2	429	34.3
2.18	-	-	21.43	21.43	2	479	38.3
3.17	0.083	7.57	21.43	29.00	212	754	60.4
4.30	1.535	140.03	21.43	161.46	1625	817	65.4
4.90	1.969	179.62	21.43	201.05	2613	821	65.7
5.12	2.128	194.12	21.43	215.55	3028	904	72.4
5.35	2.295	209.36	21.43	230.79	3393	1030	82.4
5.68	2.534	231.16	21.43	252.59	3853	1070	85.6
5.75	2.584	235.72	21.43	257.15	-	-	-
Postrun					4359	1113.5	89.2

RUN NUMBER: 5

TIME Hour	INLET PRESS. Psig	THERMOCOUPLES, °C																
		Inlet	1	2	3	4	5	6	7	8	9	10	11	12	13	14	15	
2.187	508.0	21.4	21.6	22.0	22.0	22.1	22.2	22.3	22.2	22.2	22.3	21.4	22.3	21.4	22.5	22.6	22.4	
2.353	496.5	245.3	47.7	22.3														
2.520	529.3	248.2	78.8	30.1	23.7	22.3												
2.687	514.3	246.7	104.9	44.1	30.8	23.4	22.7											
2.853	511.7	246.7	121.6	61.6	43.7	27.0	23.8	22.7										
3.02	502.1	245.5	144.0	79.2	60.2	34.5	27.7	23.4	22.8									
3.19	493.3	248.7	166.4	96.9	79.1	45.2	35.7	25.4	23.6	22.7								
3.35	491.8	252.5	182.0	114.7	96.6	57.8	45.5	29.4	25.8	23.2	22.9							
3.52	497.6	247.4	195.5	132.0	115.8	72.0	57.6	35.6	30.1	24.5	23.5	22.9						
3.69	529.0	251.0	204.3	148.9	133.3	87.2	71.4	43.8	35.9	27.0	24.9	23.3						
3.85	487.3	254.9	243.6	166.7	161.0	104.9	97.0	56.2	46.2	31.7	28.9	24.6						
4.02	519.8	249.5	247.1	214.5	229.6	123.2	109.8	71.8	57.6	38.7	33.4	26.8			23.5	23.2		
4.187	487.0	250.3	243.3	242.6	243.4	188.9	243.3	89.6	85.0	50.6	45.9	32.7			24.9	-	23.5	
4.353	489.4	246.6	243.7	243.6	243.7	243.5	243.5	156.0	115.0	64.3	59.6	40.5			27.5	-	24.1	23.8
4.520	505.0	262.4	245.4	245.5	245.4	245.3	245.4	209.5	245.3	106.0	82.5	50.0	42.7	31.7	-	25.4	24.8	
4.687	502.2	263.4	245.2	245.2	245.2	245.0	245.0	245.0	245.0	197.3	244.9	79.8	55.4	37.9	-	27.8	26.3	
4.853	517.6	265.9	246.8	246.7	246.9	246.7	246.7	246.7	246.7	244.4	246.7	224.3	118.9	50.6	42.2	31.5	28.8	
5.02	512.5	251.6	246.6	246.5	246.6	246.3	246.3	246.2	246.0	245.9	245.8	244.5	245.6	154.8	80.4	41.7	37.2	
5.187	494.5	266.6	244.2	244.2	244.2	243.9	244.0	244.0	243.9	243.6	243.8	243.8	243.7	231.9	243.7	183.5	88.2	
5.353	482.1	252.2	242.9	242.8	242.9	242.5	242.6	242.6	242.4	242.1	242.3	242.3	242.2	242.4	242.2	240.1	242.3	
5.520	498.0	267.2	244.7	244.6	244.7	244.4	244.4	244.4	244.4	243.9	244.1	244.2	244.0	243.6	244.0	242.8	244.2	
5.687	502.1	266.9	245.3	245.3	245.3	245.0	245.1	245.1	245.0	244.6	244.8	244.8	244.7	244.4	244.6	244.2	244.5	

TIME	STEAM INJECTED		GAS INJECTED	TOTAL INJECTED	WATER PRODUCED	OIL PRODUCED	OIL RECOVERY
Hour	RV	Moles	Moles	Moles	cm ³	cm ³	% OOIP
0.35	0.081	6.62	7.602	14.22	30	431	34.2
0.60	0.169	13.89	13.03	26.92	64	588	46.7
0.82	0.274	22.50	18.73	41.23	215	647	51.4
0.99	0.419	34.40	24.15	58.55	403	681	54.1
1.15	0.548	45.00	29.25	74.25	591	722	57.3
1.45	0.806	66.20	38.81	105.01	974	795	63.1
1.75	1.080	88.70	48.37	137.07	1354	853	67.8
2.02	1.339	110.00	56.97	166.97	1717	908	72.1
2.29	1.614	132.60	65.56	198.16	2100	975	77.4
2.52	1.841	151.30	72.89	224.19	2470	1035	82.2
2.74	2.068	169.90	79.90	249.80	2778	1049	83.3

Postrun

RUN NUMBER: 6

TIME Hour	INLET PRESS. Psig	THERMOCOUPLES, °C														
		Inlet	1	2	3	4	5	6	7	8	9	10	11	12	13	14
0.07	1005.1	30.7	23.0	22.7	23.0	22.7	22.9	22.8	22.8	22.7	22.8	22.8	22.8	22.8	22.8	22.9
0.15	706.9	29.4	22.7													
0.23	566.5	48.3	22.7													
0.32	655.8	258.1	23.7	22.7												
0.48	618.2	256.1	42.6	23.1												
0.57	601.5	254.5	63.0	24.5												
0.65	593.8	253.8	83.2	27.7	24.5	22.8										
0.82	650.2	260.0	209.4	43.3	43.4	23.7	23.2									
0.90	632.0	258.3	220.6	82.7	87.0	26.5	26.3	22.9								
0.98	649.5	259.8	223.3	117.4	137.6	33.7	35.9	23.6	23.2							
1.15	627.6	258.2	224.3	155.6	192.0	73.3	72.9	29.9	29.2	23.2						
1.23	587.9	255.1	224.2	166.6	207.2	105.3	126.2	37.9	37.5	24.3	24.2					
1.32	610.9	256.9	224.7	174.6	209.9	130.0	161.4	53.0	51.2	26.7	26.1	23.2				
1.48	612.9	256.9	224.5	186.2	213.6	162.7	192.5	104.5	104.5	39.0	36.9	25.6	24.0			
1.57	584.3	255.1	223.8	190.5	216.6	172.9	201.4	131.5	144.5	52.1	48.7	29.0	25.6	23.3		
1.65	581.5	254.5	224.9	194.3	218.1	180.9	206.6	152.8	174.1	71.8	67.4	34.8	28.7	24.1	23.3	
1.82	587.4	255.6	225.0	199.6	220.0	192.2	212.1	178.6	198.9	122.6	147.0	61.4	42.8	28.3	25.3	23.5
1.90	563.8	256.1	224.3	201.1	220.0	195.6	214.0	187.1	204.5	144.5	178.4	91.1	61.6	33.5	27.8	24.3
1.98	556.9	260.8	224.0	202.6	220.5	198.3	215.4	193.1	208.2	161.4	193.2	123.0	105.2	44.8	32.6	25.9
2.15	537.7	263.1	223.6	204.0	220.3	202.3	215.9	201.2	212.5	183.5	206.2	170.2	186.9	103.8	71.0	38.3
2.23	541.9	254.8	222.8	206.7	224.0	205.6	216.8	205.1	212.0	189.4	208.1	184.1	197.7	132.8	118.7	63.1
2.32	537.4	263.8	223.4	206.2	220.5	206.2	216.1	207.3	213.9	194.2	210.6	192.3	204.2	156.7	173.5	101.6
2.48	507.2	262.5	222.1	207.4	220.9	210.0	217.8	211.8	215.1	200.1	212.2	202.6	209.3	185.5	204.1	168.1
2.57	511.0	252.9	221.6	207.8	219.6	210.7	218.3	212.5	215.7	202.0	213.7	205.0	210.7	192.6	207.4	182.7
2.65	503.7	259.9	221.1	210.0	219.7	211.4	217.2	212.5	215.4	203.5	213.5	206.7	211.7	197.3	209.6	192.8
2.73	528.6	257.4	224.0	211.5	220.7	211.4	217.7	212.4	215.8	204.7	214.0	206.9	212.6	200.5	210.6	197.7

TIME Hour	STEAM INJECTED		GAS INJECTED	TOTAL INJECTED	WATER PRODUCED	OIL PRODUCED	OIL RECOVERY
	PV	Moles	Moles	Moles	cm ³	cm ³	% OOIP
0.22	0.107	9.29	1.50	10.8	12	201	15.8
0.30	0.149	12.93	2.04	14.97	99	343	26.9
0.38	0.197	17.10	2.59	19.69	137	464	36.4
0.50	0.288	24.99	3.40	28.39	222	563	44.2
0.65	0.409	35.49	4.42	39.91	368	641	50.4
0.80	0.532	46.17	5.44	51.61	531	704	55.3
0.93	0.639	55.45	6.33	61.78	709	752	59.0
1.08	0.763	66.21	7.35	73.56	897	788	61.9
1.23	0.888	77.06	8.37	85.43	1078	829	65.1
1.37	1.010	87.65	9.32	96.97	1256	875	68.7
1.52	1.137	98.67	10.34	109.01	1442	914	71.8
1.68	1.273	110.47	11.43	121.90	1652	942	74.0
1.95	1.503	130.43	13.27	143.70	2052	995	78.1
2.30	1.803	156.46	15.65	172.11	2467	1041	81.7
2.55	2.024	175.64	17.35	192.99	2860	1090	85.6
2.75	2.202	191.08	18.71	209.79	3165	1102	86.5
Postrun					3764	1130	88.7

RUN NUMBER: 7

INLET
PRESS.

Hour	1	2	3	4	5	6	7	8	9	10	11	12	13	14
0.00	22.4	22.0	21.9	22.0	21.9	22.0	21.9	22.0	21.9	22.0	22.0	22.0	22.2	22.2
0.083	272.7	75.3	22.0											
0.167	795.9	271.2	68.0	25.0	24.9									
0.250	819.3	273.7	68.4	30.6	28.8	22.7								
0.417	621.2	256.6	229.1	63.1	42.4	25.5								
0.500	562.5	251.4	236.5	91.0	72.0	28.3								
0.583	587.4	254.9	239.2	114.2	99.4	34.4								
0.750	561.1	253.1	240.3	162.1	195.7	56.0								
0.833	557.0	258.3	240.2	177.2	221.8	73.2								
0.916	550.1	258.3	237.1	189.5	230.9	97.4								
1.083	552.3	258.5	233.9	204.8	231.3	149.9								
1.167	557.5	258.9	236.6	209.8	233.5	168.0								
1.250	549.9	256.5	236.8	213.1	234.8	183.5								
1.417	530.2	260.3	235.9	216.7	234.6	204.0								
1.500	544.4	258.8	237.0	219.0	236.4	210.4								
1.583	520.7	260.5	235.8	221.6	234.3	216.2								
1.750	538.1	257.4	237.4	225.2	235.0	221.4								
1.833	532.4	256.7	239.2	227.4	235.6	224.0								
1.916	530.4	260.9	240.3	229.4	236.2	226.3								
2.083	510.0	256.7	237.5	232.4	235.4	228.7								
2.167	522.7	262.0	239.6	231.9	236.6	229.5								
2.330	526.1	261.7	240.0	234.0	236.3	231.1								
2.417	515.7	262.1	238.9	234.0	236.0	231.7								
2.583	518.7	263.8	240.1	234.3	236.2	232.1								
2.667	517.3	264.2	239.8	235.1	236.5	233.0								
2.750	522.2	264.9	240.7	236.0	237.1	233.6								

----- THERMOCOUPLES, °C -----

Hour	1	2	3	4	5	6	7	8	9	10	11	12	13	14
0.00	22.4	22.0	21.9	22.0	21.9	22.0	21.9	22.0	21.9	22.0	22.0	22.0	22.2	22.2
0.083	272.7	75.3	22.0											
0.167	795.9	271.2	68.0	25.0	24.9									
0.250	819.3	273.7	68.4	30.6	28.8	22.7								
0.417	621.2	256.6	229.1	63.1	42.4	25.5								
0.500	562.5	251.4	236.5	91.0	72.0	28.3								
0.583	587.4	254.9	239.2	114.2	99.4	34.4								
0.750	561.1	253.1	240.3	162.1	195.7	56.0								
0.833	557.0	258.3	240.2	177.2	221.8	73.2								
0.916	550.1	258.3	237.1	189.5	230.9	97.4								
1.083	552.3	258.5	233.9	204.8	231.3	149.9								
1.167	557.5	258.9	236.6	209.8	233.5	168.0								
1.250	549.9	256.5	236.8	213.1	234.8	183.5								
1.417	530.2	260.3	235.9	216.7	234.6	204.0								
1.500	544.4	258.8	237.0	219.0	236.4	210.4								
1.583	520.7	260.5	235.8	221.6	234.3	216.2								
1.750	538.1	257.4	237.4	225.2	235.0	221.4								
1.833	532.4	256.7	239.2	227.4	235.6	224.0								
1.916	530.4	260.9	240.3	229.4	236.2	226.3								
2.083	510.0	256.7	237.5	232.4	235.4	228.7								
2.167	522.7	262.0	239.6	231.9	236.6	229.5								
2.330	526.1	261.7	240.0	234.0	236.3	231.1								
2.417	515.7	262.1	238.9	234.0	236.0	231.7								
2.583	518.7	263.8	240.1	234.3	236.2	232.1								
2.667	517.3	264.2	239.8	235.1	236.5	233.0								
2.750	522.2	264.9	240.7	236.0	237.1	233.6								

TYPE: SIMULTANEOUS STEAM/N₂

TIME Hour	STEAM INJECTED		GAS INJECTED Moles	TOTAL INJECTED Moles	WATER PRODUCED cm ³	OIL PRODUCED cm ³	OIL RECOVERY % OOIP
	PV	Moles					
0.100	0.049	4.60	2.56	7.16	8	207	16.0
0.170	0.076	6.51	4.34	10.85	46	368	28.5
0.283	0.124	11.44	7.23	18.67	93	507	39.2
0.417	0.197	18.17	10.66	28.83	196	588	45.5
0.583	0.307	28.31	14.90	43.21	350	655	50.7
0.750	0.423	39.01	19.17	58.18	540	706	54.6
0.900	0.528	48.69	22.99	71.68	740	747	57.8
1.050	0.641	59.11	26.83	85.94	943	782	60.5
1.220	0.777	71.66	31.18	102.84	1147	815	63.0
1.383	0.907	83.65	35.34	118.99	1357	846	65.4
1.520	1.018	93.88	38.84	132.72	1560	878	67.9
1.683	1.158	106.79	43.01	149.80	1770	910	70.4
2.017	1.446	133.35	51.54	184.89	2175	975	75.4
2.266	1.672	154.20	57.90	212.10	2581	1052	81.4
2.583	1.963	181.03	66.00	247.03	3057	1074	83.1
Postrun					3342	1079	83.4

RUN NUMBER: - 8

TIME Hour	INLET PRESS. Psig	THERMOCOUPLES, °C															
		Inlet	1	2	3	4	5	6	7	8	9	10	11	12	13	14	15
0.000	510.4	150.9	22.7	22.8	22.9	22.5	22.6	22.7	22.6	22.6	22.8	22.7	22.7	22.7	22.8	22.8	23.
0.167	891.4	277.7	88.3	28.4	23.9												
0.333	811.9	271.8	172.6	45.1	32.5	23.4	22.8										
0.500	702.6	263.7	217.8	84.3	71.2	28.8	25.8	22.9									
0.667	655.3	259.7	224.0	122.2	151.2	47.8	42.3	25.2	23.7	22.6							
0.750	692.4	263.1	228.5	137.4	176.6	64.3	60.0	28.4	25.9	22.9							
1.083	597.9	259.5	228.9	179.6	217.5	141.4	191.3	79.4	85.2	33.3	-	-	23.5	22.7			
1.250	573.1	258.2	228.0	191.1	219.8	168.9	210.8	125.0	166.1	55.4	-	28.6	27.5	23.4	23.3		
1.417	617.5	256.2	230.0	198.0	221.3	185.6	212.4	161.2	192.4	95.6	-	41.4	37.6	25.8	24.9	23.2	23.
1.500	557.2	257.4	226.3	200.7	224.8	191.6	215.6	175.4	204.2	119.4	-	53.3	49.3	28.8	27.4	23.7	23.
1.667	575.2	256.5	227.8	205.0	221.3	200.4	218.6	194.2	215.1	161.9	-	95.6	94.2	40.7	36.9	26.3	24.
1.833	544.1	254.0	226.7	208.3	221.6	206.1	219.8	203.8	217.8	187.0	-	150.2	183.6	72.9	66.3	34.6	30.
2.000	551.0	254.6	227.2	209.2	223.2	208.0	219.3	207.3	216.7	198.4	-	182.3	205.6	131.8	146.3	54.7	41.
2.167	525.3	254.3	226.7	211.5	224.3	210.3	221.6	210.8	220.0	204.9	-	197.8	212.8	178.1	203.8	113.1	107.
2.333	511.8	256.6	226.0	213.6	223.0	212.5	220.4	213.3	219.4	209.0	-	205.9	218.3	198.3	215.5	172.7	204.
2.500	515.0	257.7	226.7	215.4	223.4	214.7	221.6	215.5	220.5	211.3	-	209.8	219.7	206.8	218.8	197.8	214.
2.583	512.1	256.3	225.8	216.1	224.3	215.5	223.6	216.3	221.3	212.3	-	211.2	220.8	208.9	219.0	203.3	214.

TYPE: SIMULTANEOUS STEAM/CO₂/N₂ (POST WATERFLOOD)

TIME Hour	STEAM INJECTED		GAS INJECTED	TOTAL INJECTED	WATER PRODUCED	OIL PRODUCED	OIL RECOVERY
	PV	Moles	Moles	Moles	cm ³	cm ³	% ORAW
0.43	0.371	31.93	13.91	45.84	727	128	18.0
0.82	0.664	57.14	26.53	83.67	1162	193	27.2
0.98	0.791	68.07	31.71	99.78	1362	231	32.5
1.12	0.904	77.79	36.24	114.03	1526	258	36.3
1.22	0.985	84.76	39.48	124.24	1653	279	39.3
1.35	1.091	93.89	43.68	137.57	1865	310	43.7
1.48	1.197	103.01	47.89	150.90	2064	349	49.2
1.72	1.397	120.22	55.65	175.87	2368	409	57.6
1.88	1.531	131.75	60.83	192.58	2626	464	65.4
2.17	1.782	153.35	70.22	223.57	2945	525	73.9
2.33	1.921	165.31	75.39	240.70	3285	559	78.7
Postrun					3580	572	80.6

9

TIME Hour	INLET PRESS. Pslg	THERMOCOUPLES, °C															
		Inlet	1	2	3	4	5	6	7	8	9	10	11	12	13	14	15
0.000	0.00	23.5	23.5	23.5	23.5	23.5	23.4	23.5	23.2	23.3	23.2	23.3	23.3	23.3	23.3	23.5	23.7
0.167	542.8	251.0	115.2	23.9	23.7												
0.333	592.2	255.6	204.1	42.1	43.3	24.3											
0.500	589.2	255.6	213.3	88.5	98.9	33.2	37.0	24.4	24.9								
0.667	585.0	255.2	217.9	130.8	168.5	56.4	61.4	29.9	32.9	24.2							
0.833	562.3	253.0	219.5	157.9	197.3	98.7	111.2	42.7	50.3	27.5	28.3						
1.000	543.4	254.1	221.3	174.9	209.2	143.2	176.6	68.3	87.7	36.2	38.5	26.2	25.8				
1.167	540.7	252.4	223.9	187.3	215.9	172.0	201.7	109.3	160.9	54.9	64.1	32.5	32.2	25.0	24.5	23.7	
1.333	538.9	256.1	225.4	196.1	218.4	188.9	211.7	150.2	197.1	92.3	133.8	48.3	49.6	29.2	27.8	24.5	24.2
1.667	516.6	255.8	223.5	201.8	220.1	201.5	216.1	191.3	211.4	166.3	204.8	134.5	186.8	74.7	67.4	35.1	30.6
1.833	508.4	256.9	223.2	207.9	220.3	204.2	216.9	198.9	213.4	184.4	209.8	167.0	203.7	134.2	171.0	60.3	43.2
2.083	492.9	256.1	223.0	210.5	220.4	207.4	217.9	204.9	215.4	197.6	212.7	191.3	210.7	186.1	204.7	168.5	109.1
2.333	499.6	254.5	226.6	211.8	220.5	209.7	218.5	208.0	216.4	203.2	214.9	200.9	213.2	201.1	210.7	200.1	203.3

TYPE: SIMULTANEOUS STEAM/CO₂ (POST WATERFLOOD)

TIME Hour	STEAM INJECTED		GAS INJECTED	TOTAL INJECTED	WATER PRODUCED	OIL PRODUCED	OIL RECOVERY
	PV	Moles	Moles	Moles	cm ³	cm ³	% ORAW
0.133	0.120	10.24	0.90	11.14	238	8	1.2
0.183	0.165	14.08	1.25	15.33	436	11	1.6
0.467	0.421	35.94	3.18	39.12	876	107	16.0
0.617	0.557	47.55	4.20	51.75	1057	176	26.3
0.800	0.722	61.63	5.44	67.07	1309	225	33.6
0.930	0.839	71.62	6.33	77.95	1501	248	37.0
1.250	1.128	96.29	8.50	104.79	1925	291	43.5
1.38	1.245	106.27	9.39	115.66	2172	313	46.8
1.63	1.471	125.57	11.09	136.66	2455	361	53.9
1.87	1.688	144.09	12.72	156.81	2885	426	63.6
2.08	1.880	160.48	14.15	174.63	3200	478	71.4
2.25	2.03	173.28	15.31	188.59	3480	508	75.9
Postrun					3690	525	78.4

RUN NUMBER: 10

TIME Hour	INLET Psig	THERMOCOUPLES, °C														
		1	2	3	4	5	6	7	8	9	10	11	12	13	14	15
0.00	2.6	23.0	23.1	23.0	23.0	22.9	22.9	22.7	22.7	22.7	22.7	22.7	22.7	22.8	23.0	23.2
0.33	529.8	255.2	241.1	62.4	84.6	27.0	27.6	23.3	23.4	23.1	23.3	23.1	23.3	23.1	23.2	23.2
0.75	516.5	266.1	239.2	191.1	233.9	106.8	110.9	46.6	60.4	29.0	29.2	23.9	23.5	23.2	23.2	23.3
1.00	508.8	270.2	239.5	213.2	237.4	170.2	203.3	91.3	123.1	50.1	62.1	32.7	31.4	24.5	24.1	23.5
1.33	502.5	273.1	238.5	219.2	237.8	210.7	233.3	170.5	228.6	118.3	170.6	65.6	70.9	39.4	42.3	26.7
1.67	496.2	272.6	238.7	226.0	236.2	222.5	236.0	213.4	235.4	191.5	234.1	160.8	216.8	85.9	91.8	43.7
1.92	490.1	268.0	238.6	227.3	235.5	225.1	235.8	221.4	234.7	215.7	232.7	209.6	230.2	173.8	211.9	84.1
2.25	502.7	268.7	238.7	233.4	237.4	230.4	237.3	226.3	236.7	224.9	236.0	227.2	235.4	225.4	235.0	217.8

RUN NUMBER: 11

TYPE: SIMULTANEOUS STEAM/N₂ (POST WATERFLOOD)

TIME Hour	STEAM INJECTED		GAS INJECTED Moles	TOTAL INJECTED Moles	WATER PRODUCED cm ³	OIL PRODUCED cm ³	OIL RECOVERY % ORAW
	PV	Moles					
0.03	0.025	2.158	0.76	2.918	352	3	0.4
0.25	0.206	17.78	6.36	24.14	612	61	8.5
0.517	0.426	36.78	13.16	49.94	907	99	13.8
0.830	0.684	59.05	21.12	80.17	1284	168	23.5
1.05	0.865	74.68	26.72	101.40	-	-	-
1.08	0.890	76.84	27.48	104.32	1624	227	31.7
1.65	1.349	116.46	41.99	158.45	(2396)	(365)	50.9
1.83	1.496	129.15	46.57	175.72	(2671)	(432)	60.3
2.02	1.651	142.54	51.40	193.94	(2949)	(481)	67.2
2.18	1.782	153.85	55.47	209.32	(3210)	(506)	70.7
2.33	1.905	164.47	59.29	223.76	(3455)	(519)	72.5
Postrun					(3860)	(534)	74.6

() indicate production estimates.

()

١٠

RUN NUMBER: 12

TYPE: SLUG FLUE GAS/STEAMFLOOD

TIME Hour	STEAM INJECTED		GAS INJECTED	TOTAL INJECTED	WATER PRODUCED	OIL PRODUCED	OIL RECOVERY
	PV	Moles	Moles	Moles	cm ³	cm ³	% OOIP
0.033			1.07	1.07	0	274	21.8
0.167			5.40	5.40	0	369	29.4
0.95			30.74	30.74	0	453	36.1
1.58			51.12	51.12	0	489	39.0
2.42			78.30	78.30	0	517	41.2
3.15	0.351	31.10	80.89	111.99	173	559	44.5
3.40	0.532	47.14	80.89	128.03	367	587	46.8
3.68	0.738	65.40	80.89	146.29	571	606	48.3
3.92	0.907	80.37	80.89	161.26	766	620	49.4
4.30	1.185	105.00	80.89	185.89	1194	638	50.8
4.62	1.415	125.38	80.89	206.27	1657	649	51.7
4.90	1.620	143.55	80.89	224.44	2071	703	56.0
5.33	1.935	171.46	80.89	252.35	2642	828	66.0
5.60	2.128	188.56	80.89	269.45	3032	916	73.0
5.85	2.310	204.69	80.89	285.58	3395	1007	80.2
6.08	2.480	219.76	80.89	300.65	3752	1073	85.5
Postrun					3901	1099	87.6

RUN NUMBER: 12

TIME Hour	INLET PRESS. Pslg	THERMOCOUPLES, °C															
		Inlet	1	2	3	4	5	6	7	8	9	10	11	12	13	14	15
2.750	507.6	244.0	53.1	23.8	23.5												
3.000	554.3	249.7	91.4	40.5	29.4	24.1	23.6										
3.333	545.2	248.5	125.9	70.3	53.3	31.8	27.1	24.2	23.6								
3.500	532.6	248.0	139.4	83.4	66.0	38.3	30.3	25.2	24.1	23.7							
3.750	545.5	248.9	160.7	102.9	84.2	50.4	39.2	28.2	25.6	24.1	23.9	23.7					
4.083	548.4	257.8	193.9	130.5	115.2	69.9	57.5	36.9	31.6	25.8	24.9	24.1	23.9				
4.417	550.9	263.0	246.7	170.3	163.4	100.6	91.8	55.5	48.3	33.1	30.4	25.6	25.0	24.2	24.1		
4.750	572.2	257.0	251.9	237.0	252.0	150.3	128.7	83.7	76.7	49.6	44.8	32.0	30.4	26.1	25.6	24.5	24.6
5.083	560.8	254.6	250.8	250.8	250.9	233.3	250.7	173.7	156.7	75.0	68.5	45.5	42.1	32.4	30.7	26.5	26.1
5.417	560.4	254.7	250.8	250.8	242.8	250.7	250.7	235.3	250.7	214.1	250.7	78.5	86.0	45.7	43.7	31.9	30.8
5.750	537.2	262.0	248.5	248.5	248.6	248.2	241.0	248.1	242.8	248.1	229.6	248.2	144.4	159.7	55.6	50.5	
6.000	520.0	263.1	246.7	246.7	246.4	246.6	240.7	246.3	246.0	246.1	243.8	246.3	245.5	246.2	226.8	128.3	
6.167	516.4	263.2	246.3	246.3	246.5	246.1	240.1	246.0	243.1	245.8	245.8	245.9	245.5	245.8	244.4	246.2	

RUN NUMBER: 13

TYPE: SIMULTANEOUS STEAM/CO₂ (LOW RATE)

TIME Hour	STEAM INJECTED		GAS INJECTED	TOTAL INJECTED	WATER PRODUCED	OIL PRODUCED	OIL RECOVERY
	PV	Moles	Moles	Moles	cm ³	cm ³	% OOIP
0.617	0.292	23.85	2.33	26.18	83	520	41.9
0.867	0.430	35.12	3.24	38.36	178	579	46.6
1.100	0.524	42.79	3.98	46.77	305	614	49.4
1.383	0.639	52.19	4.88	57.07	470	654	52.7
1.683	0.762	62.23	5.87	68.10	662	685	55.2
1.950	0.872	71.21	6.78	77.99	848	709	57.1
2.600	1.136	92.77	8.98	101.75	1262	763	61.4
2.917	1.274	104.04	10.05	114.09	1460	799	64.3
3.233	1.405	114.74	11.12	125.86	1680	823	66.3
3.817	1.648	134.59	13.09	147.68	2069	874	70.4
4.150	1.786	145.86	14.22	160.08	2281	903	72.7
4.650	1.994	162.84	15.92	178.76	2601	953	76.7
5.150	2.202	179.83	17.74	197.57	2919	992	79.9
5.683	2.423	197.88	19.60	217.48	3236	1026	82.6
6.300	2.679	218.79	21.75	240.54	3641	1071	86.2
6.833	2.901	236.92	23.62	260.54	3980	1093	88.0
Postrun					4185	1108	89.2

RUN NUMBER: 13

TIME Hour	INLET PRESS. Pstg	THERMOCOUPLES, °C															
		Inlet	1	2	3	4	5	6	7	8	9	10	11	12	13	14	15
0.00	0.80	23.3	23.5	23.5	23.5	23.5	23.5	23.6	23.5	23.5	23.5	23.6	23.6	23.6	23.6	23.6	23.7
0.25	405.3	233.7	96.1	26.9	24.2	23.6											
0.50	538.4	249.0	85.0	39.1	28.5	24.2	23.8										
0.75	526.6	247.4	109.8	51.1	37.9	26.8	24.8										
1.00	520.3	247.0	154.1	65.8	50.2	32.0	28.3	24.6	23.7	23.8							
1.25	514.3	246.0	200.0	86.3	66.2	40.6	35.3	26.7	25.1	24.0	24.0	23.9					
1.50	513.0	246.2	209.0	116.5	87.7	52.3	44.8	31.0	27.9	24.8	24.3	24.1	24.0				
1.75	512.2	246.0	213.9	147.1	118.9	68.6	57.8	37.7	32.7	26.5	25.4	24.3	24.2	24.1			
2.00	500.2	244.7	221.1	168.0	170.1	89.0	74.7	46.3	39.2	29.7	27.4	24.9	24.5	24.2			
2.25	490.2	243.1	222.3	184.1	199.8	113.5	98.3	58.7	49.5	34.4	31.2	26.3	25.5	24.2	24.3		
2.50	506.5	245.4	224.4	195.5	208.1	140.3	124.4	74.6	61.8	41.0	35.8	28.8	26.9	25.1	24.8	24.3	
2.75	506.4	245.3	225.2	202.4	215.6	164.1	159.9	93.8	78.7	50.1	42.7	32.3	29.4	26.3	25.4	24.6	24.6
3.00	504.6	245.2	228.1	208.8	221.3	182.8	199.7	117.0	99.4	62.3	52.2	37.4	33.1	28.0	26.5	25.2	24.9
3.25	474.8	241.5	231.0	213.0	221.8	198.9	220.3	148.1	127.0	77.6	66.7	44.8	39.2	31.0	28.6	26.1	25.5
3.50	505.8	245.3	231.5	216.6	226.1	206.9	223.6	174.2	157.6	95.0	81.3	53.7	45.8	34.9	31.2	27.4	26.1
3.75	505.7	245.2	233.4	218.7	228.4	212.3	226.1	194.0	202.6	119.7	99.3	65.5	55.0	40.2	35.0	29.4	27.2
4.00	499.7	244.5	232.0	220.7	228.5	215.4	226.5	205.2	220.0	151.5	123.7	79.5	66.9	47.1	40.5	32.2	29.3
4.25	500.4	244.7	232.8	221.9	231.9	216.8	224.9	211.4	220.4	180.6	163.4	98.0	80.8	56.1	47.0	36.3	31.9
4.58	475.3	241.8	230.5	223.3	228.9	220.0	227.6	217.8	228.9	200.5	213.3	133.2	108.5	71.4	61.0	43.4	38.1
4.92	503.7	245.3	235.7	224.5	230.8	221.2	228.8	220.0	228.5	211.9	221.3	177.9	152.0	94.0	76.5	53.7	43.9
5.25	508.7	245.5	236.0	224.8	230.4	222.7	230.3	221.1	228.5	216.5	224.7	203.9	207.4	132.2	101.4	68.4	54.7
5.58	504.1	244.9	233.9	226.5	232.8	224.1	229.6	222.4	229.6	218.6	226.8	212.4	219.6	176.6	140.6	89.1	67.5
5.92	509.2	245.4	237.5	226.5	229.9	225.0	230.5	223.0	229.4	220.1	227.9	216.9	224.0	203.8	191.2	123.9	88.9
6.25	508.6	244.9	237.1	226.8	228.9	225.2	230.6	223.9	230.3	221.1	228.4	219.4	226.1	214.7	216.9	171.7	118.2
6.58	501.4	244.7	236.8	227.1	228.9	225.2	229.8	223.6	229.6	221.8	228.9	220.7	227.3	219.0	222.6	203.3	164.8
6.83	485.3	242.7	232.9	228.1	233.3	225.8	230.4	223.4	229.8	222.2	229.7	221.4	227.8	220.7	224.2	212.7	200.1

RUN NUMBER: 14

TYPE: SIMULTANEOUS STEAM/CO₂/N₂ (LOW RATE)

TIME Hour	STEAM INJECTED		GAS INJECTED	TOTAL INJECTED	WATER PRODUCED	OIL PRODUCED	OIL RECOVERY
	PV	Moles	Moles	Moles	cm ³	cm ³	% OOIP
0.20	0.093	7.81	3.25	11.06	5	325	25.5
0.38	0.147	12.34	6.18	18.52	15	467	36.7
0.60	0.222	18.64	9.76	28.40	90	548	43.0
0.88	0.323	27.11	14.31	41.92	229	623	48.9
1.13	0.418	35.09	18.37	53.46	363	675	53.0
1.45	0.544	45.67	23.58	69.25	539	715	56.2
2.10	0.811	68.08	34.14	102.22	951	774	60.8
2.43	0.950	79.75	39.51	119.26	1157	800	62.8
2.80	1.080	90.66	45.53	136.19	1392	829	65.1
3.42	1.354	113.66	55.61	169.27	1798	887	69.7
3.83	1.536	128.94	62.27	191.21	2075	924	72.6
4.32	1.754	147.24	70.24	217.48	2379	975	76.6
4.78	1.958	164.36	77.72	242.08	2702	1033	81.1
5.30	2.189	183.75	86.17	269.92	3037	1081	84.9
5.87	2.442	204.99	95.44	300.43	3433	1112	87.4
6.58	2.758	231.52	106.98	338.50	3903	1135	89.2
Postrun					4103	1155	90.7

14

INLET
TIME PRESS.

RUN NUMBER: 15

TYPE: SIMULTANEOUS STEAM/CO₂/N₂ (HIGH PRESSURE)

TIME Hour	STEAM INJECTED		GAS INJECTED	TOTAL INJECTED	WATER PRODUCED	OIL PRODUCED	OIL RECOVERY
	PV	Moles	Moles	Moles	cm ³	cm ³	% OOIP
0.233	0.283	23.93	7.58	31.51	27	482	37.6
0.400	0.331	27.99	13.02	41.01	97	593	46.3
0.867	0.517	43.72	28.22	71.94	415	724	56.5
1.050	0.629	53.19	34.17	87.36	583	753	58.7
1.233	0.834	70.52	40.13	110.65	873	793	61.9
1.483	1.115	94.28	48.26	142.54	1268	834	65.1
1.617	1.267	107.13	52.62	159.75	1463	861	67.2
1.750	1.418	119.90	56.95	176.85	1682	891	69.5
1.883	1.514	128.02	61.28	189.30	1880	925	72.2
2.030	1.673	141.46	66.07	207.53	2091	960	74.9
2.250	1.846	156.09	73.23	229.32	2413	1012	78.9
2.417	1.978	167.25	78.66	245.91	2671	1051	82.0
2.633	2.148	181.63	85.69	267.32	2937	1085	84.6
2.767	2.254	190.59	90.05	280.64	3115	1100	85.8
2.900	2.359	199.47	94.38	293.85	3287	1104	86.1
3.000	2.438	206.15	97.63	303.78	3424	1111	86.7
Postrun					3934	1136	88.6

RUN NUMBER: 15

TIME Hour	INLET Psig	THERMOCOUPLES, °C															
		Inlet	1	2	3	4	5	6	7	8	9	10	11	12	13	14	15
0.00	339.6	85.4	23.6	23.6	23.6	23.6	23.6	23.7	23.6	23.6	23.7	23.7	23.7	23.7	23.7	23.8	23.9
0.25	1110.6	293.0	79.6	32.7	32.8	24.5											
0.50	1058.4	289.7	137.8	55.4	50.4	29.5	28.8	24.5									
0.75	1039.8	288.4	174.7	85.0	78.7	42.0	40.7	27.7	26.9	24.2							
1.00	1037.8	288.2	195.8	114.6	110.2	61.0	59.3	35.6	33.9	26.3	25.6	24.2					
1.25	1039.2	294.6	252.4	180.0	229.2	107.5	146.9	57.6	64.9								
1.50	1044.2	289.3	253.3	212.3	242.5	172.6	218.3	118.3	149.4	64.6	72.8	37.7	39.1	28.1	27.6	24.9	24.9
1.75	1031.0	294.7	255.2	224.7	244.2	205.5	236.7	181.3	215.4	124.4	152.9	62.7	77.8	40.4	40.5	28.6	28.4
2.00	1019.6	295.7	251.8	232.1	247.2	218.7	242.5	212.9	234.2	181.3	213.2	125.0	149.9	71.8	72.5	40.5	41.0
2.25	1018.4	288.0	252.8	235.2	246.8	226.2	242.7	222.7	237.1	209.0	228.9	180.0	205.8	132.0	134.2	66.4	64.0
2.50	995.2	286.0	247.5	236.0	245.3	228.9	240.3	225.6	237.2	220.4	232.9	208.1	225.0	187.7	203.1	121.3	116.1
2.75	1015.0	287.4	248.7	237.1	244.7	230.4	241.6	226.9	238.1	224.7	234.6	218.5	229.6	211.2	221.6	176.8	193.0
3.00	1010.2	286.9	250.2	238.1	245.8	232.0	242.1	229.5	239.6	227.1	236.2	223.6	232.5	220.4	228.2	204.4	218.1

RUN NUMBER: 16

TYPE: SIMULTANEOUS STEAM/CO₂ (CO₂ PRESATURATED)

TIME Hour	STEAM INJECTED		GAS INJECTED Moles	TOTAL INJECTED Moles	WATER PRODUCED cm ³	OIL PRODUCED cm ³	OIL RECOVERY % OOIP
	PV	Moles					
0.200	0.203	17.59	1.36	18.95	169	448	38.1
0.333	0.347	30.07	2.27	32.34	322	569	48.4
0.483	0.513	44.46	3.29	47.75	587	634	54.0
0.683	0.735	63.70	4.65	68.35	942	704	59.9
0.850	0.920	79.73	5.78	85.51	1232	759	64.6
1.033	1.122	97.24	7.03	104.27	1587	826	70.3
1.250	1.334	114.75	8.50	123.25	1895	877	74.6
1.467	1.545	133.90	9.98	143.88	2238	927	78.9
1.700	1.754	152.01	11.57	163.58	2640	985	83.8
1.950	1.970	170.73	13.27	184.00	2896	1028	87.5
2.100	2.097	181.74	14.29	196.03	3089	1045	88.9
2.167	2.153	186.59	14.74	201.33	3201	1054	89.7
Postrun					3354	1071	91.1

RUN NUMBER: 16

TIME Hour	INLET PRESS. Psig	THERMOCOUPLES, °C														
		1	2	3	4	5	6	7	8	9	10	11	12	13	14	15
0.000	646.6	56.0	22.7	22.7	22.8	22.7	22.8	22.6	22.8	22.7	22.8	23.0	22.9	23.0	23.0	23.2
0.167	590.4	254.7	225.2	51.5	30.5	23.4	23.0	23.0	22.8							
0.333	548.0	250.4	242.9	124.1	138.0	40.8	37.0	24.5	23.8	22.8						
0.500	550.2	250.7	241.8	176.4	230.0	86.8	82.3	35.6	37.0	25.1	24.8					
0.667	537.8	249.4	239.5	201.9	236.2	145.3	185.9	58.5	68.0	33.5	36.8	25.6				
0.833	548.4	250.8	240.7	217.2	238.5	187.1	233.9	121.9	129.3	51.2	56.4	33.9	25.6	26.8		
1.000	512.8	253.0	235.7	224.8	233.6	210.7	233.1	187.5	232.5	90.5	98.3	49.0	33.2	38.8	26.3	29.9
1.167	543.6	251.9	235.9	226.8	235.1	219.0	235.3	209.7	234.1	155.2	176.6	76.8	44.1	48.3	31.9	35.4
1.333	531.2	251.6	237.7	229.6	236.1	224.1	236.2	221.2	236.0	199.6	233.4	135.0	147.1	62.3	64.7	45.1
1.500	537.2	252.9	238.6	231.6	238.1	228.7	237.8	226.7	237.4	218.1	236.4	193.3	228.1	103.7	116.7	60.9
1.667	486.4	246.3	234.6	231.0	233.3	230.1	232.4	228.2	232.5	227.4	232.7	221.6	233.1	167.8	222.3	85.5 104.9
1.833	530.6	249.0	236.7	231.2	234.4	229.4	234.3	228.5	235.2	227.4	235.0	224.7	234.0	201.8	229.6	129.9 151.6
2.000	527.0	249.1	236.8	236.4	235.6	231.5	234.7	229.4	235.3	229.3	235.5	228.0	235.0	216.0	233.6	191.9 216.6
2.167	525.4	248.9	237.3	237.1	236.0	232.2	235.7	229.1	236.0	230.6	236.0	229.7	234.9	222.1	233.9	222.6 233.6

RUN NUMBER: 17

TYPE: SLUG CO₂/STEAMFLOOD

TIME Hour	STEAM INJECTED		GAS INJECTED	TOTAL INJECTED	WATER PRODUCED	OIL PRODUCED	OIL RECOVERY
	PV	Moles	Moles	Moles	cm ³	cm ³	% OOIP
0.467			3.18	3.18	5	215	17.1
2.500			17.01	17.01	5	225	17.9
2.767	0.065	5.51	17.01	22.52	68	321	25.5
2.900	0.371	31.43	17.01	48.44	198	370	29.4
3.050	0.510	43.21	17.01	60.22	370	403	32.0
3.200	0.649	54.98	17.01	71.99	569	428	34.0
3.367	0.804	68.12	17.01	85.13	769	447	35.5
3.500	0.927	78.54	17.01	95.55	961	470	37.3
3.633	1.050	88.96	17.01	105.97	1156	491	39.0
3.750	1.159	98.19	17.01	115.18	1367	511	40.6
4.017	1.406	119.12	17.01	136.13	1770	562	44.6
4.133	1.514	128.27	17.01	145.28	1948	591	46.9
4.400	1.761	149.20	17.01	166.21	2331	685	54.4
4.650	1.993	168.85	17.01	185.86	2714	787	62.5
4.900	2.225	188.51	17.01	205.52	3083	901	71.6
5.167	2.472	209.43	17.01	226.44	3189	1007	80.0
Postrun					3240	1058	84.0

—

TIME Hour	INLET PRESS. Psig	THERMOCOUPLES, °C															
		Inlet	1	2	3	4	5	6	7	8	9	10	11	12	13	14	15
2.583	524.4	247.1	60.9	25.1	24.1	23.7											
2.833	518.0	248.0	137.6	74.4	62.4	33.0	29.0	24.8	24.2								
3.083	507.4	247.5	194.8	108.7	91.2	49.8	43.2	29.9	27.7	24.9							
3.333	517.8	252.1	219.2	142.2	126.6	68.9	64.7	37.8	36.2	27.2	26.7	24.9					
3.583	516.4	252.7	246.7	189.0	174.2	96.7	103.7	54.0	61.8	34.5	36.3	27.4	26.6	25.1	24.7		
3.833	503.6	248.5	245.0	230.7	245.2	168.0	178.3	82.5	99.7	51.3	58.9	36.3	36.0	28.6	26.8	25.4	25.0
4.083	515.6	249.3	246.5	245.9	246.7	226.2	246.7	157.4	183.6	76.3	89.6	50.0	49.8	36.1	32.7	28.0	26.3
4.333	510.2	253.3	245.8	242.9	245.9	235.7	246.0	227.5	245.9	172.3	136.3	75.6	69.4	45.8	39.4	32.0	29.0
4.583	488.0	251.9	243.3	240.4	243.4	238.1	243.5	242.3	243.3	229.0	243.1	191.9	151.5	80.4	78.8	44.2	37.5
4.833	490.3	249.1	243.6	243.5	243.6	239.2	243.7	239.6	243.5	242.0	243.3	239.6	243.5	242.4	212.7	62.8	52.1
5.083	497.6	255.1	244.4	244.4	244.5	238.9	244.5	244.4	244.4	243.9	244.2	244.1	244.3	244.2	244.7	244.1	213.4
5.167	490.7	248.2	243.6	243.7	243.8	238.6	243.8	243.1	243.6	243.1	243.5	243.5	243.5	243.5	243.9	243.8	244.0

RUN NUMBER: 18

TYPE: STEAM ONLY (POST WATERFLOOD)

TIME Hour	STEAM INJECTED		GAS INJECTED	TOTAL INJECTED	WATER PRODUCED	OIL PRODUCED	OIL RECOVERY
	PV	Moles	Moles	Moles	cm ³	cm ³	% ORAW
0.217	0.191	16.36	-	16.36	244	4	0.58
0.400	0.353	30.24	-	30.24	486	8	1.16
0.583	0.514	44.00	-	44.00	736	12	1.74
0.767	0.676	57.91	-	57.91	984	16	2.33
0.950	0.837	71.70	-	71.70	1231	19	2.76
1.117	0.984	84.30	-	84.30	1475	23	3.34
1.250	1.102	94.40	-	94.40	1717	27	3.92
1.367	1.205	103.22	-	103.22	1962	30	4.36
1.517	1.337	114.53	-	114.53	2209	33	4.80
1.767	1.557	133.38	-	133.38	2684	57	8.28
1.883	1.660	142.21	-	142.21	2884	104	15.11
2.167	1.910	163.62	-	163.62	3278	216	31.40
2.417	2.130	182.47	-	182.47	3668	331	48.11
2.700	2.380	203.89	-	203.89	4058	443	64.39
2.766	2.438	208.86	-	208.86	4139	460	66.86
2.833	2.497	213.91	-	213.91	4226	472	68.60
Postrun					4704	514	74.70

RUN NUMBER: 18

TIME Hour	INLET PRESS. Psig	THERMOCOUPLES, °C														
		1	2	3	4	5	6	7	8	9	10	11	12	13	14	15
0.083	509.6	244.9	24.6	24.1	24.0	23.9	-	23.7	23.5	23.5	23.5	23.5	23.6	23.6	23.7	23.9
0.333	532.0	248.7	40.2	26.7	24.1	-	-	-	-	-	-	-	-	-	-	-
0.583	504.3	246.0	156.3	83.2	58.6	30.1	24.1	-	-	-	-	-	-	-	-	-
0.833	503.4	246.9	184.1	118.9	96.5	50.3	27.2	25.1	23.8	-	-	-	-	-	-	-
1.083	505.8	248.2	154.8	134.3	78.7	-	38.7	34.1	25.9	24.8	-	-	-	-	-	-
1.333	517.2	251.6	246.3	245.9	215.4	114.6	61.1	57.5	34.3	32.1	25.8	24.8	24.1	-	-	-
1.583	522.0	250.0	246.7	246.9	246.9	211.2	94.8	92.3	52.3	49.7	33.3	30.4	25.9	24.9	24.2	24.2
1.833	516.8	249.7	246.4	246.6	246.5	233.5	212.9	246.5	85.5	100.4	50.6	49.7	32.7	30.1	25.4	25.0
2.083	515.4	254.8	246.2	246.3	246.3	237.8	242.6	246.1	237.1	246.2	113.9	85.0	50.2	42.1	30.6	28.4
2.333	494.7	256.3	243.6	243.8	243.8	242.7	242.6	243.6	241.5	243.6	242.5	243.7	242.3	144.7	55.9	47.1
2.583	504.0	251.6	245.0	245.2	245.0	242.0	243.8	244.9	244.8	244.8	244.5	244.8	244.8	245.2	129.0	84.8
2.833	501.1	252.1	244.4	244.6	244.5	243.1	244.4	244.3	244.4	244.3	244.3	244.4	244.4	244.8	242.7	244.9

RUN NUMBER: 19

TYPE: SIMULTANEOUS STEAM/N₂ (POST WATERFLOOD)

TIME Hour	STEAM INJECTED		GAS INJECTED	TOTAL INJECTED	WATER PRODUCED	OIL PRODUCED	OIL RECOVERY
	PV	Moles	Moles	Moles	cm ³	cm ³	% OOIP
0.083	0.074	6.34	2.12	8.46	395	4	0.6
0.283	0.251	21.52	7.23	28.75	745	46	6.9
0.617	0.548	46.98	15.77	62.75	1174	126	19.0
0.867	0.770	66.01	22.15	88.16	1482	179	27.0
1.083	0.962	82.46	27.67	110.13	1774	222	33.5
1.250	1.111	95.24	31.94	127.18	2017	256	38.6
1.417	1.259	107.92	36.21	144.13	2219	276	41.6
1.533	1.362	116.75	39.17	155.92	2390	299	45.1
1.767	1.570	134.58	45.15	179.73	2780	421	63.5
1.883	1.673	143.41	48.12	191.53	2970	455	68.6
2.017	1.792	153.61	51.54	205.15	3172	479	72.2
2.133	1.895	162.44	54.51	216.95	3364	492	74.2
2.250	1.999	171.36	57.50	228.86	3533	501	75.6
Postrun					3908	516	77.8

RUN NUMBER: 19

TIME Hour	INLET PRESS. Psig	THERMOCOUPLES, °C															
		Inlet	1	2	3	4	5	6	7	8	9	10	11	12	13	14	15
0.000	17.47	23.4	24.2	23.7	23.5	23.5	23.3	23.1	23.0	23.0	23.0	22.9	22.9	22.9	23.0	23.2	
0.167	589.0	253.5	163.9	31.0	27.6	23.7											
0.333	642.7	258.9	219.2	69.6	73.2	29.6	29.2	23.7									
0.500	619.2	257.4	227.2	118.8	153.1	52.8	53.1	27.2	26.9								
0.667	602.5	255.6	229.6	154.1	200.5	100.9	119.5	41.0	40.1	25.5	25.6	23.5					
0.833	584.1	254.3	229.1	171.9	208.6	143.6	182.8	74.4	71.4	32.7	32.7	24.9					
1.000	571.6	252.8	228.4	183.4	215.4	170.2	205.3	120.2	150.9	51.1	50.7	29.5	28.3	24.2			
1.167	562.1	253.3	228.9	191.9	219.5	187.3	214.1	156.9	195.6	92.1	111.4	42.0	39.1	27.0	25.9	23.9	
1.333	548.4	254.3	229.3	198.4	223.2	197.4	218.9	181.6	210.8	137.0	189.7	76.8	76.1	34.9	32.5	25.5	24.8
1.500	535.9	253.4	228.3	203.2	224.0	203.8	220.7	197.3	216.4	169.8	210.2	131.6	179.2	59.2	57.0	30.6	27.9
1.667	507.9	265.2	227.0	205.4	225.2	206.7	222.7	202.8	219.2	188.3	216.6	173.8	209.8	122.3	145.0	52.1	41.1
1.833	509.0	251.2	227.4	208.4	225.4	207.5	223.0	208.4	220.3	199.8	219.7	195.4	217.2	167.2	209.9	104.1	96.9
2.000	496.1	260.3	225.4	209.7	224.7	208.7	223.1	211.2	220.4	205.2	219.3	204.7	217.5	191.2	215.4	164.7	192.1
2.167	510.0	260.4	227.6	211.2	225.8	212.1	223.0	213.3	222.4	208.3	221.3	208.4	218.5	201.6	217.5	192.6	212.1
2.250	509.9	251.8	226.5	212.1	225.3	212.9	224.4	213.9	222.7	209.4	221.1	210.0	219.8	204.7	217.9	199.5	214.7

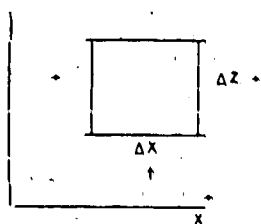
TIME Hour	STEAM INJECTED		GAS INJECTED	TOTAL INJECTED	WATER PRODUCED	OIL PRODUCED	OIL RECOVERY
	PV	Moles	Moles	Moles	cm ³	cm ³	% OOIP
0.45	0.513	43.32	3.06	46.38	360	494	39.6
0.55	0.607	51.26	3.74	55.00	493	551	44.2
0.65	0.702	59.28	4.42	63.70	627	597	47.8
0.783	0.828	69.92	5.33	75.25	829	651	52.2
0.917	0.955	80.64	6.24	86.88	999	713	57.1
1.133	1.165	98.38	7.71	106.09	1328	814	65.2
1.300	1.325	111.89	8.84	120.73	1585	852	68.3
1.483	1.502	126.84	10.09	136.93	1858	891	71.4
1.700	1.711	144.48	11.57	156.05	2191	963	77.2
1.900	1.904	160.78	12.93	173.71	2509	1010	80.9
2.133	2.131	179.95	14.51	194.46	2875	1070	85.7
2.167	2.164	182.74	14.74	197.48	2903	1078	86.4
Postrun					2953	1090	87.3

RUN NUMBER: 20

TIME Hour	INLET PRESS. Psig	THERMOCOUPLES, °C													
		1	2	3	4	5	6	7	8	9	10	11	12	13	14
0.000	49.5	23.0	22.2	22.2	22.3	22.2	22.3	22.2	22.3	22.2	22.3	22.2	22.3	22.3	22.5
0.167	380.3	231.8	141.3	81.5	102.7	41.3	27.8	22.8							
0.417	535.4	249.5	232.9	140.0	110.5	60.1	49.8	28.6	27.2	22.8	22.9	22.7			
0.750	535.3	250.2	240.1	195.5	235.9	136.1	102.7	50.4	50.3	31.2	34.4	25.4	27.0	23.4	23.1
1.000	530.2	250.7	238.9	214.9	236.3	201.6	231.0	98.3	90.1	47.6	50.4	33.4	34.5	26.5	23.9
1.250	516.3	250.4	234.9	224.0	235.7	224.0	235.1	192.0	230.8	90.4	101.3	49.7	51.7	34.4	27.0
1.500	510.3	259.9	235.1	225.4	237.9	226.7	235.5	217.9	234.5	181.2	228.9	100.6	113.5	51.7	34.4
1.750	516.4	262.3	238.1	228.2	238.5	228.6	238.0	226.8	236.4	214.5	236.1	193.9	232.6	105.2	51.9
2.000	510.7	262.9	238.3	230.5	237.5	228.6	237.5	230.3	237.3	224.6	237.4	224.4	236.4	216.6	105.3
2.167	503.3	263.9	237.5	231.0	237.4	229.1	237.6	230.6	237.6	228.4	238.1	229.5	237.4	228.0	213.4

APPENDIX D

DERIVATION OF PARTIAL DIFFERENTIAL EQUATIONS FOR THE MATHEMATICAL MODEL



Q_1 = external source or sink (+ve for injection)
units: moles/time

Let N_{ij} = molar flow rate of component i in phase j (units: moles/time).

The molar flow rates of component i at the various faces of the element are:

- x - direction inlet $(N_{ia} + N_{io} + N_{iv})_x$
- x - direction outlet $(N_{ia} + N_{io} + N_{iv})_{x+\Delta x}$
- z - direction inlet $(N_{ia} + N_{io} + N_{iv})_z$
- z - direction outlet $(N_{ia} + N_{io} + N_{iv})_{z+\Delta z}$

Let c_{ij} = molar concentration of component i in phase j (units: moles/volume).

The amounts of component i present in the element are given by:

$$\begin{aligned} \text{at time } t & \quad [\phi V_b (c_{ia}S_a + c_{io}S_o + c_{iv}S_v)]_t \\ \text{at time } t+\Delta t & \quad [\phi V_b (c_{ia}S_a + c_{io}S_o + c_{iv}S_v)]_{t+\Delta t} \end{aligned}$$

A molar balance on component i over time increment Δt may be written as:

$$\begin{aligned} (\text{Output} - \text{Input}) + \text{Accumulation} &= 0 \\ \left[(N_{ia} + N_{io} + N_{iv})_{x+\Delta x} - (N_{ia} + N_{io} + N_{iv})_x \right] \Delta t &+ \left[(N_{ia} + N_{io} + N_{iv})_{z+\Delta z} - (N_{ia} + N_{io} + N_{iv})_z \right] \Delta t \\ &- Q_1 \Delta t + [\phi V_b (c_{ia}S_a + c_{io}S_o + c_{iv}S_v)]_{t+\Delta t} - [\phi V_b (c_{ia}S_a + c_{io}S_o + c_{iv}S_v)]_t = 0 \end{aligned} \quad (D-1)$$

The equation may be rewritten as:

$$\begin{aligned} & \frac{(N_{ia} + N_{io} + N_{iv})_{x+\Delta x} - (N_{ia} + N_{io} + N_{iv})_x}{\Delta x} \cdot \Delta x \\ & + \frac{(N_{ia} + N_{io} + N_{iv})_{z+\Delta z} - (N_{ia} + N_{io} + N_{iv})_z}{\Delta z} \cdot \Delta z + Q_1 \\ & - \frac{[\phi V_b (c_{ia}S_a + c_{io}S_o + c_{iv}S_v)]_{t+\Delta t} - [\phi V_b (c_{ia}S_a + c_{io}S_o + c_{iv}S_v)]_t}{\Delta t} = 0 \end{aligned} \quad (D-2)$$

$$= \frac{\partial}{\partial x} (N_{1a} + N_{1o} + N_{1v}) \cdot \Delta x + \frac{\partial}{\partial z} (N_{1a} + N_{1o} + N_{1v}) \cdot \Delta z + Q_1 = V_b \frac{\partial}{\partial t} [\phi (x_{1a} S_a + x_{1o} S_o + x_{1v} S_v)] \quad (D-3)$$

$$\text{Now } N_{1j} = \frac{x_{1j} \rho_j u_j}{M_j} \cdot A \quad (D-4)$$

$$\text{and } C_{1j} = \frac{x_{1j} \rho_j}{M_j} \quad (D-5)$$

Substituting (D-4) and (D-5) into (D-3), we obtain:

$$\begin{aligned} &= \frac{\partial}{\partial x} \left(\frac{x_{1a} \rho_a u_a}{M_a} A_x + \frac{x_{1o} \rho_o u_o}{M_o} A_x + \frac{x_{1v} \rho_v u_v}{M_v} A_x \right) \cdot \Delta x \\ &+ \frac{\partial}{\partial z} \left(\frac{x_{1a} \rho_a u_a}{M_a} A_z + \frac{x_{1o} \rho_o u_o}{M_o} A_z + \frac{x_{1v} \rho_v u_v}{M_v} A_z \right) \cdot \Delta z + Q_1 \\ &= V_b \frac{\partial}{\partial t} \left[\phi \left(\frac{x_{1a} \rho_a S_a}{M_a} + \frac{x_{1o} \rho_o S_o}{M_o} + \frac{x_{1v} \rho_v S_v}{M_v} \right) \right] \end{aligned} \quad (D-6)$$

Phase velocities, U_j , are given by Darcy's Law as follows:

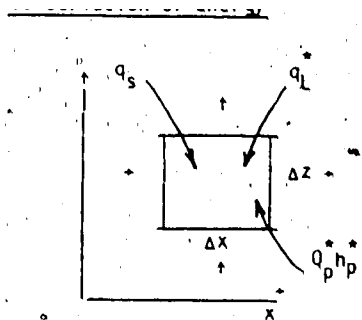
$$\begin{aligned} u_{ax} &= - \frac{k_x k_{ra}}{\mu_a} \frac{\partial \phi_a}{\partial x} & u_{az} &= - \frac{k_z k_{ra}}{\mu_a} \frac{\partial \phi_a}{\partial z} \\ u_{ox} &= - \frac{k_x k_{ro}}{\mu_o} \frac{\partial \phi_o}{\partial x} & u_{oz} &= - \frac{k_z k_{ro}}{\mu_o} \frac{\partial \phi_o}{\partial z} \\ u_{vx} &= - \frac{k_x k_{rv}}{\mu_v} \frac{\partial \phi_v}{\partial x} & u_{vz} &= - \frac{k_z k_{rv}}{\mu_v} \frac{\partial \phi_v}{\partial z} \end{aligned} \quad (D-7)$$

Substituting (D-7) into (D-6), we obtain:

$$\begin{aligned} &\frac{\partial}{\partial x} \left(x_{1a} \frac{A_x k_x k_{ra} \rho_a}{M_a \mu_a} \frac{\partial \phi_a}{\partial x} + x_{1o} \frac{A_x k_x k_{ro} \rho_o}{M_o \mu_o} \frac{\partial \phi_o}{\partial x} + x_{1v} \frac{A_x k_x k_{rv} \rho_v}{M_v \mu_v} \frac{\partial \phi_v}{\partial x} \right) \cdot \Delta x \\ &+ \frac{\partial}{\partial z} \left(x_{1a} \frac{A_z k_z k_{ra} \rho_a}{M_a \mu_a} \frac{\partial \phi_a}{\partial z} + x_{1o} \frac{A_z k_z k_{ro} \rho_o}{M_o \mu_o} \frac{\partial \phi_o}{\partial z} + x_{1v} \frac{A_z k_z k_{rv} \rho_v}{M_v \mu_v} \frac{\partial \phi_v}{\partial z} \right) \cdot \Delta z + Q_1 \\ &= V_b \frac{\partial}{\partial t} \left[\phi \left(\frac{x_{1a} \rho_a S_a}{M_a} + \frac{x_{1o} \rho_o S_o}{M_o} + \frac{x_{1v} \rho_v S_v}{M_v} \right) \right] \end{aligned} \quad (D-8)$$

Using the del operator, equation (D-8) may be written as:

$$\begin{aligned} &\nabla \cdot \left(x_{1a} \frac{A k k_{ra} \rho_a}{M_a \mu_a} \nabla \phi_a + x_{1o} \frac{A k k_{ro} \rho_o}{M_o \mu_o} \nabla \phi_o + x_{1v} \frac{A k k_{rv} \rho_v}{M_v \mu_v} \nabla \phi_v \right) \cdot \Delta + Q_1 \\ &= V_b \frac{\partial}{\partial t} \left[\phi \left(\frac{x_{1a} \rho_a S_a}{M_a} + \frac{x_{1o} \rho_o S_o}{M_o} + \frac{x_{1v} \rho_v S_v}{M_v} \right) \right] \end{aligned} \quad (D-9)$$



q_L = heat loss from the element (units: energy/time)
(-ve for loss)

q_s = extra heat source/sink term (units: energy/time)
(+ve for input)

$Q_p h_p$ = heat gained or lost due to production or injection
of phase p (+ve if injected) (units: energy/time)

Let q_{cond} = rate of heat conduction

Using Fourier's Law:

$$x - \text{direction inlet } q_{\text{cond}_x} = \left(-\lambda A \frac{\partial T}{\partial x} \right)_x$$

$$x - \text{direction outlet } q_{\text{cond}_{x+\Delta x}} = \left(-\lambda A \frac{\partial T}{\partial x} \right)_{x+\Delta x}$$

$$z - \text{direction inlet } q_{\text{cond}_z} = \left(-\lambda A \frac{\partial T}{\partial z} \right)_z$$

$$z - \text{direction outlet } q_{\text{cond}_{z+\Delta z}} = \left(-\lambda A \frac{\partial T}{\partial z} \right)_{z+\Delta z}$$

Let q_{conv} = rate of heat convection

$$x - \text{direction inlet } q_{\text{conv}_x} = \left(\frac{\rho_a h_a u_a}{M_a} \cdot A_x + \frac{\rho_o h_o u_o}{M_o} \cdot A_x + \frac{\rho_v h_v u_v}{M_v} \cdot A_x \right)_x$$

$$x - \text{direction outlet } q_{\text{conv}_{x+\Delta x}} = \left(\frac{\rho_a h_a u_a}{M_a} \cdot A_x + \frac{\rho_o h_o u_o}{M_o} \cdot A_x + \frac{\rho_v h_v u_v}{M_v} \cdot A_x \right)_{x+\Delta x}$$

$$z - \text{direction inlet } q_{\text{conv}_z} = \left(\frac{\rho_a h_a u_a}{M_a} \cdot A_z + \frac{\rho_o h_o u_o}{M_o} \cdot A_z + \frac{\rho_v h_v u_v}{M_v} \cdot A_z \right)_z$$

$$z - \text{direction outlet } q_{\text{conv}_{z+\Delta z}} = \left(\frac{\rho_a h_a u_a}{M_a} \cdot A_z + \frac{\rho_o h_o u_o}{M_o} \cdot A_z + \frac{\rho_v h_v u_v}{M_v} \cdot A_z \right)_{z+\Delta z}$$

The amounts of energy contained in the element are given by:

$$\text{at time } t \quad \left[V_b (1 - \phi) \bar{\rho}_r U_r + \phi V_b \left(\frac{S_a \rho_a U_a}{M_a} + \frac{S_o \rho_o U_o}{M_o} + \frac{S_v \rho_v U_v}{M_v} \right) \right]_t$$

$$\text{at time } t+\Delta t \quad \left[V_b (1 - \phi) \bar{\rho}_r U_r + \phi V_b \left(\frac{S_a \rho_a U_a}{M_a} + \frac{S_o \rho_o U_o}{M_o} + \frac{S_v \rho_v U_v}{M_v} \right) \right]_{t+\Delta t}$$

An energy balance over time interval Δt may be written considering that:

$$\text{Output} - \text{Input} + \text{Accumulation} = 0$$

$$\begin{aligned} & - \left[\left(\lambda A_x \frac{\partial T}{\partial x} \right)_{x+\Delta x} - \lambda A_x \frac{\partial T}{\partial x} \Big|_x \right] + \left[\left(\lambda A_z \frac{\partial T}{\partial z} \right)_{z+\Delta z} - \lambda A_z \frac{\partial T}{\partial z} \Big|_z \right] \cdot \Delta t \\ & + \left[\frac{\rho_a h_a U_a}{M_a} \cdot A_x + \frac{\rho_o h_o U_o}{M_o} \cdot A_x + \frac{\rho_v h_v U_v}{M_v} \cdot A_x \right]_{x+\Delta x} - \\ & - \left[\frac{\rho_a h_a U_a}{M_a} \cdot A_x + \frac{\rho_o h_o U_o}{M_o} \cdot A_x + \frac{\rho_v h_v U_v}{M_v} \cdot A_x \right]_x \cdot \Delta t \\ & + \left[\frac{\rho_a h_a U_a}{M_a} \cdot A_z + \frac{\rho_o h_o U_o}{M_o} \cdot A_z + \frac{\rho_v h_v U_v}{M_v} \cdot A_z \right]_{z+\Delta z} - \\ & - \left[\frac{\rho_a h_a U_a}{M_a} \cdot A_z + \frac{\rho_o h_o U_o}{M_o} \cdot A_z + \frac{\rho_v h_v U_v}{M_v} \cdot A_z \right]_z \cdot \Delta t \\ & + \left[v_b (1 - \phi) \bar{p}_r U_r + \phi v_b \left(\frac{S_a \rho_a U_a}{M_a} + \frac{S_o \rho_o U_o}{M_o} + \frac{S_v \rho_v U_v}{M_v} \right) \right]_{t+\Delta t} \\ & - \left[v_b (1 - \phi) \bar{p}_r U_r + \phi v_b \left(\frac{S_a \rho_a U_a}{M_a} + \frac{S_o \rho_o U_o}{M_o} + \frac{S_v \rho_v U_v}{M_v} \right) \right]_t \\ & - q_s \cdot \Delta t - q_L \cdot \Delta t - (Q_a^* h_a^* + Q_o^* h_o^* + Q_v^* h_v^*) \cdot \Delta t = 0 \end{aligned} \quad (D-10)$$

Equation (D-10) may be rearranged to yield:

$$\begin{aligned} & \left(\frac{\lambda A_x \frac{\partial T}{\partial x} \Big|_{x+\Delta x} - \lambda A_x \frac{\partial T}{\partial x} \Big|_x}{\Delta x} \right) \cdot \Delta x + \left(\frac{\lambda A_z \frac{\partial T}{\partial z} \Big|_{z+\Delta z} - \lambda A_z \frac{\partial T}{\partial z} \Big|_z}{\Delta z} \right) \cdot \Delta z \\ & - \left[\frac{\rho_a h_a U_a}{M_a} \cdot A_x + \frac{\rho_o h_o U_o}{M_o} \cdot A_x + \frac{\rho_v h_v U_v}{M_v} \cdot A_x \right]_{x+\Delta x} - \\ & - \left[\frac{\rho_a h_a U_a}{M_a} \cdot A_x + \frac{\rho_o h_o U_o}{M_o} \cdot A_x + \frac{\rho_v h_v U_v}{M_v} \cdot A_x \right]_x \cdot \Delta x \\ & + \left[\frac{\rho_a h_a U_a}{M_a} \cdot A_z + \frac{\rho_o h_o U_o}{M_o} \cdot A_z + \frac{\rho_v h_v U_v}{M_v} \cdot A_z \right]_{z+\Delta z} - \\ & - \left[\frac{\rho_a h_a U_a}{M_a} \cdot A_z + \frac{\rho_o h_o U_o}{M_o} \cdot A_z + \frac{\rho_v h_v U_v}{M_v} \cdot A_z \right]_z \cdot \Delta z \end{aligned}$$

$$\begin{aligned}
& + q_s + q_L + (Q_a^* h_a^* + Q_o^* h_o^* + Q_v^* h_v^*) \\
& = \left[v_b (1 - \phi) \bar{\rho}_r U_r + \phi v_b \left(\frac{S_a \rho_a U_a}{M_a} + \frac{S_o \rho_o U_o}{M_o} + \frac{S_v \rho_v U_v}{M_v} \right) \right]_{t+\Delta t} \\
& - \left[v_b (1 - \phi) \bar{\rho}_r U_r + \phi v_b \left(\frac{S_a \rho_a U_a}{M_a} + \frac{S_o \rho_o U_o}{M_o} + \frac{S_v \rho_v U_v}{M_v} \right) \right]_t \bigg/ \Delta t
\end{aligned} \tag{D-11}$$

Taking the limits as Δx , Δz and Δt approach zero, we may write:

$$\begin{aligned}
& \frac{\partial}{\partial x} \left(\lambda A_x \frac{\partial T}{\partial x} \right) \Delta x + \frac{\partial}{\partial z} \left(\lambda A_z \frac{\partial T}{\partial z} \right) \Delta z - \frac{\partial}{\partial x} \left(\frac{\rho_a h_a U_a}{M_a} A_x + \frac{\rho_o h_o U_o}{M_o} A_x + \frac{\rho_v h_v U_v}{M_v} A_x \right) \Delta x \\
& - \frac{\partial}{\partial z} \left(\frac{\rho_a h_a U_a}{M_a} A_z + \frac{\rho_o h_o U_o}{M_o} A_z + \frac{\rho_v h_v U_v}{M_v} A_z \right) \Delta z \\
& + q_s + q_L + (Q_a^* h_a^* + Q_o^* h_o^* + Q_v^* h_v^*) \\
& = v_b \frac{\partial}{\partial t} \left[(1 - \phi) \bar{\rho}_r U_r + \phi \left(\frac{S_a \rho_a U_a}{M_a} + \frac{S_o \rho_o U_o}{M_o} + \frac{S_v \rho_v U_v}{M_v} \right) \right]
\end{aligned} \tag{D-12}$$

Substituting equations (D-7) for the phase velocities in (D-12), we obtain:

$$\begin{aligned}
& \frac{\partial}{\partial x} \left(\lambda A_x \frac{\partial T}{\partial x} \right) \Delta x + \frac{\partial}{\partial z} \left(\lambda A_z \frac{\partial T}{\partial z} \right) \Delta z + \frac{\partial}{\partial x} \left(\frac{A_x k_x k_{ra} \rho_a h_a}{M_a u_a} \frac{\partial \phi_a}{\partial x} + \frac{A_x k_x k_{ro} \rho_o h_o}{M_o u_o} \frac{\partial \phi_o}{\partial x} \right. \\
& + \left. \frac{A_x k_x k_{rv} \rho_v h_v}{M_v u_v} \frac{\partial \phi_v}{\partial x} \right) \Delta x + \frac{\partial}{\partial z} \left(\frac{A_z k_z k_{ra} \rho_a h_a}{M_a u_a} \frac{\partial \phi_a}{\partial z} + \frac{A_z k_z k_{ro} \rho_o h_o}{M_o u_o} \frac{\partial \phi_o}{\partial z} \right. \\
& + \left. \frac{A_z k_z k_{rv} \rho_v h_v}{M_v u_v} \frac{\partial \phi_v}{\partial z} \right) \Delta z + q_s + q_L + (Q_a^* h_a^* + Q_o^* h_o^* + Q_v^* h_v^*) \\
& = v_b \frac{\partial}{\partial t} \left[(1 - \phi) \bar{\rho}_r U_r + \phi \left(\frac{S_a \rho_a U_a}{M_a} + \frac{S_o \rho_o U_o}{M_o} + \frac{S_v \rho_v U_v}{M_v} \right) \right]
\end{aligned} \tag{D-13}$$

Using the del operator, equation (D-13) may be written as:

$$\begin{aligned}
& \nabla \cdot (A \lambda \nabla T) \Delta + \nabla \cdot \left(\frac{A k k_{ra} \rho_a h_a}{M_a u_a} \nabla \phi_a + \frac{A k k_{ro} \rho_o h_o}{M_o u_o} \nabla \phi_o + \frac{A k k_{rv} \rho_v h_v}{M_v u_v} \nabla \phi_v \right) \Delta + q_s + q_L \\
& + (Q_a^* h_a^* + Q_o^* h_o^* + Q_v^* h_v^*) = v_b \frac{\partial}{\partial t} \left[(1 - \phi) \bar{\rho}_r U_r + \phi \left(\frac{S_a \rho_a U_a}{M_a} + \frac{S_o \rho_o U_o}{M_o} + \frac{S_v \rho_v U_v}{M_v} \right) \right]
\end{aligned} \tag{D-14}$$

APPENDIX E

MATHEMATICAL MODEL IN FINITE DIFFERENCE FORM

MATHEMATICAL MODEL IN FINITE DIFFERENCE FORM

The set of seven simultaneous equations describing the present problem may be written in finite difference form as:

1. Gas Phase Mole Fraction Constraint

$$x_{1v} + x_{2v} + x_{3v} + x_{4v} + x_{5v} - 1.0 = 0.0 \quad (E-1)$$

2. Continuity Equation for Water

$$\Delta (T_a x_{1a} \Delta \phi_a + T_o x_{1o} \Delta \phi_o + T_v x_{1v} \Delta \phi_v) + Q_1^* - \frac{V_b}{\Delta t} \delta \left[\phi \left(\frac{x_{1a} \rho_a S_a}{M_a} + \frac{x_{1o} \rho_o S_o}{M_o} + \frac{x_{1v} \rho_v S_v}{M_v} \right) \right] = 0 \quad (E-2)$$

3. Continuity Equations for Oil Components Summed

$$\begin{aligned} & \Delta (T_a x_{2a} \Delta \phi_a + T_o x_{2o} \Delta \phi_o + T_v x_{2v} \Delta \phi_v) + Q_2^* \\ & - \frac{V_b}{\Delta t} \delta \left[\phi \left(\frac{x_{2a} \rho_a S_a}{M_a} + \frac{x_{2o} \rho_o S_o}{M_o} + \frac{x_{2v} \rho_v S_v}{M_v} \right) \right] \\ & + \Delta (T_a x_{3a} \Delta \phi_a + T_o x_{3o} \Delta \phi_o + T_v x_{3v} \Delta \phi_v) + Q_3^* \\ & - \frac{V_b}{\Delta t} \delta \left[\phi \left(\frac{x_{3a} \rho_a S_a}{M_a} + \frac{x_{3o} \rho_o S_o}{M_o} + \frac{x_{3v} \rho_v S_v}{M_v} \right) \right] = 0 \end{aligned} \quad (E-3)$$

4. Energy Conservation Equation

$$\begin{aligned} & \Delta (T_c \Delta T) + \Delta (T_a h_a \Delta \phi_a + T_o h_o \Delta \phi_o + T_v h_v \Delta \phi_v) \\ & + q_s + q_l + (Q_a^* h_a^* + Q_o^* h_o^* + Q_v^* h_v^*) \\ & - \frac{V_b}{\Delta t} \delta \left[(1 - \phi) \bar{\rho}_r U_r + \phi \left(\frac{S_a \rho_a U_a}{M_a} + \frac{S_o \rho_o U_o}{M_o} + \frac{S_v \rho_v U_v}{M_v} \right) \right] = 0 \end{aligned} \quad (E-4)$$

5. Continuity Equation for CO₂

$$\begin{aligned} & \Delta (T_a x_{4a} \Delta \phi_a + T_o x_{4o} \Delta \phi_o + T_v x_{4v} \Delta \phi_v) + Q_4^* \\ & - \frac{V_b}{\Delta t} \delta \left[\phi \left(\frac{x_{4a} \rho_a S_a}{M_a} + \frac{x_{4o} \rho_o S_o}{M_o} + \frac{x_{4v} \rho_v S_v}{M_v} \right) \right] = 0 \end{aligned} \quad (E-5)$$

6. Continuity Equation for N₂

$$\begin{aligned} & \Delta (T_a x_{5a} \Delta \phi_a + T_o x_{5o} \Delta \phi_o + T_v x_{5v} \Delta \phi_v) + Q_5^* \\ & - \frac{V_b}{\Delta t} \delta \left[\phi \left(\frac{x_{5a} \rho_a S_a}{M_a} + \frac{x_{5o} \rho_o S_o}{M_o} + \frac{x_{5v} \rho_v S_v}{M_v} \right) \right] = 0 \end{aligned} \quad (E-6)$$

7. Continuity Equation for Heavy Oil

$$\Delta (T_a x_{3a} \Delta \phi_a + T_o x_{3o} \Delta \phi_o + T_v x_{3v} \Delta \phi_v) + O_3^* - \frac{V_b}{\Delta t} \left(x_{3a} \frac{\rho_a S_a}{M_a} + x_{3o} \frac{\rho_o S_o}{M_o} + x_{3v} \frac{\rho_v S_v}{M_v} \right) = 0 \quad (E-7)$$

The transmissibilities are defined as:

$$\begin{aligned} T_a &= \frac{A k k_{ra} \rho_a}{M_a \mu_a L} \\ T_o &= \frac{A k k_{ro} \rho_o}{M_o \mu_o L} \\ T_v &= \frac{A k k_{rv} \rho_v}{M_v \mu_v L} \\ T_c &= \frac{\lambda L}{L} \end{aligned} \quad (E-8)$$

To illustrate the expansion of finite difference form for the fully implicit case we use the Energy Conservation equation (E-4). The other equations may be written in a similar manner. For the general case of solubility of all components in all phases and writing in three spatial dimensions, we obtain:

$$\begin{aligned} & T_{cx}^{n+1} \left(T_{1+1/2,j,k}^{n+1} - T_{1,j,k}^{n+1} - T_{1,j,k}^{n+1} - T_{cx}^{n+1} T_{1-1/2,j,k}^{n+1} T_{1,j,k}^{n+1} - T_{1-1,j,k}^{n+1} \right) \\ & + T_{cy}^{n+1} \left(T_{1,j+1/2,k}^{n+1} - T_{1,j+1,k}^{n+1} - T_{1,j,k}^{n+1} - T_{cy}^{n+1} T_{1,j-1/2,k}^{n+1} T_{1,j,k}^{n+1} - T_{1,j-1,k}^{n+1} \right) \\ & + T_{cz}^{n+1} \left(T_{1,j,k+1/2}^{n+1} - T_{1,j,k+1}^{n+1} - T_{1,j,k}^{n+1} - T_{cz}^{n+1} T_{1,j,k-1/2}^{n+1} T_{1,j,k}^{n+1} - T_{1,j,k-1}^{n+1} \right) \\ & + T_{ax}^{n+1} \left(h_a^{n+1} \phi_{a,1+1/2,j,k}^{n+1} - \phi_{a,1+1,j,k}^{n+1} - \phi_{a,1,j,k}^{n+1} - T_{ax}^{n+1} h_a^{n+1} \phi_{a,1-1/2,j,k}^{n+1} - \phi_{a,1,j,k}^{n+1} - \phi_{a,1-1,j,k}^{n+1} \right) \\ & + T_{ox}^{n+1} \left(h_o^{n+1} \phi_{o,1+1/2,j,k}^{n+1} - \phi_{o,1+1,j,k}^{n+1} - \phi_{o,1,j,k}^{n+1} - T_{ox}^{n+1} h_o^{n+1} \phi_{o,1-1/2,j,k}^{n+1} - \phi_{o,1,j,k}^{n+1} - \phi_{o,1-1,j,k}^{n+1} \right) \\ & + T_{vx}^{n+1} \left(h_v^{n+1} \phi_{v,1+1/2,j,k}^{n+1} - \phi_{v,1+1,j,k}^{n+1} - \phi_{v,1,j,k}^{n+1} - T_{vx}^{n+1} h_v^{n+1} \phi_{v,1-1/2,j,k}^{n+1} - \phi_{v,1,j,k}^{n+1} - \phi_{v,1-1,j,k}^{n+1} \right) \\ & + T_{ay}^{n+1} \left(h_a^{n+1} \phi_{a,1,j+1/2,k}^{n+1} - \phi_{a,1,j+1,k}^{n+1} - \phi_{a,1,j,k}^{n+1} - T_{ay}^{n+1} h_a^{n+1} \phi_{a,1,j-1/2,k}^{n+1} - \phi_{a,1,j,k}^{n+1} - \phi_{a,1,j-1,k}^{n+1} \right) \end{aligned}$$

$$+ T_{oy}^{n+1} h_o^{n+1} \phi_o^{n+1} 1,j+1,k - \phi_o^{n+1} 1,j,k - T_{oy}^{n+1} h_o^{n+1} \phi_o^{n+1} 1,j,k - \phi_o^{n+1} 1,j-1,k$$

$$+ T_{vy}^{n+1} h_v^{n+1} \phi_v^{n+1} 1,j+1,k - \phi_v^{n+1} 1,j,k - T_{vy}^{n+1} h_v^{n+1} \phi_v^{n+1} 1,j,k - \phi_v^{n+1} 1,j-1,k$$

$$+ T_{az}^{n+1} h_a^{n+1} \phi_a^{n+1} 1,j,k+1 - \phi_a^{n+1} 1,j,k - T_{az}^{n+1} h_a^{n+1} \phi_a^{n+1} 1,j,k - \phi_a^{n+1} 1,j,k-1$$

$$+ T_{oz}^{n+1} h_o^{n+1} \phi_o^{n+1} 1,j,k+1 - \phi_o^{n+1} 1,j,k - T_{oz}^{n+1} h_o^{n+1} \phi_o^{n+1} 1,j,k - \phi_o^{n+1} 1,j,k-1$$

$$+ T_{vz}^{n+1} h_v^{n+1} \phi_v^{n+1} 1,j,k+1 - \phi_v^{n+1} 1,j,k - T_{vz}^{n+1} h_v^{n+1} \phi_v^{n+1} 1,j,k - \phi_v^{n+1} 1,j,k-1$$

$$+ q_s^{n+1} + q_L^{n+1} + (Q_a^* h_a^* + Q_o^* h_o^* + Q_v^* h_v^*)^{n+1}$$

$$- \frac{V_o}{\Delta t} \left[(1 - \phi) \bar{\rho}_r U_r + \phi \left(\frac{S_a \rho_a U_a}{M_a} + \frac{S_o \rho_o U_o}{M_o} + \frac{S_v \rho_v U_v}{M_v} \right) \right]^{n+1}$$

$$- \frac{V_b}{\Delta t} \left[(1 - \phi) \bar{\rho}_r U_r + \phi \left(\frac{S_a \rho_a U_a}{M_a} + \frac{S_o \rho_o U_o}{M_o} + \frac{S_v \rho_v U_v}{M_v} \right) \right]^\eta = 0$$

where $T_{cx}^{n+1} 1,j+1/2,k = T_{cx}^{n+1} 1,j+1/2,k \lambda^{n+1} 1,j+1/2,k$ and $T_{cx}^{n+1} 1,j-1/2,k = T_{cx}^{n+1} 1,j-1/2,k \lambda^{n+1} 1,j-1/2,k$

$$T_{cx}^{n+1} 1,j+1/2,k = \frac{2 A_{1+1,j,k} A_{1,j,k}}{A_{1,j,k} \Delta X_{1+1,j,k} + A_{1+1,j,k} \Delta X_{1,j,k}} \text{ and}$$

$$T_{cx}^{n+1} 1,j-1/2,k = \frac{2 A_{1-1,j,k} A_{1,j,k}}{A_{1-1,j,k} \Delta X_{1,j,k} + A_{1,j,k} \Delta X_{1-1,j,k}}$$

also $T_{cy}^{n+1} 1,j+1/2,k = T_{cy}^{n+1} 1,j+1/2,k \lambda^{n+1} 1,j+1/2,k$ and $T_{cy}^{n+1} 1,j-1/2,k = T_{cy}^{n+1} 1,j-1/2,k \lambda^{n+1} 1,j-1/2,k$

$$T_{cy}^{n+1} 1,j+1/2,k = \frac{2 A_{1,j,k} A_{1,j+1,k}}{A_{1,j,k} \Delta Y_{1,j+1,k} + A_{1,j+1,k} \Delta Y_{1,j,k}} \text{ and}$$

$$T_{cy}^{n+1} 1,j-1/2,k = \frac{2 A_{1,j-1,k} A_{1,j,k}}{A_{1,j-1,k} \Delta Y_{1,j,k} + A_{1,j,k} \Delta Y_{1,j-1,k}}$$

$$\text{and } T_{cz,1,J,k+1/2}^{n+1} = T_{cz,1,J,k+1/2}^{n+1} \lambda_{1,J,k+1/2}^{n+1} \quad \text{and} \quad T_{cz,1,J,k-1/2}^{n+1} = T_{cz,1,J,k-1/2}^{n+1} \lambda_{1,J,k-1/2}^{n+1}$$

$$T_{cz,1,J,k+1/2}^{n+1} = \frac{2 A_{1,J,k} \cdot A_{1,J,k+1}}{A_{1,J,k} \cdot \Delta Z_{1,J,k+1} + A_{1,J,k+1} \cdot \Delta Z_{1,J,k}} \quad \text{and}$$

$$T_{cz,1,J,k-1/2}^{n+1} = \frac{2 A_{1,J,k-1} \cdot A_{1,J,k}}{A_{1,J,k-1} \cdot \Delta Z_{1,J,k} + A_{1,J,k} \cdot \Delta Z_{1,J,k-1}}$$

$$\text{furthermore } T_{ax,1+1/2,J,k}^{n+1} = T_{ax,1+1/2,J,k}^{n+1} \left(\frac{k_{ra} \rho_a}{M_a u_a} \right)_{1+1/2,J,k}^{n+1} \quad \text{and}$$

$$T_{ax,1-1/2,J,k}^{n+1} = T_{ax,1-1/2,J,k}^{n+1} \left(\frac{k_{ra} \rho_a}{M_a u_a} \right)_{1-1/2,J,k}^{n+1}$$

$$T_{x,1+1/2,J,k}^{n+1} = \frac{2 A_{1,J,k} \cdot A_{1,J,k+1} \cdot k_{1,J,k} \cdot k_{1+1,J,k}}{A_{1,J,k} \cdot k_{1,J,k} \cdot \Delta X_{1+1,J,k} + A_{1+1,J,k} \cdot k_{1+1,J,k} \cdot \Delta X_{1,J,k}} \quad \text{and}$$

$$T_{x,1-1/2,J,k}^{n+1} = \frac{2 A_{1-1,J,k} \cdot A_{1,J,k} \cdot k_{1-1,J,k} \cdot k_{1,J,k}}{A_{1-1,J,k} \cdot k_{1-1,J,k} \cdot \Delta X_{1,J,k} + A_{1,J,k} \cdot k_{1,J,k} \cdot \Delta X_{1-1,J,k}}$$

$$\text{also } T_{ox,1+1/2,J,k}^{n+1} = T_{ox,1+1/2,J,k}^{n+1} \left(\frac{k_{ro} \rho_o}{M_o u_o} \right)_{1+1/2,J,k}^{n+1} \quad \text{and} \quad T_{ox,1-1/2,J,k}^{n+1} = T_{ox,1-1/2,J,k}^{n+1} \left(\frac{k_{ro} \rho_o}{M_o u_o} \right)_{1-1/2,J,k}^{n+1}$$

$$T_{vx,1+1/2,J,k}^{n+1} = T_{vx,1+1/2,J,k}^{n+1} \left(\frac{k_{rv} \rho_v}{M_v u_v} \right)_{1+1/2,J,k}^{n+1} \quad \text{and} \quad T_{vx,1-1/2,J,k}^{n+1} = T_{vx,1-1/2,J,k}^{n+1} \left(\frac{k_{rv} \rho_v}{M_v u_v} \right)_{1-1/2,J,k}^{n+1}$$

$$\text{In the y-direction } T_{ay,1,J+1/2,k}^{n+1} = T_{ay,1,J+1/2,k}^{n+1} \left(\frac{k_{ra} \rho_a}{M_a u_a} \right)_{1,J+1/2,k}^{n+1} \quad \text{and}$$

$$T_{ay,1,J-1/2,k}^{n+1} = T_{ay,1,J-1/2,k}^{n+1} \left(\frac{k_{ra} \rho_a}{M_a u_a} \right)_{1,J-1/2,k}^{n+1}$$

$$\text{where } T_{y,1,J+1/2,k}^{n+1} = \frac{2 A_{1,J,k} \cdot A_{1,J+1,k} \cdot k_{1,J,k} \cdot k_{1,J+1,k}}{A_{1,J+1,k} \cdot k_{1,J+1,k} \cdot \Delta Y_{1,J,k} + A_{1,J,k} \cdot k_{1,J,k} \cdot \Delta Y_{1+1,k}}$$

$$T_{y,1,J-1/2,k}^{n+1} = \frac{2 A_{1,J,k} \cdot A_{1,J-1,k} \cdot k_{1,J,k} \cdot k_{1,J-1,k}}{A_{1,J,k} \cdot k_{1,J,k} \cdot \Delta Y_{1,J-1,k} + A_{1,J-1,k} \cdot k_{1,J-1,k} \cdot \Delta Y_{1,J,k}}$$

The oleic and vapour phase transmissibilities in the Y-direction and the transmissibilities in the Z-direction may be obtained similarly. One hundred percent upstream weighting of physical properties and mole fractions was employed. For example:

$$\frac{k_{ra} \rho_a}{M_a \mu_a}^{n+1}_{i+1/2,j,k} = \frac{k_{ra} \rho_a}{M_a \mu_a}^{n+1}_{i+1,j,k} \quad \text{if } \phi_{i+1,j,k} > \phi_{i,j,k}$$

$$\frac{k_{ra} \rho_a}{M_a \mu_a}^{n+1}_{i,j,k} \quad \text{if } \phi_{i,j,k} > \phi_{i+1,j,k}$$

In the case of thermal conductivity,

$$\lambda_{i+1/2,j,k}^{n+1} = \lambda_{i+1,j,k}^{n+1} \quad \text{if } T_{i+1,j,k} > T_{i,j,k}$$

$$\lambda_{i,j,k}^{n+1} \quad \text{if } T_{i,j,k} > T_{i+1,j,k}$$

APPENDIX F

MATHEMATICAL MODEL EQUATIONS IN STANDARD FORM

APPENDIX F

MATHEMATICAL MODEL EQUATIONS IN STANDARD FORM

The set of 7 simultaneous equations may be written in a standard form as follows:

$$\begin{aligned}
 & ZC(I) \cdot T_{1,J,k-1}^{n+1} + BC(I) \cdot T_{1,J-1,k}^{n+1} + DC(I) \cdot T_{1-1,J,k}^{n+1} + EC(I) \cdot T_{1,J,k}^{n+1} + FC(I) \cdot T_{1+1,J,k}^{n+1} + HC(I) \cdot T_{1,J+1,k}^{n+1} \\
 & \quad + VC(I) \cdot T_{1,J,k+1}^{n+1} \\
 & + ZA(I) \cdot \phi_a^{n+1}{}_{1,J,k-1} + BA(I) \cdot \phi_a^{n+1}{}_{1,J-1,k} + DA(I) \cdot \phi_a^{n+1}{}_{1-1,J,k} + EA(I) \cdot \phi_a^{n+1}{}_{1,J,k} + FA(I) \cdot \phi_a^{n+1}{}_{1+1,J,k} \\
 & \quad + HA(I) \cdot \phi_a^{n+1}{}_{1,J+1,k} + VA(I) \cdot \phi_a^{n+1}{}_{1,J,k+1} \\
 & + ZO(I) \cdot \phi_o^{n+1}{}_{1,J,k-1} + BO(I) \cdot \phi_o^{n+1}{}_{1,J-1,k} + DO(I) \cdot \phi_o^{n+1}{}_{1-1,J,k} + EO(I) \cdot \phi_o^{n+1}{}_{1,J,k} + FO(I) \cdot \phi_o^{n+1}{}_{1+1,J,k} \\
 & \quad + HO(I) \cdot \phi_o^{n+1}{}_{1,J+1,k} + VO(I) \cdot \phi_o^{n+1}{}_{1,J,k+1} \\
 & + ZV(I) \cdot \phi_v^{n+1}{}_{1,J,k-1} + BV(I) \cdot \phi_v^{n+1}{}_{1,J-1,k} + DV(I) \cdot \phi_v^{n+1}{}_{1-1,J,k} + EV(I) \cdot \phi_v^{n+1}{}_{1,J,k} + FV(I) \cdot \phi_v^{n+1}{}_{1+1,J,k} \\
 & \quad + HV(I) \cdot \phi_v^{n+1}{}_{1,J+1,k} + VV(I) \cdot \phi_v^{n+1}{}_{1,J,k+1}
 \end{aligned}$$

$$QF(I) - GF(I)/\Delta t + GN(I)/\Delta t + RF(I) = 0 \quad \text{where } I = 1,7 \text{ representing the seven equations.}$$

In Equation 1, $RF(1) = x_{1v} + x_{2v} + x_{3v} + x_{4v} + x_{5v} = 1.0$ with all other standard form coefficients being zero. Coefficients for the other six equations are as follows:

$$ZA(2) = T_{az}^{n+1} \chi_{1a}^{n+1}$$

$$ZO(2) = T_{oz}^{n+1} \chi_{1o}^{n+1}$$

$$BA(2) = T_{ay}^{n+1} \chi_{1a}^{n+1}$$

$$BO(2) = T_{oy}^{n+1} \chi_{1o}^{n+1}$$

$$DA(2) = T_{ax}^{n+1} \chi_{1a}^{n+1}$$

$$DO(2) = T_{ox}^{n+1} \chi_{1o}^{n+1}$$

$$EA(2) = -(ZA(2) + BA(2) + DA(2) + FA(2) + HA(2) + VA(2))$$

$$EO(2) = -(ZO(2) + BO(2) + DO(2) + FO(2) + HO(2) + VO(2))$$

$$FA(2) = T_{ax}^{n+1} \chi_{1a}^{n+1}$$

$$FO(2) = T_{ox}^{n+1} \chi_{1o}^{n+1}$$

$$HA(2) = T_{ay}^{n+1} \chi_{1a}^{n+1}$$

$$HO(2) = T_{oy}^{n+1} \chi_{1o}^{n+1}$$

$$VA(2) = T_{az}^{n+1} \chi_{1a}^{n+1}$$

$$VO(2) = T_{oz}^{n+1} \chi_{1o}^{n+1}$$

$$QF(2) = (Q_1^{n+1})_{1,j,k}$$

$$GF(2) = V_{D,1,j,k} \left[\phi \left(\frac{\chi_{1a} \rho_a S_a}{M_a} + \frac{\chi_{1o} \rho_o S_o}{M_o} + \frac{\chi_{1v} \rho_v S_v}{M_v} \right) \right]_{1,j,k}^{n+1}$$

$$ZV(2) = T_{vz}^{n+1} \chi_{1v}^{n+1}$$

$$BV(2) = T_{vy}^{n+1} \chi_{1v}^{n+1}$$

$$DV(2) = T_{vx}^{n+1} \chi_{1v}^{n+1}$$

$$EV(2) = -(ZV(2) + BV(2) + DV(2) + FV(2) + HV(2) + VV(2))$$

$$FV(2) = T_{vx}^{n+1} \chi_{1v}^{n+1}$$

$$HV(2) = T_{vy}^{n+1} \chi_{1v}^{n+1}$$

$$VV(2) = T_{vz}^{n+1} \chi_{1v}^{n+1}$$

$$GN(2) = V_{D,1,j,k} \left[\phi \left(\frac{\chi_{1a} \rho_a S_a}{M_a} + \frac{\chi_{1o} \rho_o S_o}{M_o} + \frac{\chi_{1v} \rho_v S_v}{M_v} \right) \right]_{1,j,k}^n$$

$$ZA(3) = T_{az}^{n+1} \chi_{1,J,k-1/2}^{n+1} + \chi_{2a}^{n+1} + \chi_{3a}^{n+1}$$

$$BA(3) = T_{ay}^{n+1} \chi_{1,J-1/2,k}^{n+1} + \chi_{2a}^{n+1} + \chi_{3a}^{n+1}$$

$$DA(3) = T_{ax}^{n+1} \chi_{1-1/2,J,k}^{n+1} + \chi_{2a}^{n+1} + \chi_{3a}^{n+1}$$

$$EA(3) = - (ZA(3) + BA(3) + DA(3) + FA(3) + HA(3) + VA(3))$$

$$FA(3) = T_{ax}^{n+1} \chi_{1+1/2,J,k}^{n+1} + \chi_{2a}^{n+1} + \chi_{3a}^{n+1}$$

$$HA(3) = T_{ay}^{n+1} \chi_{1,J+1/2,k}^{n+1} + \chi_{2a}^{n+1} + \chi_{3a}^{n+1}$$

$$VA(3) = T_{az}^{n+1} \chi_{1,J,k+1/2}^{n+1} + \chi_{2a}^{n+1} + \chi_{3a}^{n+1}$$

$$OF(3) = (Q_2^* + Q_3^*)_{1,J,k}^{n+1} \quad GF(3) = V_D \left[\phi \left(\frac{(\chi_{2a} + \chi_{3a}) \rho_a S_a}{M_a} + \frac{(\chi_{20} + \chi_{30}) \rho_0 S_0}{M_0} + \frac{(\chi_{2v} + \chi_{3v}) \rho_v S_v}{M_v} \right) \right]_{1,J,k}^{n+1}$$

$$ZV(3) = T_{vz}^{n+1} \chi_{1,J,k-1/2}^{n+1} + \chi_{2v}^{n+1} + \chi_{3v}^{n+1}$$

$$BV(3) = T_{vy}^{n+1} \chi_{1,J-1/2,k}^{n+1} + \chi_{2v}^{n+1} + \chi_{3v}^{n+1}$$

$$DV(3) = T_{vx}^{n+1} \chi_{1-1/2,J,k}^{n+1} + \chi_{2v}^{n+1} + \chi_{3v}^{n+1}$$

$$EV(3) = - (ZV(3) + BV(3) + DV(3) + FV(3) + HV(3) + VV(3))$$

$$FV(3) = T_{vx}^{n+1} \chi_{1+1/2,J,k}^{n+1} + \chi_{2v}^{n+1} + \chi_{3v}^{n+1}$$

$$HV(3) = T_{vy}^{n+1} \chi_{1,J+1/2,k}^{n+1} + \chi_{2v}^{n+1} + \chi_{3v}^{n+1}$$

$$VV(3) = T_{vz}^{n+1} \chi_{1,J,k+1/2}^{n+1} + \chi_{2v}^{n+1} + \chi_{3v}^{n+1}$$

$$GN(3) = V_D \left[\phi \left(\frac{(\chi_{2a} + \chi_{3a}) \rho_a S_a}{M_a} + \frac{(\chi_{20} + \chi_{30}) \rho_0 S_0}{M_0} + \frac{(\chi_{2v} + \chi_{3v}) \rho_v S_v}{M_v} \right) \right]_{1,J,k}^n$$

$$ZO(3) = T_{oz}^{n+1} \chi_{1,J,k-1/2}^{n+1} + \chi_{20}^{n+1} + \chi_{30}^{n+1}$$

$$BO(3) = T_{oy}^{n+1} \chi_{1,J-1/2,k}^{n+1} + \chi_{20}^{n+1} + \chi_{30}^{n+1}$$

$$DO(3) = T_{ox}^{n+1} \chi_{1-1/2,J,k}^{n+1} + \chi_{20}^{n+1} + \chi_{30}^{n+1}$$

$$EO(3) = - (ZO(3) + BO(3) + DO(3) + FO(3) + HO(3) + VO(3))$$

$$FO(3) = T_{ox}^{n+1} \chi_{1+1/2,J,k}^{n+1} + \chi_{20}^{n+1} + \chi_{30}^{n+1}$$

$$HO(3) = T_{oy}^{n+1} \chi_{1,J+1/2,k}^{n+1} + \chi_{20}^{n+1} + \chi_{30}^{n+1}$$

$$VO(3) = T_{oz}^{n+1} \chi_{1,J,k+1/2}^{n+1} + \chi_{20}^{n+1} + \chi_{30}^{n+1}$$

$$ZC(4) = T_{cz}^{n+1}_{1,j,k-1/2}$$

$$BC(4) = T_{cy}^{n+1}_{1,j-1/2,k}$$

$$DC(4) = T_{cx}^{n+1}_{1-1/2,j,k}$$

$$EC(4) = - (ZC(4) + BC(4) + DC(4) + FC(4) + HC(4) + VC(4))$$

$$FC(4) = T_{cx}^{n+1}_{1+1/2,j,k}$$

$$HC(4) = T_{cy}^{n+1}_{1,j+1/2,k}$$

$$VC(4) = T_{cz}^{n+1}_{1,j,k+1/2}$$

$$ZO(4) = T_{oz}^{n+1}_{1,j,k-1/2} h_o^{n+1}$$

$$BO(4) = T_{oy}^{n+1}_{1,j-1/2,k} h_o^{n+1}$$

$$DO(4) = T_{ox}^{n+1}_{1-1/2,j,k} h_o^{n+1}$$

$$EO(4) = - (ZO(4) + BO(4) + DO(4) + FO(4) + HO(4) + VO(4))$$

$$FO(4) = T_{ox}^{n+1}_{1+1/2,j,k} h_o^{n+1}$$

$$HO(4) = T_{oy}^{n+1}_{1,j+1/2,k} h_o^{n+1}$$

$$VO(4) = T_{oz}^{n+1}_{1,j,k+1/2} h_o^{n+1}$$

$$OF(4) = q_{s1,j,k}^{n+1} + q_{L1,j,k}^{n+1} + (Q_a^* h_a^* + Q_o^* h_o^* + Q_v^* h_v^*)_{1,j,k}^{n+1}$$

$$GF(4) = v_{b1,j,k} \left[(1-\phi) \bar{p}_r U_r + \phi \left(\frac{S_a \rho_a U_a}{M_a} + \frac{S_o \rho_o U_o}{M_o} + \frac{S_v \rho_v U_v}{M_v} \right) \right]_{1,j,k}^{n+1}$$

$$GN(4) = v_{b1,j,k} \left[(1-\phi) \bar{p}_r U_r + \phi \left(\frac{S_a \rho_a U_a}{M_a} + \frac{S_o \rho_o U_o}{M_o} + \frac{S_v \rho_v U_v}{M_v} \right) \right]_{1,j,k}^n$$

$$ZA(4) = T_{az}^{n+1}_{1,j,k-1/2} h_a^{n+1}$$

$$BA(4) = T_{ay}^{n+1}_{1,j-1/2,k} h_a^{n+1}$$

$$DA(4) = T_{ax}^{n+1}_{1-1/2,j,k} h_a^{n+1}$$

$$EA(4) = - (ZA(4) + BA(4) + DA(4) + FA(4) + HA(4) + VA(4))$$

$$FA(4) = T_{ax}^{n+1}_{1+1/2,j,k} h_a^{n+1}$$

$$HA(4) = T_{ay}^{n+1}_{1,j+1/2,k} h_a^{n+1}$$

$$VA(4) = T_{az}^{n+1}_{1,j,k+1/2} h_a^{n+1}$$

$$ZV(4) = T_{vz}^{n+1}_{1,j,k-1/2} h_v^{n+1}$$

$$BV(4) = T_{vy}^{n+1}_{1,j-1/2,k} h_v^{n+1}$$

$$DV(4) = T_{vx}^{n+1}_{1-1/2,j,k} h_v^{n+1}$$

$$EV(4) = - (ZV(4) + BV(4) + DV(4) + FV(4) + HV(4) + VV(4))$$

$$FV(4) = T_{vx}^{n+1}_{1+1/2,j,k} h_v^{n+1}$$

$$HV(4) = T_{vy}^{n+1}_{1,j+1/2,k} h_v^{n+1}$$

$$VV(4) = T_{vz}^{n+1}_{1,j,k+1/2} h_v^{n+1}$$

$$ZA(5) = T_{az}^{n+1} \chi_{1,j,k-1/2,a}^{n+1}$$

$$BA(5) = T_{ay}^{n+1} \chi_{1,j-1/2,k,a}^{n+1}$$

$$DA(5) = T_{ax}^{n+1} \chi_{1-1/2,j,k,a}^{n+1}$$

$$EA(5) = - (ZA(5) + BA(5) + DA(5) + FA(5) + HA(5) + VA(5))$$

$$FA(5) = T_{ax}^{n+1} \chi_{1+1/2,j,k,a}^{n+1}$$

$$HA(5) = T_{ay}^{n+1} \chi_{1,j+1/2,k,a}^{n+1}$$

$$VA(5) = T_{az}^{n+1} \chi_{1,j,k+1/2,a}^{n+1}$$

$$ZO(5) = T_{oz}^{n+1} \chi_{1,j,k-1/2,o}^{n+1}$$

$$BO(5) = T_{oy}^{n+1} \chi_{1,j-1/2,k,o}^{n+1}$$

$$DO(5) = T_{ox}^{n+1} \chi_{1-1/2,j,k,o}^{n+1}$$

$$EO(5) = - (ZO(5) + BO(5) + DO(5) + FO(5) + HO(5) + VO(5))$$

$$FO(5) = T_{ox}^{n+1} \chi_{1+1/2,j,k,o}^{n+1}$$

$$HO(5) = T_{oy}^{n+1} \chi_{1,j+1/2,k,o}^{n+1}$$

$$VO(5) = T_{oz}^{n+1} \chi_{1,j,k+1/2,o}^{n+1}$$

$$ZV(5) = T_{vz}^{n+1} \chi_{1,j,k-1/2,v}^{n+1}$$

$$BV(5) = T_{vy}^{n+1} \chi_{1,j-1/2,k,v}^{n+1}$$

$$DV(5) = T_{vx}^{n+1} \chi_{1-1/2,j,k,v}^{n+1}$$

$$EV(5) = - (ZV(5) + BV(5) + DV(5) + FV(5) + HV(5) + VV(5))$$

$$FV(5) = T_{vx}^{n+1} \chi_{1+1/2,j,k,v}^{n+1}$$

$$HV(5) = T_{vy}^{n+1} \chi_{1,j+1/2,k,v}^{n+1}$$

$$VV(5) = T_{vz}^{n+1} \chi_{1,j,k+1/2,v}^{n+1}$$

$$QF(5) = (Q_a^*)_{1,j,k}^{n+1}$$

$$GF(5) = v_{b,1,j,k} \left[\phi \left(\frac{X_{a,a} \rho_a S_a}{M_a} + \frac{X_{o,o} \rho_o S_o}{M_o} + \frac{X_{v,v} \rho_v S_v}{M_v} \right) \right]_{1,j,k}^{n+1}$$

$$GN(5) = v_{b,1,j,k} \left[\phi \left(\frac{X_{a,a} \rho_a S_a}{M_a} + \frac{X_{o,o} \rho_o S_o}{M_o} + \frac{X_{v,v} \rho_v S_v}{M_v} \right) \right]_{1,j,k}^n$$

$$ZA(6) = T_{az}^{n+1} X_{sa}^{n+1}$$

$$BA(6) = T_{ay}^{n+1} X_{sa}^{n+1}$$

$$DA(6) = T_{ax}^{n+1} X_{sa}^{n+1}$$

$$EA(6) = - (ZA(6) + BA(6) + DA(6) + FA(6) + HA(6) + VA(6))$$

$$FA(6) = T_{ax}^{n+1} X_{sa}^{n+1}$$

$$HA(6) = T_{ay}^{n+1} X_{sa}^{n+1}$$

$$VA(6) = T_{az}^{n+1} X_{sa}^{n+1}$$

$$ZO(6) = T_{oz}^{n+1} X_{so}^{n+1}$$

$$BO(6) = T_{oy}^{n+1} X_{so}^{n+1}$$

$$DO(6) = T_{ox}^{n+1} X_{so}^{n+1}$$

$$EO(6) = - (ZO(6) + BO(6) + DO(6) + FO(6) + HO(6) + VO(6))$$

$$FO(6) = T_{ox}^{n+1} X_{so}^{n+1}$$

$$HO(6) = T_{oy}^{n+1} X_{so}^{n+1}$$

$$VO(6) = T_{oz}^{n+1} X_{so}^{n+1}$$

$$ZV(6) = T_{vz}^{n+1} X_{sv}^{n+1}$$

$$BV(6) = T_{vy}^{n+1} X_{sv}^{n+1}$$

$$DV(6) = T_{vx}^{n+1} X_{sv}^{n+1}$$

$$EV(6) = - (ZV(6) + BV(6) + DV(6) + FV(6) + HV(6) + VV(6))$$

$$FV(6) = T_{vx}^{n+1} X_{sv}^{n+1}$$

$$HV(6) = T_{vy}^{n+1} X_{sv}^{n+1}$$

$$VV(6) = T_{vz}^{n+1} X_{sv}^{n+1}$$

$$QF(6) = (Q_s)^{n+1}$$

$$GF(6) = v_{b1,j,k} \left[\phi \left(\frac{x_{sa} \rho_a S_a}{M_a} + \frac{x_{so} \rho_o S_o}{M_o} + \frac{x_{sv} \rho_v S_v}{M_v} \right) \right]_{1,j,k}^{n+1}$$

$$GN(6) = v_{b1,j,k} \left[\phi \left(\frac{x_{sa} \rho_a S_a}{M_a} + \frac{x_{so} \rho_o S_o}{M_o} + \frac{x_{sv} \rho_v S_v}{M_v} \right) \right]_{1,j,k}^n$$

$$ZA(7) = T_{az}^{n+1} \chi_{1,J,k-1/2,3a}^{n+1}$$

$$BA(7) = T_{ay}^{n+1} \chi_{1,J-1/2,k,3a}^{n+1}$$

$$DA(7) = T_{ax}^{n+1} \chi_{1-1/2,J,k,3a}^{n+1}$$

$$EA(7) = - (ZA(7) + BA(7) + DA(7) + FA(7) + HA(7) + VA(7))$$

$$FA(7) = T_{ax}^{n+1} \chi_{1+1/2,J,k,3a}^{n+1}$$

$$HA(7) = T_{ay}^{n+1} \chi_{1,J+1/2,k,3a}^{n+1}$$

$$VA(7) = T_{az}^{n+1} \chi_{1,J,k+1/2,3a}^{n+1}$$

$$ZO(7) = T_{oz}^{n+1} \chi_{1,J,k-1/2,3o}^{n+1}$$

$$BO(7) = T_{oy}^{n+1} \chi_{1,J-1/2,k,3o}^{n+1}$$

$$DO(7) = T_{ox}^{n+1} \chi_{1-1/2,J,k,3o}^{n+1}$$

$$EO(7) = - (ZO(7) + BO(7) + DO(7) + FO(7) + HO(7) + VO(7))$$

$$FO(7) = T_{ox}^{n+1} \chi_{1+1/2,J,k,3o}^{n+1}$$

$$HO(7) = T_{oy}^{n+1} \chi_{1,J+1/2,k,3o}^{n+1}$$

$$VO(7) = T_{oz}^{n+1} \chi_{1,J,k+1/2,3o}^{n+1}$$

$$ZV(7) = T_{vz}^{n+1} \chi_{1,J,k-1/2,3v}^{n+1}$$

$$BV(7) = T_{vy}^{n+1} \chi_{1,J-1/2,k,3v}^{n+1}$$

$$DV(7) = T_{vx}^{n+1} \chi_{1-1/2,J,k,3v}^{n+1}$$

$$EV(7) = - (ZV(7) + BV(7) + DV(7) + FV(7) + HV(7) + VV(7))$$

$$FV(7) = T_{vx}^{n+1} \chi_{1+1/2,J,k,3v}^{n+1}$$

$$HV(7) = T_{vy}^{n+1} \chi_{1,J+1/2,k,3v}^{n+1}$$

$$VV(7) = T_{vz}^{n+1} \chi_{1,J,k+1/2,3v}^{n+1}$$

$$QF(7) = (Q_3)^{n+1} \chi_{1,J,k}^{n+1}$$

$$GF(7) = v_{b,1,J,k} \left[\phi \left(\frac{x_{3a} \rho_a S_a}{M_a} + \frac{x_{3o} \rho_o S_o}{M_o} + \frac{x_{3v} \rho_v S_v}{M_v} \right) \right]_{1,J,k}^{n+1}$$

$$GN(7) = v_{b,1,J,k} \left[\phi \left(\frac{x_{3a} \rho_a S_a}{M_a} + \frac{x_{3o} \rho_o S_o}{M_o} + \frac{x_{3v} \rho_v S_v}{M_v} \right) \right]_{1,J,k}^n$$

APPENDIX G

EXAMPLE SIMULATION DATA SET AND COMPUTER OUTPUT

[illegible]

FLUID/ROCK PHYSICAL PROPERTY DATA

COMPONENT	MOLECULAR WEIGHT (MG/MOL)	CRITICAL PRESSURE (KG/CM ²)	CRITICAL TEMPERATURE (K)	CRITICAL Z-FACTOR	ACENTRIC FACTOR	BOILING POINT (K)
COMPONENT 1	0.01802	22104.59	647.44	0.231	-0.100	373.30
COMPONENT 2	0.07215	3374.86	469.96	0.258	-0.277	308.40
COMPONENT 3	0.14228	2206.32	619.44	0.258	-0.465	271.30
COMPONENT 4	0.04401	7398.07	304.44	0.275	-0.284	194.83
COMPONENT 5	0.02802	3382.22	126.20	0.231	-0.437	77.56

CONSTANTS FOR AQUEOUS PHASE VISCOSITY CALCULATION

AW= 0.00000+000 BV= 0.00000+000

CONSTANTS FOR OILIC PHASE VISCOSITY CALCULATION

COMPONENT	AW	BV
1	0.1000-004	0.1160-003
2	0.1920-001	0.2870-003
3	0.1620-001	0.2870-003
4	0.4130-000	0.5780-003
5	0.14130+000	0.90300+002

CONSTANTS FOR VAPOR PHASE VISCOSITY CALCULATION

COMPONENT	AW	BV
1	0.1000-004	0.1160-003
2	0.1920-001	0.2870-003
3	0.1620-001	0.2870-003
4	0.4130-000	0.5780-003
5	0.25300-003	0.74500+000

DATA REQUIRED FOR PHASE DENSITY CALCULATIONS

DATA REQUIRED FOR LIQUID PHASE DENSITY CALC

COMPONENT	CHE (L/KG)	CRH (L/KG)	CRH (ML/KG)	CRH (L/KG)
1	0.8220-003	0.4480-006	0.5500+005	0.10132+003
2	0.7200-003	0.7200-006	0.8730+004	0.10132+003
3	0.7200-003	0.7200-006	0.5140+004	0.10132+003
4	0.7200-003	0.7200-006	0.5140+004	0.10132+003
5	0.72000-003	0.7200-006	0.5500+005	0.10132+003

1203100

DRY ROCK DENSITY=
ROCK HEAT CAPACITY=

ONE-PROBLEM FORMULATION CONSTANTS

PLATE COMPONENT

TEMPERATURE-DEPENDENT PERMEABILITY DATA

Variable	Mean	Std. Dev.	Minimum	Maximum
KGRO1=	1.0000	0.0000	1.0000	1.0000
SGRO1=	0.0000	0.0000	0.0000	0.0000
SGRO2=	0.0000	0.0000	0.0000	0.0000
SGRO3=	0.0000	0.0000	0.0000	0.0000
KGRO4=	1.0000	0.0000	1.0000	1.0000
SGRO4=	0.0000	0.0000	0.0000	0.0000
SGRO5=	0.0000	0.0000	0.0000	0.0000
SGRO6=	0.0000	0.0000	0.0000	0.0000
SGRO7=	0.0000	0.0000	0.0000	0.0000
SGRO8=	0.0000	0.0000	0.0000	0.0000
SGRO9=	0.0000	0.0000	0.0000	0.0000
SGRO10=	0.0000	0.0000	0.0000	0.0000
SGRO11=	0.0000	0.0000	0.0000	0.0000
SGRO12=	0.0000	0.0000	0.0000	0.0000
SGRO13=	0.0000	0.0000	0.0000	0.0000
SGRO14=	0.0000	0.0000	0.0000	0.0000
SGRO15=	0.0000	0.0000	0.0000	0.0000
SGRO16=	0.0000	0.0000	0.0000	0.0000
SGRO17=	0.0000	0.0000	0.0000	0.0000
SGRO18=	0.0000	0.0000	0.0000	0.0000
SGRO19=	0.0000	0.0000	0.0000	0.0000
SGRO20=	0.0000	0.0000	0.0000	0.0000
SGRO21=	0.0000	0.0000	0.0000	0.0000
SGRO22=	0.0000	0.0000	0.0000	0.0000
SGRO23=	0.0000	0.0000	0.0000	0.0000
SGRO24=	0.0000	0.0000	0.0000	0.0000
SGRO25=	0.0000	0.0000	0.0000	0.0000
SGRO26=	0.0000	0.0000	0.0000	0.0000
SGRO27=	0.0000	0.0000	0.0000	0.0000
SGRO28=	0.0000	0.0000	0.0000	0.0000
SGRO29=	0.0000	0.0000	0.0000	0.0000
SGRO30=	0.0000	0.0000	0.0000	0.0000
SGRO31=	0.0000	0.0000	0.0000	0.0000
SGRO32=	0.0000	0.0000	0.0000	0.0000
SGRO33=	0.0000	0.0000	0.0000	0.0000
SGRO34=	0.0000	0.0000	0.0000	0.0000
SGRO35=	0.0000	0.0000	0.0000	0.0000
SGRO36=	0.0000	0.0000	0.0000	0.0000
SGRO37=	0.0000	0.0000	0.0000	0.0000
SGRO38=	0.0000	0.0000	0.0000	0.0000
SGRO39=	0.0000	0.0000	0.0000	0.0000
SGRO40=	0.0000	0.0000	0.0000	0.0000
SGRO41=	0.0000	0.0000	0.0000	0.0000
SGRO42=	0.0000	0.0000	0.0000	0.0000
SGRO43=	0.0000	0.0000	0.0000	0.0000
SGRO44=	0.0000	0.0000	0.0000	0.0000
SGRO45=	0.0000	0.0000	0.0000	0.0000
SGRO46=	0.0000	0.0000	0.0000	0.0000
SGRO47=	0.0000	0.0000	0.0000	0.0000
SGRO48=	0.0000	0.0000	0.0000	0.0000
SGRO49=	0.0000	0.0000	0.0000	0.0000
SGRO50=	0.0000	0.0000	0.0000	0.0000
SGRO51=	0.0000	0.0000	0.0000	0.0000
SGRO52=	0.0000	0.0000	0.0000	0.0000
SGRO53=	0.0000	0.0000	0.0000	0.0000
SGRO54=	0.0000	0.0000	0.0000	0.0000
SGRO55=	0.0000	0.0000	0.0000	0.0000
SGRO56=	0.0000	0.0000	0.0000	0.0000
SGRO57=	0.0000	0.0000	0.0000	0.0000
SGRO58=	0.0000	0.0000	0.0000	0.0000
SGRO59=	0.0000	0.0000	0.0000	0.0000
SGRO60=	0.000			

0.00000

	0.00000	0.00000	0.00000	0.00000	0.00000
	0.00000	0.00000	0.00000	0.00000	0.00000

LABORATORY HEAT LOSS DATA

OVERALL HEAT TRANSFER COEFFICIENTS UG- 2.00000 UEL- 5.00000
 SYSTEM RADIUS- 0.07620 AMBIENT TEMP- 288.16000
 INITIAL TEMP- 298.16000 LIMITED CONSTANT- 0.00300
 TRANSFER COEFF- 2500.00000 TRANSFER AREA- 0.00314
 1 THERMAL MODEL INITIALIZATION DATA

NUMBER OF GRID BLOCKS NM-17 NZ- 5
 NUMBER OF PHASES AND COMPONENTS NC- 3
 NUMBER OF LIQUID PHASE COMPONENTS NL- 3
 NUMBER OF GAS PHASE COMPONENTS NG- 2
 MAX ALLOWED ITERATIONS ITERIM- 8
 MAX ALLOWED STEP OUTF- 8
 MAX ALLOWED TIME STEPS MAXSTA- 10
 MAX ALLOWED TOTAL ITERATIONS NSTAT- 5000
 TIME STEP PRINT CONTROL VARIABLE NSTPR- 5
 TIME STEP SELECTION NORMS
 SATURATION 0.1000000-001
 PRESSURE 0.5000000+003
 TEMPERATURE 0.5000000+001
 MOLE FRACTION 0.3500000-001
 MAXIMUM TIME STEP DIMAX- 0.3000000+003
 MAX TIME ALLOWED TMAX- 0.2000000+005

GRID BLOCK NO.	WELL INDEX	BLOCK LOCATION	BLOCK LENGTH (M)	BLOCK HEIGHT (M)	BLOCK ELEVATION (M)	ABS. PERM. X-DIRECTION (Darcy)	ABS. PERM. Z-DIRECTION (Darcy)	POROSIITY (FRAC)
1	1	0.00	0.08	0.08	0.00	10.0000	10.0000	0.4500
2	1	0.08	0.08	0.08	0.00	10.0000	10.0000	0.4500
3	1	0.16	0.08	0.08	0.00	10.0000	10.0000	0.4500
4	1	0.24	0.08	0.08	0.00	10.0000	10.0000	0.4500
5	1	0.32	0.08	0.08	0.00	10.0000	10.0000	0.4500
6	1	0.40	0.08	0.08	0.00	10.0000	10.0000	0.4500
7	1	0.48	0.08	0.08	0.00	10.0000	10.0000	0.4500
8	1	0.56	0.08	0.08	0.00	10.0000	10.0000	0.4500
9	1	0.64	0.08	0.08	0.00	10.0000	10.0000	0.4500
10	1	0.72	0.08	0.08	0.00	10.0000	10.0000	0.4500
11	1	0.80	0.08	0.08	0.00	10.0000	10.0000	0.4500
12	1	0.88	0.08	0.08	0.00	10.0000	10.0000	0.4500
13	1	0.96	0.08	0.08	0.00	10.0000	10.0000	0.4500
14	1	1.04	0.08	0.08	0.00	10.0000	10.0000	0.4500
15	1	1.12	0.08	0.08	0.00	10.0000	10.0000	0.4500
16	1	1.20	0.08	0.08	0.00	10.0000	10.0000	0.4500
17	1	1.28	0.08	0.08	0.00	10.0000	10.0000	0.4500

THIRD DIMENSION DV- 0.06

GRID BLOCK SATURATIONS, PRESSURES AND TEMPERATURES

BLOCK NO.	SA	SO	SV	PRESSURE (MPa)	TEMPERATURE (K)	HEAT LOSS (J)	HEAT SINK (J)
-----------	----	----	----	----------------	-----------------	---------------	---------------

GRID BLOCK AQUEOUS, OLEIC AND VAPOUR PHASE MOLE FRACTIONS

[illegible]

TIME STEP SUMMARY

```

TIME = 0.11574-006 DAYS NSTEP = 1
TIME STEP = 0.11574-006 DAYS NSTEP = 4

```

MAXIMUM CHANGES OVER GRID
 DEPMAX = 0.5167-003 DEPMAX = 0.12799-003 DEPMAX = 0.44080-001
 DPMAX = 0.21091-005 DPMAX = 0.21049-005 DPMAX = 0.60414-002
 MASS AND ENERGY BALANCES
 WATER = -0.62462-008 H OIL = -0.10322-008 L OIL = 0.23842-009 CO2 = 0.39913-008 N2 = 0.28949-008 ENERGY = -0.94240-005

TIME STEP SUMMARY

TIME = 0.25793-006 DAYS NSTEP = 2
 TIME STEP = 0.14219-006 DAYS NITER = 4 NEASS = 0 NICUM = 8
 MAXIMUM CHANGES OVER GRID
 DEPMAX = 0.45841-003 DEPMAX = 0.10171-003 DEPMAX = 0.44735-001
 DPMAX = 0.25770-005 DPMAX = 0.25769-005 DPMAX = 0.14691-002
 MASS AND ENERGY BALANCES
 WATER = -0.65369-010 H OIL = -0.10800-010 L OIL = 0.33754-011 CO2 = 0.44022-010 N2 = 0.24527-010 ENERGY = -0.19702-006

TIME STEP SUMMARY

TIME = 0.43547-006 DAYS NSTEP = 3
 TIME STEP = 0.17755-006 DAYS NITER = 4 NEASS = 0 NICUM = 12
 MAXIMUM CHANGES OVER GRID
 DEPMAX = 0.44693-003 DEPMAX = 0.95639-002 DEPMAX = 0.50526-001
 DPMAX = 0.32072-005 DPMAX = 0.25671-005 DPMAX = 0.74882-003
 MASS AND ENERGY BALANCES
 WATER = -0.14605-010 H OIL = -0.23990-011 L OIL = 0.93531-012 CO2 = 0.10286-010 N2 = 0.32618-011 ENERGY = -0.55922-007

TIME STEP SUMMARY

TIME - 0.65801-006 DAYS NSTEP - 4
 TIME STEP - 0.72254-006 DAYS NITER - 3 NPA55 - 0 NIGUM - 15
 MAXIMUM CHANGES OVER GRID
 DEWAX - 0.4833-003 DEWAX - 0.94624+002 DIFFAX - 0.59021-001
 DEWAX - 0.40060-005 DEWAX - 0.40059-005 DIFFAX - 0.62358-003
 MASS AND ENERGY BALANCES
 WATER - 0.73706-008 H OIL - 0.12900-008 L OIL - 0.28794-010 CO2 - 0.43124-008 N2 - 0.11497-007 ENERGY - 0.32809-004

TIME STEP SUMMARY

TIME - 0.93712-006 DAYS NSTEP - 5
 TIME STEP - 0.27911-006 DAYS NITER - 3 NPA55 - 0 NIGUM - 18
 MAXIMUM CHANGES OVER GRID
 DEWAX - 0.25744-003 DEWAX - 0.92456+002 DIFFAX - 0.70043-001
 DEWAX - 0.50048-005 DEWAX - 0.50046-005 DIFFAX - 0.77311-003
 MASS AND ENERGY BALANCES
 WATER - 0.61584-008 H OIL - 0.10825-008 L OIL - 0.22100-010 CO2 - 0.36337-008 N2 - 0.97025-008 ENERGY - 0.27202-004

INJECTION/PRODUCTION SUMMARY

BLOCK	PRESSURE	COMPONENT1	COMPONENT2	COMPONENT3	COMPONENT4	COMPONENT5	WATER	OIL	GAS	ENERGY
RATES PER WELL										
1	616.75	0.15430-001	0.00000+000	0.00000+000	0.17820-003	0.53470-003	0.27802-006	0.00000+000	0.17497-004	0.69766+003
VOLUMES PER WELL										
1	616.75	0.37210-003	0.00000+000	0.00000+000	0.42973-005	0.12894-004	0.67045-008	0.00000+000	0.42193-006	0.16824+002
CUMULATIVE VOLUMES PER WELL										
1	616.75	0.12493-002	0.00000+000	0.00000+000	0.14428-004	0.43293-004	0.22510-007	0.00000+000	0.14167-005	0.56488+002

RATES PER WELL

14 1.00000 0.00000 0.00000 0.00000 0.00000 0.00000 0.00000 0.46338 0.53102 0.00000 0.00000 0.01104 0.00007 0.00000 0.00000 0.00000
 15 1.00000 0.00000 0.00000 0.00000 0.00000 0.00000 0.00000 0.46338 0.53102 0.00000 0.00000 0.01104 0.00007 0.00000 0.00000 0.00000
 16 1.00000 0.00000 0.00000 0.00000 0.00000 0.00000 0.00000 0.46338 0.53102 0.00000 0.00000 0.01104 0.00007 0.00000 0.00000 0.00000
 17 1.00000 0.00000 0.00000 0.00000 0.00000 0.00000 0.00000 0.46338 0.53102 0.00000 0.00000 0.01104 0.00007 0.00000 0.00000 0.00000

TIME STEP SUMMARY

TIME = 0.12670-005 DAYS NSTEP = 6
 TIME STEP = 0.34988-006 DAYS NITER = 3 NPA55 = 0 NIGM = 21
 MAXIMUM CHANGES OVER GRID
 DEPRX = 0.6253-003 DEPRX = 0.96659-002 DEPRX = 0.83832-001
 DOWRX = 0.62455-005 DOWRX = 0.62453-005 DOWRX = 0.10267-002
 MASS AND ENERGY BALANCES
 WATER = -0.59283-008 H OIL = -0.10460-008 L OIL = 0.24477-010 CO2 = 0.35387-008 N2 = 0.91994-008 ENERGY = -0.24924-004

TIME STEP SUMMARY

TIME = 0.17253-005 DAYS NSTEP = 7
 TIME STEP = 0.43827-006 DAYS NITER = 3 NPA55 = 0 NIGM = 24
 MAXIMUM CHANGES OVER GRID
 DEPRX = 0.77650-003 DEPRX = 0.97799-002 DEPRX = 0.19095-000
 DOWRX = 0.77817-005 DOWRX = 0.77814-005 DOWRX = 0.12502-002
 MASS AND ENERGY BALANCES
 WATER = -0.64607-008 H OIL = -0.11438-008 L OIL = -0.35885-010 CO2 = 0.39090-008 N2 = 0.95815-008 ENERGY = -0.24648-004

TIME STEP SUMMARY

TIME = 0.22739-005 DAYS NSTEP = 8
 TIME STEP = 0.54859-006 DAYS NITER = 3 NEASS = 0 NICUM = 27
 MAXIMUM CHANGES OVER GRID
 DSWAX = 0.9120-003 DEFWAX = 0.98756+002 DIFFMAX = 0.12218+000
 DROWAX = 0.56793-005 DROWAX = 0.56790-005 DIFFMAX = 0.13614-002
 MASS AND ENERGY BALANCES
 WATER = -0.79109-008 H OIL = -0.14033-008 L OIL = 0.63705-010 CO2 = 0.48536-008 N2 = 0.10838-007 ENERGY = -0.26235-004

TIME STEP SUMMARY

TIME = 0.29601-005 DAYS NSTEP = 9
 TIME STEP = 0.68627-006 DAYS NITER = 3 NEASS = 0 NICUM = 30
 MAXIMUM CHANGES OVER GRID
 DSWAX = 0.1120-003 DEFWAX = 0.92789-002 DIFFMAX = 0.14856+000
 DROWAX = 0.12018-004 DROWAX = 0.12018-004 DIFFMAX = 0.12895-002
 MASS AND ENERGY BALANCES
 WATER = -0.10212-007 H OIL = -0.18064-008 L OIL = 0.12493-009 CO2 = 0.63653-008 N2 = 0.12440-007 ENERGY = -0.28497-004

TIME STEP SUMMARY

TIME = 0.38181-005 DAYS NSTEP = 10
 TIME STEP = 0.85795-006 DAYS NITER = 3 NEASS = 0 NICUM = 33
 MAXIMUM CHANGES OVER GRID
 DSWAX = 0.1357-003 DEFWAX = 0.10134+003 DIFFMAX = 0.18138+000
 DROWAX = 0.11893-004 DROWAX = 0.14892-004 DIFFMAX = 0.13163-002
 MASS AND ENERGY BALANCES
 WATER = -0.12651-007 H OIL = -0.22178-008 L OIL = 0.22701-009 CO2 = 0.80377-008 N2 = 0.13228-007 ENERGY = -0.28895-004

INJECTION/PRODUCTION SUMMARY

BLOCK	PRESSURE	COMPONENT1	COMPONENT2	COMPONENT3	COMPONENT4	COMPONENT5	WATER	OIL	GAS	ENERGY
RATES PER WELL										
1	1111.09	0.15430-001	0.00000+000	0.00000+000	0.17820-003	0.53470-003	0.27802-006	0.00000+000	0.17497-004	0.69766+003
VOLUMES PER WELL										
1	1111.09	0.11438-002	0.00000+000	0.00000+000	0.13209-004	0.39636-004	0.20609-007	0.00000+000	0.12970-005	0.51715+002
CUMULATIVE VOLUMES PER WELL										
1	1111.09	0.50901-002	0.00000+000	0.00000+000	0.58785-004	0.17639-003	0.91713-007	0.00000+000	0.57718-005	0.23015+003
RATES PER WELL										
17	101.33	0.00000+000	0.00000+000	0.00000+000	0.00000+000	0.00000+000	0.00000+000	0.00000+000	0.00000+000	0.00000+000
VOLUMES PER WELL										
17	101.33	0.00000+000	0.00000+000	0.00000+000	0.00000+000	0.00000+000	0.00000+000	0.00000+000	0.00000+000	0.00000+000
CUMULATIVE VOLUMES PER WELL										
17	101.33	0.00000+000	0.00000+000	0.00000+000	0.00000+000	0.00000+000	0.00000+000	0.00000+000	0.00000+000	0.00000+000

GRID BLOCK SATURATIONS, PRESSURES AND TEMPERATURES

BLOCK NO.	SA	SO	SV	PRESSURE (KPA)	TEMPERATURE (K)	HEAT LOSS (KJ)	HEAT SINK (KJ)
1	0.20138	0.79141	0.00723	1111.09	299.07	0.82248-001	-0.71051+001
2	0.20120	0.79151	0.00079	1115.77	298.20	-0.67488-002	0.00000+000
3	0.20039	0.78870	0.00090	102.16	298.16	-0.47521-003	0.00000+000
4	0.20040	0.78870	0.00091	101.33	298.16	-0.25844-004	0.00000+000
5	0.20040	0.78869	0.00091	101.33	298.16	-0.14917-005	0.00000+000
6	0.20040	0.78869	0.00091	101.33	298.16	-0.12187-005	0.00000+000
7	0.20040	0.78869	0.00091	101.33	298.16	-0.27311-006	0.00000+000
8	0.20040	0.78869	0.00091	101.33	298.16	-0.27119-006	0.00000+000
9	0.20040	0.78869	0.00091	101.33	298.16	-0.27119-006	0.00000+000
10	0.20040	0.78869	0.00091	101.33	298.16	-0.27119-006	0.00000+000
11	0.20040	0.78869	0.00091	101.33	298.16	-0.27119-006	0.00000+000
12	0.20040	0.78869	0.00091	101.33	298.16	-0.27119-006	0.00000+000
13	0.20040	0.78869	0.00091	101.33	298.16	-0.27119-006	0.00000+000
14	0.20040	0.78869	0.00091	101.33	298.16	-0.27119-006	0.00000+000
15	0.20040	0.78869	0.00091	101.33	298.16	-0.27119-006	0.00000+000
16	0.20040	0.78869	0.00091	101.33	298.16	-0.27119-006	0.00000+000
17	0.20040	0.78869	0.00091	101.33	298.16	-0.13559-008	0.00000+000

•GRID BLOCK AQUEOUS, OLEIC AND VAPOUR PHASE MOLE FRACTIONS

VITA

NAME: Thomas Grant Harding
PLACE OF BIRTH: Calgary, Alberta, Canada
YEAR OF BIRTH: 1951

POST-SECONDARY EDUCATION AND DEGREES:

University of Calgary
Calgary, Alberta Canada,
1969-1973
B.Sc. Chemical Engineering

University of Calgary
Calgary, Alberta, Canada
1973-1976
M.Sc. Chemical Engineering

HONOURS AND AWARDS:

AOSTRA Scholarship 1981-1983

RELATED WORK EXPERIENCE:

Teaching Assistant
University of Calgary
1973-1976

Reservoir Engineer
Oil Sands Department
BP Canada Inc.
1976-1980

Teaching Assistant
University of Alberta
1980-1983

Supervisor, Technical Development
Oil Sands Department
BP Canada Inc.
1983-1986

PUBLICATIONS:

Harding, T. G. and Ejiogu, G. C.: "Pilot to Commercial Production of Bitumen in the Wolf Lake Area", presented at Advances in Petroleum Recovery and Upgrading Technology 1986, Calgary, June 12-13, 1986.

VITA (continued)

Pethrick, W. D., Sennhauser, E. S. and Harding, T. G.: "Numerical Modelling Optimization of Cyclic Steam Stimulation in Cold Lake Oil Sands", paper no. 86-37-21 presented at the 37th Annual CIM Technical Meeting, Calgary, June 9-11, 1986.

Harding, T. G. and Farouq Ali, S. M.: "Mine-Assisted Heavy Oil Recovery Technology", SPE 12787 presented at the 1984 SPE California Regional Meeting, Long Beach, April 11-13, 1984.

Harding, T. G., Farouq Ali, S. M. and Flock, D. L.: "Steamflood Performance in the Presence of Carbon Dioxide and Nitrogen", Journal of Canadian Petroleum Technology, Sept.-Oct. 1983, pp. 30-37.

Harding, T. G.: "Marguerite Lake Phase A Project", presented at the AOSTRA Seminar on Non-Conventional Oil Recovery Technology, Calgary, May 29-30, 1980, 24 pp.

Grabowski, J. W., Rubin, B. and Harding, T. G.: "A Preliminary Numerical Simulation Study of In-Situ Combustion in a Cold Lake Oil Sands Reservoir", Journal of Canadian Petroleum Technology, April-June, 1981, pp. 79-89.

Harding, T. G., Moore, R. G., Bennion, D. W. and Donnelly, J. K.: "Adiabatic Combustion Tube Evaluation of In-Situ Processes for Oil Sands", presented at the 26th Annual Meeting of the Canadian Society for Chemical Engineering, Toronto, Oct. 3-6, 1976, 17 pp.